Molecular Mechanisms of B Cell Activation

Tim Schnyder

University College London (UCL)

Submitted for the degree of PhD

To Katrin. This is for you.

Declaration

I, Tim Schnyder, confirm that the work presented in this thesis is my own. Where information has been derived from other sources, I confirm that this has been indicated in the thesis.

Tim Schnyder London, November 2012

Abstract

Our body is under constant attack by pathogens such as viruses or bacteria. The immune system has evolved to efficiently counteract these attacks using an array of cells and soluble proteins. In particular, B cells support the immune system by producing high-affinity antibodies, which target pathogens for destruction by recognition of antigenic structures. B cells furthermore contribute to immunological memory to quickly mount responses to secondary challenges by the same pathogen.

In order to produce antibodies, B cells need to get activated in secondary lymphoid organs by a two-step process: First, B cells sense antigen molecules on the surface of antigen-presenting cells using their B cell receptor (BCR), which leads to intracellular signalling and antigen acquisition. B cells then present processed antigen molecules to specific helper T cells. Both BCR ligation and adequate T cell help lead to full B cell activation and the production of antigen-specific antibodies.

This thesis investigates the early molecular events of B cell activation. Using a combination of genetics, lipid bilayers and high-resolution microscopy we identify a role for the adaptors Grb2 and Dok-3 alongside the ubiquitin ligase Cbl in antigen gathering by B cells. Moreover, we show recruitment of Grb2, Dok-3 and Cbl to the signalling BCR and establish Grb2 as a central downstream adaptor. We further assess the role of several motor proteins in antigen gathering and find that dynein is recruited to the signalling BCR driving antigen gathering by the movement of antigen-containing BCR microclusters on the underlying microtubule network. Interestingly, recruitment of dynein to BCR microclusters is impaired in B cells lacking Grb2, Dok-3 or Cbl. As the amount of antigen acquired by B cells directly correlates with the extent of T cell help, the data presented significantly contributes to our understanding of the early molecular events underlying B cell activation.

Acknowledgments

This thesis would not exist without the help of so many people both near and far. It has been a team effort really and I cannot say how much I appreciate the help and motivation I have received from you!

First of all I would like to thank my previous tutors Laurence Bugeon, Fiona Culley, Maggie Dallman and Dan Davis for lighting the fire in me by getting me interested in immunology and the power of imaging. Further, I would like to thank Cancer Research UK and everybody at the London Research Institute for providing an excellent working environment. Facilities like FACS or biological resources, our lab aides Chris and Ian and the whole admin team including Alice, Catalina, Sabina and Erin have made life so much easier. In this context I would also like to thank Sally for her continuous support and understanding throughout the years at the LRI. In addition, I very much appreciate the help provided by my thesis committee, Jürgen and Caetano, who made me think harder on my research.

Regarding the lymphocyte interaction lab, I do not know where to start or to end. It has been an incredible experience working with all of you and apart from being great colleagues you have also been good friends helping me out whenever I needed you. In particular I would like to thank: Selina, for being enthusiastic about my work and willing to continue with it; Olivier, for providing the bigger picture and for saving my humor during the write-up period by introducing me to Eddie Izzard; Carol and Irene, for providing a taste of human immunology; Elo, for being a true Argentinian football fan and always in a good mood; Julia, for passing on her knowledge about particles and helping me to understand *in vivo* work; Patricia, for being an outstanding scientist and always up for a coffee; Michele, for setting the foundation of my work, for being very good fun at nights out or at concerts and for helping me settle in the lab; David, for being an incredible teacher, always calm, and for being a good friend and amazing chef; Beb, for being a tough cookie and a fantastic teacher and for making me understand that the cell is not just a bag of enzymes, I'll never forget that; Pieta,

for being similarly tough as Beb, but also incredibly supportive and good fun whenever we went out; Angelo, for introducing style and drama in the lab; Christoph, for being German and a good pal to discuss current issues of all sorts with; Andreas, for being so supportive and reliable during the paper writing phase and for developing analysis tools for everything I needed in no time; Bea, for a constant provision of chewing gum, the organisation of everything in the lab, but also for being unintentionally funny and slightly chaotic at times; Naomi, for the fantastic support during the generation of the paper and this thesis and for her almost unbelievable efficiency and sharpness and finally Aitor for teaching me how to set up experiments properly, for sharing his music and for being good fun and of course a dear friend.

Last but not least I would like to thank you, Facundo. I guess we both know why… Not only have you taught me how to do great science, but also how to interpret and present it. In addition, you have taught me that scientific life is not only about good experiments, but also about trust; trust in yourself, trust in your data and trust in other people. You have provided so much and I thank you for it!

In addition to my working environment I have received at least as much support from people outside the institute. In this respect I would like to thank my good friends near and far for providing a balance and for being there for me. You know who you are and I would not have achieved this without you!

A very fond thank you also goes to my family including my grandparents and Heike and Jürgen, who have been very supportive although I have hardly been in touch. That is going to change soon… Last but not least I would like to thank my parents Liane and Achim and my sister Claire. You have been so incredibly supportive all these years and coping so well with me not being around. I cannot say how much that has meant to me and I wish that one day I can live by your example. Thank you!

Table of Contents

List of Figures, Videos and Appendices

Videos	**Title**
Video 1	Bjab B cells spread on anti-human IgM-coated glass
Video2	DT40 B cells lacking Grb2, Dok-3 or Cbl do not gather antigen-containing BCR microclusters in a central aggregate
Video 3	Grb2 colocalises with antigen-containing BCR microclusters over time
Video 4	Grb2 recruitment to antigen-containing BCR microclusters is altered in *Dok-3*$^{-/-}$ B cells
Video 5	SLP65 colocalises with antigen-containing BCR microclusters over time
Video 6	CIN85 colocalises with antigen-containing BCR microclusters over time
Video 7	Myosin IIa does not colocalise with antigen-containing BCR microclusters over time
Video 8	Myosin VI does not colocalise with antigen-containing BCR microclusters over time
Video 9	Myosin VI does not mediate centripetal movement of antigen-containing BCR microclusters
Video 10	Dynein colocalises with antigen-containing BCR microclusters over time
Video 11	Inhibition of dynein activity or expression affects centripetal movement of antigen-containing BCR microclusters
Video 12	Single particles of BCR are immobilized in tubulin-rich regions upon BCR cross-linking
Video 13	The microtbule network in B cells is highly dynamic
Video 14	The tubulin network is unaffected in cells lacking Grb2, Dok-3 or Cbl
Video 15	Dynein colocalises with antigen-containing BCR microclusters in DT40 B cells over time
Video 16	Recruitment of dynein to antigen-containing BCR microclusters requires Grb2, Dok-3 or Cbl

All supplementary videos can be found as mov-files on the CD-ROM attached to this thesis. They can be read using Quicktime or VLC player for PC or Macintosh.

Appendices	**Title**
Appendix 1	List of abbreviations
Appendix 2	Supplementary video legends

Chapter 1 : Introduction

The process of B cell activation in the context of an immune response is both highly specific and tightly regulated. This thesis describes the early molecular events during B cell activation and reveals new insights into the mechanisms by which B cells gather antigen to allow full activation.
To appreciate the importance of B cell activation during an immune response, this chapter introduces the underlying concepts in light of the relevant literature.

1.1 The Immune System: Who fights who?

Our body is constantly challenged by harmful pathogens such as viruses, bacteria or parasites from the environment (Janeway et al., 2008). We use physical barriers such as the skin to keep pathogens out of our organism (Gallo et al., 2002). However, in some occasions pathogenic particles make their way into the body and cause an infection (Hornef et al., 2002). Typical entry routes are the airway, the digestive system or lesions in the skin. Once pathogens have entered the organism, cells of our immune system get activated in order to clear the infection. The immune system of higher vertebrates is composed of a large number of different cell types of the hematopoietic lineage. Immune cells constantly patrol the body and induce an immune response upon encounter of a pathogen. The initiation of an immune response relies on a functional and complex network of cellular interactions ensuring appropriate activation of immune cells and clearance of pathogens (Janeway et al., 2008).
Apart from dealing with infections, our immune system also maintains homeostasis by eliminating old cells that have undergone programmed cell death. Furthermore, immune cells provide a basal protection from cancer by continuously removing genetically transformed cells, which can potentially give rise to tumors. On the flip-side, dysregulated activation of immune cells can cause

severe clinical conditions such as lymphomas, leukemia or a variety of auto-immune diseases (Ehrlich and Morgenroth, 1957; Plotz, 2003; Shlomchik et al., 1987 and Kato et al., 2009). It is therefore apparent that the initiation of an immune response represents a careful balance of activatory and inhibitory signals (Acuto et al., 2008).

In the context of an infection with a pathogen, the corresponding immune response is broadly separated into two branches: innate and adaptive immunity. The combination of innate and adaptive immunity and their interplay allows our body to react to an infection both quickly and in a highly specific manner. The following pages will provide an introduction to the two branches of immunity and underline the different concepts of pathogen recognition by cells of the innate or adaptive immune system. In particular, we will explain the role of B cells during an immune response and highlight critical stages in their maturation and activation.

1.1.1 The innate immune system serves as a first line of defence

The innate immune system serves as a first line of defense against pathogenic organisms and uses mechanisms such as ingestion of pathogens, apoptosis of infected cells and unspecific killing by toxic granules (Aderem and Underhill, 1999; Harrison and Grinstein, 2002 and Chertov et al., 2000). An immune response is initially triggered by cells of the innate immune system such as Macrophages residing in tissues, which can be challenged by an infectious organism. Macrophages carry an array of pattern recognition recptors (PRRs) such as mannose, glucan, scavenger and toll-like receptors on their surface (Janeway and Medzhitov, 2002; Medzhitov and Janeway, 2000 and Gough and Gordon, 2000). These receptors represent a fixed repertoire of specificities and are able to sense the presence of common pathogen-associated molecular patterns (PAMPs) such as lipopolysaccharide (LPS) found in the outer membrane of gram-negative bacteria (Medzhitov and Janeway, 2000). Apart from providing an activatory signal, PRRs furthermore allow Macrophages to engulf and eventually kill bacteria in an intracellular structure called the phagolysosome.

Once activated *via* their surface receptors, Macrophages secret a variety of cytokines such as tumor necrose factor-α (TNF-α), interleukin-1 and -6 (IL-1 and IL-6) and prostaglandins (Brightbill et al., 1999, Heine and Lien, 2003 and Pfeffer, 2003). The secretion of these soluble factors signals the presence of an infectious agent and activates other immune cells such as granulocytes including neutrophils, basophils or eosinophils. The latter are recruited from the blood stream and adjacent tissues to the site of infection by secretion of chemoatractants such as interleukin-8 (IL-8) by macrophages (Kunkel and Butcher, 2002 and Bochenska-Marciniak et al., 2003). The activation and recruitment of immune cells is concomitant with the common global signs of infection like pain, swelling, increase of temperature and blushing. The primary role of granulocytes is the release of toxic granules at the site of infection to eliminate pathogenic organisms. However, the random secretion of toxic granules inevitably also leads to the killing of host cells and thus represents a very crude and unspecific means of fighting infections.

In contrast to bacterial challenges, viral infections are mainly cleared by cell-mediated cytotoxicity provided by natural killer (NK) cells and others. NK cells constantly patrol our tissues by attaching to host cells and scanning their surface for the presence of molecules, which can be induced by viral infections, cellular stress or malignant transformations (Biron et al., 1999 and Orange et al., 2002). One member of this family is the major histocompatibility complex class I polypeptide-related sequence A (MICA) that is specifically recognised by the activating NK cell receptor NKG2D (Robbins and Brossay, 2002 and McCann et al., 2007). Upon activation by MICA NK cells release toxic agents at the interface between the infected host cell and themselves to initiate cell-mediated killing. This mechanism of cytotoxicity only targets the cell under surveillance and thus leads to less unspecific damage compared to the release of toxic granules by granulocytes as described earlier.

In addition to cell-mediated immunity the complement system represents an array of soluble plasma proteins that interact with pathogens and mark them for destruction by phagocytic cells such as Macrophages (Frank and Fries, 1991 and Tomlinson, 1993). Complement uses conserved recognition patterns such as

certain sugar molecules on the surface of pathogens to initiate a cascade of proteolytic cleavages of numerous proteins subsequently leading to opsonisation of pathogenic organisms and their eventual clearance (Bhakdi and Tranum-Jensen, 1991 and Ehlers, 2000).

In summary, the innate immune system makes use of numerous strategies to fight pathogens quickly after an infection has occurred. These mechanisms include phagocytosis, release of cytotoxic agents, cell-mediated cytotoxicity or opsonisation by the complement system. These first stages of an immune response are important to limit the pathogenic load and also to induce adaptive immunity. However, the innate immune system relies on the expression of receptors on the surface of immune cells, which have a limited specificity inherited in the genome and only recognise conserved molecular patterns. Driven by evolution pathogens have developed many ways to subvert the surveillance provided by the innate immune system. Luckily, adaptive immunity provides our body with a means to fight pathogens, which are difficult to detect with the limited repertoire of receptors expressed by cells of the innate immune system.

1.1.2 Adaptive immunity:

The diversity of lymphocyte receptors allows adequate immune responses

Our defense mechanisms rely on adaptive immunity in case of a challenge with a pathogen that cannot be detected by cells of the innate immune system expressing a restricted set of PRRs. Therefore our body is equipped with cells, which constitute the adaptive immune system and are called lymphocytes. Lymphocytes are generated from a common lymphoid progenitor (CLP) and are mainly sub-divided into T and B cells (Akashi et al., 1999). The differentiation of a CLP into T or B cells is driven by extracellular cues such as the presence of interleukin-7 (IL-7) and the cellular environment. Although both T and B cells are generated from CLPs, they mature in different tissues: T cells develop in the thymus, whereas B cells predominantly mature in the bone marrow (Nagasawa, 1996 and Carlyle, 1998).

The striking feature of lymphocytes is the surface expression of immunoreceptors, which are encoded in multiple gene segments and are able to recognise a wide variety of molecular structures (Clark and Kupper, 2005) (Figure 1.1.). Genetic re-arrangements of immunoreceptor genes during T and B cell development lead to the generation of lymphocyte pools consisting of cell clones each expressing an immunoreceptor of unique specificity (Talmage, 1957 and Potworowski and Nairn, 1967). The large diversity of receptor specificities thus provides the immune system with a vast repertoire of immune cells able to identify and fight a plethora of pathogenic structures.

T and B cell clones whose receptors recognise ubiquitous self-antigens originating from host tissues are eliminated from the pool by a process called clonal deletion involving apoptosis (Cornall et al., 1995 and Zinkernagel et al., 1978). This process is of great importance to prevent the development of autoimmune diseases such as rheumatoid arthritis or diabetes once mature lymphocytes patrol the body. In the particular case of B cells there is a mechanism in place that allows some self-reactive B cell clones to be rescued from apoptosis, however. By further genetic rearrangement of the immunoreceptor loci, self-reactive B cells retain the capability to change the specificity of their receptor. Hence, this mechanism is called receptor editing (Tiegs, 1993 and Casellas, 2001).

Upon completion of maturation T and B cells leave the thymus or the bone marrow, respectively, and home to secondary lymphoid organs such as the spleen, lymph nodes or smaller structures like the tonsils or Peyer's patches (Mebius, 2003). There they can encounter pathogenic structures, which are broadly called antigens, in the context of an infection.

Antigens are recognised by immunoreceptors expressed on the surface of lymphocytes (Ager, 1996). Given the large pool of lymphocytes expressing immunoreceptors with a wide variety of specificities, it is likely that one ore more lymphocyte clones are able to sense the presence of antigenic structures through their receptor. Ligation of immunoreceptors by antigen leads to activation of the particular lymphocyte clone and triggers a process of clonal expansion. This process involves proliferation and differentiation of lymphocytes leading to the generation of effector cells bearing the same antigen specificity as their ancestors.

A

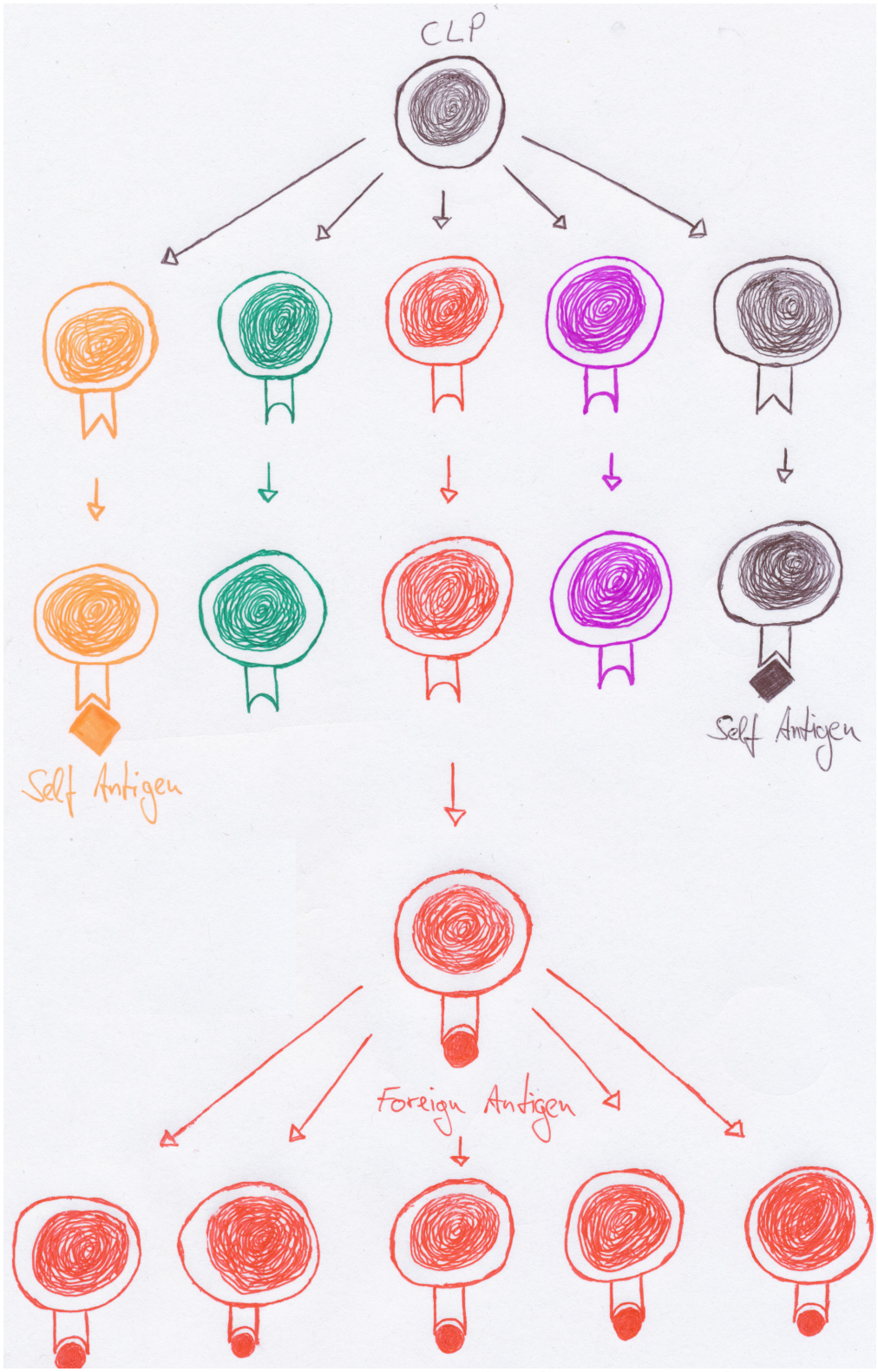

Figure 1.1. Immunoreceptor expression on lymphocytes is crucial for survival, self-tolerance and appropriate immune responses against a plethora of pathogens

(A) A common lymphoid progenitor (CLP) gives rise to a large number of lymphocytes each expressing a unique immunoreceptor. During maturation the immunoreceptor can deliver survival signals. Maturation of self-reactive lymphocytes recognising self-antigens derived from host tissue is halted and cells are removed from the pool by apoptosis or anergy. In order to circumvent deletion from the pool, self-reactive lymphocytes can edit their receptor and render it non-specific for host tissue. Foreign antigen triggers a specific immunoreceptor on a lymphocyte during an immune response and initiates a process of clonal expansion. Antigen specificity is thus maintained as the progeny proliferates and differentiates into effector cells. Adapted from Janeway et al., 2008.

Large numbers of effector cells are generated within a few days, which in turn target pathogens for destruction or eliminate infected cells. Moreover, certain sub-populations of effector cells provide immunological memory by the generation of long-lived memory cells (Mitchell and Chan, 1972). These are of great importance in the case of a second challenge with the same pathogen and equip the host with a quick and efficient mechanism of fighting the same pathogen again.

Adaptive immunity thus provides the immune system with pools of B and T cell clones, which express immunoreceptors specific for a vast variety of antigens. Upon activation of B and T cells in secondary lymphoid organs antigen-specific lymphocytes undergo clonal expansion yielding large numbers of effector cells. This allows us to efficiently fight a plethora of pathogenic organisms and supplies immunological memory for future challenges with identical pathogens.

1.1.3 The role of B cells during an immune response and the special structure of the BCR

B cells are lymphocytes that get activated during an immune response. They are part of the adaptive immune system and help the host organism to fight pathogens such as viruses or bacteria by producing antibodies, also called immunoglobulins (Tiselius and Kabat, 1938 and Fagraeus, 1948). Antibodies are proteins characterised by their unique Y-shaped structure and their ability to bind antigens with great affinity (Frangione et al., 1969 and Harris et al., 1992) (Figure 1.2. A). During the course of an immune response antibodies are released into the extracellular space by specialised B cells and they are used by the immune system to recognise antigenic structures such as whole pathogens or toxins and target them for destruction by phagocytes, NK cells or the complement system (Figure 1.2. B). Apart from antibody production for the fight against pathogens, activated B cells furthermore differentiate into memory cells providing long-term protection against pathogens. This immunological memory is crucial for mounting a fast and efficient immune response against pathogens, which might have challenged the host before (Mitchell and Chan, 1972).

B cells express an immunoreceptor on their surface, which is a membrane-bound version of an antibody: the B cell receptor (BCR). The BCR is an immunoglobulin composed of two heavy and two light chains (Edelman, 1991) (Figure 1.2. C). Disulfide bonds at the hinge region covalently connect the heavy chains (Frangione and Milstein, 1967). Digestion of immunoglobulins with proteases such as papain yields one Fc fragment containing the membrane proximal portion of both heavy chains and two Fab fragments comprised of the light chains and residual heavy chains (Porter, 1991). In contrast to the T cell receptor, the Y-shaped structure of the BCR with one Fc and two Fab portions linked at the hinge region allows it to bind multivalent, intact antigens independent of accessory molecules (Poljak, 1991). Antigen specificity of the BCR is achieved by juxtaposition of the variable domains of both heavy and light chains, which form antigen-binding pockets, also called complimentary-determining regions (CDRs) (Al-Lazikani et al., 1997 and North et al., 2010).

Transmembrane domains found in both heavy chains ensure plasma membrane tethering of the BCR. Importantly, the BCR itself cannot trigger intracellular signals upon cross-linking by antigen. Therefore it non-covalently associates with the Igα and Igβ molecules (CD79a and CD79b, respectively), which are connected by a disulfide bond (Schamel and Reth, 2000). The Igα/β sheath possesses immunoreceptor tyrosine activation motifs (ITAMs), which provide a platform for intracellular signalling when phosphorylated at ITAM-tyrosine residues by a kinase (Reth, 1989).

Depending on their differentiation and maturation stage, B cells can express different isotypes of immunoglobulins. Moreover, during an immune response B cells diversify the repertoire of antigen-specific antibodies produced by a process called isotype switching (Stavnezer, 1996). This results in the production of different immunoglobulin isotypes including IgM, IgD, IgG, IgE and IgA, which in turn dictate the outcome of the effector response. Another important mechanism by which activated B cells alter the repertoire of antigen-specific antibodies is the phenomenon of somatic hypermuation. This process is applied by B cells to introduce random mutations in the genes coding for the variable regions of both heavy and light chains. After a selection process, somatic hypermutation eventually leads to the production of antibodies that can bind the specific antigen with greater affinity thus helping the immune system to target pathogens more efficiently (MacLennan, 1994 and Rajewsky, 1996).

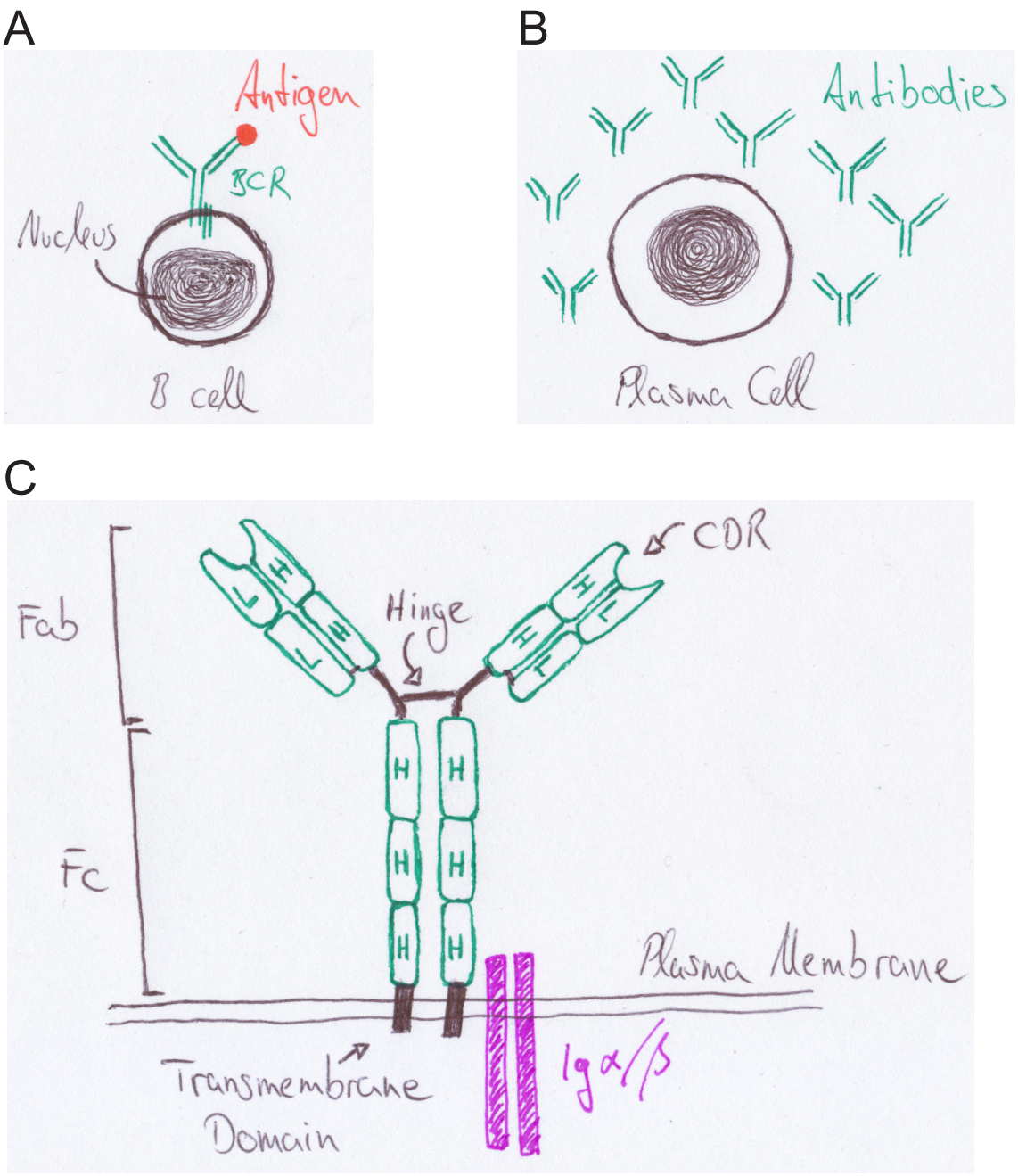

Figure 1.2. B cells produce antibodies upon activation
(A) B cells are lymphocytes derived from the bone marrow. Each B cell clone expresses a B cell receptor (BCR) with unique specificity for an antigen. Antigens can be derived from the host tissue (self antigen) or from pathogens such viruses or bacteria. (B) Upon activation in the context of an immune response B cell clones undergo a maturation process involving differentiation and proliferation. The resulting plasma cells produce a soluble, high-affinity version of their BCR to target pathogenic structures for clearance. (C) The BCR immunoglobulin consists of two heavy (H) and two light (L) chains. Chains are covalently linked by disulfide bonds at the Hinge region, which can be digested with proteases to yield two Fab fragments and one Fc fragment. The heavy chains contain transmembrane domains and thus confer membrane anchoring of the BCR. Antigen binding is mediated by the two complimentary-determining regions (CDR) by juxtaposition of the variable domains of the heavy and light chains. Adapted from Janeway et al., 2008.

To sum up, B cells are a sub-population of lymphocytes, which produce antibodies during an adaptive immune response. Antibodies help the immune system to neutralise harmful structures such as pathogens or toxins by targeting them for destruction. Over the course of an immune response the repertoire of antigen-specific antibodies can be varied. The processes of isotype switching and somatic hypermutation yield several classes of antibodies with higher affinity for the antigen triggering a wide variety of effector functions by other cells of the immune system. Lastly, B cells express an immunoreceptor, which is a membrane-bound version of an antibody called the BCR. The special Y-shaped structure of the BCR allows B cells to bind native antigens in a multivalent fashion without the need for other accessory molecules. The expression of the BCR and its subclass is furthermore linked to the maturation and differentiation stage of B cells.

1.1.4 B cell development and differentiation is linked to BCR expression

Hematopoietic stem cells resdiding in the bone marrow can commit to the lymphoid lineage by differentiating into common lymphoid progenitors (CLPs). The latter give rise to lymphocytes such as T and B cells mainly driven by signalling through the interleukin-7 receptor (IL-7R). The development of B cells in particular is characterised by several stages and linked to the re-arrangement of gene segments coding for the BCR and its subsequent expression (Gathings et al., 1977) (Figure 1.3. A).

Pro B cells can be phenotypically identified by surface expression of the markers CD19 and B220 (CD45R) (Coffman, 1982). While B220 is also expressed by some subsets of splenic dendritic cells, CD19 is widely regarded as a unique B cell marker further to its role as the BCR co-receptor. During the pro B cell stage, gene segments coding for the BCR heavy chains are re-arranged. This is achieved by the random fusion of inherited gene elements from the variable (V), diverse (D) and joining (J) regions. This process is referred to as VDJ recombination and is orchestrated by enzymes of the recombination activating genes (RAG) family, which introduce DNA double-strand breaks to enable gene segment shuffling and re-joining (Schatz et al., 1989; Agrawal and Schatz, 1997 and Grawunder et al., 1998). VDJ recombination creates a wide variety of immunoglobulin heavy chains and is thus the first process leading to immunoreceptor diversification (Brack et al., 1978). Upon expression of a functional heavy chain the pro B cell progresses to the next maturation stage and becomes a pre B cell.

In order to progress to the pre B cell stage, the newly created immunoglobulin heavy chain needs to associate with a surrogate light chain. This association leads to surface expression of the pre-BCR, which associates with the Igα/β sheath on the cell surface. Expression of the pre-BCR is a hallmark of the pre B cell stage and is crucial for B cell development in several ways: First, surface expression of the pre-BCR is part of a selection process, which singles out heavy chains that are capable of assembling as homodimers and associating with light chains, thus having the potential to form a functional BCR (Kitamura et al., 1992 and Shimizu et al., 2002). Second, signalling through the pre-BCR triggers proliferation and stops any further re-arrangements within the heavy chain locus. This process is

called allelic exclusion and ensures expression of only one unique BCR by any given B cell clone (Loffert et al., 1996). Finally, pre-BCR signalling leads to downregulation of surrogate light chain expression and initiates gene re-shuffling within the light chain locus characterised by recombination of V and J gene segments. Upon completion of V and J gene re-arrangement the resulting light chains associate with the previously created heavy chains to form a functional BCR, which is expressed at the cell surface and associates with the Igα/β sheath (Arakawa et al., 1996). Surface expression of a fully functional BCR initiates the progression to the next developmental stage.

Immature B cells express a functional BCR allowing them to detect antigen and become activated. However, before leaving the bone marrow B cells have to be selected based on their potential to cause auto-immunity. Ubiquitous self-antigens are therefore presented to immature B cells in order to select clones, which do not get activated by host tissues, as this would have severe consequences. When recognising self-antigens, immature B cells can either become anergic, a state of long-lasting unresponsiveness, or they can be removed from the B cell pool by clonal deletion involving apoptosis (Nemazee and Burki, 1989). The outcome of the selection process in the bone marrow relies on the nature of self-antigens: Whereas mulitivalent, membrane-bound antigen triggers apoptosis of autoreactive B cells, soluble monovalent antigen promotes entry into anergy (Hartley et al., 1991 and Goodnow, 1996). B cell clones, which do not react to self-antigens, are allowed to leave the bone marrow. After a transitional maturation stage in the periphery (T1 and T2 B cells) (Loder et al., 1999), mature B cells home to secondary lymphoid organs to fulfil their main function, the production of antibodies in the context of an immune response.

Mature B cells express BCRs of two different isotypes, IgM and IgD (Figure 1.3. B). The ratio of IgM to IgD surface expression differs between organisms and subtypes: While follicular B cells express high amounts of IgD and intermediate levels of IgM, marginal zone B cells in the spleen show high levels of IgM and low amounts of IgD (Loder et al., 1999 and Makowska et al., 1999). The expression of both IgM and IgD is crucial for steady-state B cell survival as they transduce low-level, tonic signals into the intracellular space (Lam et al., 1997

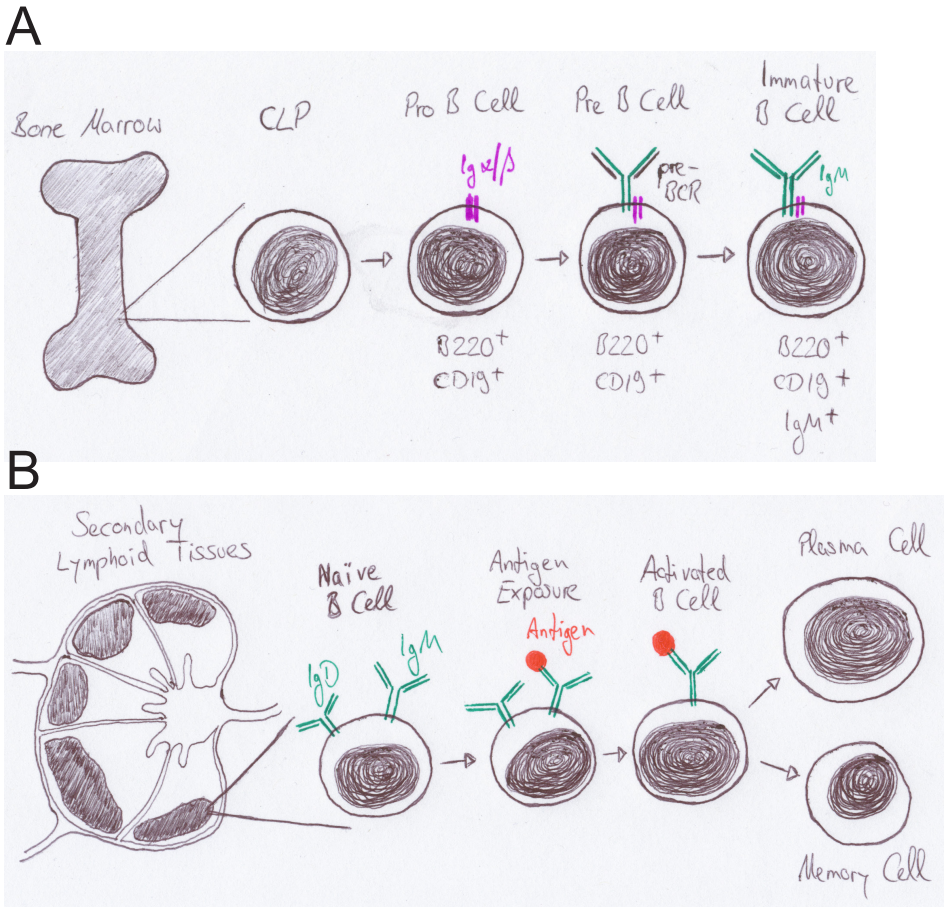

Figure 1.3. B cell differentiation and proliferation are linked to BCR expression

(A) Hematopoietic stem cells in the bone marrow give rise to common lymphoid progenitors (CLP). IL-7 drives differentiation of CLPs into pro B cells expressing the B cell markers B220 and CD19. Re-arrangement of immunoglobulin genes leads to the expression of a pre-BCR on the surface of pre B cells. Further genetic re-arrangements lead to the expression of a functional IgM BCR on the surface of the now immature B cell. The latter leave the bone marrow and home to secondary lymphoid organs. The expression of both IgM and IgD on the cell surface characterises mature B cells. (B) Mature B cells encounter antigen molecules in secondary lymphoid organs such as lymph nodes. Once antigen triggers the BCR and adequate T cell help is provided, B cells downregulate BCR surface expression. Fully activated B cells undergo a complex process of differentiation and proliferation leading to effector cells such as antibody-producing plasma cells and long-lived memory cells. Adapted from M. Weber.

and Kraus et al., 2004). Upon recognition of foreign antigen during an immune response mature B cells downregulate surface expression of both IgM and IgD and start a complex process of maturation and differentiation to become effector and memory cells. The main B effector cells are called plasma cells and produce an array of antigen-specific antibodies to target pathogens. Plasma cells are terminally differentiated and do not express a surface BCR. However, after initial downregulation, memory cells re-express a BCR with the same antigen specificity and of IgG isotype. This re-expression is crucial for the future activation of memory B cells in the context of a second challenge with the same pathogen.

In summary, B cells undergo several maturation stages, which mainly take place in the bone marrow and are characterised by vast genetic re-arrangements. Immature B cells expressing a functional BCR are selected for non-reactivity to self-antigens and are released into the periphery where they circulate and home to secondary lymphoid organs. Here, they get activated by foreign antigens and differentiate into effector and memory cells. Overall, the life and death of B cells is dictated by the expression of a functional BCR, which both provides a tool for the selection of auto-reactive B cells and triggers activation signals upon recognition of foreign antigen.

1.2 B cell activation in the context of an immune response

B cells circulate through the body and frequently home to secondary lymphoid organs like lymph nodes or the spleen. Theoretically, expression of a BCR that recognises unprocessed antigen molecules independently of any accessory molecules allows B cells to get activated at all times. However, multiple cellular interactions are needed for full B cell activation and the eventual production of high-affinity antibodies. Secondary lymphoid organs provide a platform for these interactions and are thus widely regarded as the site of B cell activation and the initiation of adaptive immunity (Junt et al., 2008).

1.2.1 B cells get activated in secondary lymphoid organs

Secondary lymphoid organs (SLOs) are found throughout the body in the form of glandular structures such as lymph nodes or bigger organs like the spleen. They are connected to both the lymph system and blood stream and function to concentrate antigen molecules entering through afferent lymphatics. Furthermore, SLOs provide an extracellular structure that allows compartmentalisation and facilitates cellular interactions (Gowans and Knight, 1964).

In particular, lymph nodes are characterised by a specialised architecture showing an outer region, the cortex, and an inner zone called the medulla (Figure 1.4. upper panel). The cortex is surrounded by the subcapsular sinus (SCS), which collects lymph fluids from afferent lymphatics and mainly contains macrophages and dendritic cells. The cortex is comprised of B cell follicles and distinct T cell zones and is located below a macrophage-rich area lining the SCS (Fossum and Ford, 1985). The medulla consists of draining sinuses and marks the site of lymphocyte egress into efferent lymphatics (Pham et al., 2008). Homing of immune cells to SLOs and the compartmentalisation within lymph nodes is maintained by chemokine gradients and other extracellular cues (von Andrian and Mempel, 2003 and Cyster, 2005). The continuous draining of fluids by SLOs and their highly organised architecture ensure concentration of antigen molecules in the context of an infection and mediate efficient cell-cell interactions (Catron et al., 2004).

B cells reside in follicles located between the SCS and the paracortex, which mainly contains T cells. The location of follicles allows B cells to interact with both macrophages lining the SCS and T cells occupying the paracortex (Carrasco and Batista, 2007). During an immune response antigen molecules enter the lymph node through afferent lymphatics by passive flow (Nossal et al., 1968). Antigen molecules can occur as either soluble, intact structures such as toxins or bound to antibodies and complement fragments named immune complexes (Batista and Harwood, 2009). Once concentrated in the SCS, antigen can access B cell follicles in several ways. One possible route of antigen entry into B cell follicles is *via* small pores between SCS macrophages (Clark, 1962 and Farr et al., 1980). This allows B cells to directly interact with antigen molecules without the need of accessory cells (Pape et al., 2007) (Figure 1.4. lower panel). However, the existence of pores between SCS macrophages remains controversial. Given the documented size of these pores of 0.1-1 μm, this would only allow small, low-molecular weight antigens to passively diffuse into B cell follicles. Bearing in mind that the shape and size of antigens can be very variable, the existence of alternative ways of antigen-presentation to B cells appears therefore likely.

Indeed, it is now widely accepted that the main route of antigen-recognition by B cells *in vivo* is through cell-mediated presentation by antigen-presenting cells (APCs) (Szakal et al., 1983 and Gonzalez et al., 2009). APCs constitute a family of cells including Macrophages and several subsets of dendritic cells. Interestingly, a role for basophils in antigen presentation has recently been reported as well (Yoshimoto et al., 2009 and Sokol et al., 2009). In the context of B cell activation macrophages can extent their processes into the SCS and are thus able to retain antigen molecules or immune complexes (Martinez-Pomares et al., 1996). In order to bind and present antigen, macrophages use an array of inherited receptors including macrophage receptor 1 (MAC1) recognising complement-opsonised antigen or the DC-specific ICAM3-grabbing non-integrin (DC-SIGN), which senses the presence of glycosylated antigens (Phan et al., 2007 and Koppel et al., 2005). Further receptors used by macrophages are the families of Fc and complement receptors, which can bind immune complexes and opsonised antigen (Bergtold et al., 2005). Once SCS Macrophages have bound antigen they

A

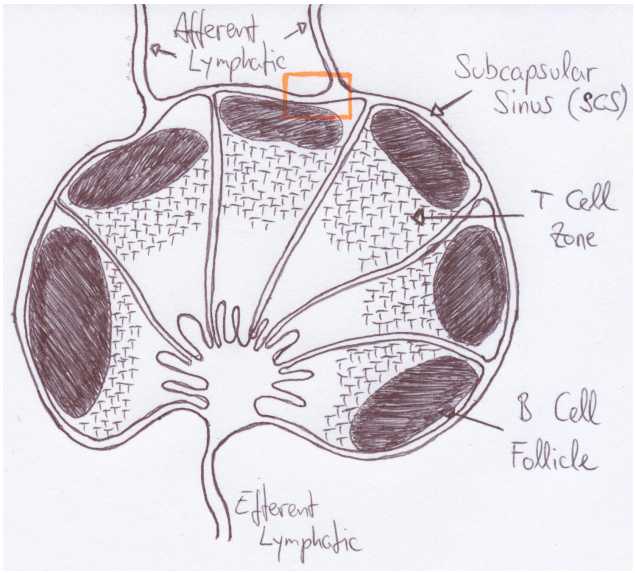

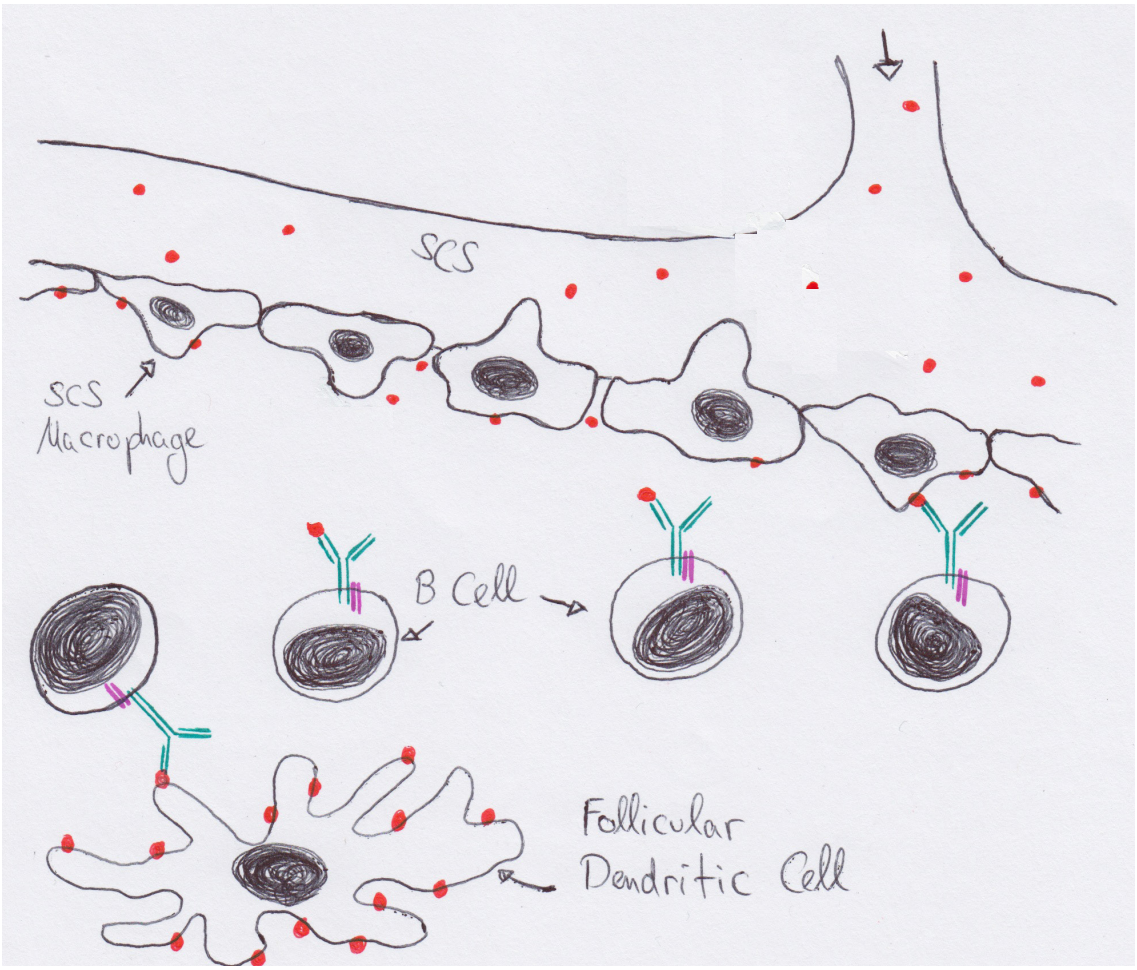

Figure 1.4. B cell activation in secondary lymphoid tissues
(A, upper panel) B cells home to secondary lymphoid organs such as lymph nodes and reside in B cell follicles. B cell follicles are found between the subcapsular sinus (SCS) and the T cell zones enabling B cells to interact with macrophages lining the SCS, CD4 T cells and follicular dendritic cells (FDCs). (lower panel, representing magnified area indicated by orange box in upper panel)Antigen molecules enter the lymph node *via* afferent lymphatics either on the surface of an antigen-presenting cell or as soluble molecules. SCS macrophages and FDCs have the capability of binding soluble or complexed antigen and in turn present antigen molecules to B cells in the follicle. Once a B cell clone has specifically recognised an antigen on the surface of an APC, it extracts antigen molecules and migrates towards the T cell zone to receive appropriate T cell help for full activation. Adapted from Batista and Harwood, 2009.

are able to present to B cells in the follicle (Junt et al., 2007 and Cyster, 2010). However, it is unclear whether this mode of antigen presentation is mediated by the simple retention of antigen molecules on the surface of Macrophages or if it involves the phagocytic uptake into non-degradative intracellular compartments and the subsequent presentation on the cell surface. Upon specific recognition of antigen on the surface of Macrophages B cells stop moving and extract antigen followed by the directed migration towards the T cell zone to receive appropriate T cell help (Garside et al., 1998; Okada et al., 2005 and Carrasco and Batista, 2007). The concept of T cell help will be introduced later in this chapter (paragraph 1.2.3).

Another potential cell-mediated route of antigen-presentation to B cells is through dendritic cells (DCs), which are professional APCs and can enter the lymph node from the blood stream through high endothelial venules (HEVs) (Dudziak, 2007). Similar to SCS Macrophages they use an inherited set of surface receptors to bind antigen such as FcγRIIB and DC-SIGN. As B cells also enter the lymph node through HEVs, it would seem ideal to encounter antigen in the paracortex on the surface of DCs. However, B cells sense antigen in its unprocessed state and presentation to B cells by DCs would therefore imply mechanisms whereby antigen is retained on the cell surface or internalised into non-degradative intracellular compartments. These mechanisms remain to be formally established. Still, presentation of native antigen by conventional DCs might represent a fast way for B cells to access antigen.

Importantly, more prolonged antigen presentation to B cells is carried out by a particular subset of DCs, follicular dendritic cells (FDCs). These reside in B cell follicles and have classically been regarded as central APCs for B cells in the context of a germinal centre response (see paragraph 1.2.4) (Tew et al., 1980; Tew et al., 2001 and Suzuki et al., 2009). FDCs as well express high levels of innate receptors like complement or Fc receptors and are able to retain and present antigen for long periods of time (Papamichail et al., 1975 and Yoshida et al., 1993).

To sum up, secondary lymphoid organs (SLOs) provide a unique architecture that supports the concentration of antigen molecules during an infection and allows interactions between immune cells to occur. These interactions are crucial for the initiation of a humoral immune response as the predominant way of antigen presentation to B cells *in vivo* is through the contact with APCs.

1.2.2 B cells recognise antigen molecules on the surface of antigen presenting cells and form an immune synapse upon recognition

During an immune response B cells sense antigen using their BCR. Unlike the T cell receptor, the BCR recognises unprocessed, native antigen using a wide range of affinities without the need of accessory proteins. The affinity of the BCR for its ligand is a crucial parameter that determines whether an activation threshold can be overcome and thus dictates the outcome of B cell activation (Batista and Neuberger, 1998). Another central concept of antigen recognition by B cells is the context of its presentation. Similar to the process of clonal deletion of auto-reactive B cells during maturation, foreign antigen can occur in a soluble form or tethered to the surface of an APC and this determines the nature of the B cell response. Thus, the strength of the stimulus provided by antigen molecules - either self or foreign - is regulated by the way it is presented. Importantly, it has been shown that the functional range of B cell activation is wider when antigen molecules are bound to an antigen-presenting surface or to a particle (Batista and Neuberger, 2000 and Eckl-Dorna and Batista, 2009).

Further to the presentation of membrane-bound antigen, the threshold for B cell activation can be further modulated by adhesion molecules such as integrins and co-receptors like CD19 (Carrasco et al., 2004; Batista et al., 2007; Arana et al., 2008 and Depoil et al., 2008). Adhesion molecules and co-receptors are expressed on the surface of B cells and their distribution during the resting state is mostly random and less organised. However, upon recognition of antigen on an APC, the distribution of surface molecules at the interface between the B cell and APC is dramatically changed: Soon after the initial contact, surface molecules show a molecular segregation pattern called the immune synapse (IS, Figure 1.5.) (Batista et al., 2001). Immune synapses have first been described for T cells when

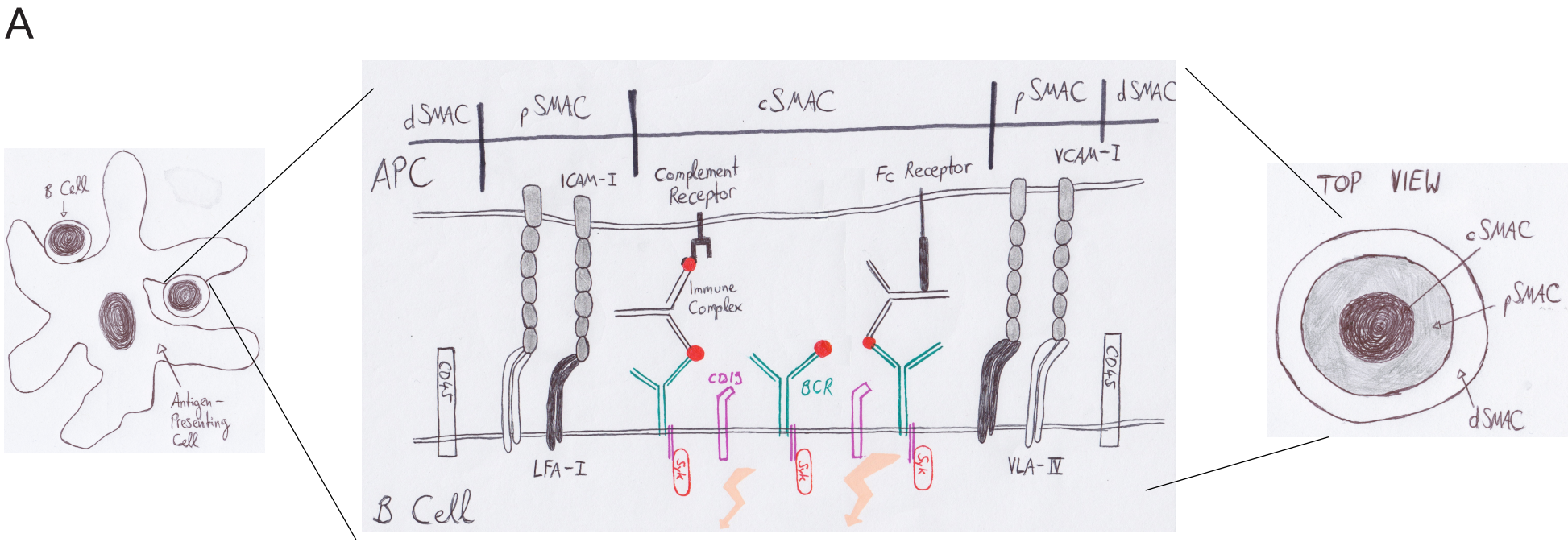

Figure 1.5. Antigen recognition by B cells on the surface of APCs and immune synapse formation
(A) The predominant way of antigen recognition by B cells *in vivo* is on the surface of an antigen-presenting cell (APC) such as a follicular dendritic cell (FDC). Recognition of membrane-bound antigen by the BCR is accompanied by the re-arrangement of surface receptors into a highly organised structure called the immune synapse. The mature immune synapse shows a characteristic molecular segregation pattern with ligated BCRs accumulating in the centre. This central aggregate is called the central supramolecular activation cluster (cSMAC) and constitutes a site for signalling and possibly antigen extraction. The sSMAC is surrounded by a ring of adhesion molecules such as the integrins LFA-1 andVLA-4. This ring is commonly referred to as the peripheral SMAC (pSMAC) and it confers stability to the immune synapse as well as integrin signalling. Large molecules such as the phosphatase CD45 are excluded from both cSMAC and pSMAC and accumulate in a more distant area called the distal SMAC (dSMAC). Adapted from S. Fleire.

in contact with APCs, but have since then also been reported for other immune cells such as NK cells (Monks et al., 1998; Grakoui et al., 1999; Krummel et al., 2000; Potter et al., 2001; Stinchcombe et al., 2001 and Davis et al., 1999). The immune synapse is thus a common feature of lymphocytes and provides a platform for spatially organised signalling, directed secretion of lytic granules and receptor internalisation (Davanture et al., 2005; Stinchcombe et al., 2006 and Liu et al., 2009).

The B cell immune synapse is characterised by a central region called the central supramolecular activation cluster (cSMAC). Here, antigen-engaged BCRs and co-receptors accumulate and the cSMAC has thus far widely been regarded as the site of active signalling. The cSMAC is surrounded by a ring of adhesion molecules like the integrins LFA-1 and VLA-4, which form the peripheral SMAC (pSMAC) (Carrasco et al., 2004 and Carrasco and Batista, 2006). Apart from enabling the B cell to tightly adhere to the APC, integrins also lower the threshold for B cell activation by a process called outside-in signalling. During immune synapse formation large proteins such as the phosphatase CD45 are excluded from both cSMAC and pSMAC and accumulate in a more distant area named the distal SMAC (dSMAC) (Depoil et al., 2008). Further to the modulation of activation thresholds and spatial organisation of signalling the formation of an immune synapse also provides B cells with a means to gather antigen molecules in a central agglomerate, which allows efficient extraction of antigen needed for full activation (Batista et al., 2001).

In conclusion, the predominant way of antigen recognition by B cells *in vivo* takes place on the surface of antigen-presenting cells through formation of an immune synapse. Ligation of the BCR by membrane-tethered antigen modulates the activation threshold and thus dictates the outcome of B cell activation. Furthermore, the immune synapse likely provides B cells with a platform for antigen extraction, which in turn is crucial for full B cell activation.

1.2.3 Full B cell activation requires at least 2 signals

In the context of an infection B cells mainly recognise antigen tethered to the surface of an antigen-presenting cell and subsequently form an immune synapse. Ligation of the BCR transduces an activatory signal into the intracellular space *via* the Igα/β sheath. Both Igα and Igβ molecules possess ITAM motifs, which serve as a docking site for kinases and adaptors once phosphorylated (Reth, 1989). Cross-linking of the BCR thus initiates a cascade of numerous signalling events including phosphorylation, Calcium flux and the activation of transcription factors (Harwood and Batista, 2008). Intracellular signalling upon BCR ligation is considered a first step during B cell activation and is not sufficient to induce differentiation into effector cells such as plasma or memory cells, however.

For full activation to occur, B cells need to extract antigen from the surface of an APC and present it in the context of major histocompatibility complex class II (MHC II) proteins to specific $CD4^+$ T cells (Figure 1.6.) (Lanzavecchia, 1985 and Batista et al., 2001). The process of extraction and presentation is characterised by the endocytic uptake of antigen molecules and the sorting into LAMP-1-positive endosomes (Cheng et al., 1999). Endosomes constitute an intracellular compartment where antigen is degraded by acidification and antigenic peptide fragments are subsequently loaded into MHC II molecules, which traffic to the cell surface for presentation to T cells (Chesnut and Grey, 1981). While B cells extract antigen from APCs and process it intracellularly, they also need to change their location within the secondary lymphoid organ in order to be able to interact with T cells. Therefore, B cells, which have encountered antigen on APCs such as SCS macrophages, migrate towards the paracortex to get in close contact with T cells. This migration is led by a gradient of chemokines CCL19 and CCL21, which bind to the chemokine receptor CCR7 expressed by B cells (Okada et al., 2005). At the border of B and T cell areas, antigen-presenting B cells then form cell-cell conjugates with previously primed T cells, which carry T cell receptors (TCRs) recognising the specific antigen in the context of MHC II molecules (Garside et al., 1998). Once T cells have been activated by TCR ligation they provide co-stimulatory signals for B cells in the form of soluble cytokines such as interleukin-4 (IL-4) or by upregulation of the surface molecule CD40 ligand (CD40L), which

in turn activates CD40 expressed by B cells (Garside et al., 1998). This process of co-stimulation is crucial for full B cell activation leading to effector cell differentiation and is referred to as T cell help. Furthermore, the cytokine milieu created by helper T cells can determine the outcome of B cell activation leading to the production of specific immunoglobulin subtypes depending on the cytokines secreted by T cells.

B effector cell differentiation and antibody production thus rely on appropriate T cell help and antigens leading to this response are therefore called T-dependent antigens. In addition, B cells can also get activated by T-independent antigens. These are futher separated into two types: T-independent antigens of the first type (TI-1) are polyclonal activators such as LPS or CpG, which lead to B cell activation independent of the BCR using inherited receptors like toll-like receptors (TLRs) (Mosier and Subbarao, 1982 and Akira and Takeda, 2004). In contrast, the second type of T-independent antigens (TI-2) are sensed by the BCR and are of a repetitive nature often derived from viral envelopes or representing bacterial polysaccharides. Due to their repetitive structure TI-2 antigens cross-link a large amount of BCRs on the B cell surface and thereby circumvent the need for T cell help (Dintzis et al., 1976). However, while this leads to a fast and specific humoral response, B cells activated by TI-2 antigens do not undergo affinity maturation by somatic hypermutation and do not form long-term memory.

In summary, full activation of B cells by T-dependent antigens and subsequent differentiation into B effector cells requires at least two signals: First, ligation of the BCR on the surface of an APC triggers a serious of intracellular signalling events leading to antigen uptake, migration towards the T cell zone and the transcription of target genes. Second, B cells present antigen to specific T cells in the context of MHC II to receive T cell help, which is characterised by secretion of cytokines and presentation of co-stimulatory molecules. While both signals are necessary for full B cell activation, they are well separated in space and time.

A

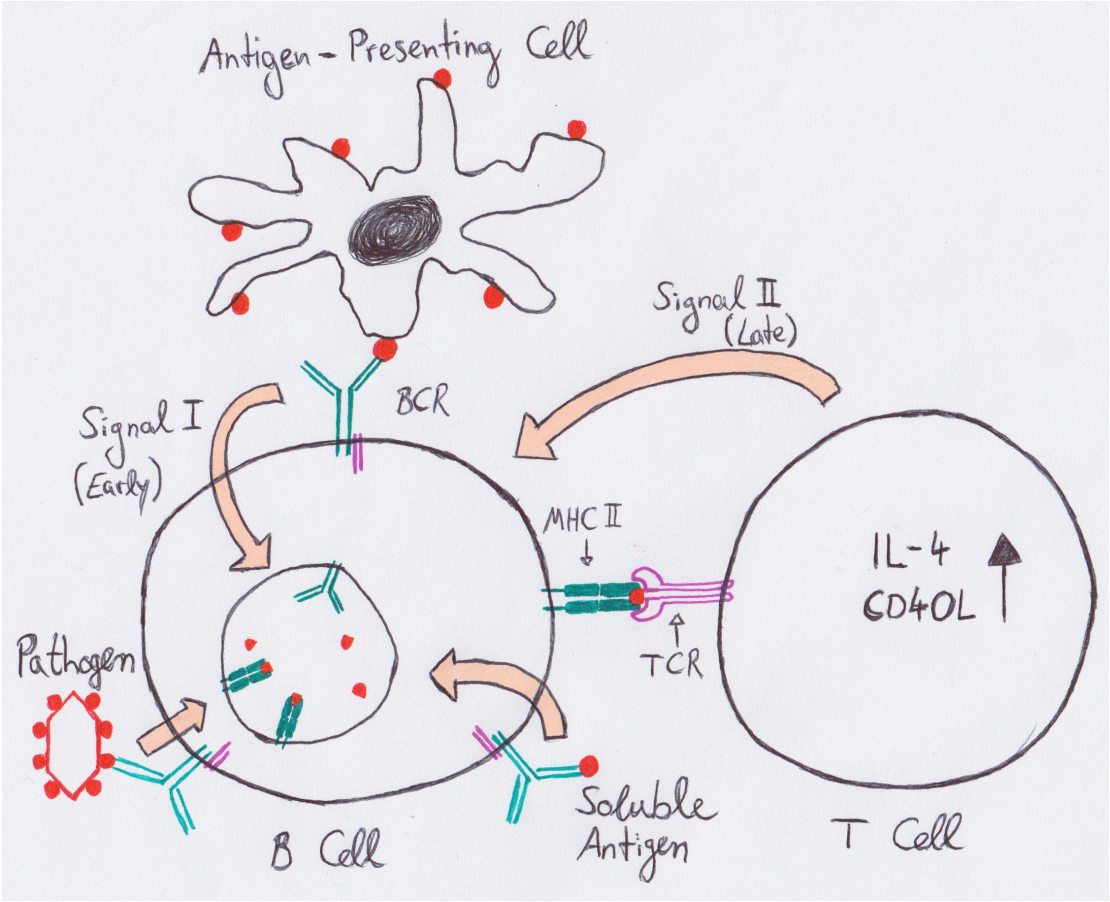

Figure 1.6. B cells require at least two signals for full activation
(A) B cells recognise pathogen-derived antigen molecules on the surface of an antigen-presenting cell (APC) through a specific interaction with their BCR. Alternatively, B cells can also sense intact, soluble antigen or whole pathogens such as viruses using the BCR. Its ligation initiates an intracellular signalling cascade involving numerous phosphorylation events and Calcium influx from the endoplasmic reticulum. B cells subsequently extract antigen from the surface of the APC and internalise the BCR-antigen complex into endosomes. Antigen molecules are further processed and loaded onto major histocompatibility complex class II (MHC II) molecules. Loaded MHC molecules are transported to the cell surface where they can be recognised by primed CD4 T cells expressing a T cell receptor (TCR) specific for the given antigen. TCR cross-linking triggers the T cell to upregulate surface expression of CD40 ligand (CD40L) and to produce interleukin-4 (IL-4). Both CD40L and IL-4 act as co-stimularoty factors for the B cell and are crucial for full B cell activation leading to antibody production.

1.2.4 Affinity maturation during the germinal centre response and B cell memory

Depending on the type of antigen B cells can follow different fates upon activation. On the one hand, they can differentiate into extrafollicular plasma cells. These can arise independently of T cell help and are typically short-lived (Smith et al., 1996). Extrafollicular plasma cells are therefore regarded as a subset of B effector cells, which are responsible to produce a first wave of specific antibodies without the ability to further diversify the immunoglobulins secreted (McHeyzer-Williams et al., 1993).

On the other hand, B cells having received appropriate T cell help undergo a complex differentiation process leading to the creation of long-lived plasma and memory cells. This differentiation process is referred to as the germinal centre response as it takes place in a special compartment within the SLO, called the germinal centre (GC) (MacLennan et al., 1994). Based on their histological appearance GCs are divided into a light and a dark zone and provide B cells with a microenvironment, which allows them to diversify the array of specific immunoglobulins secreted (Cozine et al., 2005). This diversification is mainly characterised by two phenomena changing both the subclass of the immunoglobulin and its affinity for the antigen, while antibody specificity *per se* remains unchanged.

The first process leading to the secretion of different antibody subclasses is known as isotype switching and involves genetic recombination in the switch region of the immunoglobulin heavy chain locus. As a consequence, the secretion of a variety of specific antibody isotypes dictates effector cell responses and therefore extends the diversity of the immune response against a certain antigen.

Further to isotype switching germinal centre B cells have the ability to increase the affinity of their antibodies for the specific antigen by 100-1000-fold (Eisen and Siskind, 1964 and Foote and Milstein, 1991). This is achieved by introducing random mutations in the variable regions of both heavy and light chains. This process is therefore called affinity maturation and is the consequence of a phenomenon named somatic hypermutation (Odegard and Schatz, 2006). B cells subjected to somatic hypermutation are referred to as centroblasts and reside in

the dark zone of the GC. After several rounds of proliferation and mutation, these B cells re-express the mutated BCR and migrate to the light zone of the GC where they get in contact with antigen-presenting FDCs. Here, B cells are selected based on their ability to recognise antigen on the surface of FDCs using their newly expressed BCR. Ligation of the BCR leads to the secretion of high-affinity antibodies of several subclasses. Plasma cells generated in this way are long-lived and home to the bone marrow. Moreover, B cells, which have received T cell help and have matured in a GC, can become memory cells (Zinkernagel et al., 1996). These continue to recirculate through the same SLOs that contain naive B cells, namely the spleen or lymph nodes for example. In contrast to plasma cells memory B cells express a BCR of IgG isotype to ensure fast activation upon following challenges with the same antigen.

As well as the first steps of B cell activation the GC response relies on the continuous presentation of antigen and thus ongoing cell-cell interactions. In fact, multi-photon imaging of GC responses has revealed that the organisation of GCs is highly dynamic and less static as explained by the classical model simply separating the GC in dark and light zones (Allen et al., 2007; Hauser et al., 2007 and Schwickert et al., 2007). Advanced intravital microscopy has led to a model that describes the GC response as a constant circulation of B cells expressing mutated BCRs and competing for antigen on the surface of FDCs. B cells expressing BCRs with higher affinity are thus more likely to capture higher amounts of antigen and therefore receive T cell help to a greater extent. This generates plasma cells, which produce antibodies of the highest affinity for any given antigen, and hence significantly improve the chances of clearing the pathogen from the host organism.

In conclusion, B cells produce antibodies in the context of an immune response and their activation takes place in secondary lymphoid organs. Here, antigen can occur in a soluble form or bound to the surface of an APC such as a SCS Macrophage or a FDC. It is now widely accepted that *in vivo* B cells sense antigen tethered to the surface of an APC by formation of an immune synapse (IS). The B cell IS represents a molecular segregation pattern of BCRs, co-receptors and integrins and lowers the threshold for B cell activation. Furthermore, B cells extract antigen from APCs after IS formation and receive T cell help by subsequent presentation of processed antigen in the context of MHC II to primed $CD4^+$ T helper cells. T cell help drives the formation of germinal centres where B cells diversify the repertoire of specific immunoglobulins by isotype switching and somatic hypermutation. This leads to the production of high-affinity antibodies, which in turn help the immune system to clear the specific pathogen. In addition to antibody production the GC response also leads to the generation of memory B cells that form a pool of long-lived cells in the bone marrow for secondary challenges of the host with the same pathogen.

1.3 Early events during B cell activation

As described earlier, full B cell activation requires at least two signals. These are characterised by antigen-induced BCR ligation and subsequent T cell help. In order to receive adequate T cell help, B cells need to process and present antigen acquired from antigen-presenting cells. BCR-mediated antigen recognition and and associated signalling events are therefore regarded as early steps during B cell activation and will be introduced in the following sections.

1.3.1 Cytoskeletal control of BCR diffusion and signalling in resting B cells

B cells are considered resting prior to BCR ligation with antigen. The state of the BCR in resting B cells remains unclear and is controversially discussed. Earlier work employing fluorescence energy transfer (FRET) of differentially labelled Igα molecules showed a monomeric distribution of the BCR within the membrane

(Tolar et al., 2005). In contrast, Reth and colleagues recently showed that BCR molecules form oligomers on the surface of B cells (Yang et al., 2010). The authors propose that BCR oligomerisation provides resting B cells with a mechanism for auto-inhibition. As the initial steps of B cell activation are associated with a dramatic re-distribution of BCRs on the cell surface, it is paramount to understand its dynamic organisation within the membrane of resting B cells. In light of this issue, work from the T cell field has established a link between the TCR and the organisation of cholesterol-containing protein islands, which were also rich in cortical actin (Lillemeier et al., 2006). It was thus assumed that the cytoskeleton plays a critical role in the formation and distribution of protein islands in the membrane of lymphocytes. In line with this, simultaneous dual-colour high-speed total internal fluorescence (TIRF) microscopy has been used to show that cortical actin restricts the lateral diffusion of single BCR molecules in the B cell membrane (Treanor et al., 2010). BCRs were observed to diffuse slower in actin-rich regions, whereas they exhibited faster diffusion in areas low in cortical actin. Interestingly, disruption of the actin network with depolymerising agents induced robust Calcium flux, phosphorylation of signalling proteins such as Extracellular signal-regulated kinsase (Erk) and up-regulation of the activation marker CD86. Importantly, these events were BCR-dependent, as they did not occur in B cells lacking signalling molecules downstream of the BCR such as PLCγ2. One explanation for the initiation of intracellular signalling by disruption of the actin cytoskeleton might be the release of BCR molecules from actin-rich regions and a consequently higher extent of spontaneous BCR clustering.

In summary, the cytoskeleton plays an important role in the molecular organisation and compartmentalisation of the lymphocyte cell membrane. Cortical actin furthermore restricts BCR diffusion and thus controls the extent of basal signalling potentially caused by receptor clustering.

1.3.2 Signal initiation:
Assembly of the BCR signalosome and microcluster formation

Signal transduction into the intracellular space by antigen recognition

B cell activation is initiated by antigen-mediated BCR ligation on the cell surface. Receptor crosslinking leads to an intracellular signalling cascade, which involves Calcium flux, activation of specific transcription factors and cytoskeletal re-arrangements. However, it is not clear how the BCR transmits the initial activating signal from the extracellular milieu into the intracellular space. In T cells two prominent models have been used to explain the process of signal transduction by the TCR. One model assumes an intramolecular conformational change of the TCR upon ligand binding and has thus been termed the conformational change model (Kuhns et al., 2006 and Schamel et al., 2006). It has been reported that structural changes within the TCR complex can lead to the intracellular exposure of certain amino acid residues of the CD3 molecule. This in turn allowed binding of adaptor molecules such as Nck or phosphorylation of ITAM tyrosines by the Src kinase Lck (Gil et al., 2002 and Xu et al., 2008). On the contrary, earlier studies applying X-ray crystallography only detected few conformational changes of the TCR being transmitted to membrane-proximal regions leading to some controversy regarding the conformational change model (Garcia et al., 1999 and Hennecke and Wiley, 2001).

A second model describing the initial signal transduction by the TCR has subsequently been introduced by Davis and van der Merwe and has been termed kinetic segregation model (Choudhuri et al., 2005 and Davis and Van Der Merwe, 2006). The kinetic segregation model assumes that the TCR randomly diffuses in the cell membrane and frequently gets into brief contact with Src kinases and membrane-anchored phosphatases. This leads to a finely tuned balance of phosphorylation and dephosphorylation of the TCR. In line with this, treatment of resting T cells with the phosphatase inhibitor pervanadate leads to TCR activation and intracellular signalling (Secrist et al., 1993). Upon antigen recognition on the surface of an APC, TCR complexes together with adhesion molecules get in close proximity to the APC establishing areas of tight adhesion. The kinetic segregation

model proposes that proteins with large extracellular domains such as bulky phosphatases are forced out of these areas allowing for an accumulation of Src kinases to occur (Irles et al., 2003). The increased accessibility of the TCR for kinases consequently tips the balance towards phosphorylation and initiates downstream signalling cascades.

Although experimental data provides evidence for the kinetic segregation model, the exact mechanisms of initial signal transduction by the TCR remain unclear. With regards to the BCR it is important to note that B cells bind antigen in a multivalent manner and with higher affinity. Furthermore, in addition to common phosphatases such as CD45 B cells also express the phosphatase CD148, which is comprised of an even bulkier extracellular domain (Zhu et al., 2008). It is therefore likely that aspects of the kinetic segregation model could potentially hold true for B cells.

Signal initiation and microcluster formation

Upon binding to antigen the BCR transmits a signal into the intracellular space, which is characterised by numerous phosphorylation events and Calcium flux. As the BCR itself does not possess any intrinsic signalling capabilities, it associates with the Igα/β sheath. These molecules contain ITAM motifs and can thus be phosphorylated by kinases (Reth, 1989). The major kinase thought to be providing initial ITAM phosphorylation immediately after antigen recognition is the Src kinase Lyn (Kurosaki, 1999 and Dal Porto et al., 2004). Phosphorylated ITAMs provide a docking site for other molecules containing Src homology 2 (SH2) domains and it has been established that the spleen tyrosine kinase Syk predominantly binds the phosphorylated ITAMs of the Igα/β sheath (Taniguchi et al., 1991; Flaswinkel et al., 1995 and Rolli et al., 2002). Binding of Syk to the phosphorylated Igα/β molecule by virtue of its two SH2 domains releases the kinase from an auto-inhibited state by a mechanism involving auto-phophorylation and the eventual exposure of the kinase domain (Deindl et al., 2007). The concerted action of Lyn and Syk downstream of the ligated BCR is thought to be the driving force for phosphorylation events leading to formation of

the BCR signalosome. However, it remains unclear how substrate specificity is achieved and how both kinases act in a spatiotemporally resolved manner.

In recent years high-resolution TIRF microscopy of B cells settled on antigen-loaded planar lipid bilayers has provided important insights into the spatiotemporal regulation of signalling events downstream of the BCR (Depoil et al., 2008; Weber et al., 2008; Tolar et al., 2009; Treanor et al., 2010 and Treanor et al., 2011). This has led to the discovery of BCR microclusters, which represent clusters of BCR molecules that form in the plasma membrane upon BCR ligation by membrane-bound antigen. Work in primary murine B cells has shown that BCR microclusters can consist of IgM or IgD alone, or a mixture of both (Depoil et al., 2008). Furthermore, BCR microclusters exclude the phosphatase CD45 and show an accumulation of phosphotyrosine (Fleire et al., 2006 and Depoil et al., 2008). The existence of microclusters had previously been shown in T cells (Bunnell et al., 2002; Campi et al., 2005 and Yokosuka et al., 2005) and microclusters have therefore been established as discrete signalling units forming in the plasma membrane driving lymphocyte activation.

BCR microclusters are maintained by the cortical cytoskeleton

Formation of BCR microclusters represents the earliest observable step in B cell activation. Importantly, this process does not depend on BCR signalling as microclusters have been observed in Lyn-deficient B cells settled on antigen-bearing lipid bilayers (Weber et al., 2008). This is potentially caused by diffusion trapping of BCR molecules by antigen tethered to the lipid bilayer. As diffusion of the BCR is controlled by actin, our laboratory has recently also established a critical role for the cortical cytoskeleton in BCR microcluster formation and maintenance (Treanor et al., 2011). When B cells were settled on antigen-loaded lipid bilayers, TIRF microscopy revealed that the cortical actin dynamically re-arranged forming corrals around BCR microclusters. In line with this, BCR microclusters lost integrity when cells were treated with the actin depolymerising agent Latrunculin A. Interestingly, the same dynamic re-organisation was observed for the ezrin-radixin-moeisin (ERM)-family protein ezrin. ERM proteins link the plasma membrane with the cortical cytoskeleton by simultaneously

binding F-actin and membrane proteins (Fievet et al., 2007). This link can be released by de-phosphorylation of ERM proteins in their C-terminus and it has indeed been suggested that ezrin plays a role in membrane microdomain coalescence upon BCR ligation (Gupta et al., 2006 and Gupta and DeFranco, 2007). In light of these observations, ERM proteins have also been reported to be important during T cell activation allowing membrane relaxation upon TCR cross-linking and thus fascilitating T cell-APC conjugate formation (Allenspach et al., 2001; Roumier, et al., 2001 and Delon et al., 2001).

In conclusion, the BCR transmits activatory signals into the intracellular space upon ligation with membrane-bound antigen. The mechanism of initial signal transduction may involve a series of intramolecular conformational changes and the kinetic segregation of bulky phosphatases from the BCR complex resulting in an increased net phosphorylation of ITAM motifs within the Igα/β sheath. Initial ITAM phosphorylation is achieved by Src kinases such as Lyn followed by recruitment and activation of the spleen tyrosine kinase Syk. Early phosphorylation events are concomitant with the formation of BCR microclusters, which represent clusters of immunoreceptors and have been established as discrete signalling units driving lymphocyte activation. Formation and maintenance of BCR microclusters is controlled by the ezrin-defined cortical actin cytoskeleton indicating a critical role for the cytoskeleton during lymphocyte activation.

1.3.3 Signal propagation:
B cell spreading drives signal amplification and integration

BCR microclusters provide a platform for signalosome assembly

BCR microclusters form quickly after antigen recognition on an antigen-presenting surface such as an APC. This process is concomitant with initial phosphorylation events at the BCR signalosome mainly carried out by the kinases Lyn and Syk. These early steps of B cell activation are immediately followed by the recruitment of numerous signalling and adaptor molecules to the BCR signalosome including the B cell linker protein (BLNK), the lipase PLCγ2, the Tec kinase Btk, the B cell

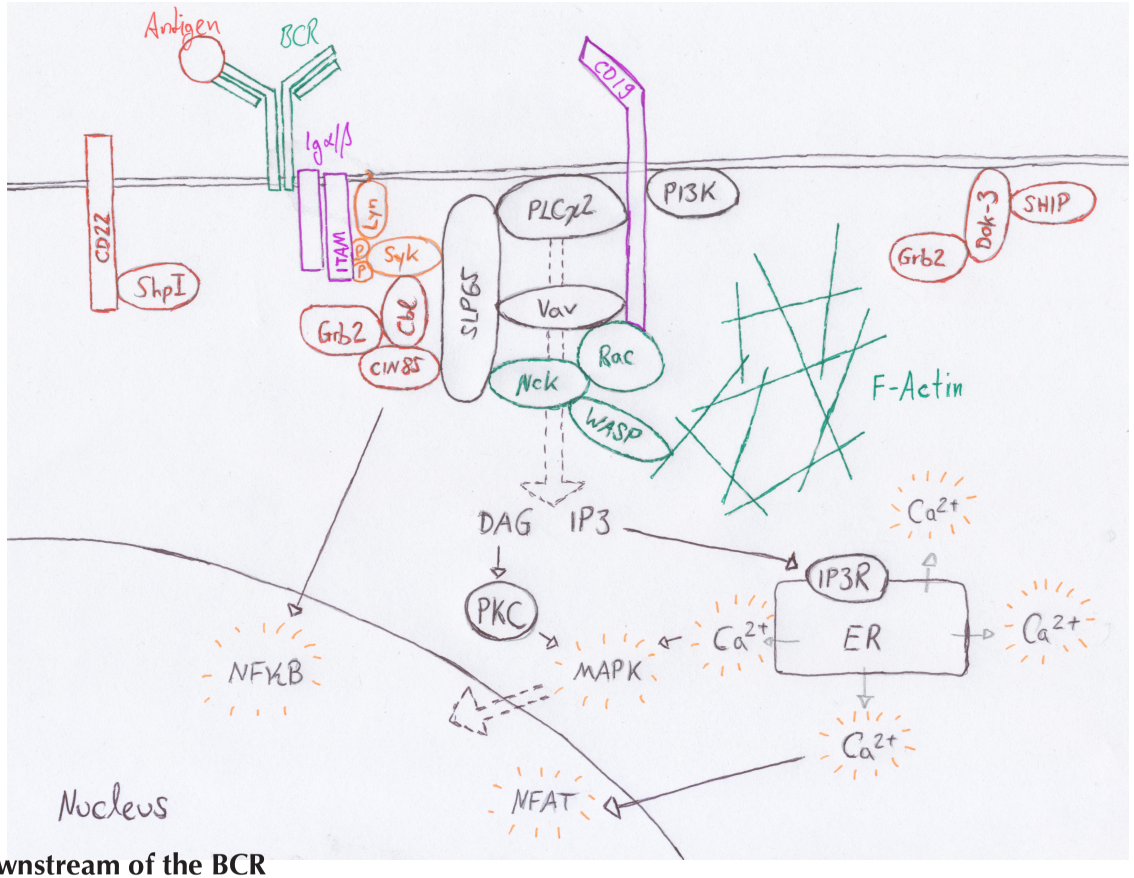

Figure 1.7. Signalling events downstream of the BCR

BCR ligation by foreign antigen triggers the recruitment of the src-kinase Lyn to the BCR. Lyn phosphorylates tyrosine residues in the immunoreceptor tyrosine activation motifs (ITAMs) of the Igα/β sheath, which in turn allows binding of Syk kinase to Igα/β. Lyn and Syk phosphorylate numerous downstream targets such as the signal integrator SLP65, the lipase PLCγ2, the adaptor Dok-3 or the ubiquitin ligase Cbl. SLP65 serves as a central adaptor molecule allowing binding of several other mediators at the same time. Activated PLCγ2 hydrolyses membrane lipids yielding the second messengers diacylglycerol (DAG) and inositol-tri-phosphate (IP3). IP3 binds to the IP3 receptor (IP3R) on the endoplasmic reticulum and triggers Calcium influx leading to activation of transcription factors such as NFAT or MAP kinases (MAPK). In addition, the adaptor CIN85 links the BCR to survival signals *via* the NFκB pathway. The B cell co-receptor CD19 amplifies signalling by recruiting downstream signalling molecules such as Vav and a protein complex involving Nck and WASP driving actin polymerisation and ultimately B cell spreading. BCR signalling is negatively regulated by the adaptors Dok-3 and Grb2 recruiting the lipid phosphatase SHIP and the ubiquitin ligase Cbl, respectively. Negative regulation of BCR signalling is further achieved by recruitment of the protein phosphatase Shp1 by the transmembrane protein CD22.

adaptor molecule of 32kDa (Bam32) and the cytoskeletal regulator Vav (Fu et al., 1998; Niiro and Clark, 2002 and Weber et al., 2008). The concerted recruitment of these adaptor and signalling molecules to the BCR signalosome provides activatory signals through phosphorylation of downstream proteins like Erk and the production of second messengers such as diacylglycerol (DAG) or inositol triphosphate (IP_3). The latter induce the release of Calcium ions from intracellular stores, which in turn activate transcription factors like NFAT or members of the MAP kinase pathway such as p38 (Kurosaki, 2002 and Scharenberg et al., 2007). Taken together, BCR microclusters provide a platform for the assembly of the BCR signalosome, which leads to signal diversification by activation of numerous downstream signalling pathways and ultimately results in B cell activation (Figure 1.7).

BCR-mediated spreading propagates BCR microclusters

BCR microcluster formation and Calcium influx are among the first events linked to B cell activation. As B cells need to overcome a sharp threshold for activation, the B cell starts to spread over the antigen-presenting surface soon after the first BCR microclusters have formed (Fleire et al., 2006). This spreading response is driven by the actin cytoskeleton and allows engagement of further BCR molecules by antigen at the leading edge of the B cell membrane and thus leads to the formation of new microclusters (Figure 1.8) (Fleire et al., 2006). BCR microcluster propagation by cell spreading is crucial for B cell activation and clearly depends on BCR signalling as B cells treated with the Src kinase inhibitor PP1 or the actin depolymerising agent Latrunculin A do not spread. Moreover, B cells lacking the kinases Lyn or Syk or the co-receptor CD19 also show impaired spreading in response to membrane-bound antigen (Weber et al., 2008 and Depoil et al., 2008). Additional work involving a panel of knockout B cells identified a co-operative role for PLCγ2 and the cytoskeletal regulator Vav in B cell spreading (Weber et al., 2008). Apart from signal amplification through the propagation of BCR microclusters, spreading also allows the B cell to discriminate between different antigen densities and affinities (Fleire et al., 2006). The extent of

A

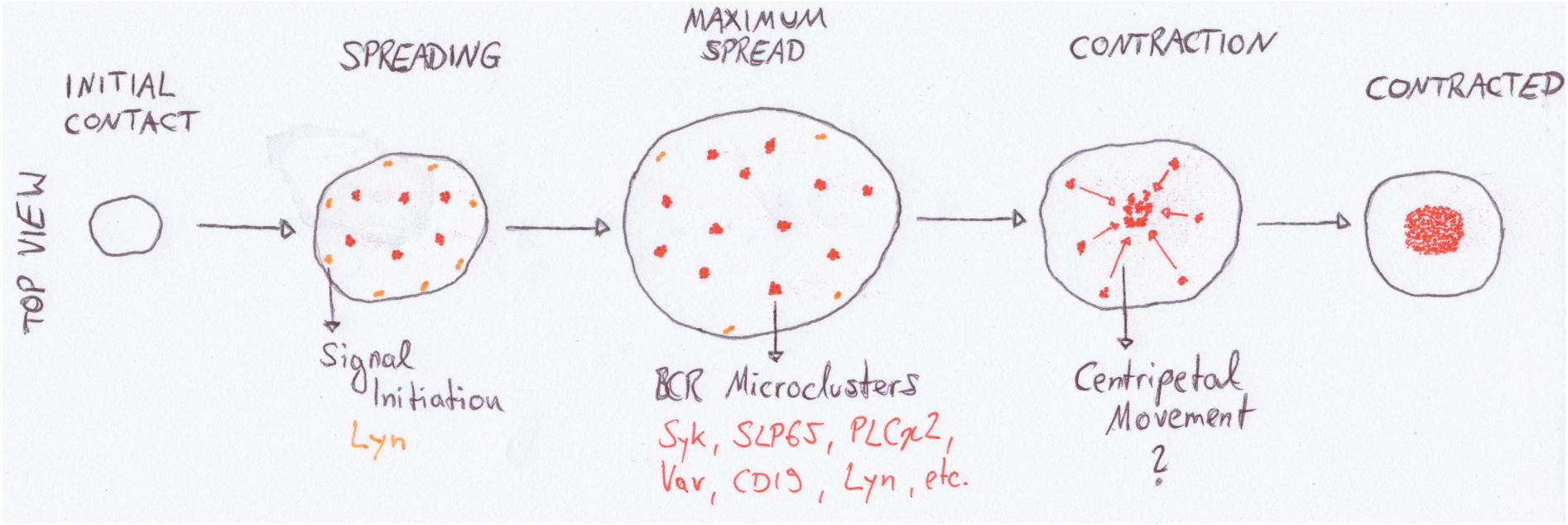

Figure 1.8. Antigen-containing BCR microclusters form during spreading and are gathered in the cSMAC through a process of centripetal movement
(A) Upon contact with an antigen-presenting cell (APC) specific recognition of antigen through the BCR initiates intracellular signalling *via* the src-kinase Lyn. This leads to the recruitment of numerous intracellular signalling molecules to the cross-linked BCRs. This recruitment is characterised by the formation of signalling-competent BCR microclusters. BCR microclusters serve as platform for signal amplification and drive B cell spreading. Once fully spread, antigen-containing BCR microclusters start to move towards the cSMAC area in a centripetal manner. This directional movement provides the B cell with a mechanism for antigen gathering, which allows antigen extraction and subsequent presentation to T cells for full B cell activation and thus antibody production.

spreading directly correlates with the amount of antigen gathered by B cells and consequently dictates the level of adequate T cell help.

In summary, B cells spread in response to membrane-bound antigen in order to form new BCR microclusters and thus overcome a threshold for activation. B cell spreading depends on BCR signalling and involves central signalling molecules such as Lyn, Syk, PLCγ2, Vav and CD19. As for BCR microcluster formation and integrity, the cortical actin cytoskeleton plays a critical role in B cell spreading by driving the extension of membrane lamellipodia at the leading edge.

BCR signalling is shaped by the co-receptor CD19

In response to membrane-bound antigen B cells spread over the antigen-presenting surface in order to propagate BCR microclusters and overcome a threshold for activation. Previous work has established a crucial role for the surface molecule CD19 in B cell spreading when recognising antigen tethered to a membrane as likely occurs *in vivo* (Depoil et al., 2008). CD19 has classically been known to associate with CD21 to form the complement receptor 2 (CR2) (Fearon and Carrell, 2000). It was thus assumed that CD19 amplifies BCR signalling in the context of antigen coated with proteins of the complement system. However, recent unpublished work by Batista and colleagues employing high-speed TIRF microscopy has shown that CD19 potentially amplifies BCR signalling by transiently associating with BCR microclusters. CD19 bears several intracellular tyrosine motifs, which get phosphorylated upon BCR ligation and serve as a docking site for signalling molecules like Vav, PI3K and PLCγ2 (Tuveson et al., 1993 and Li et al., 1997). By interacting with BCR microclusters, CD19 could thus help to recruit further signalling molecules to the BCR signalosome and consequently drive B cell spreading. Interestingly, mice lacking CD19 fail to mount a humoral immune response when immunised highlighting both the importance of CD19 as a co-receptor and B cell spreading in response to membrane-bound antigen (Engel et al., 1995 and Rickert et al., 1995).

To conclude, BCR microclusters form in response to membrane-bound antigen. They provide a platform for the coordinated assembly of the BCR signalosome and their formation and maintenance are controlled by the cortical cytoskeleton.

Recruitment of signalling molecules to the microcluster activates several intracellular mediators such as Calcium, MAP kinases or cytoskeletal regulators. The latter induce B cell spreading, which provides a mechanism for microcluster propagation and affinity discrimination through the BCR. Spreading is furthermore driven by the B cell co-receptor CD19, which transiently associates with BCR microclusters in order to assist the recruitment of signalling molecules. This increased recruitment leads to an amplification of the BCR signal and is therefore crucial for B cell activation.

1.3.4 Signal termination: Dephosphorylation, ubiquitination and internalisation

When B cells get activated by membrane-bound antigen, they form signalling-active BCR microclusters and spread over the antigen-presenting surface in order to propagate microclusters and overcome a threshold for activation. B cell spreading is followed by a more prolonged contraction phase, during which BCR microclusters move in a centripetal manner and fuse in the cSMAC area (Figure 1.8) (Fleire et al., 2006). Antigen gathering in a central aggregate potentially provides B cells with a mechanism for both antigen uptake and negative regulation of BCR signalling. It is likely that activating signals initially provided by kinases such as Syk or Btk need to be reversed so that the B cell does not enter into a hyperactive state. Several means of signal termination in B cells have been reported and they mainly include post-translational modifcations such as dephosphorylation and ubiquitination. In line with this, transmembrane proteins such as CD22 or the Fcγ receptor IIB, which contain immunoreceptor tyrosine inhibitory motifs (ITIMs), have been shown to recruit the phosphatases Shp1 and SHIP to the BCR signalosome (Nitschke, 2005). Shp1 has been indicated to act on BCR-proximal proteins like Lyn, Syk, Btk and BLNK whereas SHIP dephosphorylates membrane lipids (Maeda et al., 1999; Mizuno et al., 2000 and Liu et al., 1998). Other molecules including the protein phosphatases CD45 and CD148 could potentially also contribute to signal termination in B cells (Mustelin et al., 2005). However, questions about substrate specificity and the

spatiotemporally resolved action of phosphatases after BCR ligation remain unanswered.

Another possible mode of negative regulation of BCR signalling is ubiquitination. Depending on the number of ubiquitin molecules attached to a given protein by an ubiquitin ligase, this process can lead to proteasomal degradation or intracellular translocation of the modified protein. In particular, the E3 ubiquitin ligase Cbl has been reported to directly associate and subsequently ubiquitinate Syk kinase (Lupher et al., 1998 and Sohn et al., 2003). Interestingly, B cells from mice lacking Cbl are hyper-responsive to antigen and show elevated intracellular signalling in response to BCR activation (Kitaura et al., 2007). Given the size of the family of ubiquitin ligases and thus a potential redundancy, their exact role during immunoreceptor signalling remains to be elucidated (Rao et al., 2002 and Huang and Gu, 2008).

Further to dephosphorylation and ubiquitination, internalisation of the BCR itself constitutes an important mechanism for signal termination. Previous work has shown that the BCR triggers transport of monovalent antigens to endosomal MHC-loading compartments by a mechanism involving clathrin-mediated endocytosis (West et al., 1994 and Song et al., 1995). This process required functional actin filaments and the association of the clathrin-associated adaptor proteins 1 and 2 with the ITAM motif of the Igα molecule (Ohno et al., 1995; Cassard et al., 1998 and Brown and Song, 2000). In contrast, multivalent antigen increased the internalisation rate by 10-fold and endocytosis was independent of the ITAM motif within Igα (Song et al., 1995). It is therefore likely that mono- and multivalent antigens induce different pathways for internalisation. However, the exact process of BCR internalisation and the concomitant termination of signalling remain poorly understood.

In summary, B cells can apply different mechanisms to achieve negative regulation of BCR signalling. These include the dephosphorylation of signalling molecules, the ubiquitination and subsequent degradation of signalosome components or the internalisation of the BCR itself. The relative contribution of each of these processes to signal termination and their regulation is poorly understood and needs to be addressed in future work.

1.4 Aims of this study

The initiation of an immune response is characetrised by the highly co-ordinated and well-regulated activation of immune cells. In particular, the process of lymphocyte activation relies on the presentation of antigen molecules through diverse cell-cell interactions. While classical microscopy and biochemical methods have provided valuable insights for our understanding of lymphocyte activation, it was the introduction of life cell imaging, which has allowed us to appreciate the complexity and spatiotemporal dynamics of cell-cell interactions during an immune response. On the smaller scale, high-resolution microscopy has helped us to understand the orchestration of intracellular signalling events following immunoreceptor ligation in real-time.

This thesis focuses on the early events of B cell activation immediately after BCR triggering by membrane-tethered antigen. We use a combination of biochemical means, genetics and advanced high-resolution imaging to gain further insights into the B cell spreading response, the composition of BCR microclusters and the process of antigen gathering by B cells. We therefore provide valuable information on the molecular mechanisms underlying B cell activation in the context of an immune response.

The specific aims were:

1. To set up a siRNA screening to identify novel cytoskeletal regulators, which potentially drive B cell spreading.
2. To screen a panel of knockout B cells in order to identify proteins, which could orchestrate antigen gathering.
3. To investigate, which molecular motor(s) could be responsible for the centripetal movement of antigen-containing BCR microclusters, which provides B cells with a mechanism for antigen gathering.

Chapter 2 : Materials and Methods

This chapter provides information on the materials and methods used to generate the data presented in this thesis. For a list of abbreviations used please refer to appendix 1.

2.1 Materials

2.1.1 Antibodies

All antibodies listed in the following table were sorted according to their application.

Reactivity (Conjugation)	Host	Isotype	Product Code	Manufacturer/ Originator	Application
human IgM	goat	IgG	I0759	Sigma	microscopy
chicken IgM, clone M1	mouse	IgG_{2b}	Hybridoma	T. Kurosaki	microscopy
mouse kappa light chain (clone HB-58)	rat	IgG_1	Hybridoma	ATCC	microscopy
chicken IgM, clone M4	mouse	IgM	Hybridoma	T. Kurosaki	stimulations
mouse IgM (biotin)	goat	IgG	1020-08	Southern Biotech	stimulations
GFP	rabbit	total serum	ab290	Abcam	IP
Myosin IIa	rabbit	IgG	ab24762	Abcam	IP
Myosin VI	rabbit	IgG	ab106288	Abcam	IP
phospho-JNK T183/185	rabbit	IgG	9251	Cell Signaling	WB
phospho-p38 T180/182	rabbit	IgG	9211	Cell Signaling	WB
phospho-Syk Y323	rabbit	IgG	2715	Cell Signaling	WB
phospho-Syk Y352	rabbit	IgG	2701	Cell Signaling	WB

phospho-Syk Y525/526	rabbit	IgG	2710	Cell Signaling	WB
Cbl	mouse	IgG_1	610442	BD	WB
p50 dynamitin	mouse	IgG_1	611002	BD	WB
p150Glued	mouse	IgG_1	610473	BD	WB
GFP, clone 3E1	mouse	IgG_1	Hybridoma	CRUK	WB
mDia1	mouse	IgG_1	610848	BD	WB
DYNC1I1, clone 70.1	mouse	IgM	ab6304	Abcam	WB
DYNC1H1, clone R-325	rabbit	IgG	sc-9115	Santa Cruz	WB
rabbit IgG (HRP)	goat	IgG	31460	Pierce	WB
mouse IgG1 (HRP)	goat	IgG	1070-05	Southern Biotech	WB
Actin	mouse	IgG_1	A1978	Sigma	WB
Tubulin (HRP)	rabbit	IgG	ab6046	Abcam	WB
human CD19 (Alexa Fluor488)	mouse	IgG_1	53-0199	eBioscience	FC
mouse CD19, clone 1D3 (APC)	rat	IgG_{2a}	550992	BD	FC
mouse B220 (Alexa Fluor488)	rat	IgG_{2a}	557669	BD	FC
rat kappa light chain-FITC	mouse	IgG_{2a}	553872	BD	FC
mouse IL-2, clone JES6-1A12	rat	IgG_{2a}	554424	BD	ELISA (capture)
mouse IL-2, clone JES6-5H4 (biotin)	rat	IgG_{2b}	554426	BD	ELISA (detection)
Lamin	mouse	IgG_1	ab8984	Abcam	IF
goat IgG (Alexa Fluor488)	donkey	IgG	A11055	Invitrogen	IF

2.1.2 DNA constructs

Most DNA constructs used in this thesis were contributions from our collaborators J. Wienands, M. Engelke and M. Reth. Other constructs mentioned in the table below were either commercially available or kind gifts from various researchers.

Construct	Parental vector	Originator	Reference
pMAX-GFP	N.A.	Amaxa (Lonza)	N.A.
YFP-GPI	N.A.	B. Nichols	Nichols et al., 2001
Grb2-GFP	pEGFP-N1	M. Engelke	Stork et al., 2004
Dok-3-GFP	pEGFP-N1	M. Engelke	Stork et al., 2007
Dok-3-Y331F-GFP	pEGFP-N1	M. Engelke	Stork et al., 2007
Cbl-YFP	pEYFP-N1	L. Samelson	Balagopalan et al., 2007
Grb2R86K-GFP	pEGFP-N1	M. Engelke	Stork et al., 2004
Dok-3-Grb2cSH3-GFP	pEGFP-N1	M. Engelke	N.A.
Dok-3-Grb2cSH3-W193K-GFP	pEGFP-N1	M. Engelke	N.A.
MoysinVI-GFP	pEGFP-N1	F. Buss	Warner et al., 2003
MyosinIIa-GFP	pTRE-GFP	R. Adelstein	Wei et al., 2000
dynein-GFP	z4MSCV	M. Huse	Quann et al., 2009
dynamitin-GFP	pEGFP-N1	R. Vallee	Döhner et al., 2002
Tubulin-Cherry	pcDNA3.1	B. Treanor	Schnyder et al., 2011
LifeAct-GFP	pEGFP-N1	M. Sixt	Riedl et al., 2008
α-tubulin-RFP	p2MSCV	M. Huse	Quann et al., 2009
GST-Grb2	pGEX	M. Engelke	Grabbe et al., 2006
GST-Grb2nSH3	pGEX	M. Engelke	Grabbe et al., 2006
GST-Grb2cSH3	pGEX	M. Engelke	Grabbe et al., 2006
GST-Grb2SH2	pGEX	M. Engelke	Grabbe et al., 2006
Syk-GFP	pcDNA3.1	M. Reth	Kulathu et al., 2008
Syk2F-GFP	pcDNA3.1	M. Reth	this thesis
Syk3F-GFP	pcDNA3.1	M. Reth	Kulathu et al., 2008
Syk2F3F-GFP	pcDNA3.1	M. Reth	this thesis

Dync1h1 shRNA	pRetro-U6G	R. Vallee	Tsai et al., 2007
pGIPZ control shRNA	N.A.	Open Biosystems	N.A.
CD2ap-GFP		J. Wienands	Oellerich et al., 2011
Slp65-GFP		J. Wienands	Oellerich et al., 2011
CIN85-GFP		J. Wienands	Oellerich et al., 2011

2.1.3 Buffers

All chemicals were from Fisher Scientific, apart from PBS (Invitrogen), FCS (Invitrogen), Tween-20 (Sigma), BSA (Sigma), and milk powder (Marvel).

Buffer	**Components**
Imaging buffer	1x PBS, 0.5 % FCS, 2 mM $MgCl_2$, 0.5 mM $CaCl_2$, 1 g/l D-glucose, pH 7.4
SDS lysis buffer	62.5 mM Tris pH 6.8, 2 % SDS, 10 % glycerol, 50 mM DTT
NP-40 lysis buffer	20 mM Tris pH 8, 5 mM EDTA, 1 % NP-40, 200 mM NaCl, 1x Roche protease inhibitors, 1 µg/ml Nocodazole
SDS-Page buffer	12.1 g Tris, 23.8 g HEPES, 1 g SDS; fill to 1 l with dH_2O
Transfer buffer	14.4 g Glycine, 3 g Tris, 20 % Methanol; fill to 1 l with dH_2O
WB wash buffer	1x TBS, 0.1 % Tween-20
WB blocking buffer	1x TBS, 0.1 % Tween-20, 5 % w/v milk powder
FACS buffer	1x PBS, 1 % FCS, 1 % BSA
MACS buffer	1x PBS, 0.5 % FCS, 2 mM EDTA
Red Blood Cell lysis buffer	1 vol. Tris-HCl pH 7.6, 9 vol. NH_4Cl pH 7.2

2.1.4 Media

All components were from Invitrogen apart from 2-mercaptoethanol (Sigma) and DMSO (Fisher Scientific).

Medium	Components
Complete medium	1x RPMI 1640 supplemented with 10 % FCS, 1x GlutaMAX, 25 mM HEPES, 10 U/ml penicillin / streptomycin, 50 µM 2-mercaptoethanol
Complete chicken medium	1x RPMI 1640 supplemented with 10 % FCS, 1 % chicken serum, 1x GlutaMAX, 25 mM HEPES, 10 U/ml penicillin / streptomycin, 50 µM 2-mercaptoethanol
Stimulation medium	1x IMDM
Freezing medium	90 % FCS, 10 % DMSO
SOC	2 % bacto-tryptone, 0.5 % bacto yeast extract, 8.56 mM NaCl, 2.5 mM KCl, 10 mM $MgCl_2$, 20 mM Glucose

2.1.5 Reagents

All reagents listed in the table below were sorted based on their application.

Reagent	Product Code	Manufacturer/ Originator	Application
Streptavidin Alexa Fluor-633	S21375	Invitrogen	microscopy
PKH-26	PKH26GL	Sigma	microscopy
EZ-Link-Sulfo-NHS-LC-LC-Biotin	21338	Pierce	microscopy
1,2-dioleoyl-*sn*-glycero-3-phsphocholine (DOPC)	850375C	Avanti Polar Lipids	microscopy
1,2-dioleoyl-*sn*-glycero-3-phsphoethanolamine-N-(Cap Biotinyl) (Biotin-DOPC)	870273C	Avanti Polar Lipids	microscopy
ICAM-1-GPI DOPC	-	D. Depoil (CRUK)	microscopy
Taxol	T7402	Sigma	microscopy
Nocodazole	M1404	Sigma	microscopy
Fibronectin	F1141	Sigma	microscopy

Streptavidin polystyrene beads 0.13 µm	L090304C	Bangs Laboratories	stimulations
HEL	L-6876	Sigma	stimulations
CpG-biotin	custom made	Isogen	stimulations
CpG			stimulations
CFSE	C34554	Invitrogen	FC
Streptavidin polystyrene beads 5.6 µm	L090216J	Bangs Laboratories	FC
Extravidin-Alkaline Phosphatase (AP)	E-2336	Sigma	ELISA
p-Nitrophenyl phosphate tablets	N-2770	Sigma	ELISA
Complete protease inhibitors	11 873 580 001	Roche	IP
Dynabeads protein G	100.04D	Invitrogen	IP
DynaMag-2 (magnet)	123.21D	Invitrogen	IP
Dual-colour protein marker	310005174	BioRad	WB
LDS sample buffer	NP0008	Invitrogen	WB
kit V	VACA-1003	Amaxa (Lonza)	transfections
kit T	VACA-1002	Amaxa (Lonza)	transfections
Lipofectamine	15338-500	Invitrogen	transfections
DreamFect Gold	DG80500	OZ Biosciences	transfections
Lullaby	LL70500	OZ Biosciences	transfections
TransIT-TKO	MIR 2154	Mirus	transfections
Genesilencer	T500020	Genlantis	transfections
FuGENE HD	E2311	Promega	transfections
N-TER Nanoparticle	N2913-120UL	Sigma	transfections
Lipofectamine Plus	15338-100	Invitrogen	transfections
siIMPORTER	64-101	Millipore	transfections
TransPass R2	M2552S	NEB	transfections
293 Fectin	12347-500	Invitrogen	transfections

2.1.6 Mice

Mice listed in the table below were imported from the sources given and re-derived from quarantine through embryo transfer. Animals were used for experiments at an age of 8-24 weeks. All experiments involving mice were approved by the Cancer Research UK Animal Ethics Committee and the United Kingdom Home Office.

Mouse strain	Background	Source	Reference
wildtype	C57BL/6	Charles River	www.criver.com

2.1.7 Cell lines

All cell lines (apart from DT40) listed in the table below were kept at 37 °C and 5 % CO_2 in a humidified and sterile environment. Human and mouse cell lines were grown in complete medium (s.a.). Human cells were split every 72 hours to a concentration of 100,000 cells per ml. A20 and LK cell lines were split every 72 hours to a concentration of 200,000 cells per ml. T cell hybridomas were split every 48 hours to a concentration of 200,000 cells per ml. DT40 B cells were maintained in complete chicken medium (s.a.) at 39.5 °C and 5 % CO_2. Cells were split every 48 hours to a concentration of 100,000 cells per ml.

Cell line	Species	Description	Reference
Bjab	human	Burkitt's lymphoma derived, EBV^-, IgM^+, κ	Tedder et al., 1984
Raji	human	Burkitt's lymphoma derived, EBV^+, IgM^+, κ	Pulvertaft et al., 1964
Ramos	human	Burkitt's lymphoma derived, EBV^-, IgM^+, λ	Benjamin et al., 1982
A20 D1.3	mouse	BALB/c lymphoma derived, IgG_{2a}^+, κ, stably expressing the D1.3 BCR (see below)	Kim et al., 1979
DT40	chicken	ALV-induced bursal lymphoma, IgM^+	Baba et al., 1985
DT40*Cbl*$^{-/-}$	chicken	DT40 cells deficient for Ubiquitin ligase c-Cbl	Yasuda et al., 2000

DT40*Dok3*$^{-/-}$	chicken	DT40 cells deficient for adaptor Dok-3	Stork et al., 2007
DT40*Grb2*$^{-/-}$	chicken	DT40 cells deficient for adaptor Grb2	Hashimoto et al., 1998
DT40*Lyn*$^{-/-}$	chicken	DT40 cells deficient for kinase Lyn	Takata et al., 1994
DT40*Slp65*$^{-/-}$	chicken	DT40 cells deficient for adaptorSLP65	Ishiai et al., 1999
DT40*Syk*$^{-/-}$	chicken	DT40 cells deficient for kinase Syk	Takata et al., 1994
Plat-E	human	packaging cell line used for production of viral particles	Morita et al., 2000

The D1.3 transgenic BCR shows high affinity for HEL antigen and consists of a murine IgM heavy chain paired with a rat κ light chain (Aluvihare et al., 1997).

2.1.8 DT40 B cells as a model system

DT40 B cells constitute a very versatile cellular system as knockout cell lines can be created with relative ease. This is due to elevated rates of homologous recombination and - as a result - the higher probability to successfully insert targeting constructs for exon disruption (Shinohara and Kurosaki, 2006). Apart from knockout cell lines, DT40 cells can be easily used to generate B cell pools or clones stably expressing fluorescently-tagged molecules (see section 2.2.4). However, as DT40 cells were originally isolated from the bursa of fabricus of a chicken, they represent an avian B cell line (Baba et al., 1985). Given the evolutionary distance between birds and mammals one has to be aware of the potential differences in overall B cell biology. For example, DT40 B cells do not express the surface protein CD19, which is characteristic for B cells in mammals.

2.2 Methods

2.2.1 Isolation of naïve B cells from mouse spleen

Primary B cells were magnetically purified using negative selection. For this purpose, murine spleens were harvested under sterile conditions and passed through a 70 µm cell strainer. The suspension was spun and subjected to red blood cell lysis using red blood cell lysis buffer for five minutes at room temperature. Tubes were filled with complete medium, spun and cells resuspended in 400 µl MACS buffer. 100 µl of B cell isolation kit antibody cocktail (Miltenyi Biotec) were added and incubated on ice for ten minutes. Suspensions were topped up with 300 µl MACS buffer and 200 µl B cell isolation kit anti-biotin MicroBeads (Miltenyi Biotec). The suspension was incubated on ice for a further ten minutes. Cells were spun, resuspended in 1 ml MACS buffer and loaded on a previously equilibrated MACS LS separation column (Miltenyi Biotech). Columns were washed twice with 5 ml MACS buffer and the flow-through was collected, spun and plated in complete medium in 10 cm tissue culture dishes. The resulting population of B cells was tested for purity using flow cytometry assessing the surface expression of CD19 and B220 (Figure 2.1). Typically, isolated B cells were 95-99 % pure.

2.2.2 Flow cytometry

For flow cytometric analysis cells were washed and resuspended at a concentration of 10^7 cells per ml in FACS buffer in 5 ml polystyrene tubes (Falcon). To discriminate live and dead cells a drop of a 100 µg/ml Propidium Iodide (PI) solution was added to cell suspensions. PI penetrates dead cells and binds to DNA, thus conferring fluorescence to dead cells. All samples were read on a FACSCalibur II or a LSR II system (both BD).

For cell sorting, cells were resuspended at the concentration given above and passed through a 70 µm strainer to remove clumps. Filtered cell suspensions were transferred to FACS tubes and cells were sorted under sterile conditions using the FACS Aria system (BD) with laser excitation at 488 nm and 70 µm nozzle. Cells were sorted into 5 ml polypropylene tubes (Falcon) containing complete medium.

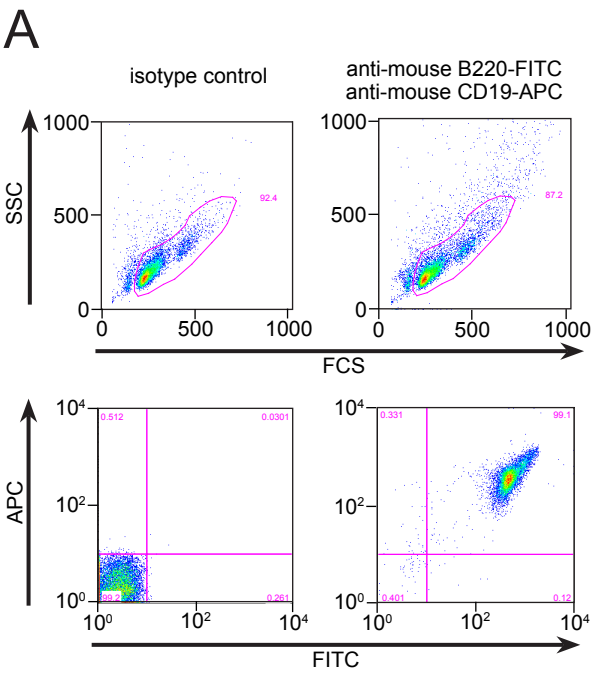

Figure 2.1. Purity of magnetically purified primary murine B cells
(A) Primary murine B cells were magnetically purified using a negative selection kit. Purified B cells were stained either with isotype controls or with monoclonal antibodies against B220 and CD19. B220 and CD19 expression was analysed using flow cytometry. Cells were identified based on their scatter profile (top row). FITC- and APC-fluorescence within the gated populations are shown (bottom row).

2.2.3 Amplification and purification of DNA plasmids

50 µl of library efficient DH5α competent bacteria (Invitrogen) were thawed on ice and subsequently incubated with 10 ng of plasmid DNA for 10 min. Bacteria were heat-shocked at 42 °C for 30 sec. 200 µl of SOC medium was added immediately after heat shock. Bacteria were incubated for one hour at 37 °C and 220 rpm and then plated on LB Agar plates containing 50 µg/ml of either Ampicillin or Kanamycin (both Sigma). Plates were incubated overnight at 37 °C. LB cultures of 400 ml supplemented with the appropriate antibiotic were started the next day using single colonies. Cultures were grown for at least 16 hours at 37 °C and 220 rpm. Bacteria were harvested by centrifugation and plasmid DNA was purified using Maxi purification kits (Qiagen). Concentration of resulting DNA solutions was measured using a NanoDrop spectrophotometer (Thermo Scientific).

2.2.4 Transfections

Transient transfection of cell lines using nucleofection (electroporation)

One day prior to electroporation B cells were split to a concentration of 500,000 cells per ml. $5x10^6$ cells were harvested, spun and resuspended in electroporation solution (kit T or V, Amaxa). 2 µg of plasmid DNA was added and the cell suspension was transferred to an electroporation cuvette. Cells were electroporated in a Nucleofector II device (Amaxa) using the appropriate electroporation programme for the specific cell type. Immediately after electroporation cells were transferred into pre-warmed complete medium. Expression of specific proteins was assessed 16-24 hours later using flow cytometry.

For electroporation of siRNA 1 µg of either RISCfree control siRNA or siRNA targeting mDia1, Syk or CD19 (all Dharmacon) was used per electroporation. Pools of four siRNA oligos were used to target CD19 or Syk.

CD19 target sequences:

Oligo 1: 5′-AAAGAAAGCGAAUGACUGAUU

Oligo 2: 5′-GCCUAGAGCUGAAGGACGAUU

Oligo 3: 5′-CAGCUGUGACUUUGGCUUAUU

Oligo 4: 5′-AGAGAUAUGUGGGUAAUGGUU

Syk target sequences:

Oligo 1: 5′-AGAAAUGUGUUGCUAGUUAUU

Oligo 2: 5′-CGGAAUGCAUCAACUACUAUU

Oligo 3: 5′-GAGCAAAUUGUCCUGAUAGUU

Oligo 4: 5′-GCUGCGCAAUUACUACUAUUU

mDia1 target sequence:

Oligo 1: 5′-AGGCAGAGCCACACUUCCUUU

Chemical transfection of siRNA into Bjab cells

Bjab B cells were split to a concentration of 500,000 cells per ml one day prior to transfection. Chemical transfection reagents were prepared according to manufacturer's instructions and different amounts of reagent (0.15 µl, 0.3 µl, 0.5 µl) were incubated with either RISCfree control siRNA or siRNA targeting Lamin or mDia1 (all Dharmacon) at a concentration of 50 nM in 48-well plates. A total of 200,000 Bjab B cells was added to each well and plates were incubated at 37 °C and 5 % CO_2 for 48 hours. Cells were harvested and processed for IF or WB analysis. To measure knockdown of Lamin, cells were transferred in 96-well glass bottom plates, permeabilised and stained with a fluorescent anti-human Lamin antibody. Lamin fluorescence was measured on the Cellomics automated fluorescence microscope. To assess knockdown of mDia1, cells were lysed using SDS-lysis buffer. Lysates were sonicated and boiled for 10 min at 95 °C. Samples were spun in a tabletop centrifuge (Eppendorf) at full speed for 5 min and loaded on SDS-Page gels.

For transfection with Accell siRNA targeting CD19 (Dharmacon) cells were grown in Accell delivery medium supplemented with 10 % FCS. FCS was diluted 1/2 when cells were split and cells were maintained at a final concentration of FCS of 2.5 %. Accell siRNA was added to the cell culture at a concentration of 1 µM and

cells were cultured in presence of siRNA for 72 hours. After this time cells were harvested and CD19 expression was measured using flow cytometry. A pool of four siRNA oligos was used.

CD19 target sequences:

Oligo 1: 5′-CUUUUCAUCUUCAACGUCU

Oligo 2: 5′-GCUGUGACUUUGGCUUAUC

Oligo 3: 5′-GUGGAAUGUUUCGGACCUA

Oligo 4: 5′-GCCAGAGAUAUGUGGGUAA

Transfection of DT40 B cells to generate stable cell lines

10^7 DT40 cells were harvested, spun and washed with PBS. Cells were resuspended in 500 µl PBS and incubated with 30 µg of plasmid DNA for 5 min. Cell suspensions were transferred to an electroporation cuvette (Cell Projects) and electroporated in a Gene Pulser apparatus (Bio-Rad) at 570 mV and 25 µFd. After electroporation cells were immediately transferred to a tissue culture dish containing 20 ml pre-warmed complete medium and left at 37 °C overnight. The next day, appropriate antibiotics (G418, Puromycin or Hygromycin B) were added at a concentration of 2 mg/ml (Puromycin at 0.5 µg/ml). The volume was adjusted to 70 ml and cells were plated into 96-well flat-bottom dishes at 180 µl per well (yield = 4 plates). Stable clones were picked 10-14 days after plating, expanded and screened for expression of the transgene by flow cytometry.

Transfection of primary murine B cells

Primary murine B cells were transiently transfected using retroviral particles. For this purpose, retroviral vectors were transfected into the packaging cell line Plat-E using 293 Fectin and virus particles were harvested 48 hours after transfection using ultracentrifugation. Magnetically purified splenic B cells were cultured in complete medium containing 25 µg/ml LPS for 36 hours. $1.5x10^6$ B cells were subsequently infected with supernatant containing virus particles by centrifugation at 1500 x g at 33 °C for four hours.

2.2.5 SDS-Page and Western blotting

10-50 µl of cleared cell lysate and 5 µl of protein marker were loaded on 8 % or 12 % pre-cast LongLife gels (NuSep). Gels were run in an electrophoresis tank (Bio-Rad) using SDS-Page buffer at 100 V for one hour. To resolve the cytoplasmic dynein heavy chain, 3-8 % NuPAGE Tris-Acetate gels and Tris-Acetate SDS running buffer (both Invitrogen) were used. Proteins were blotted onto a Hybond-P PVDF membrane (GE Healthcare), which was previously activated in pure Methanol. Proteins were blotted in wet conditions using transfer buffer in a blotting apparatus (Bio-Rad) at 100 V for one hour. Membranes were subsequently blocked in WB blocking buffer at room temperature for one hour. Primary antibodies were diluted in blocking buffer and incubated with the membrane overnight at 4 °C. Following three washes with WB wash buffer the primary antibody was detected using a HRP-linked secondary antibody diluted in blocking buffer for one hour at room temperature. Membranes were washed and incubated with ECL solution (GE Healthcare) for 1 min at room temperature. Chemiluminescence was detected with Hyperfilm (GE Healthcare) and developed in a JP-33 (Jpi) film processor.

2.2.6 Immunoprecipitations

For immunoprecipitations from resting or activated DT40 cells expressing proteins coupled to GFP, 10^7 cells per condition were starved in IMDM without serum at 37 °C for 15 min. Cells where left to rest or stimulated with 5 µg/ml anti-chicken IgM antibody (clone M4) for 5 min. Samples were subsequently spun at 0.5 x g and lysed in NP-40 lysis buffer on ice for 45 min. In the meantime, magnetic protein A/G Dynabeads were coated with an excess of a polyclonal anti-GFP antibody for 10 min at room temperature. Dynabeads were washed three times with PBS and 50 µl of bead slurry was used per sample. Lysates were cleared by centrifugation at 10,000 x g for 15 min at 4 °C. GFP-tagged proteins were immunoprecipitated from lysates using the anti-GFP coupled Dynabeads overnight at 4 °C. The following day beads were harvested from lysates using a magnet and immunoprecipitated complexes were washed in ice-cold PBS three times. Beads were finally incubated in LDS sample buffer and boiled at 95 °C for

10 min. Samples were subsequently loaded on SDS-Page gels and transferred to PVDF membranes as described.

2.2.7 Affinity purification of Syk from SILAC labelled DT40 B cells

DT40 cells were cultured in SILAC-Medium as described before (Oellerich et al., 2009). For identification of the Syk interactome, One-STrEP-tagged Syk expressing DT40 cells were cultured in SILAC medium containing ^{13}C, ^{15}N labelled Lysine (Lys+8) and 13C, 15N labelled Arginine (Arg+10) while DT40 wildtype cells expressing untagged Syk served as control and were grown in the presence of non-labelled amino acids (Lys+0 and Arg+0). $2x10^8$ B cells from both populations (labelled and non-labelled) were stimulated for 5 min with an anti-chicken IgM antibody, lysed and lysates were passed over a Strep-Tactin column for affinity purification of tagged Syk. Eluates were pooled at a 1:1 ratio after washing and pooled samples were concentrated by ultracentrifugation using spin columns (Sartorius, Göttingen). Protein samples were separated by 1-D PAGE and entire gel lanes were cut into pieces of equal size and subjected to trypsin digest. Extracted peptides were separated and subsequently analysed by liquid chromatography-coupled tandem mass spectrometry (LC-MS/MS) on an Orbitrap XL ESI mass spectrometer (ThermoFisherScientific). Proteins were identified in the database and subsequently quantified using Mascot as search engine and MaxQuant software,respectively (Cox et al., 2009).

2.2.8 Stimulation of DT40 B cells and intracellular signalling

To assess intracellular signalling in DT40 cells upon BCR-activation, 24-well tissue culture plates were coated with 0.3 or 3 µg/ml of an anti-chicken IgM antibody (clone M4) at 4 °C overnight. The next day, plates were washed three times with PBS. DT40 B cells were harvested, washed once and starved in serum-free IMDM medium for 15 min at 37 °C. Cells were then seeded into coated wells at a concentration of 10^6 cells per well. Plates were briefly spun to allow cells to make contact with the anti-IgM coated surface. Cells were lysed with SDS-lysis buffer 1, 5, 15 and 30 min after seeding. Cells in non-coated wells served as timepoint 0. After lysis, samples were sonicated and boiled at 95 °C for 10 min.

After a 5 min spin in a tabletop centrifuge at full speed, cleared samples were loaded on SDS-Page gels (equivalent of 500,000 cells per lane). Gels were run and blotted as described and membranes were probed with antibodies specific for p-JNK, p-p38 and p-Syk (Y352).

2.2.9 Inhibitor treatment

For treatment of primary murine B cells with Taxol, cells were washed once in PBS and subsequently incubated in complete medium containing 50 µg/ml Taxol at 37 °C for 80 min. Inhibition of the microtubule network using Nocodazole was carried out by pre-incubating DT40 cells with the drug at a concentration of 1 µg/ml at 37 °C for 10 min. Inhibitors were washed out, cells resuspended in imaging buffer and immediately used for imaging experiments.

2.2.10 Lipid bilayers

Generation of liposomes

DOPC and Biotin-DOPC lipids (see Materials) were purchased as 10 mg/ml stock solutions in chloroform. Liposomes were prepared by the detergent dialysis method described by Brian and McConnell (Brian and McConnell, 1984). Chloroform was evaporated using N_2 and traces of solvent were removed under vacuum for three hours. Dried lipids were resuspended in Tris/NaCl buffer containing 2 % octylglucoside to obtain a 2 mM 10x stock solution. The lipid solution was then sonicated until clear and the stock was diluted 1/10 in Tris/NaCl buffer containing 2 % octylglucoside and dialysed against Tris/NaCl buffer at 4 °C for 24 hours. Buffer was changed three times during dialysis. The final liposome solution was passed through a 0.22 µm filter, overlaid with Argon gas and stored at 4 °C until use.

Monobiotinylation of antibodies

Monoclonal antibodies used for mono-biotinylation were first dialysed against PBS for 24 hours at 4 °C to remove any traces of free amines. Antibodies were then biotinylated at a concentration of 1 mg/ml using the EZ Link Sulfo-NHS-biotin reagent (stock solution at 100 mg/ml in DMSO). A final concentration of NHS-biotin reagent of 0.01 µg/ml typically yielded in mono-biotinylation of antibodies. Antibodies and NHS-biotin reagent were incubated at the concentrations mentioned above for 30 min at room temperature and subsequently dialysed against PBS for 24 hours at 4 °C. Dialysis was carried out to remove all traces of free NHS-biotin reagent.

To verify mono-biotinylation of antibodies, these were coupled to 5.6 µm streptavidin polystyrene beads. A poly-biotinylated antibody served as control. Antibodies coupled to beads were detected using a specific secondary antibody linked to FITC. Additional biotin-sites on antibodies were detected by incubation of beads with Streptavidin Alexa Fluor633. Beads were washed three times with PBS and passed through a flow cytometer to read FITC and Alexa Fluor633 fluorescence. See Figure 2.2 for flow cytometry data showing mono-biotinylation of monoclonal antibodies.

Generation of lipid bilayers for microscopy

Glass-supported planar lipid bilayers were established in FCS2 microaqueduct chambers (Bioptechs) by fusion of liposomes as previously described (Dustin et al., 1996). One day prior to experiments glass coverslips were incubated in sulphochromic acid overnight to remove any traces of dirt or dust. Coverslips were rinsed three times with dH_2O and acetone to remove the acid. Biotin-DOPC liposomes were diluted in DOPC liposomes at various dilutions (1/500 to 1/2000) and 0.8 µl droplets of the lipid mixture were pipetted on the cleaned glass coverslips. FCS2 chambers were then assembled according to manufacturer's instructions and liposomes were allowed to fuse on the glass for 15 min. Established lipid bilayers were blocked for one hour at room temperature using imaging buffer. Streptavidin Alexa Fluor633 stock solution at 1 mg/ml was diluted in imaging buffer 1/1000 and incubated with blocked lipid bilayers.

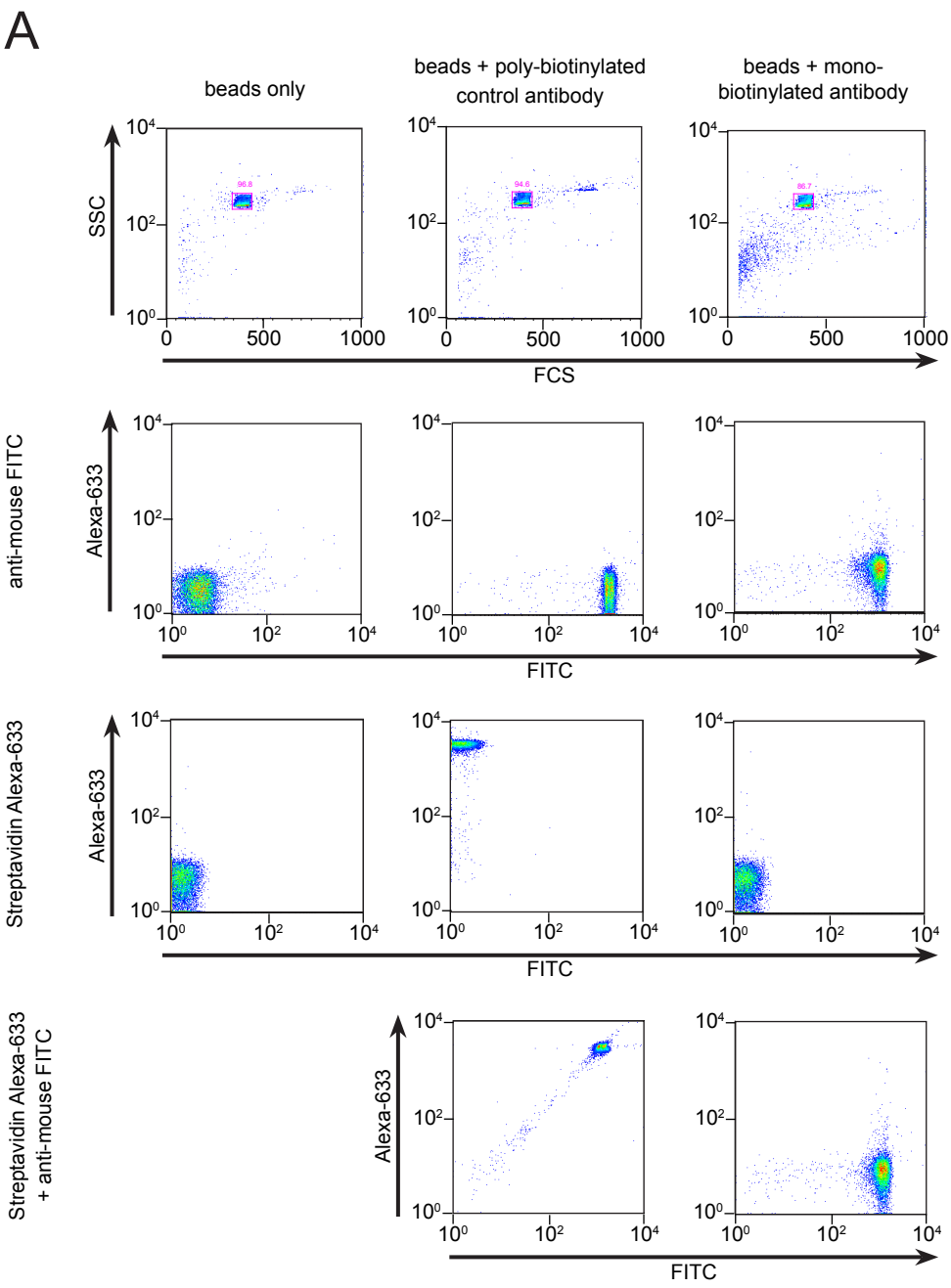

Figure 2.2. Flow cytometric test of mono-biotinylation of antibody
(A) Streptavidin-coated polystyrene beads were left alone or incubated with poly- or mono-biotinylated antibodies. Antibodies will bind to beads by virtue of the streptavidin-biotin interaction. Binding of antibody to beads was assessed by incubation with a FITC-conjugated secondary antibody. Additional biotin binding-sites on bound antibodies were detected by incubation with streptavidin coupled to Alexa-633. Beads were identified based on their scatter profile (top row).

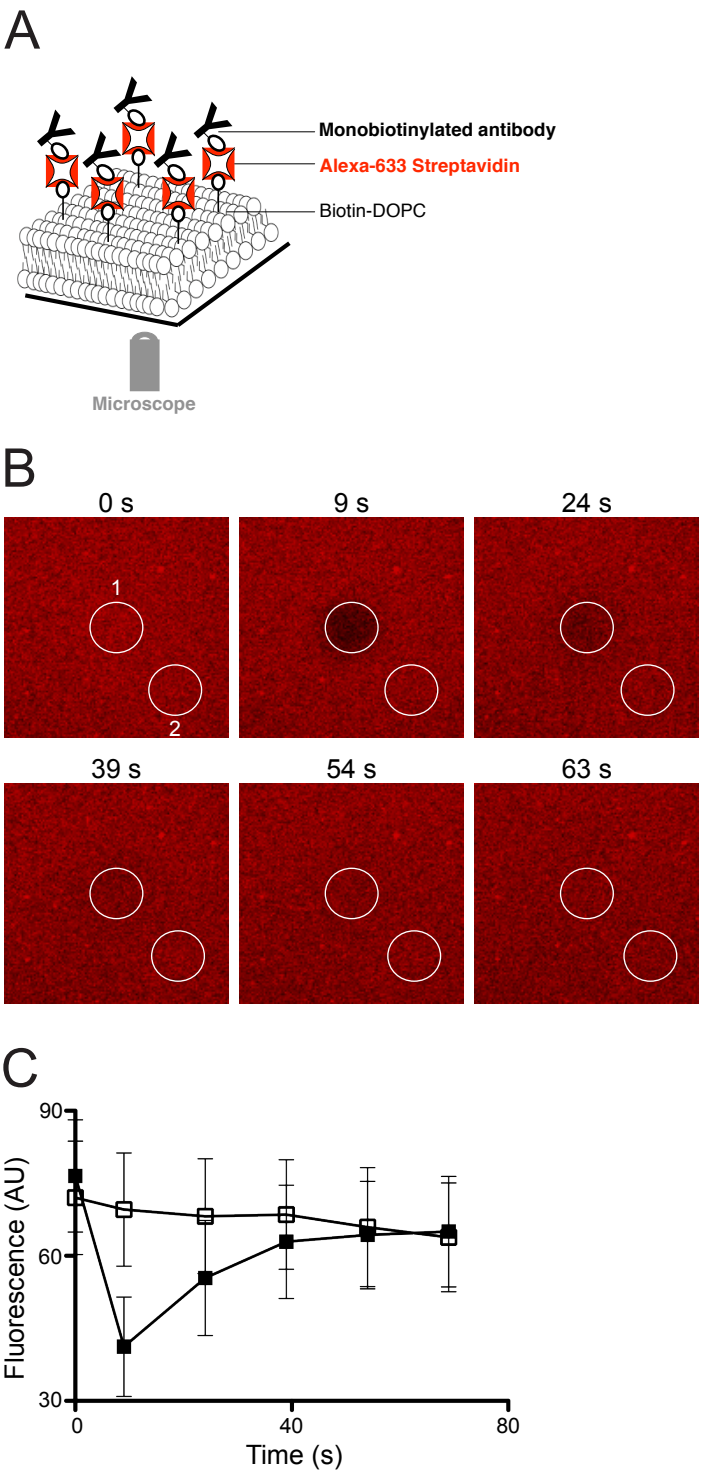

Figure 2.3. Bleaching experiment to verify fluidity of planar lipid bilayers
(A) Schematic representation of a supported lipid bilayer using biotin-DOPC lipids diluted in DOPC lipids, fluorescent streptavidin and mono-biotinylated monoclonal anti-BCR antibody. (B) Planar lipid bilayers were prepared as described in the Methods. Bilayers were bleached using a confocal microscope at a wavelength of 633 nm. Circle 1 highlights the bleached area before, immediately after and later after bleaching to show recovery of the fluorescent signal. The area highlighted by circle 2 was used to monitor fluorescence outside the bleached area. (C) The total fluorescence of areas 1 (filled squares) and 2 (empty squares) was measured using ImageJ software and plotted as a function of time.

Fluorescent streptavidin was allowed to bind to biotin-DOPC incorporated in lipid bilayers for 10 min at room temperature and was subsequently washed using imaging buffer. The 1 mg/ml stock solution of mono-biotinylated antibody was diluted 1/25 in imaging buffer and incubated with lipid bilayers for 10 min at room temperature to allow binding to fluorescent streptavidin. After washing off excess antibody, lipid bilayers were ready to use. Fluidity of lipid bilayers was assessed using a confocal microscope bleaching a defined region and measuring the recovery of fluorescence over time (Figure 2.3).

2.2.11 Microscopy

Confocal microscopy

All brightfield, IRM and confocal microscopy images were acquired with an inverted Zeiss Axiovert LSM 510 META microscope. Objectives used were 20x and 63x oil immersion objectives. For imaging of lipid bilayers pinhole sizes were set to one Airy, which yielded in an effective optical slice of 1-2 µm.

Total Internal Reflection Fluorescence microscopy (TIRF)

TIRF images were acquired with a Cascade II EMCCD camera (Photometrics) coupled to an Olympus TIRF system based on an IX-81 inverted microscope. Laser excitation at 488 nm, 561 nm and 633 nm and an Olympus 150 x 1.45 NA oil immersion objective were used. For a schematic explaining the basic principle of TIRF microscopy please refer to Figure 2.4.

To simultaneously image BCR particles and tubulin we made use of dual-view high-speed microscopy. For this purpose, Fab fragments of a monoclonal anti-chicken IgM antibody (clone M1) were labelled with Atto633 fluorophores, which contain a reactive NHS-Ester group (Atto-Tec). The reactive Ester group allows coupling of fluorophores to lysines present in antibodies. The stained M1 Fabs were used to label DT40 B cells stably expressing tubulin-RFP at a limiting dilution to visualise only a fraction of BCRs present on the surface of the cell. High-speed simultaneous acquisition of two channels was done using an Optosplit II image splitter (Cairn Research) coupled to a QuantEM CCD camera

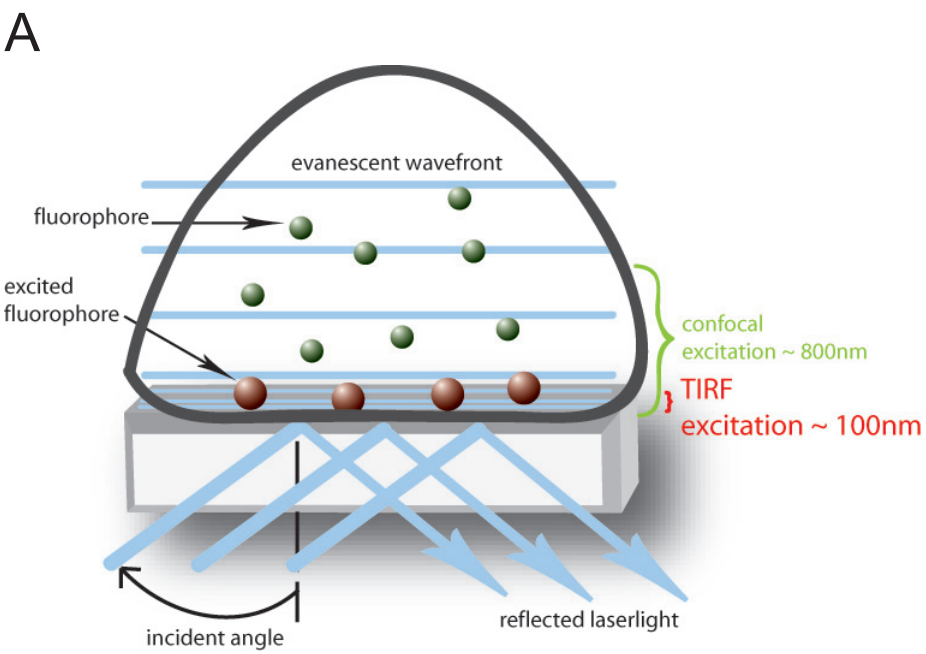

Figure 2.4. Schematic illustrating the principle of TIRF microscopy
(A) Laserlight arriving at the coverslip is totally reflected due to the incident angle. A small portion of light is not reflected, however, and penetrates the sample as an evanescent wave parallel to the glass slide. The evanescent wave looses energy in an exponential manner and thus only excites fluorophores which are very close to the glass slide (approx. 100-200 nm). This results in a significant contrast enhancement in the acquired image. Schematic adapted from B. Treanor.

(Photometrics). Frame rates of 20 frames/s were used to record image sequences of 200 frames (10 s total length). Single particle tracking of labelled BCR was done using the tracking algorithm established by Crocker and Grier (Crocker and Grier, 1996). Software used for single particle tracking was Matlab. BCR particles were scored as immobile if their diffusion coefficient was below 0.01 $\mu m^2 s^{-1}$.

2.2.12 Data analysis

Software

Software used for analysis of flow cytometry data was FlowJo (Tree Star). Imaging data was analysed using ImageJ (NIH), Imaris (Bitplane), Volocity (Improvision), and Matlab (MathWorks). Graphs and charts were created using Prism software (GraphPad). Statistical analysis was carried out using Prism.

Quantification of Western blots

Developed chemiluminescence films were scanned using a CanoScan 8800F (Canon) at a resolution of 300 dpi. Total fluorescence of bands was measured in ImageJ by drawing a box-shaped ROI around the specific band and using the background-substracted total fluorescence as a measure for band intensity. This was done for the band of interest and - using the same ROI – for the band of the loading control of the specific lane. Intensities of bands of interest were normalised to intensities of corresponding loading controls.

Microcluster colocalisation analysis

Images were cropped to the size of the cell using Imaris and both channels were background substracted with a filter width of 1 μm. To quantify colocalisation, the original Manders coefficient for the antigen channel was calculated for each cell using the Imaris colocalisation module (Manders et al., 1993).

Quantification of antigen microclusters (amount and movement)

For quantifications of the total number of antigen microclusters, cells were settled on antigen-bearing planar lipid bilayers and snapshots were taken five minutes later. Antigen microclusters were identified using the particle detector plugin for ImageJ software according to Sbalzarini and Koumoutsakos, 2005. Antigen microclusters were counted in at least 13 cells acquired in a minimum of two independent experiments. Figure 2.5A shows representative cells at maximum spread and the according particle detector mask.

In order to measure directed movement of antigen microclusters, video sequences were recorded using 633 nm excitation for one minute at a frame rate of 1 frame/s. Antigen microcluster movement was tracked on the bleaching-corrected images by the established particle-tracking algorithm by J. Crocker and D. Grier (s.a.). The centre of the cell (x_c,y_c) was approximated by the average of the starting positions of all clusters, which were evenly distributed over the cell. The distance of the first (x_1,y_1) and last (x_n,y_n) point of the microcluster track to the centre of the cell was simply calculated as $d_1 = \mathrm{sqrt}((x_1-x_c)^2+(y_1-y_c)^2)$ and $d_n = \mathrm{sqrt}((x_n-x_c)^2+(y_n-y_c)^2)$, which is the radius of a circle around the centre, which goes through the point (blue and red lines in Figure 2.5 B). The distance to the centre is then given by $d_c = d_1 - d_n$ which is positive when the cluster shows any net movement towards the centre and negative if it moves towards the edge of the cell.

Quantification of contact area and antigen accumulation

IRM images were used to quantify the contact area between cells and lipid bilayers. An ROI was manually drawn around the edge of the cell using Volocity software. The size of the ROI (in μm^2) was given by the software. To quantify antigen accumulation a ROI was manually drawn around the edge of each cell using the fluorescence confocal image representing the antigen-bearing lipid bilayer. The total amount of fluorescence within the ROI was used as a value for the amount of antigen gathered by the cell.

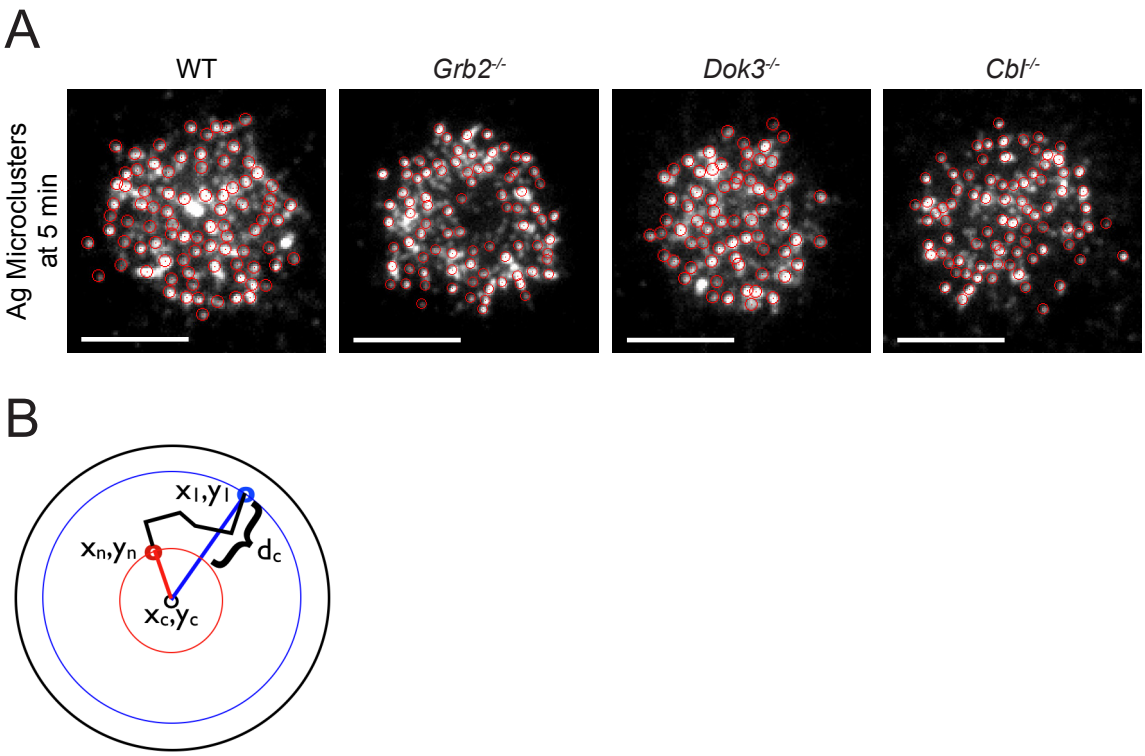

Figure 2.5. Antigen microcluster quantification in spread B cells
(A) Representative masks used for quantification of the total number of antigen microclusters formed at 5 minutes in DT40 B cells as obtained from the particle detector plugin for ImageJ software (see Methods). Scale bars equal 5 μm. (B) Schematic representation of parameters used to quantify movement of antigen microclusters.

Quantification of dynein intensities along antigen microcluster tracks

Two colour video sequences were recorded using 633 nm excitation to image the BCR microclusters and 488 nm excitation to image dynein-GFP. Intensities in the BCR channel were corrected for photobleaching by fitting an exponential decay curve to the total intensity to extract a decay length λ. The intensities were then multiplied by the function exp(1/λ t). Antigen microcluster movement was tracked on the bleaching-corrected images by the particle-tracking algorithm by J. Crocker and D. Grier, 1996 in the Matlab implementation by Daniel Blair and Eric Dufresne (http://physics.georgetown.edu/matlab/).

The dynein image sequences were background subtracted using a disk shaped structure element; the size of the disk was adjusted to match the diameter of dynein structures, typically 5-7 pixels. For each of the tracked antigen microcluster the dynein-GFP intensity was measured over time at the position of the microcluster. Given is the average intensity over a 5-pixel diameter circular region of the background-subtracted image. These intensities were normalized by the mean background intensity of the cell resulting in high values for well-resolved features and lower values for less well resolved features, independent of the expression levels of the cells. The analysis was performed in Matlab using the image processing and optimisation toolboxes.

Chapter 3 : Establishing a siRNA Library Screen to Identify Novel Regulators of B Cell Spreading

B cells recognise pathogen-derived antigen molecules by their BCR. Triggering of the BCR transmits a signal into the cell and initiates B cell activation. Previous work in our laboratory has manifested the importance of the cytoskeleton during this process (Fleire et al., 2006; Weber et al., 2008 and Treanor et al., 2011). When presented with antigen on the surface of an antigen-presenting cell, as predominantly occurs *in vivo* (Batista and Harwood, 2009 and Carrasco and Batista, 2007), B cells undergo a rapid spreading response, which is followed by cellular contraction (Fleire et al., 2006).

This two-step process allows B cells to discriminate between different antigen affinities and it is as well crucial for antigen gathering in the centre of the mature immune synapse. The extent of spreading directly correlates with the amount of antigen gathered, internalised and presented to T cells and thus dictates B cell activation (Fleire et al., 2006). For spreading to occur, signalling through the BCR involving signalling molecules such as PLCγ2 or Vav (Weber et al., 2008) is needed. BCR signalling then translates into significant changes of B cell morphology driven by the cytoskeleton. To gain further insight into the molecular mechanisms driving B cell spreading, we decided to use a siRNA library screening approach.

The screen was initiated in collaboration with the CRUK London Research Institute high-throughput facility and was based on a human genome-wide library consisting of 22,000 siRNAs. RNAi-mediated knockdown of proteins would be achieved by transfection of B cells with siRNA pools targeting specific proteins in a high-throughput manner. Once transfected with siRNA, B cells would be subjected to a functional assay to measure the potential effect of protein knockdown. As our aim was to identify novel regulators of B cell spreading this necessitated establishing a robust B cell spreading assay, which could be carried out and quantified in an automated fashion. This chapter summarises the efforts

made setting up the siRNA screen to reveal new insights into the molecular mechanism of B cell spreading.

3.1 Setting up a screening assay

3.1.1 Choice of human B cell lines

An important factor when setting up an RNAi screen is the choice of a suitable cellular system. The available siRNA library was designed to target human genes. We therefore decided to focus on human B cell lines and initially used three cell types, which were available from the CRUK London Research Institute cell production facility: Bjab, Raji and Ramos. All three B cell lines were initially isolated from Burkitt's lymphomas and can be readily grown and expanded using standard cell culture methods. Sufficient numbers of cells for a triplicate genome-wide library screen were thus easily obtainable. Bjab, Raji and Ramos cells all express surface IgM (see Materials), which should lead to cell spreading when cross-linked on a planar surface. Regarding large numbers of cells for experiments the chosen human B cell lines appeared superior to primary human B cells from blood. The use of the latter would have additionally been difficult, given the short lifespan of primary B cells after isolation. Depending on the targeted protein and its half-life, knockdown using RNAi can take up to 96 hours. We were not confident that primary human B cells could resist the crude conditions of a large-scale RNAi screen over a period of several days. Once hits from the screen would have been verified, we were planning to use other systems such as primary human and murine B cells to confirm our results.

3.1.2 Human B cells spread on anti-BCR coated glass surfaces

Given the size of the siRNA library screen our first aim was to establish a robust cellular assay, which could be carried out in a high-throughput manner using human B cell lines. As our primary interest was the regulation of B cell spreading, we sought to create a straightforward and reproducible spreading assay in a 96-well format. Before using 96-well plates, however, we had to verify that the B

cells chosen would spread on glass surfaces coated with a ligand for their BCR. We therefore coated glass coverslips with different amounts of an anti-human IgM antibody, which would serve as a surrogate antigen. We subsequently used a fluorescent secondary antibody to detect the antibody used for coating (Figure 3.1 A) and assessed fluorescence of the coated glass with a confocal microscope. To verify that resulting fluorescence was indeed due to antibody binding and not reflection from the glass, we bleached a certain region using the 488 nm Argon laser at high power. Given the titrating fluorescence correlating with the amount of anti-human IgM antibody used for coating and successful bleaching in Figure 3.1 A, we were confident that glass was sufficiently coated with anti-BCR antibody.

Next, we wanted to test the ability of the three human B cell lines to spread on anti-IgM coated glass. For this purpose, we either incubated clean coverslips with 10 µg/ml of anti-human IgM for one hour or used PBS without antibody as control. To visualise cells using confocal microscopy we labelled them with a fluorescent membrane dye, which allowed us to identify the edge of spreading cells. We seeded labelled cells on coated glass slides and left them to spread for 10 min at room temperature and subsequently acquired a single confocal slice at the interface between cells and glass using a 20x magnification objective (Figure 3.1 B). Based on the acquired images it became apparent that Bjab cells responded to anti-human IgM antibody by spreading on the glass surface. This effect was less clear for Raji and Ramos cells and we thus decided to assess spreading of Bjab cells in more detail.

In order to visualise spreading of Bjab cells with higher resolution, we coated glass coverslips as explained above, seeded cells at a density of 10^6 per ml and monitored spreading using interference reflection microscopy (IRM). IRM makes use of a phase-shift of laser light reflected by the glass or the specimen attached to it. Areas covered by cells result in a dark signal in the resulting image. As shown in Figure 3.1 C Bjab cells did not spread on control glass coverslips incubated with PBS alone. When settled on glass coated with anti-human IgM antibody, however, Bjab cells did spread significantly over the course of 20 min (Supplementary Video 1). Cells contacted the coated glass at different time points

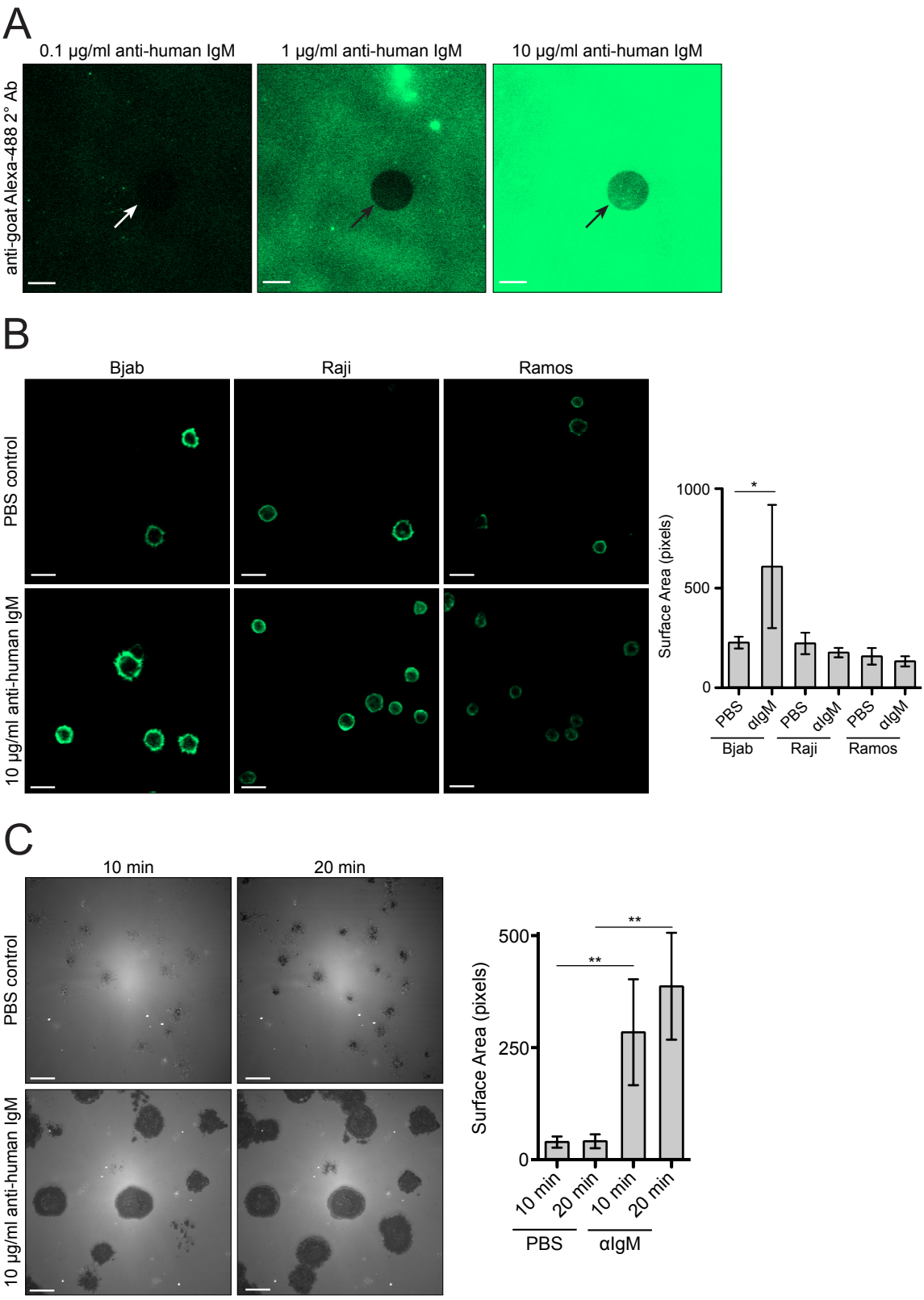

Figure 3.1. Bjab B cells spread on anti-BCR-coated glass coverslips
(A) Glass coverslips were coated with anti-human IgM antibody at different concentrations. Bound antibody was detected with an anti-donkey antibody coupled to Alexa-488. Coating was assessed using confocal microscopy. Bleaching was carried out (arrows) to verify the fluorescence was due to labelling and not reflection from the glass. (B) Human B cells (Blab, Raji, Ramos) were labelled with a membrane dye and settled on glass coverslips coated with anti-human IgM or PBS as control. Spreading was assessed 10 min after seeding using a confocal microscope and quantified (right panel). (C) Bjab B cells were settled on glass coverslips as in (B) and spreading was monitored using Interference Reflection Microscopy (IRM). Images were acquired 10 and 20 min after seeding of cells and the contact area bewteen cells and glass was quantified (right panel). Scale bars equal 5 µm.

and the initiation of spreading was not synchronised. However, after 20 min all cells had made contact with the glass coverslip and no further spreading was observed. This is likely due to the physical constraints of cells. Given their specific size, resources to push the cell membrane further must get exhausted at some point.

It is important to note that Bjab cells did not contract after spreading in this experimental setup. This was expected, as the surrogate antigen used for coating was tightly bound to the glass surface and was thus immobile. Once bound to the coated glass, B cells cannot gather antigen as they normally would on the surface of an antigen-presenting cell. As our primary focus was to screen for novel regulators of B cell spreading, however, the lack of contractility in this particular assay could be overlooked.

Among three different human B cell lines, Bjab were the most competent in BCR-mediated spreading experiments on glass. This was a first requirement to transfer the assay to a high-throughput platform for a siRNA screen.

3.1.3 Electroporation optimisation for Bjab cells to express foreign DNA

As the eventual spreading assay would be carried out and analysed in an automated fashion using the Cellomics ArrayScan fluorescence microscope, we decided to express fluorescent YFP molecules coupled to a GPI-anchor in Bjab cells. YFP proteins insert into the plasma membrane by virtue of their GPI-anchor and confer fluorescence to the membrane, which could in turn be detected using a fluorescent microscope such as the ArrayScan.

To be able to express a YFP-GPI construct in Bjab cells we had to optimise the transfection protocol for this particular cell line using the Amaxa Nucleofector system. This system works by combining cell specific transfection solutions and electroporation with the Nucleofector II device set to a certain transfection programme (see Methods). As there was no specific transfection programme defined for Bjab cells, we used a series of different programmes (C-009, L-029, O-017, T-001, X-001, Y-005) recommended to us by Amaxa to transfect a vector coding for soluble GFP (pMAX-GFP) as a high-efficiency test plasmid into Bjab cells. Cells were electroporated in the presence of pMAX-GFP vector in transfection solution 'T' using the Nucleofector programmes specified. 16 hours later GFP-expression was assessed using flow cytometry (Figure 3.2 A). Viability of cells and level of GFP-expression varied significantly depending on the transfection programme used. Viability was measured by staining cells with the DNA-binding dye propidium iodide (PI), which confers fluorescence to dead cells. Cells were defined as alive if they were negative for PI-fluorescence within the cellular population, which was defined based on the forward and side scatter profiles. GFP-fluorescence was measured within the live cell population. Figure 3.2 B shows values for cell viability and GFP-fluorescence 16 hours post-transfection depending on the programme used. Transfection programme C-009 yielded the best combination of cell viability and GFP expression. Other programmes such as O-017 or Y-005 either showed high expression with low viability or *vice versa*. Based on these data, we decided to use transfection programme C-009 for subsequent transient transfections of Bjab B cells.

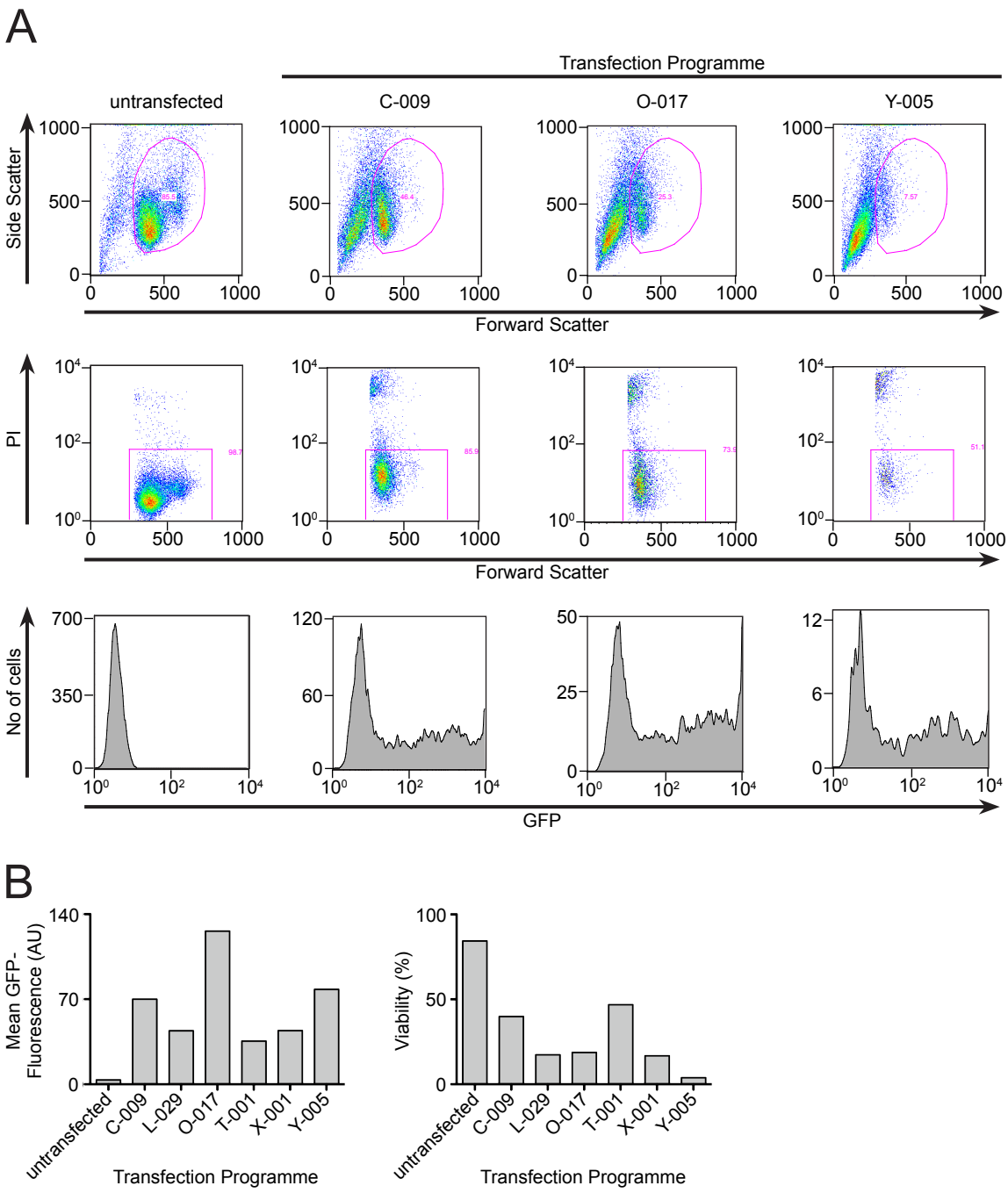

Figure 3.2. Optimisation of electroporation protocol for Bjab B cells
(A) Bjab cells were transfected with the Amaxa Nucleofector II device using kit 'T' and the indicated electroporation programmes. Three representative transfections are shown. 5 x 10^6 Cells were transfected with 1 µg of pMAX-GFP vector DNA and GFP-expression was assessed 16 h later using flow cytometry. Cells were identified by their scatter profile (top row). Live and dead cells were distinguished using Propidium Iodide (PI) which binds to DNA in dead cells (middle row). GFP-fluorescence of the living population is shown in histograms (bottom row). (B) Quantification of GFP-fluorescence for all transfections based on mean fluorescence obtained from flow cytometer. (C) Quantification of cell viability for all transfections based on percentage of cells (A, top row) and percentage of live cells within that population (A, middle row).

3.1.4 Spreading of Bjab cells can be measured in a high-throughput manner

To test the possibility of using Bjab cells expressing YFP-GPI in a high-throughput spreading assay, we expressed YFP-GPI in Bjab cells by electroporation and seeded them on anti-human IgM coated glass coverslips 16 hours after transfection. Spreading of cells was monitored using IRM and confocal microscopy simultaneously (Figure 3.3 A). YFP-GPI expression was clearly visible in the fluorescence images. Interestingly, both IRM and fluorescence signals did exactly match allowing us to use YFP-GPI as a marker to measure the extent of cellular spreading in our high-throughput screen.

We next attempted to transfer the established spreading assay from glass coverslips to 96-well glass-bottom plates, as this would be the format used in the siRNA library screen. Plates were coated with anti-human IgM in the same manner as coverslips and Bjab cells expressing YFP-GPI were seeded and left to spread at room temperature for 20 min. Plates were analysed using a 40x magnification objective coupled to the Cellomics ArrayScan fluorescence microscope (Figure 3.3 B). Built-in Cellomics software created an edge-detection mask based on the fluorescence signal and provided a mean value for the size of detected objects (Figure 3.3 C). To compare these data to our results provided by the manual assay using glass coverslips and a confocal microscope (Figure 3.3 A), we quantified the surface area covered by spread cells using YFP-GPI fluorescence and Volocity software. Volocity identified objects based on their fluorescence intensity and provided a value for their size (Figure 3.3 C). When comparing the mean values for surface area covered by Bjab cells for both manual and automatic quantification (Figure 3.3 C), there is no significant difference between manual or automated quantification based on confocal microscopy or the ArrayScan, respectively.

In summary, we have established a BCR-mediated spreading assay using the human cell line Bjab. YFP-GPI was used to detect cell edges and to quantify the surface area covered by spread B cells. The assay worked robustly and across different microscopy platforms enabling us to use it in a high-throughput manner in the context of an siRNA screen.

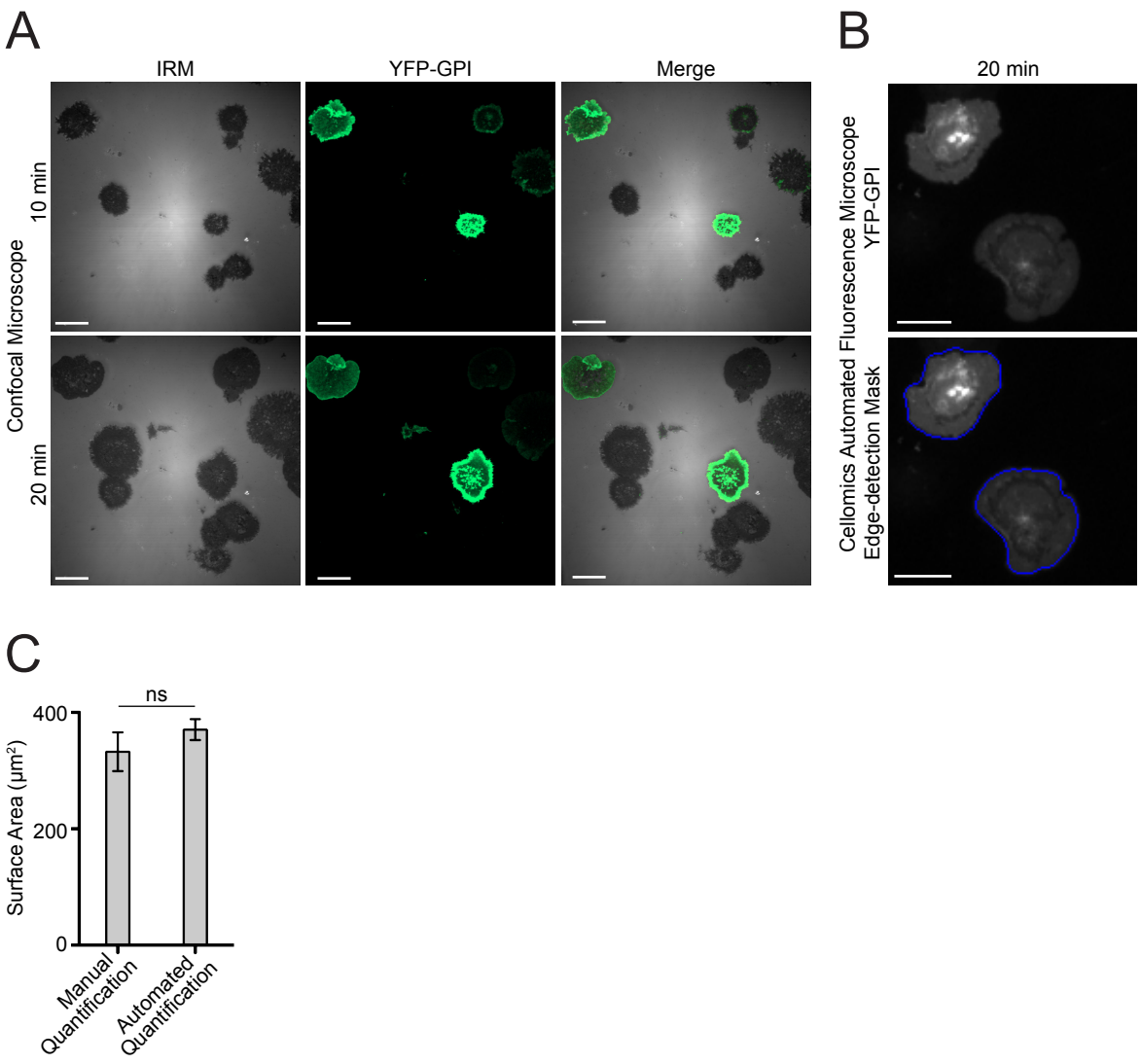

Figure 3.3. Spreading of Bjab YFP-GPI can be measured in an automated manner
(A) Bjab B cells transiently expressing YFP-GPI were settled on glass coverslips coated with 10 µg/ml anti-human IgM and spreading was monitored using Interference Reflection Microscopy (IRM) and confocal microscopy. (B) Bjab B cells transiently expressing YFP-GPI were settled on 96-well glass-bottom plates coated with 10 µg/ml anti-human IgM and spreading was monitored using the Cellomics automated fluorescence microscope. (C) Quantification of surface covered by spread Bjab cells based on fluorescence intensity of YFP-GPI 20 min after settling on anti-BCR coated glass coverslips. Data obtained in A was quantified manually using Volocity software. Images acquired in B were automatically quantified with Cellomics software. Scale bars equal 5 µm.

3.2 Investigating high-throughput transfection of B cells with siRNA

3.2.1 siRNA-induced knockdown of Lamin by chemical transfection of Bjab cells

Having a robust screening assay in place we next sought to explore routes of reliably transfecting Bjab B cells with siRNA. The efficient delivery of siRNA and subsequent knockdown of target proteins is a crucial factor when setting up RNAi-based screens. Transfection methods commonly used in library-sized RNAi screens are based on chemicals such as liposomes or peptides. These transfection reagents bind siRNA and subsequently fuse with the plasma membrane of cells for intracellular delivery.

In collaboration with the high-throughput screening facility we tested 10 different chemical transfection reagents for their ability to downregulate expression of the nuclear envelope protein Lamin. Lamin knockdown is often used as a tool to identify ideal transfection conditions (Chen et al., 2005). Different amounts of transfection reagent were mixed with a RISCfree control siRNA or siRNA targeting Lamin and incubated at room temperature for one hour to allow binding of siRNA to the transfection reagent. Bjab B cells were incubated with the mix for 48 hours and subsequently processed to measure Lamin knockdown. For this purpose, transfected cells were washed, fixed and stained with a fluorescent antibody specific for Lamin. Lamin fluorescence was analysed for each condition on an automated microscope and values for mean fluorescence were plotted to approximate the relative level of knockdown. Figure 3.4. shows the results obtained for a duplicate experiment using the same conditions. The only consistent knockdown (50 – 70 %) of Lamin was seen for siRNA incubated with either Lullaby or LipofectaminePlus (arrows in Figure 3.4.). Interestingly, protein knockdown was inversely proportional to the amount of transfection reagent used. In many cases, however, incubation of B cells with transfection reagents even increased the expression of Lamin when compared to conditions using control siRNA. Most importantly, levels of Lamin-fluorescence in control samples varied significantly among experiments. Given the high variability of Lamin-fluorescence in the controls, we were not confident that Lamin was a good marker to measure protein knockdown in B cells.

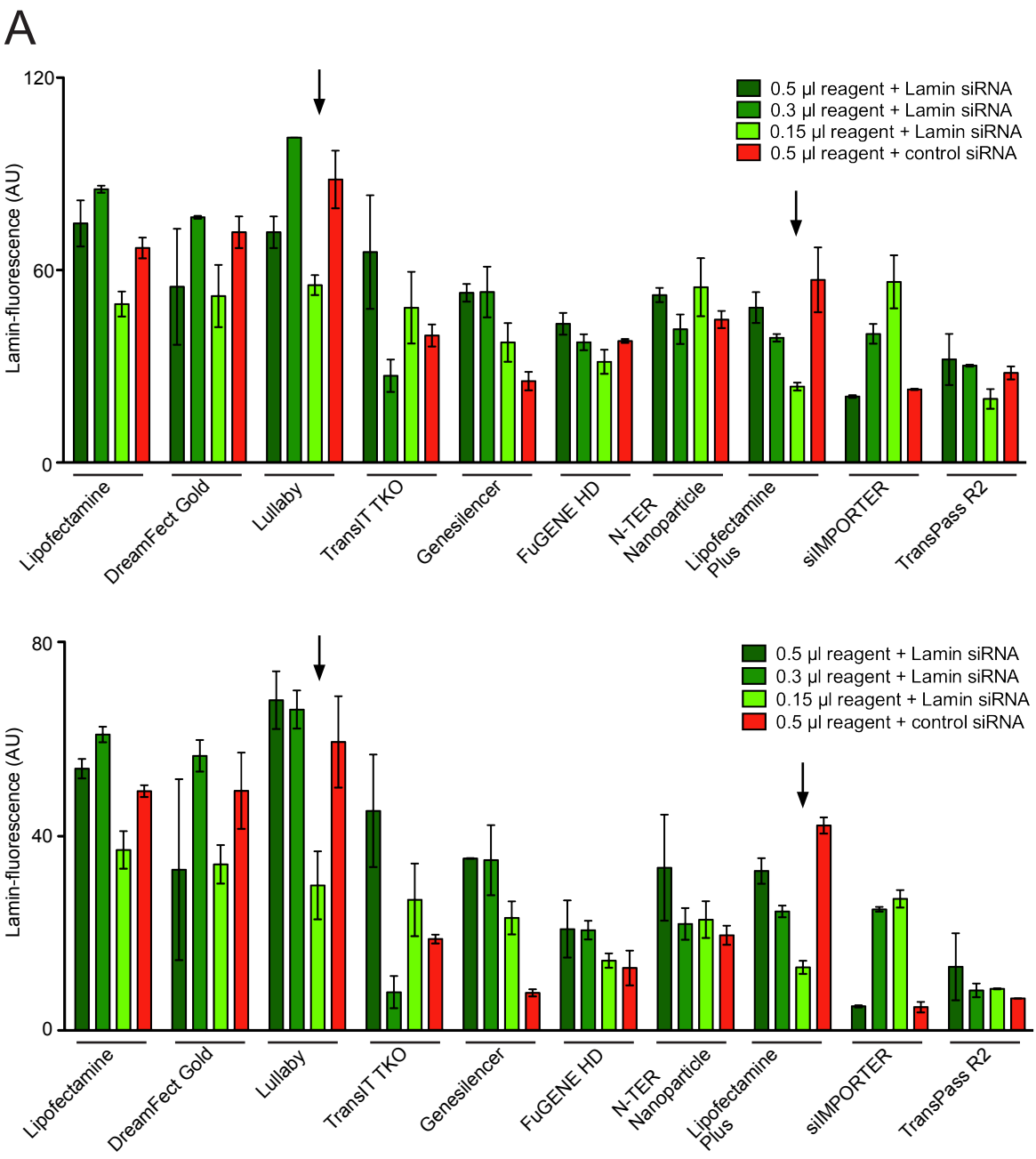

Figure 3.4. Chemical transfection of Bjab cells with siRNA targeting Lamin predominantly yields inconsistent knockdown

(A) Indicated volumes of chemical transfection reagents (x-axis) were pre-incubated in 24-well plates with siRNA targeting Lamin A or with control siRNA. Bjab B cells were added to the mixture and left at 37° C for 48 hours. Lamin A expression was subsequently measured by staining with a Lamin A antibody. Images of cells were acquired using the Cellomics automated fluorescent microscope to obtain values for Lamin A-fluorescence. The top and bottom graphs show Lamin A fluorescence for all conditions as duplicate experiment.

3.2.2 Knockdown of Syk, CD19 and mDia1 in B cells using electroporation

In view of our results with lamin, we looked for an alternative probe to optimise transfection conditions for B cells. In order to find an alternative, we wanted to test the possibility of downregulating expression of BCR-proximal proteins such as the co-receptor CD19 or the kinase Syk. Both CD19 and Syk propagate BCR signalling and it has been shown by our laboratory that cells deficient for either of the two proteins do not spread in response to membrane-bound antigen (Depoil et al., 2008 and Weber et al., 2008). For this reason, cells with significantly lower protein levels of Syk or CD19 could potentially serve as internal controls in a library-sized siRNA screen. In addition, we investigated the possibility to downregulate protein expression of the cytoskeletal regulator mDia1 against which we had a validated siRNA sequence available. mDia1 belongs to the protein family of formins, it is a Rho effector and induces actin polymerisation by interacting with barbed ends of actin filaments (Rose et al., 2005 and Kovar et al., 2006). As B cell spreading heavily depends on actin polymerisation, downregulating mDia1 expression could potentially lead to diminished spreading. To find a more robust and quantitative alternative to measure protein levels, we went on to assess RNAi-mediated knockdown of target proteins using other techniques including flow cytometry and Western blot.

We had previously established that nucleic acids such as DNA plasmids could be delivered into Bjab cells by electroporation. We thus took the same approach to test a potential knockdown of CD19. We electroporated either RISCfree control siRNA or a pool of four siRNA oligos targeting CD19 into Bjab cells using the Amaxa electroporation system. CD19 surface expression was measured 48 hours after transfection by staining with a specific anti-human CD19 antibody. Binding of antibody was analysed using flow cytometry gating on live cells identified by PI staining (Figure 3.5. A). When comparing levels of CD19 surface expression in control and CD19-targeted samples we only found a very mild downregulation of about 10 % (based on mean fluorescence values). This could be due to a long half-life of CD19 on the surface of B cells or insufficient delivery of siRNA by means of electroporation.

In an attempt to measure total protein levels by Western blot, we tested the possibility to downregulate expression of the spleen tyrosine kinase Syk. As for CD19, we electroporated Bjab cells in the presence of different amounts of siRNA targeting Syk or RISCfree control siRNA. Cells were cultured for 24 hours and processed for Western blot measuring total protein levels of Syk. In one condition we subjected Bjab cells to two electroporations with 2 µg of siRNA with a 24-hour incubation between electroporations. Figure 3.5 B summarises our efforts to downregulate expression of Syk kinase. Total amounts of Syk protein largely remained unchanged and only when using high amounts of siRNA (3 µg) or when electroporating twice we were able to downregulate Syk protein levels by 17 % and 16 %, respectively. This indicated an insufficient delivery of siRNA or a low efficiency of this particular pool of siRNA oligos to target Syk mRNA and activate the RNAi pathway.

To rule out problems with efficient activation of RNAi due to oligo sequence, we made use of a siRNA oligo that had successfully been used in the past to downregulate the highly conserved actin regulator mDia1 (Hotulainen et al., 2006). We therefore wanted to investigate the possibility to deliver siRNA targeting mDia1 by electroporation and measure potential downregulation of protein expression by Western blot. For this purpose, Bjab B cells were electroporated as explained above in the presence of 2 µg of siRNA targeting mDia1. Protein levels of mDia1 were measured using Western blot 24, 48 and 72 hours after electroporation (Figure 3.5. C). We obtained significant mDia1 knockdown (>90 %) for all three timepoints, which proved sufficient delivery of siRNA by electroporation and successful induction of RNAi. Based on this result we assumed that both delivery of siRNA *via* electroporation and RNAi-mediated downregulation of mDia1 protein levels could be used with the human B cell line Bjab. We had therefore identified a useful alternative to the previous method measuring Lamin downregulation by immunofluorescence and were equipped with an assay that could be used for the optimisation of transfection of Bjab cells with chemical transfection reagents.

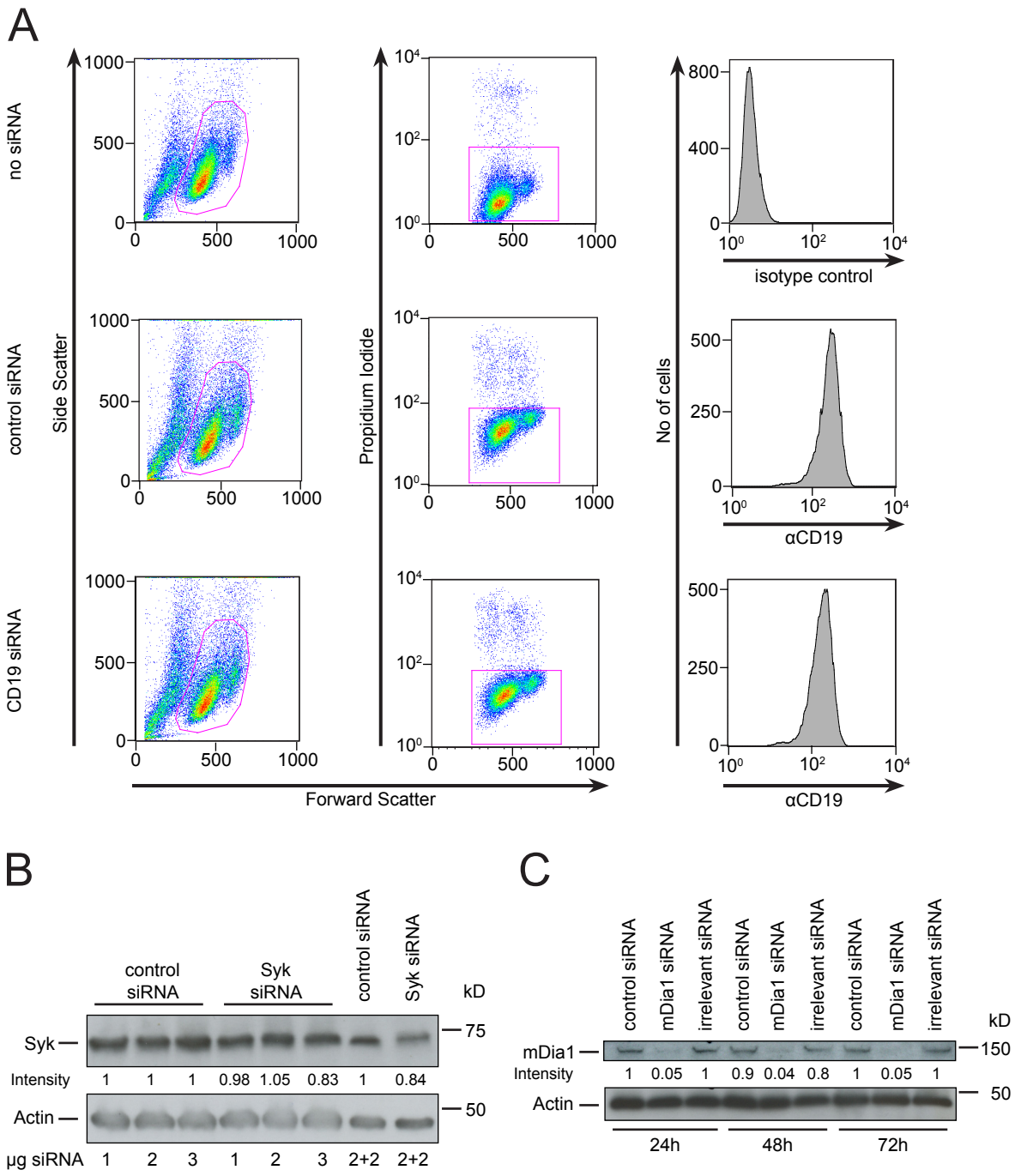

Figure 3.5. Downregulation of proteins in B cells using siRNA delivered by electroporation

(A) Bjab cells were electroporated using the settings obtained as shown in Figure 1.2. in the presence of 2 µg siRNA targeting CD19 or control siRNA. CD19 expression was assessed using flow cytometry. Cells were identified by their scatter profile (left column). Life and dead cells were distinguished using Propidium Iodide which binds to DNA in dead cells (middle column). Control cells were stained with an isotype control and CD19 on siRNA-treated cells was detected using a monoclonal antibody coupled to Alexa488. Alexa488-fluorescence of the living population is shown in histograms (right column). (B) Bjab cells were electroporated as in A using siRNA targeting Syk or control siRNA. Syk expression was assessed 24 hours later by Western blot. Amounts of siRNA used are indicated. In two conditions cells were electroporated with 2 µg of siRNA followed by another electroporation with the same amount 24 hours later (2+2). Syk expression was measured 48 hours after the second electroporation. Actin serves as loading control. Each lane represents a total of 500,000 lysed cells. (C) Bjab cells were electroporated as in A using 2 µg siRNA targeting mDia1, an irrelevant siRNA targeting p34 or control siRNA. mDia1 expression was assessed at indicated timepoints using Western blot. Numbers between blots in B and C indicate the Syk or mDia1 band intensities for siRNA treated cells relative to respective control samples.

3.2.3 Knockdown of mDia1 protein levels in Bjab cells by chemical transfection

Having established significant knockdown of mDia1 using electroporation, we next used the same siRNA oligo in combination with various chemical transfection reagents. We had previously used the same reagents in an attempt to downregulate expression of Lamin (see Figure 3.4.), which did not prove a suitable system to measure RNAi-mediated protein knockdown due to unreliable control samples.

Different amounts of transfection reagents were pre-mixed with siRNA targeting mDia1. Bjab cells were incubated with the mix in complete medium for 48 hours and knockdown of mDia1 was subsequently measured by Western blot (Figure 3.6. A). RISCfree siRNA and equal amounts of total lysate of untreated Bjab cells served as controls. In the case of two out of ten reagents (TransIT TKO and Lipofectamine Plus) a potential knockdown was observed. The results for two reagents (Genesilencer and FuGENE HD) could not be quantified, as control samples on the edge of the gel would not produce bands for mDia1. This was possibly due to problems during protein transfer. To confirm the results obtained in the first experiment using mDia1 siRNA in combination with chemical transfection reagents and to rule out technical problems with protein transfer, we repeated the experiment with the same conditions using the transfection reagents mentioned above (Figure 3.6. B). In summary, no downregulation of mDia1 expression was observed using DreamFect Gold. Furthermore, results obtained for TransIT TKO, TransPass R2 and FuGENE HD were not consistent with the first experiment. Only in the case of Lipofectamine Plus knockdown of mDia1 appeared to be reproducible and ranged from 48 % to 63 %.

In conclusion we have identified mDia1 as a useful probe to measure RNAi-mediated knockdown. We observed lower protein levels of mDia1 following transfection of siRNA with chemical transfection reagents. The level of knockdown was, however, not as substantial as achieved by means of electroporation. Furthermore, the level of knockdown was not sufficient to be used in a high-throughput screen. We therefore looked for other potential methods to deliver siRNA into Bjab B cells.

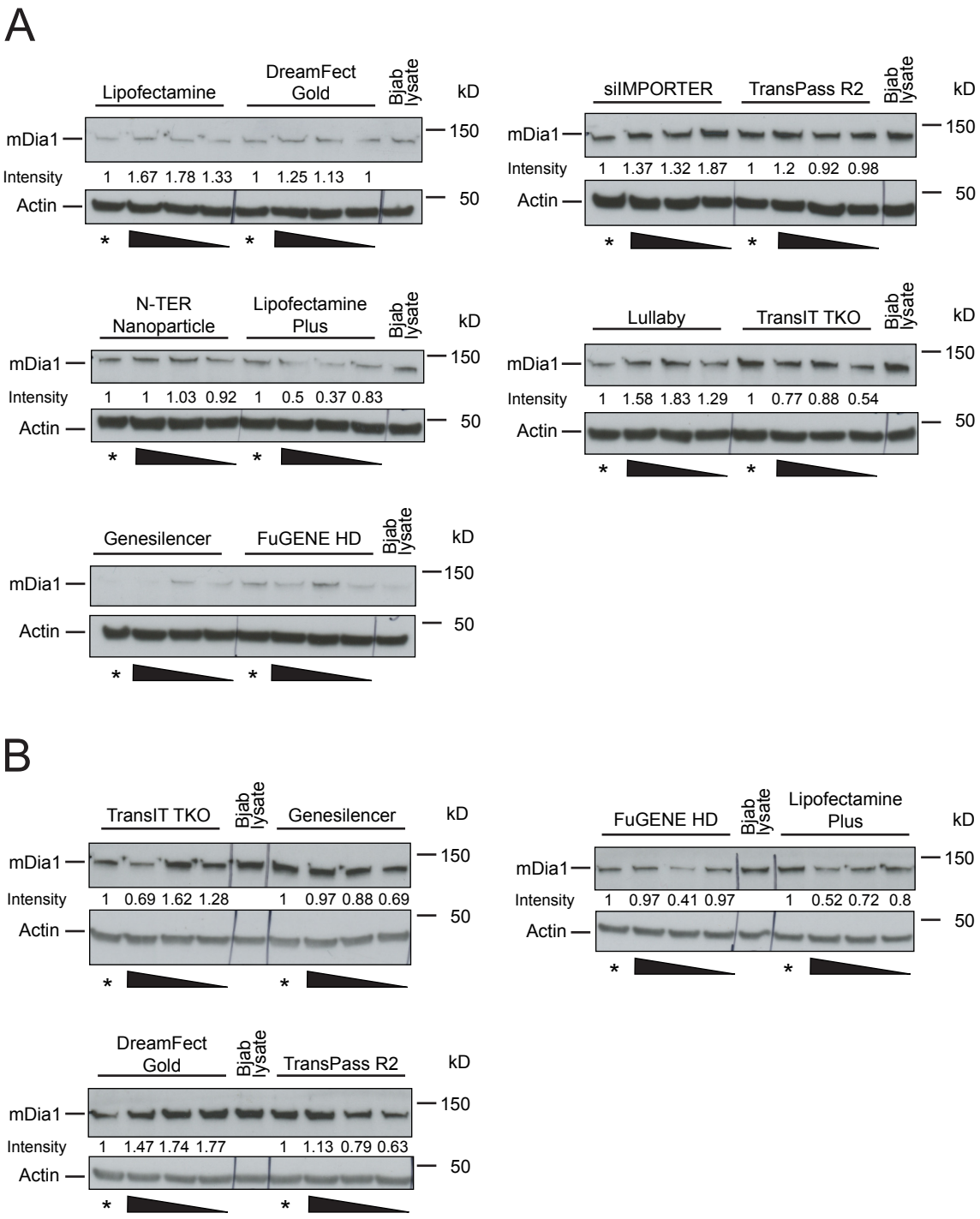

Figure 3.6. Chemical transfection of siRNA targeting mDia1 in Bjab cells leads to inconsistent knockdown

(A) Decreasing volumes (0.5 µl, 0.3 µl, 0.15 µl; triangle symbol in figure) of indicated chemical transfection reagents were pre-incubated in 24-well plates with siRNA targeting mDia1. Control siRNA was pre-incubated with 0.5 µl of transfection reagent (*). Bjab B cells were added to the mixture and left at 37° C for 48 hours. mDia1 expression was subsequently measured by Western blot; each lane represents a total of 200,000 lysed cells. Along siRNA-treated cells lysate of untreated Bjab cells was also loaded on the gel (Bjab lysate). Actin was used as loading control. Numbers between blots indicate mDia1 band intensities for siRNA treated cells relative to respective control samples.

3.2.4 RNAi-mediated targeting of CD19 expression using 'Accell' siRNA

To find an alternative approach for sufficient delivery of siRNA and subsequent knockdown of protein, we made use of a new method called 'Accell'. Special Accell siRNA is delivered into cells by passive transport when cells are cultured in a special serum-low delivery medium and at presence of siRNA at 1 µM. We first adapted Bjab cells to lower concentrations of FCS by gradually diluting the amount of serum when cells were split. Figure 3.7. A shows the dilution of FCS present in the medium as a function of the number of passages. In addition, we also measured cell viability when cells were split and observed that cells died when cultured in conditions containing less than 2.5 % FCS (Figure 3.7. A). This meant that a minimum FCS concentration of 2.5 % in the medium was needed to keep Bjab cells viable. So we chose these conditions for further Bjab cell culture during Accell siRNA delivery.

The Accell system utilises the uptake of modified siRNA oligos by cells from the surrounding culture medium. With Bjab cells previously adapted to low-serum conditions and the special Accell delivery medium, it was consequently possible to culture cells in the presence of siRNA for any desired time. This would be particularly useful to assess the downregulation of proteins with a potentially long half-life. We therefore wanted to investigate, whether the Accell system was capable of downregulating surface expression of the B cell co-receptor CD19. Bjab cells were maintained in optimised culture conditions in the presence of siRNA targeting CD19 for 96 hours. Media was replaced every 48 hours to ensure cell survival and to maintain a high concentration of siRNA present for uptake. Surface expression of CD19 was assessed using flow cytometry (Figure 3.7. B). Levels of CD19 expression for control and siRNA-treated samples can be seen in the right column. Unfortunately, there was no significant downregulation of CD19 expression using Accell siRNA. The slight shift of the histogram for cells incubated with CD19 siRNA represents a change of surface expression of approximately 5 % (based on mean fluorescence values). The Accell system therefore did not appear to be a suitable platform to run a library-sized siRNA screen.

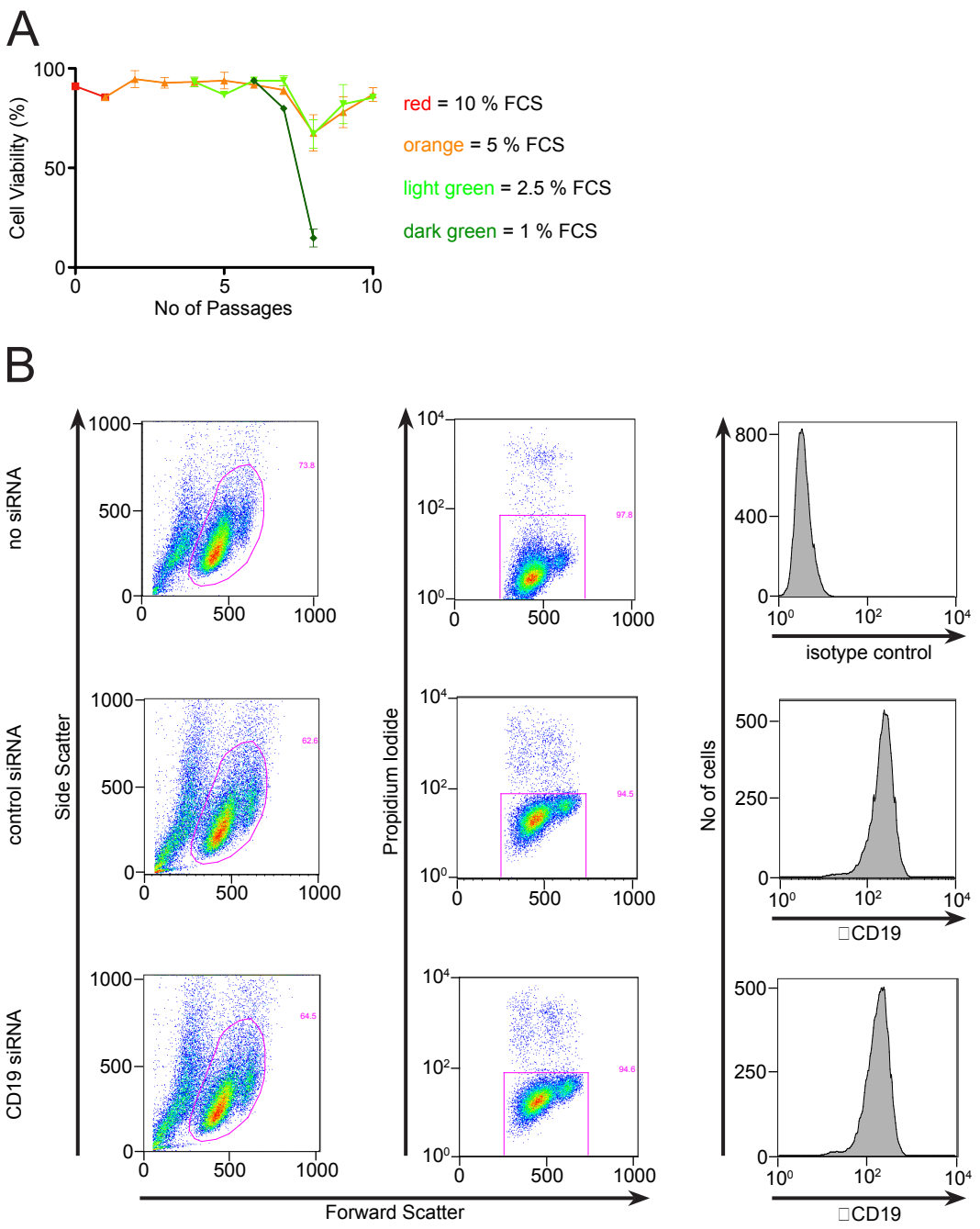

Figure 3.7. Chemical transfection of Bjab cells with 'Accell' siRNA targeting CD19 does not result in reduced surface expression of CD19

(A) Bjab cells were adapted to 'Accell' transfection medium by gradually lowering the concentration of fetal calf serum (FCS). Cell viability was monitored by Tripan Blue staining which binds to DNA of dead cells. The concentration of FCS was reduced when cells were split (red = 10 %, orange = 5 %, light green = 2.5 %, dark green = 1 %). (B) Bjab cells were cultured in 'Accell' transfection medium containing 2.5 % FCS and 1 µM 'Accell' siRNA targeting CD19 or control siRNA for 96 hours. CD19 expression was assessed using flow cytometry. Cells were identified by their scatter profile (left column). Life and dead cells were distinguished using Propidium Iodide which binds to DNA in dead cells (middle column). Control cells were stained with an isotype control and CD19 on siRNA-treated cells was detected using a monoclonal antibody coupled to Alexa488. Alexa488-fluorescence of the living population is shown in histograms (right column).

To sum up our efforts towards siRNA delivery and subsequent protein knockdown in Bjab B cells, we have assessed the RNAi-mediated knockdown of Lamin, CD19, Syk and the cytoskeletal regulator mDia1 by means of immunofluorescence, flow cytometry and Western blot. We have identified mDia1 as a suitable candidate for transfection optimisation as total protein levels and knockdown could reliably be measured using Western blot. However, sufficient levels of mDia1 knockdown were only detected when Bjab cells were transfected with siRNA oligos by electroporation. All other methods tested did not yield a satisfactory downregulation of protein levels suitable for a large-scale siRNA screen.

3.3 Discussion

A successful large-scale high-throughput siRNA screen requires a robust cellular assay and reliable delivery of siRNAs, which leads to efficient knockdown of target proteins. This chapter summarises our efforts made towards a siRNA screen to identify novel regulators of B cell spreading. We have established Bjab cells as a suitable human B cell line for use in a robust spreading assay. The fluorescent membrane probe YFP-GPI expressed by Bjab cells enabled us to develop a BCR-stimulation based spreading assay in 96-well platesthat could be analysed in an automated fashion. The data obtained by automatic quantification was consistent with our previous data generated manually employing glass coverslips and a confocal microscope.

With regards to transfection of Bjab cells with siRNA we considered electroporation, chemical transfection or a method based on passive transport (‘Accell’). In particular, electroporation-induced RNAi targeting mDia1 showed the only significant reduction of protein levels among all our experiments. However, electroporation of cells on a sample-by-sample basis was not feasible for a screen aiming to investigate several thousands of genes. Knockdown of either Lamin or mDia1 using chemical transfection reagents proved to be either

too low or inconsistent. Indeed, most large-scale screens have been carried out using adherent cell lines (Fox et al., 2011; Chong et al., 2011 and Kitchens et al., 2011). Suspension cells such as B cells – or lymphocytes in general – have been regarded as difficult to transfect and the literature describing RNAi in B cells by chemical means is scarce (Heinonen et al., 2002). Possible reasons for this include a tightly regulated uptake of extracellular material possibly due to a particularly rigid cortical cytoskeleton. In addition, immune cells express numerous receptors sensing the presence of foreign nucleic acids such as RNA. They might thus be better equipped to bypass activation of the RNAi pathway.

3.3.1 Future directions

Poor delivery of siRNA oligos into B cells appears to be the limiting factor when setting up large-scale RNAi screens. One opportunity to successfully use siRNA screening approaches in B cells in the future might arise from a novel electroporation apparatus, which works on a 96-well basis. Using this platform one could potentially be able to reach sufficient and reliable knockdown of proteins in a high-throughput manner. Another possibility for efficient RNAi-mediated protein knockdown could be the retroviral transduction of B cells. Recent work has demonstrated that protein knockdown in human B cells can be achieved with an inducible small hairpin RNA (shRNA) system based on viral delivery on a large-scale basis (Davis et al., 2010).

Furthermore, one could elucidate the BCR interactome by affinity purification of activated BCR complexes and subsequent mass spectrometric analysis as has been carried out in T cells (Brockmeyer et al., 2011). This could reveal novel cytoskeletal regulators downstream of the BCR.

A complimentary screening approach to identify novel regulators of the actin cytoskeleton in B cells could be an *in silico* bioinformatics method. By creating a primary list of known cytoskeletal regulators and actin-binding domains one could screen for novel regulators by running a genome-wide domain homology search. Found targets would then have to be verified by confirming their expression in B cells, which could be done using publicly available microarray data.

Chapter 4 : A Complex of Grb2, Dok-3 and Cbl Promotes Antigen Gathering in B Cells

B cells gather antigen on the surface of antigen-presenting cells (APC) by a process, which involves an initial spreading phase and a subsequent contraction response (Fleire et al., 2006). During spreading B cells form discrete signalling-competent antigen-containing BCR microclusters, which recruit signalling molecules such as the kinase Syk or PLCγ2 (Depoil et al., 2008 and Weber et al., 2008). Concomitant with cellular contraction antigen microclusters are gathered in the centre of the contact interface between the B cell and APC (Fleire et al., 2006). For full activation to occur, B cells need to internalise gathered antigen and present it to specific T cells in order to obtain T cell help. Importantly, the amount of antigen presented to T cells is proportional to the extent of B cell spreading and subsequent antigen gathering (Fleire et al., 2006). Gathering of antigen molecules by directed movement and fusion of antigen-containing microclusters for internalisation is thus a crucial step in B cell activation as it dictates the extent of T cell help.

We therefore focussed on the process of antigen gathering and utilised DT40 chicken B cells deficient for key signalling molecules in combination with artificial lipid bilayers mimicking APCs. DT40 B cells constitute a very versatile cellular system as knockout cell lines can be created with relative ease. This is due elevated rates of homologous recombination and the resulting higher probability to successfully insert targeting constructs for exon disruption (Shinohara and Kurosaki, 2006). To investigate the process of B cell antigen gathering by cellular contraction we used planar lipid bilayers as a tool, because antigen tethered to a fluid film is laterally mobile (Brian and McConnell, 1984). In contrast to glass coated with immobile antigen, the system of artificial lipid bilayers thus enabled us to assess the distribution of antigen in a dynamic manner. In addition, fluorescently labelled antigen molecules allowed usto couple this system to different means of fluorescent microscopy. A pre-existing panel of DT40 knockout B cells in combination with lipid bilayers for antigen presentation and

high-resolution microscopy therefore equipped us with a powerful tool to investigate the process of antigen gathering in B cells.

4.1 Grb2, Dok-3 and Cbl control directed antigen microcluster movement for antigen gathering by B cells

4.1.1 B cells require Grb2, Dok-3 and Cbl for antigen gathering by cellular contraction

A previous screen of DT40 knockout B cells in conjunction with lipid bilayers and high-resolution microscopy had concentrated on B cell spreading in response to membrane-bound antigen (Weber et al., 2008). The screen had provided significant insights into how spreading is driven by the BCR and proximal signalling molecules such as Syk, PLCγ2 and Vav. The foregoing work had also produced preliminary information on the importance of two molecules for cellular contraction (M. Weber, PhD thesis submitted to UCL, 2009). Those molecules were the small adaptor protein growth factor receptor-bound protein 2 (Grb2) and a member of the ubiquitin ligation machinery Casitas B cell lymphoma (Cbl). We consequently used the data on DT40 B cells deficient for Grb2 and Cbl as a starting point to investigate the mechanisms of antigen gathering in B cells.

We assessed cell spreading and contraction by settling wildtype DT40 B cells on lipid bilayers containing an anti-chicken IgM antibody (clone M1) as surrogate antigen (Figure 4.1. A). To visualise their response to membrane antigen we monitored the contact area between glass coverslip and cell using IRM. The fluorescent bilayer was imaged by acquisition of one confocal slice in the same focal plane as the IRM image. Cells made contact with the lipid bilayer shortly after seeding and spreading could be observed in the IRM images over the course of five minutes. During spreading fluorescent antigen molecules present in the lipid bilayer were clustered by the B cells and could be visualised using the fluorescence image. Once maximum spread was reached, cells started to contract and showed a small area of tight adhesion 15 minutes after seeding on the lipid

bilayer. Simultaneous with cellular contraction, clustered antigen molecules were gathered in a single central cluster (Figure 4.1. A). We next settled DT40 B cells deficient for either Grb2 or Cbl on antigen-loaded bilayers in the same manner as wildtype cells (Figure 4.1. B and C). Indeed, both Grb2- and Cbl-deficient cells spread and clustered antigen comparable to wildtype cells. In contrast, Grb2 and Cbl knockout B cells did not exhibit a contraction phase and did not gather antigen molecules in a central cluster over time.

We wanted to extent our knowledge of important molecules involved in B cell antigen gathering and consequently focussed on the adaptor downstream of kinase-3 (Dok-3), which has been shown to directly interact with Grb2 in the context of BCR signalling (Stork et al., 2007). We assessed the behaviour of DT40 B cells lacking Dok-3 when settled on antigen-bearing lipid bilayers. Interestingly, *Dok3*$^{-/-}$ cells resembled the results obtained for *Grb2*$^{-/-}$ and *Cbl*$^{-/-}$ cells: The extent of spreading and initial antigen clustering appeared similar to wildtype cells, whereas cellular contraction and antigen gathering were impaired (Figure 4.1. D).

We quantified the contact area between cells and the lipid bilayer by measuring the size of the IRM image for each cell over time. All cell types covered approximately 75 μm^2 per cell when fully spread (Figure 4.1. E). In the case of wildtype cells this value decreased to 43 μm^2 upon completion of contraction. In stark contrast, the contact area of cells lacking Grb2, Dok-3 or Cbl did not decrease showing a significant difference to wildtype cells. We also quantified the extent of antigen gathering by all cell types used in this assay. For this purpose, we defined the contact area between cells and antigen-containing lipid bilayer based on the IRM image and measured the total fluorescence of antigen molecules within this area (Figure 4.1. F). The value of total fluorescence thus directly correlates with the amount of antigen gathered by the cells. Fluorescence values for wildtype B cells increased over time and reached a plateau at 46 x 10^4 fluorescence units. Despite of being able to gather antigen over time, the maximum fluorescence values obtained for Grb2, Dok-3 or Cbl knockout cells were approximately 40 % lower compared to wildtype.

Our experiments thereby confirmed a crucial role for Grb2, Cbl and the adaptor Dok-3 in antigen gathering by B cells in response to membrane-bound antigen.

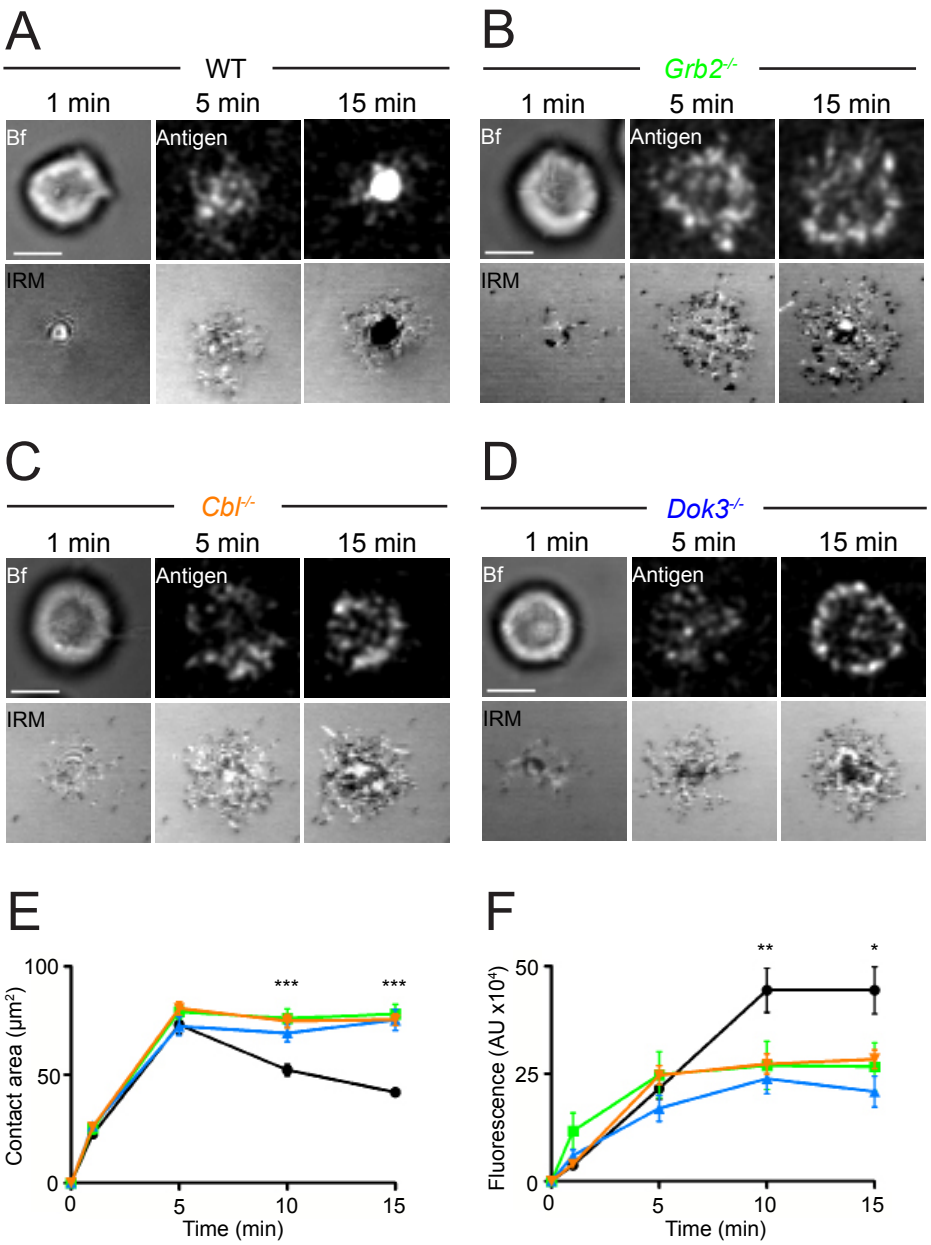

Figure 4.1. Grb2, Dok-3 and Cbl play a role in B cell contraction and antigen gathering
(A) DT40 wildtype (WT) B cells were settled on planar lipid bilayers containing fluorescently labelled anti-chicken IgM as surrogate antigen. The brightfield (bf) image was used to identify cells and antigen was visualised by confocal microscopy. In parallel, the contact area between cells and bilayer was monitored utilising interference reflection microscopy (IRM). (B-D) DT40 B cells lacking Grb2, Dok-3 or Cbl were settled on antigen-bearing bilayers and imaged as in A. (E) Quantification of the contact area between cells and lipid bilayers using IRM over time as shown in A-D (wildtype, black circles; *Grb2*$^{-/-}$, green squares; *Dok3*$^{-/-}$, blue triangles; *Cbl*$^{-/-}$, orange triangles). For each condition a minimum of 25 cells acquired in at least 3 independent experiments were examined. (F) Quantification of antigen gathered expressed as arbitraty fluorescence units (AU) using confocal microscopy as shown in A-D (labelling and number of cells quantified as in E). Statistical analysis was carried out using t-test; ***$p < 0.0001$; **$p < 0.005$; *$p < 0.02$. All scale bars equal 5 μm.

4.1.2 Directed antigen microcluster movement is impaired in B cells lacking Grb2, Dok-3 or Cbl

We wanted to study the process of antigen gathering in B cells by directed movement of antigen microclusters in greater detail. However, the resolution of standard confocal microscopy is not sufficient to visualise antigen microclusters on a sub-micrometre scale. We therefore employed Total Internal Reflection Fluorescence (TIRF) microscopy in combination with antigen-containing lipid bilayers. TIRF increases the effective resolution utilising reflected laser light and the generation of an evanescent wave front (see Methods). This provided us with a tool to image antigen-containing microclusters at significantly greater spatiotemporal resolution.

We settled either wildtype DT40 B cells or cells lacking Grb2, Cbl or Dok-3 on antigen-loaded lipid bilayers and took snapshots using TIRF microscopy when cells were fully spread (5 min). In addition we acquired TIRF images of the lipid bilayer after completion of cellular contraction (15 min, Figure 4.2. A). We observed that all cell types formed antigen-containing BCR microclusters when fully spread. By using a particle detector plugin for ImageJ software we counted the number of antigen microclusters formed by each cell. Comparing wildtype cells to DT40 cells lacking Grb2, Dok-3 or Cbl, the total number of microclusters per cell was not significantly different (Figure 4.2. B). As cell spreading had been shown to be similar among all cell types tested (Figure 4.1. E), this confirmed the model that the number of microclusters directly correlates with the extent of spreading and that Grb2, Dok-3 and Cbl were dispensable for microcluster formation on an antigen-presenting surface.

15 minutes after settling on lipid bilayers only wildtype cells displayed a single large cluster of antigen, whereas microclusters remained in the periphery in *Grb2*$^{-/-}$, *Dok3*$^{-/-}$ and *Cbl*$^{-/-}$ cells (Figure 4.1.). This suggested a defect in microcluster movement towards the central area in B cells lacking Grb2, Dok-3 or Cbl. We consequently investigated antigen microcluster movement by acquiring TIRF image sequences upon completion of spreading five minutes after settling on the lipid bilayer (see Supplementary Video 2). Microclusters were tracked using a tracking algorithm and tracks were represented as vectors pointing in the direction

of movement (Figure 4.2. C). In wildtype cells it was evident that most vectors were directed towards the centre of the contact area between the lipid bilayer and wildtype cells. In contrast, in *Grb2*$^{-/-}$, *Dok3*$^{-/-}$ and *Cbl*$^{-/-}$ cells vectors appeared generally shorter and often pointed in random directions. To quantify that directed movement of antigen microclusters was impaired in B cells lacking Grb2, Dok-3 or Cbl, we developed a method to quantify the movement of microclusters. We used the recorded image sequences and defined a cell centroid based on the initial distribution of antigen microclusters in the first frame. Subsequently the mean net movement of microclusters towards this centroid was measured over all frames of the image sequence (see Methods). This analysis showed a significant difference in directed microcluster movement between wildtype B cells and DT40 cells lacking Grb2, Dok-3 or Cbl (Figure 4.2. D).

In summary, we have demonstrated that the adaptors Grb2 and Dok-3 and the ubiquitin ligase Cbl play a crucial role in antigen gathering by B cells. Although B cell spreading and microcluster formation was not altered in knockout cells, the directed movement towards the central cluster was significantly impaired.

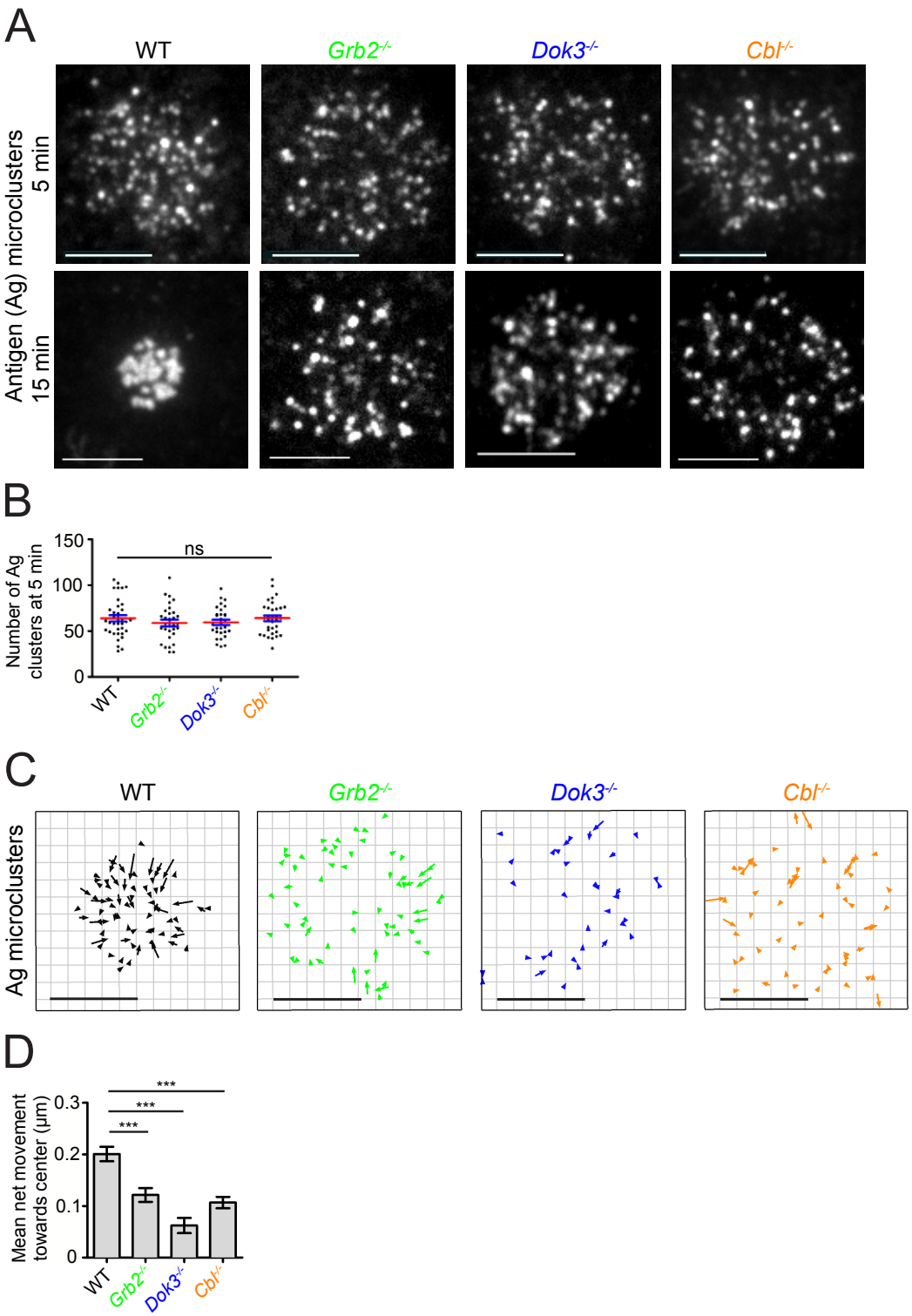

Figure 4.2. Grb2, Dok-3 and Cbl participate in the movement of antigen-containing BCR microclusters

(A) DT40 B cells were settled on planar lipid bilayers containing fluorescently labelled anti-chicken IgM as surrogate antigen. Total Internal Reflection Fluorescence (TIRF) microscopy was used to visualise antigen microclusters. Representative TIRF images showing DT40 wildtype, *Grb2*$^{-/-}$, *Dok3*$^{-/-}$ or *Cbl*$^{-/-}$ five and fifteen minutes after settling on antigen-containing bilayers. (B) Quantification of the number of antigen microclusters formed at maximum spread. Each datapoint represents one cell analysed. Red lines indicate the mean ± SEM (blue). (C) Vectorial representation of antigen microcluster movement over the course of one minute on lipid bilayers in the four different DT40 cell types. (D) Quantification of the mean net movement of antigen microclusters towards the centre of the cell over one minute. Data shown represents a minimum of 350 microcluster tracks obtained from at least 10 cells in two independent experiments. Statistical analysis was carried out using t-test; ***$p < 0.0001$. All scale bars equal 5 µm.

4.2 Grb2, Dok-3 and Cbl act in a complex recruited to antigen-containing BCR microclusters

We had previously shown that DT40 B cells lacking Grb2, Dok-3 or Cbl all showed impaired movement of antigen-containing BCR microclusters and concomitant antigen gathering. We were consequently interested, whether this phenotype was due to a mechanism involving Grb2, Dok-3 and Cbl functioning at signalling BCR microclusters.

Grb2, Dok-3 and Cbl have all been reported to play a role in BCR signalling. In particular, Grb2 has been shown to be recruited to the plasma membrane after BCR ligation by a process involving the adaptor protein NTAL (Stork et al., 2004). Another mechanism of Grb2 recruitment might involve an interaction with the kinase Lyn as Grb2 has been reported to bind the adaptor hemopoietic specific protein 1 (HS1) that in turn associates with Lyn (Takemoto et al., 1998). HS1 could therefore constitute a link between Lyn and Grb2.

Dok-3 has been shown to accumulate at the plasma membrane in response to BCR triggering and is thought to interact with Grb2 in a direct fashion (Stork et al., 2007). Its T cell homologues Dok-1 and Dok-2 have furthermore been reported as part of a complex consisting of Grb2 and the lipid phosphatase SHIP, which is recruited to the signalling TCR (Dong et al., 2006).

Cbl has been implicated to play a role downstream of the signalling BCR as it directly binds Syk kinase at Y323 *via* its PTB domain (Lupher et al., 1998). Other biochemical evidence suggested the activation of Cbl through phosphorylation by Syk and the kinase Fyn (Deckert et al., 1998). In T cells, Cbl was found to colocalise with CD3 upon TCR ligation (Wiedemann et al., 2005). Cbl furthermore colocalised and moved with LAT microclusters in activated T cells as shown by TIRF microscopy (Balagopalan et al., 2007).

While informative, previous investigations provided little insight into the role and sub-cellular localisation of Grb2, Dok-3 or Cbl following stimulation with membrane-bound antigen as occurs *in vivo* (Batista and Harwood, 2009). We therefore used the DT40 system coupled to antigen-loaded lipid bilayers and

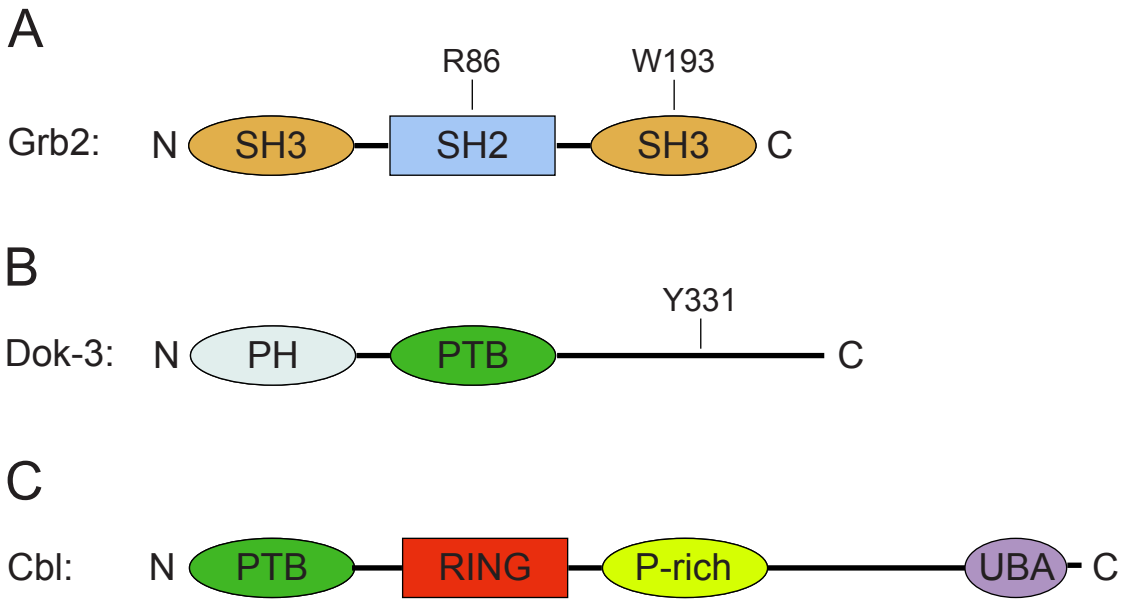

Figure 4.3. Schematic representing the domain structure of Grb2, Dok-3 and Cbl
(A) Schematic of Grb2 consisting of a central Src Homology 2 (SH2) and two flanking Src Homology 3 (SH3) domains. By mutating resiudes R86 or W193 to Lysine (K) the SH2 and C-terminal SH3 domain, respectively, can be rendered inactive. (B) Schematic of Dok-3 including Pleckstrin Homology (PH) and Phosphotyrosine-binding (PTB) domain. Y331 constitutes the binding site for the cental SH2 domain of Grb2 when phosphorylated. (C) Schematic of Ubiquitin ligase Cbl containing PTB, Really Interesting New Gene (RING) domain, Proline-rich (P-rich) region and Ubiquitin-associated (UBA) domain. The Proline-rich region constitutes a binding site for the N-terminal SH3 domain of Grb2.

high-resolution microscopy to investigate the dynamic localisation of Grb2, Dok-3 and Cbl upon BCR ligation in a spatiotemporally resolved manner. Figure 4.3. shows a schematic of structural features found in Grb2, Dok-3 and Cbl to help illustrate their possible interactions with other proteins.

4.2.1 Grb2, Dok-3 and Cbl are recruited to antigen microclusters

To assess the dynamic localisation of Grb2, Dok-3 and Cbl upon BCR ligation, we sought to investigate if all three mediators were recruited to antigen-containing BCR microclusters. For this purpose we stably expressed fluorescently tagged versions of Grb2, Dok-3 and Cbl in the respective DT40 knockout cell lines. Cells were settled on antigen-loaded lipid bilayers and images were acquired when cells were fully spread (5 min) using TIRF microscopy. We observed clustering of Grb2-GFP, Dok-3-GFP and Cbl-YFP in response to BCR stimulation by membrane-bound antigen (Figure 4.4. A to C). Importantly, these clusters colocalised with antigen microclusters as shown by scanning fluorescence intensities for both channels along randomly placed lines (right panels in Figure 4.4. A to C). Interestingly, clusters of Grb2-GFP only appeared at antigen microclusters, whereas Dok-3-GFP and Cbl-YFP were also visible at the plasma membrane outside of antigen clusters. In the case of Dok-3 this can be explained by the presence of its N-terminal PH domain allowing Dok-3 to bind to phosphorylated membrane lipids. It is important to note that expression of Grb2, Dok-3 or Cbl in the respective knockout background restored cellular contraction and antigen gathering (see Supplementary Video3).

To quantify the recruitment of Grb2, Dok-3 and Cbl to antigen-containing BCR microclusters, we carried out a colocalisation analysis using Manders coefficients (see Methods). Briefly, this method allowed us to quantify colocalisation of GFP/YFP with antigen and *vice versa*. We found that colocalisation of antigen with Grb2-GFP and Grb2-GFP with antigen was above 90 %, confirming our previous observation of Grb2 clustering at sites of antigen microclusters (Figure 4.4. D). A similar level of colocalisation was also observed for antigen with Dok-3-GFP. Colocalisation of antigen with Cbl-YFP was observed to be lower (73 %). However, values dropped to about 50 % when analysing colocalisation of Dok-3

and Cbl with antigen. This hinted at the higher abundance of Dok-3 and Cbl at the plasma membrane as the background signal in the GFP channel was less likely to overlap with the fluorescence signal generated by discrete antigen microclusters.

Hence, we have established recruitment of Grb2, Dok-3 and Cbl to the antigen-containing microcluster, implying a conjoint role downstream of the signalling BCR driving antigen gathering.

4.2.2 Grb2 and Dok-3 act in a complex with Cbl in activated B cells

The similar phenotypes of B cells deficient for Grb2, Dok-3 and Cbl regarding their role in antigen gathering and the recruitment to antigen microclusters raised the question, whether these proteins interacted at the signalling microcluster as part of a complex. To test this hypothesis, we immunoprecipitated Grb2-GFP from activated B cells using its GFP-tag with DT40*Grb2*$^{-/-}$ cells serving as control. We examined the presence of Cbl in Grb2 immunoprecipitates by Western blot and found a significant enrichment (Figure 4.4. E). We conducted the same experiment immunoprecipitating Dok-3-GFP from activated B cells and were able to co-purify Cbl (Figure 4.4. F). However, the enrichment of Cbl in Dok-3 immunoprecipitates was significantly lower compared to the co-purification with Grb2. This indicated that the interaction of Grb2 and Cbl was tighter compared to the interaction of Dok-3 and Cbl. Our findings of a strong binding of Grb2 to Cbl is in line with previous work in other cell types, which had also shown constitutive binding of the two proteins (Huang et al., 2000 and Chu et al., 1998).

Our experiments consequently support the hypothesis that Grb2, Dok-3 and Cbl are part of a functional complex at the signalling BCR microcluster.

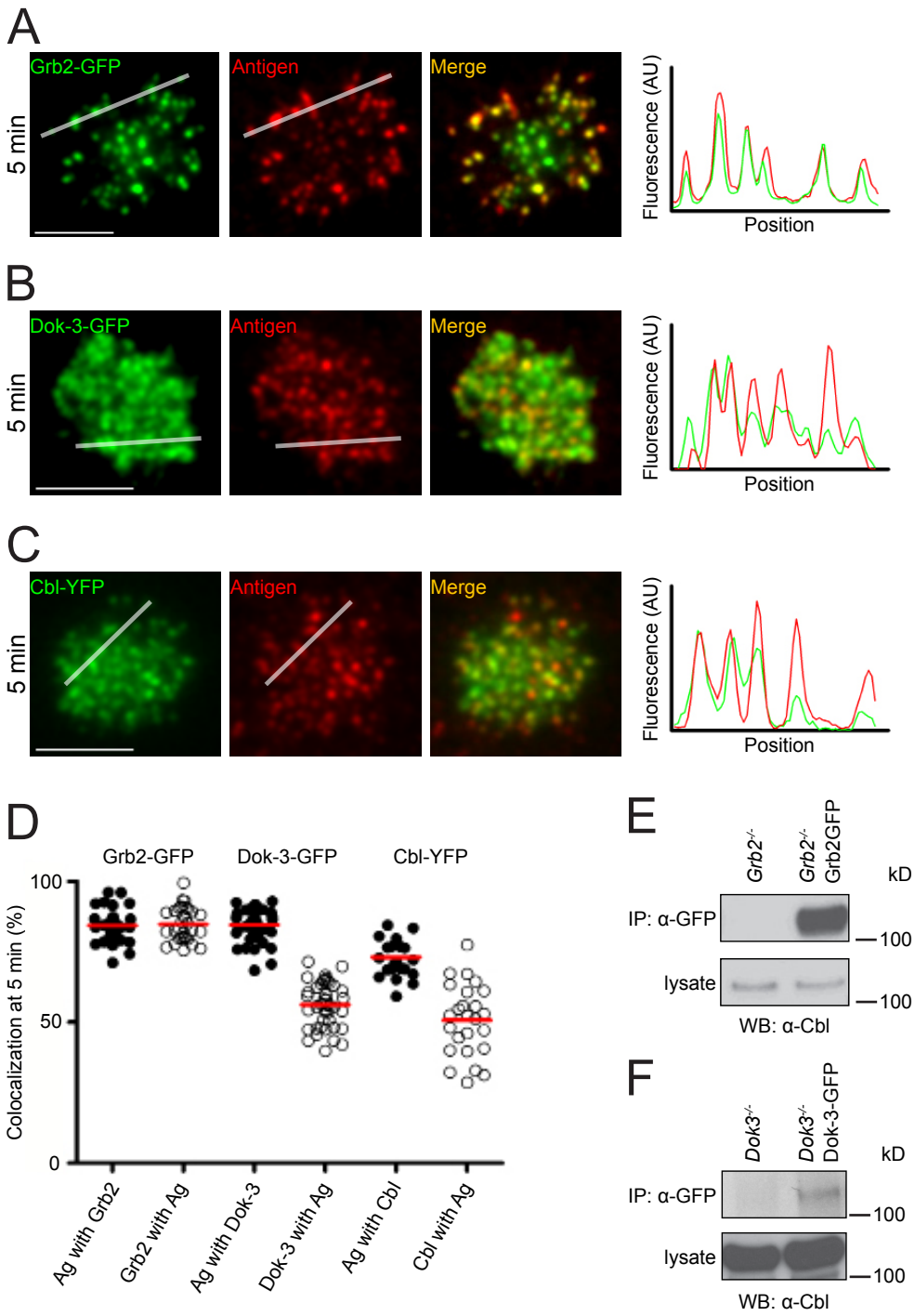

Figure 4.4. Grb2, Dok-3 and Cbl act in a complex recruited to antigen-containing BCR microclusters

(A) DT40 B cells stably expressing Grb2-GFP on a *Grb2*$^{-/-}$ background were settled on lipid bilayers containing surrogate antigen (Ag) and imaged using TIRF. Snapshots were taken at maximum spread five minutes after settling on the bilayer. To visualise colocalisation of Grb2-GFP with antigen, fluorescence was measured along translucent lines and plotted as can be seen in right panels. (B-C) Experimental setup and quantifications as in A were used to show localisation of Cbl-YFP and Dok-3-GFP in respect to antigen. All scale bars equal 5 µm. (D) Colocalisation analysis of Grb2-GFP, Cbl-YFP and Dok-3-GFP in respect to antigen microclusters (filled circles) and *vice versa* (empty circles) five minutes after settling on bilayers. One datapoint represents one cell; data was pooled from at least three independent experiments. Red lines indicate the mean. (E) Grb2 was immunoprecipitated from activated cells using an anti-GFP antibody (see Methods). Cbl was detected in immunoprecipitates with a monoclonal antibody. DT40*Grb2*$^{-/-}$ cells served as control; endogeneous expression of Cbl is shown in cell lysates (lower panels, lysate). (F) The experimental setup of E was used to immunoprecipitate Dok-3-GFP from activated B cells. Cbl was detected in Dok-3 immunoprecipitates and endogeneous expression is shown in lower panels (lysate). DT40*Dok3*$^{-/-}$ cells were used as control.

4.2.3 Stable expression of Grb2, Dok-3 and Cbl in respective knockout B cells rescues antigen microcluster movement

We had shown that Grb2, Dok-3 and Cbl mediate antigen gathering in B cells by directed movement of antigen-containing BCR microclusters. In addition we had observed recruitment of Grb2, Dok-3 and Cbl to the signalling BCR microcluster. It was thus important to assess, whether recruitment of fluorescently-tagged Grb2, Dok-3 or Cbl could rescue impaired antigen microcluster movement when expressed in the respective knockout B cell line.

We sought to address this question by stably expressing Grb2-GFP, Dok-3-GFP or Cbl-YFP in DT40 cells lacking the respective protein. We settled the reconstituted knockout B cells on antigen-loaded lipid bilayers and took snapshots of cells fifteen minutes after settling on the lipid bilayer using TIRF microscopy. This time point was chosen as our previous observations had identified that DT40 cells had fully contracted and antigen gathered within 15 minutes (Figure 4.1). We noticed that DT40*Grb2*$^{-/-}$, *Dok3*$^{-/-}$ or *Cbl*$^{-/-}$ cells reconstituted with the respective fluorescently-tagged protein all showed a large central cluster of antigen molecules in the centre of the contact site between cells and the lipid bilayer (Figure 4.5. A to C). This was likely a result of directed movement of antigen microclusters comparable to the process seen in wildtype cells (Supplementary Video 3). We furthermore observed Grb2-GFP and Cbl-YFP colocalising with both the central cluster of antigen and remaining peripheral antigen microclusters (Figure 4.5. A and C). In contrast, Dok-3-GFP did not colocalise with the central antigen cluster and was effectively excluded from that area (Figure 4.5. B). This finding indicated a spatiotemporally distinct localisation of Dok-3 compared to Grb2 and Cbl. Given our previous immunoprecipitation experiments (Figure 4.4.) this backed the notion that the interaction between Grb2 and Cbl was possibly stronger.

Taken together we have shown that Grb2, Dok-3 and Cbl mediate antigen gathering in B cells by directed movement of antigen microclusters. Grb2, Dok-3 and Cbl appear to act in a complex at antigen-containing signalling BCR microclusters. This recruitment is necessary and sufficient to rescue the phenotype of impaired antigen microcluster movement in cells lacking Grb2, Dok-3 or Cbl.

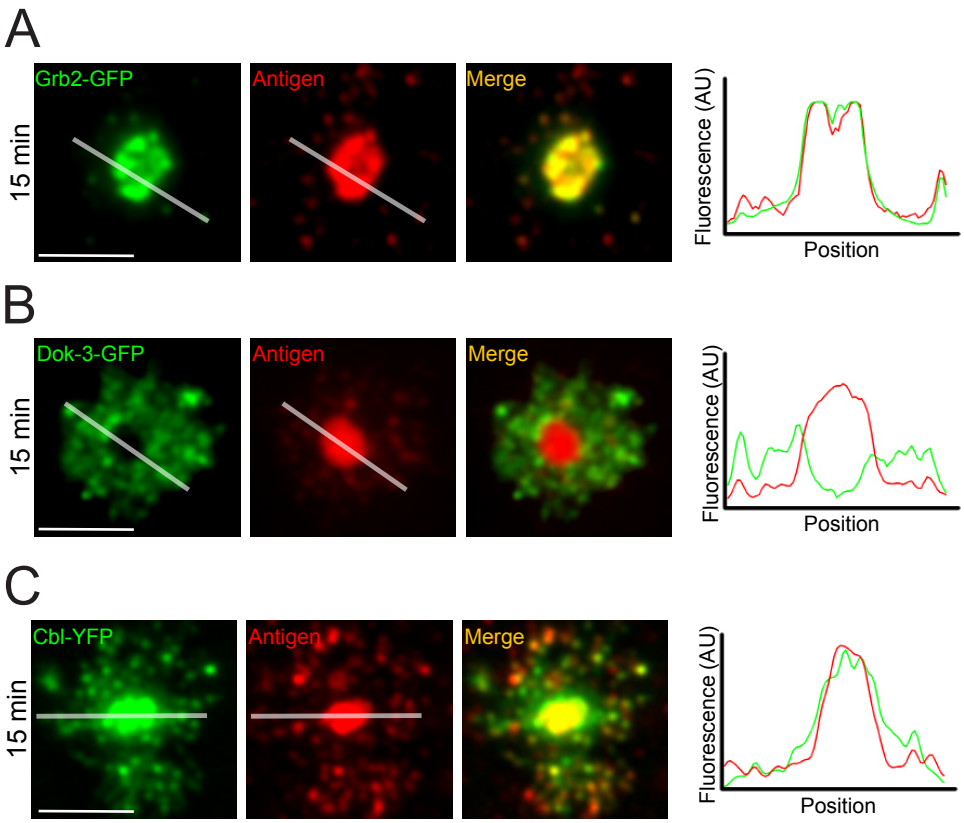

Figure 4.5. Expression of Grb2, Dok-3 and Cbl in the respective knockout B cell line rescues impaired antigen gathering in B cells

(A) DT40 B cells stably expressing Grb2-GFP on a *Grb2*$^{-/-}$ background were settled on lipid bilayers containing surrogate antigen and imaged using TIRF. Snapshots were taken fifteen minutes after settling on the bilayer. To visualise colocalisation of Grb2-GFP with antigen, fluorescence was measured along translucent lines and plotted as can be seen in right panels. (B-C) Experimental setup and quantifications as in A were used to show localisation of Cbl-YFP and Dok-3-GFP in respect to antigen fifteen minutes after settling on the lipid bilayer. All scale bars equal 5 µm.

4.3 Grb2 is a crucial BCR-proximal adaptor regulating intracellular signalling

Having established that Grb2, Dok-3 and Cbl act in a complex, which is recruited to antigen-containing BCR microclusters, we wanted to take advantage of the DT40 system as a genetic tool to further elucidate the molecular requirements for the recruitment of this complex. By combining this genetic approach with artificial lipid bilayers as antigen-presenting surfaces and high-resolution microscopy we were equipped with a powerful experimental setup to further our understanding of early signalling events in B cells.

4.3.1 Grb2 mediates the recruitment of Dok-3 and Cbl to antigen microclusters

In order to investigate the role of Grb2 in the recruitment of Dok-3 and Cbl to antigen-containing BCR microclusters, we expressed Dok-3-GFP or Cbl-YFP in B cells lacking Grb2. Cells were settled on lipid bilayers containing surrogate antigen and snapshots of cells were acquired when fully spread using TIRF microscopy (Figure 4.6. A and B). In case of Dok-3-GFP we observed cluster formation. However, the overall abundance of Dok-3 at the plasma membrane appeared lower compared to cells expressing Grb2 (Figure 4.4. B). Also, when scanning fluorescence for both GFP and antigen channels along a line, we noticed that clusters of Dok-3-GFP did not colocalise with antigen microclusters (right panel in Figure 4.6. A). To quantify our results, we measured colocalisation for Dok-3-GFP with antigen microclusters using the Manders method as before. We compared DT40 wildtype and *Grb2*$^{-/-}$ cells overexpressing Dok-3 and obtained a significant reduction in colocalisation with antigen microclusters (Figure 4.6. A, lower panel). This result indicated that Grb2 was important for recruitment of Dok-3 to antigen-containing microclusters. The formation of Dok-3 clusters can be explained by its PH domain binding to membrane lipids phosphorylated in response to BCR stimulation. These phospholipids can cluster in lipid microdomains and could thus allow the formation of Dok-3 clusters (Gupta et al., 2003). Nevertheless, Grb2 was important for colocalisation of Dok-

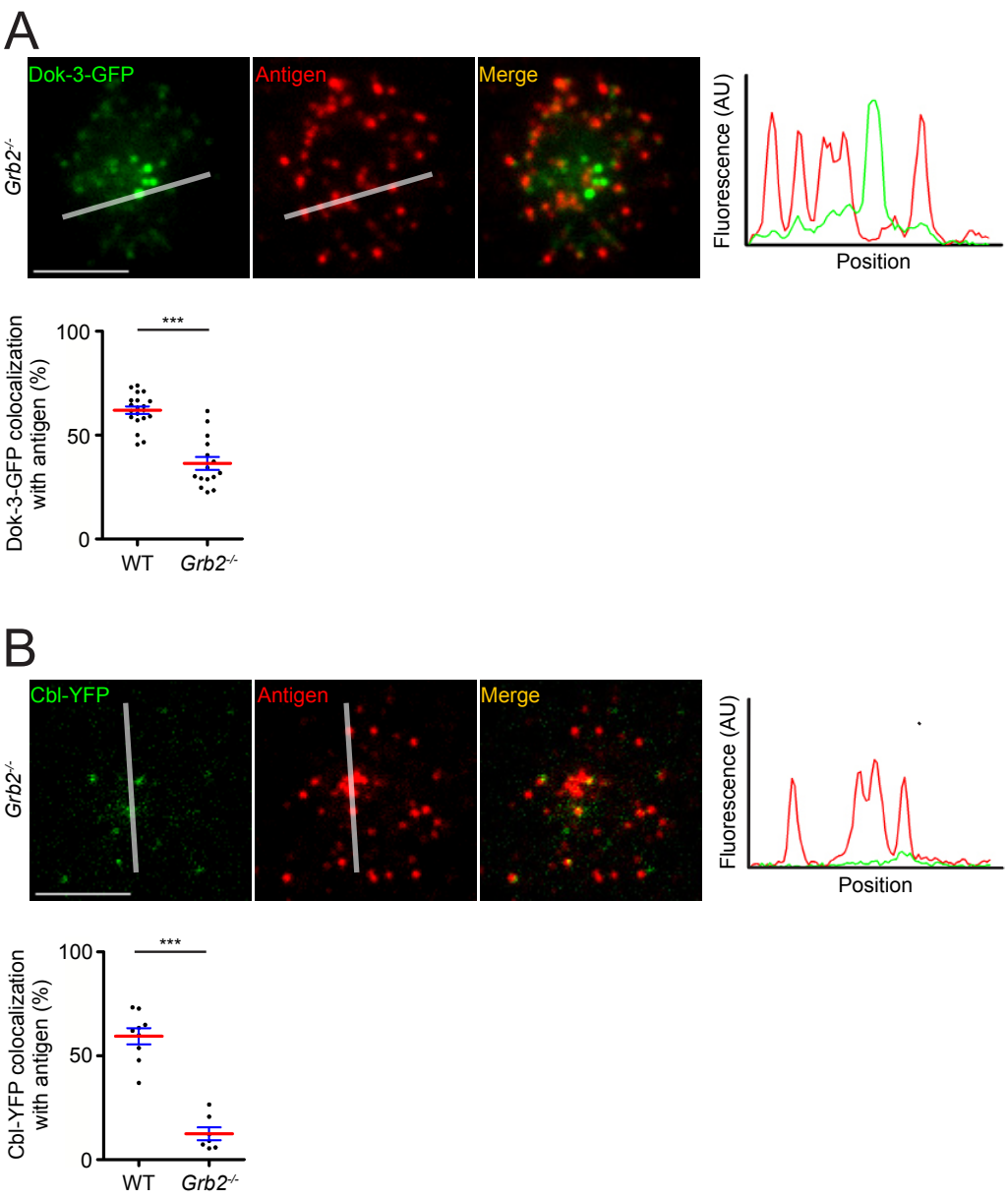

Figure 4.6. Dok-3 and Cbl recruitment to antigen-containing BCR microclusters is dependent on Grb2

(A) DT40*Grb2*$^{-/-}$ cells expressing Dok-3-GFP were settled on antigen-containing lipid bilayers and snapshots were acquired using TIRF microscopy five minutes after settling. Dok-3-GFP and antigen fluorescence was analysed along the translucent line and plotted in the right panel. The lower panel shows the quantification for co-localisation of Dok-3 with antigen microclusters either in a wildtype (WT) or *Grb2*$^{-/-}$ background. Red lines indicate the mean ± SEM (blue). (B) The experimental setup of A was used to image DT40*Grb2*$^{-/-}$ cells expressing Cbl-YFP. The same analysis as A was used to measure the co-localisation of Cbl with antigen microclusters both in wildtype and *Grb2*$^{-/-}$ cells. Statistical analysis was carried out using t-test; ***$p < 0.0001$. All scale bars equal 5 µm.

3 with antigen-containing BCR microclusters and might therefore act as an important linker between the BCR signalling complex and Dok-3.

When analysing the localisation of Cbl-YFP in B cells deficient for Grb2, we found very few and diffuse clusters of Cbl (Figure 4.6. B). This was in contrast to our previous observation in wildtype cells, which showed formation of Cbl clusters colocalising with antigen-containing microclusters (Figure 4.4.). We quantified colocalisation of Cbl-YFP and antigen microclusters as above by comparing DT40 wildtype and *Grb2*$^{-/-}$ cells overexpressing Cbl-YFP. We obtained a significant reduction in colocalisation of Cbl-YFP with antigen microclusters for B cells lacking Grb2 (Figure 4.6. B, lower panel). The difference in colocalisation between wildtype and Grb2-deficient cells expressing Cbl was more prominent as compared to Dok-3. Combined with our co-immunoprecipitation results these data again highlighted the crucial interaction of Grb2 and Cbl in the context of BCR signalling.

In summary, we have been able to show a critical function for Grb2 in the recruitment of both Dok-3 and Cbl to antigen-containing BCR microclusters. This implies a functional role for Grb2 upstream of Dok-3 and Cbl downstream of the signalling BCR.

4.3.2 Cbl is dispensable for recruitment of Grb2 and Dok-3 to antigen microclusters

To extend our analysis of the essential molecules required for recruitment of Grb2, Dok-3 and Cbl to antigen-containing BCR microclusters, we investigated the role of Cbl. For this purpose, we expressed Grb2-GFP and Dok-3-GFP in DT40 B cells lacking Cbl. We settled cells on antigen-loaded lipid bilayers and acquired snapshots five minutes after seeding. Both Grb2 and Dok-3 formed clusters to the same extent as in a wildtype background (Figure 4.7. A and B). As shown by scanning the fluorescence for both channels along randomly placed lines, Grb2 as well as Dok-3 clusters did colocalise with antigen microclusters. This result implied that Cbl was dispensable for the recruitment of both Grb2 and Dok-3 to antigen-microclusters.

4.3.3 Dok-3 is dispensable for recruitment of Cbl to antigen microclusters, but is needed for Grb2 microcluster persistence

Having established a crucial role for Grb2 in the recruitment of Dok-3 and Cbl to antigen-containing BCR microclusters, we were keen to investigate the requirement of Dok-3 for recruitment of Grb2 and Cbl. We therefore expressed a YFP-tagged version of Cbl in DT40*Dok3*$^{-/-}$ cells and imaged these using TIRF microscopy on lipid bilayers loaded with surrogate antigen (Figure 4.7. C). Snapshots of spread cells clearly showed that Cbl-YFP formed clusters in a similar manner as seen for cells expressing Dok-3 (Figure 4.4.). These clusters of Cbl-YFP did also colocalise with antigen-containing BCR microclusters as shown by scanning the fluorescence for both channels along a randomly placed line. These data showed that Dok-3 was indeed dispensable for recruitment of Cbl to antigen microclusters.

We extended our analysis on the role of Dok-3 in the recruitment of Grb2 and Cbl to antigen microclusters and expressed Grb2-GFP in DT40 wildtype B cells or in cells lacking Dok-3. Cells were settled on antigen-containing lipid bilayers and image sequences were acquired using TIRF microscopy at a frame rate of five seconds per frame for 4 minutes. In both wildtype and *Dok3*$^{-/-}$ cells Grb2-GFP formed discrete clusters while cells were spreading over the antigen-presenting surface (Supplementary Video 4). In wildtype cells Grb2-GFP clusters started to migrate towards the centre of the contact between cell and lipid bilayer upon completion of spreading. In contrary, Grb2-GFP clusters stayed in the periphery and showed random movement rather than directed migration in cells lacking Dok-3. Importantly, the majority of Grb2 clusters in *Dok3*$^{-/-}$ cells did not exist for the whole duration of the acquisition, but disappeared a few frames after they had been formed. This pointed to a possible role for Dok-3 in stabilising Grb2 at the antigen-containing BCR microcluster.

We have consequently shown that Dok-3 is dispensable for the recruitment of Cbl to antigen-containing microclusters. However, Dok-3 appeared to stabilise Grb2 in clusters formed upon BCR activation, thus possibly acting as a scaffolding protein downstream of the BCR.

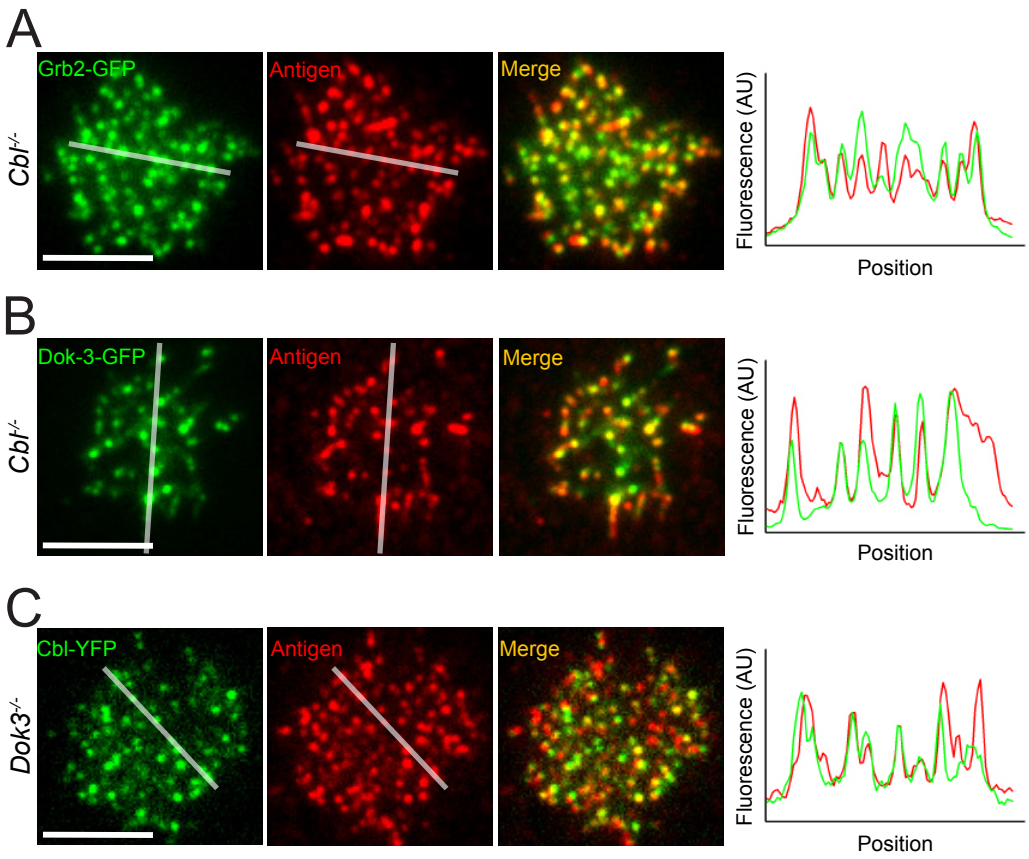

Figure 4.7. Cbl is not required for recruitment of Grb2 or Dok-3 to antigen-containing BCR microclusters

(A-C) DT40 B cells were settled on planar lipid bilayers containing surrogate antigen. (A-C) (left) TIRF images and (right) relative fluorescence intensity along translucent lines at 5 min after settling on bilayers for cells expressing (A) Grb2-GFP, (B) Dok-3-GFP on *Cbl*$^{-/-}$ background, and (C) Cbl-YFP on *Dok3*$^{-/-}$ background. All scale bars equal 5 μm.

4.3.4 A direct interaction of Grb2 and Dok-3 dictates the recruitment of Dok-3 to antigen microclusters

Our previous data showed a significantly impaired recruitment of Dok-3 to antigen-containing microclusters in the absence of Grb2. In addition, clusters of Grb2 appeared unstable over time in B cells lacking Dok-3. The mutual dependence of Grb2 and Dok-3 in respect to their recruitment to antigen microclusters encouraged us to investigate their interplay with greater detail.

The interaction between Grb2 and Dok-3 is thought to be direct and has been reported to be mediated by binding of Dok-3 Y331 to the central SH2 domain of Grb2 (Stork et al., 2007). SH2 domains are protein entities that bind to phosphorylated tyrosine residues (Figure 4.3.). We therefore utilised a Dok-3 variant, which carries the point mutation Y331 (Dok-3Y331F). By means of TIRF microscopy coupled to the lipid bilayer system for antigen presentation, we were able to show a differential recruitment of Dok-3Y331F-GFP to antigen microclusters compared to wildtype Dok-3-GFP (Figure 4.8. A). We quantified colocalisation of either Dok-3-GFP or Dok3-3Y331F-GFP with antigen microclusters and observed a significant difference (Figure 4.8. C, left panel). The mutation was, however, not sufficient to abolish Dok-3 recruitment to antigen microclusters completely. Clusters of Dok-3Y331F-GFP still formed, but these did not appear to colocalise with antigen microclusters to the same extent as for wildtype Dok-3. Interestingly, this resembled the phenotype observed in cells lacking Grb2 (Figure 4.6.). This result therefore suggested that the interaction of Dok-3 and Grb2 in the context of BCR signalling was direct and mediated by binding of the central SH2 domain of Grb2 to Dok-3Y331.

Others had shown that the C-terminal SH3 domain of Grb2 can indirectly interact with Lyn through HS1 (Takemoto et al., 1998). We therefore wanted to know whether this domain was sufficient to recruit Dok-3 to antigen-containing BCR microclusters. To address this, we expressed a chimeric protein consisting of full-length Dok-3 and the C-terminal SH3 domain of Grb2 fused to GFP in DT40 cells lacking Dok-3. Upon BCR activation on antigen-loaded lipid bilayers we observed cluster formation of the chimeric protein. Clusters of Dok-3-Grb2cSH3-GFP appeared discrete and colocalised with antigen microclusters (Figure 4.8. B,

upper panels). Yet, when introducing an inactivating point mutation in the Grb2 SH3 domain (W193K) we observed a significantly altered recruitment of Dok-3-Grb2cSH3W193K-GFP to antigen microclusters (Figure 4.8. B, lower panels). The mutated chimeric protein appeared diffuse and values for colocalisation with antigen microclusters dropped significantly when compared to the fusion protein with an intact SH3 domain (Figure 4.8. C, right panel). Our findings hence suggested an important role for the C-terminal domain of Grb2 in the recruitment of Dok-3 to antigen-containing microclusters and points at an interaction with the kinase Lyn.

In summary, by using a point mutant of Dok-3 we were able to show that a direct interaction of Dok-3 and Grb2 is necessary for the recruitment of Dok-3 to antigen microclusters. This interaction involves binding of Dok-3Y331 to the Grb2 SH2 domain and is likely to be dependent on phosphorylation of Y331 through a BCR-dependent process. Moreover, using mutagenesis of a chimeric protein consisting of Dok-3 and the C-terminal SH3 domain of Grb2 we revealed that this SH3 domain is critical for recruitment of Dok-3 to antigen-containing BCR microclusters. It is therefore anticipated that BCR-crosslinking triggers binding of Grb2 through its C-terminal SH3 domain and this is in turn needed for adequate formation of a complex consisting of Grb2 itself, Dok-3 and Cbl.

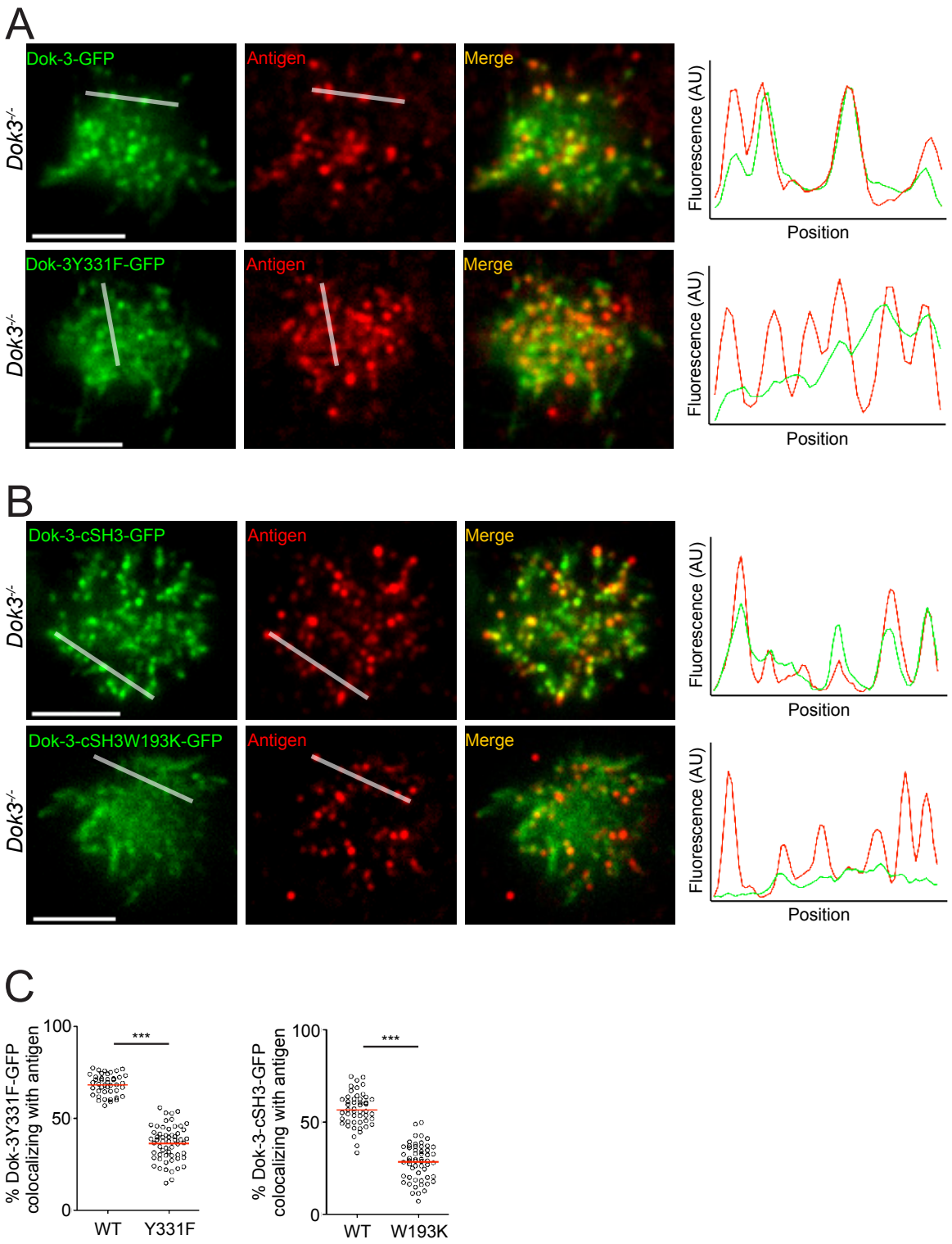

Figure 4.8. A direct interaction between Grb2 and Dok-3 is important for Dok-3 recruitment to antigen-containing BCR microclusters

(A) DT40*Dok3*$^{-/-}$ cells expressing either wildtype Dok-3-GFP (upper panels) or Dok-3Y331F-GFP (lower panels) were settled on antigen-containing lipid bilayers and snapshots were acquired five minutes after settling. Dok-3-GFP and antigen fluorescence was analysed along the translucent line and plotted in the right panel. (B) The experimental setup of A was used to image DT40*Dok3*$^{-/-}$ cells expressing a chimeric protein consisting of full-length Dok-3 and the C-terminal SH3 domain of Grb2 coupled to GFP (Dok-3-cSH3; upper panels). Lower panels show the distribution of the chimeric protein harbouring a point mutation in the SH3 domain (W193K). All scale bars equal 5 µm. (C, left) The dot plot shows co-localisation of GFP and antigen quantified for proteins used in A. Red lines indicate the mean. (C, right) The same analysis as in the left panel was used to measure the co-localisation of the chimeric proteins used in B with antigen microclusters. Statistical analysis was carried out using t-test; ***$p < 0.0001$.

4.3.5 BCR signalling is required for recruitment of Grb2 to antigen microclusters

We had previously established a crucial role for Grb2 in the recruitment of Dok-3 and Cbl to antigen-containing BCR microclusters. The importance of the C-terminal SH3 domain of Grb2 in the recruitment of Dok-3 pointed at a possibly indirect interaction with Lyn kinase.

We therefore wanted to investigate the basis of Grb2 recruitment in more detail. In particular, we were interested whether BCR signalling was indeed needed for recruitment of Grb2 to antigen microclusters. To answer this question, we expressed Grb2-GFP either in wildtype B cells or in DT40 B cells lacking the kinase Lyn. Lyn is a member of the Src family of kinases and it is crucial for the initiation of signalling in B cells as it phosphorylates the Igα and Igβ signalling subunits of the BCR. We settled cells on antigen-bearing lipid bilayers and acquired images five minutes after cells had been seeded on the bilayer. In wildtype cells Grb2-GFP formed discrete clusters colocalising with antigen microclusters as we had previously observed in DT40*Grb2*$^{-/-}$ cells (Figure 4.9. A, upper row). In the absence of Lyn, however, we could not detect any clusters of Grb2 (Figure 4.9. A, bottom row), although the expression level of Grb2-GFP was comparable between both cell lines. The complete lack of Grb2 recruitment in Lyn-deficient cells was confirmed by scanning the fluorescence along a randomly placed line resulting in almost absent fluorescence in the GFP channel (Figure 4.9. A, right panels). It is important to note that the BCR is unable to signal due to the lack of Lyn. This results in impaired spreading and the formation of a very limited amount of antigen clusters (Weber et al., 2008). In fact, clustered antigen in Figure 4.9. A (bottom row) is likely a result of BCRs diffusing on the surface of the B cells and being trapped when getting in contact with the antigen-loaded lipid bilayer. Grb2 recruitment to antigen-containing BCR microclusters thus strongly depended on the presence of Lyn kinase and implied a need for BCR signalling.

To assess whether the dependence of Grb2 on Lyn was due to its kinase activity or an adaptor function of Lyn, we used a variant of Grb2, which carries an inactivating point mutation of its central SH2 domain (Grb2R86K). This mutated SH2 domain abrogates binding of Grb2 to phosphorylated tyrosine residues

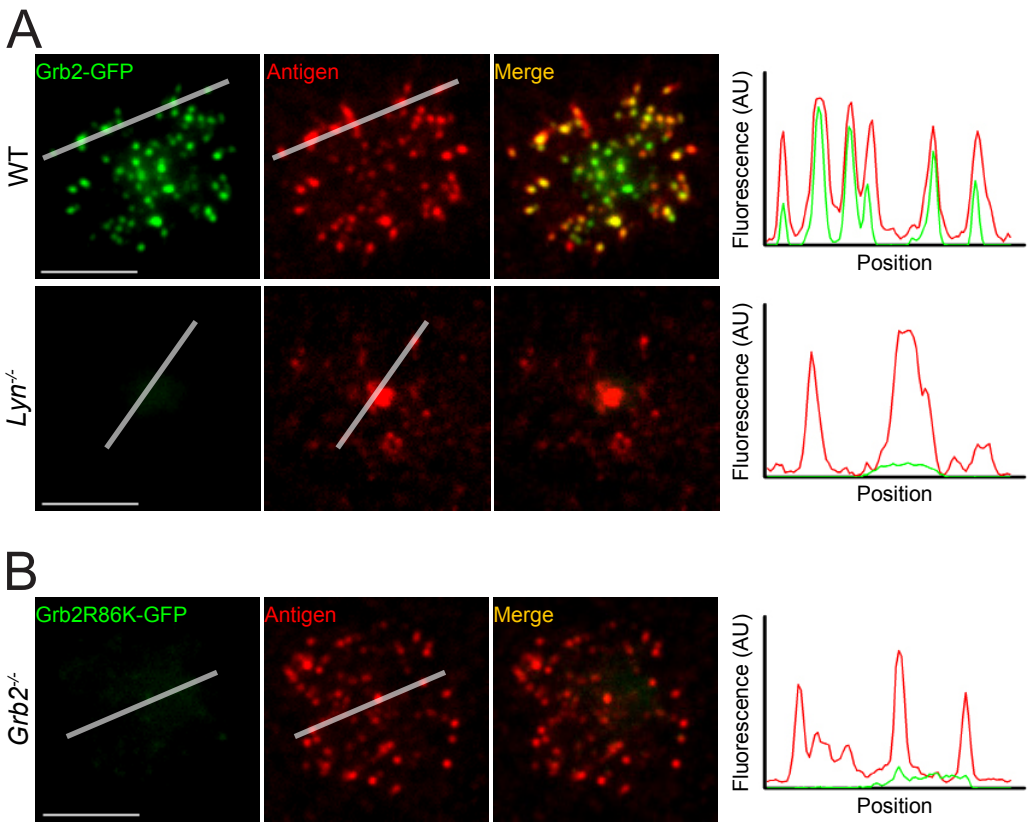

Figure 4.9. Recruitment of Grb2 to antigen-containing BCR microclusters requires BCR signalling

(A) Grb2-GFP and antigen microclusters were visualised on planar lipid bilayers in DT40 wildtype (WT) cells five minutes after settling (upper panels). The same experiment was carried out in DT40 cells deficient for Lyn (lower panels) kinase. Co-localisation of Grb2-GFP and antigen was assessed by measuring GFP and antigen fluorescence along the translucent lines and plotting the values in diagrams on the right. (B) DT40*Grb2*$^{-/-}$ cells stably expressing a point mutant of the Grb2 SH2 domain (Grb2R86K-GFP) were settled on antigen containing bilayers and images were acquired as in A. Co-localisation of Grb2R86K-GFP and antigen was analysed by plotting fluorescence for both channels as in A. All scale bars equal 5 µm.

(Tanaka et al., 1995). We expressed Grb2R86K-GFP in a DT40*Grb2*$^{-/-}$ background and settled cells on antigen-loaded lipid bilayers as before. TIRF microscopy revealed a complete absence of Grb2R86K-GFP clusters (Figure 4.9. B). This phenotype was comparable to Grb2-GFP expressed in Lyn-deficient cells and indeed demonstrated that active BCR signalling through Lyn kinase was crucial for recruitment of Grb2 to antigen microclusters.

As Grb2R86K did not appear to alter cell spreading or antigen microcluster formation, we were keen to investigate, whether this point mutant was sufficient to restore cellular contraction and antigen gathering. We therefore stably expressed either Grb2R86K-GFP or wildtype Grb2-GFP at same levels in DT40 B cells lacking endogenous Grb2 and settled these on antigen-loaded lipid bilayers. We monitored the contact area between cells and the lipid bilayer by IRM and followed antigen distribution using confocal microscopy. We observed unaltered spreading and antigen clustering within the first five minutes after seeding (Figure 4.10. A). Upon completion of spreading, however, B cells expressing Grb2R86K did not contract or gather antigen in a central agglomerate. Figures 4.10. B and C show quantifications of contact area between cells and the lipid bilayer (B) and the total amount of antigen gathered (C) by DT40*Grb2*$^{-/-}$ cells either expressing wildtype Grb2 or the point mutant Grb2R86K. It was thereby evident that Grb2R86K was not able to restore cellular contraction or antigen accumulation. In fact, there was a striking similarity to DT40*Grb2*$^{-/-}$ cells (Figure 4.1.).

In conclusion, we have shown that BCR signalling through the kinase Lyn is essential for recruitment of Grb2 to antigen microclusters. This recruitment likely depends on tyrosine phosphorylation by Lyn and is needed to restore cell contraction and antigen gathering in DT40 B cells lacking Grb2.

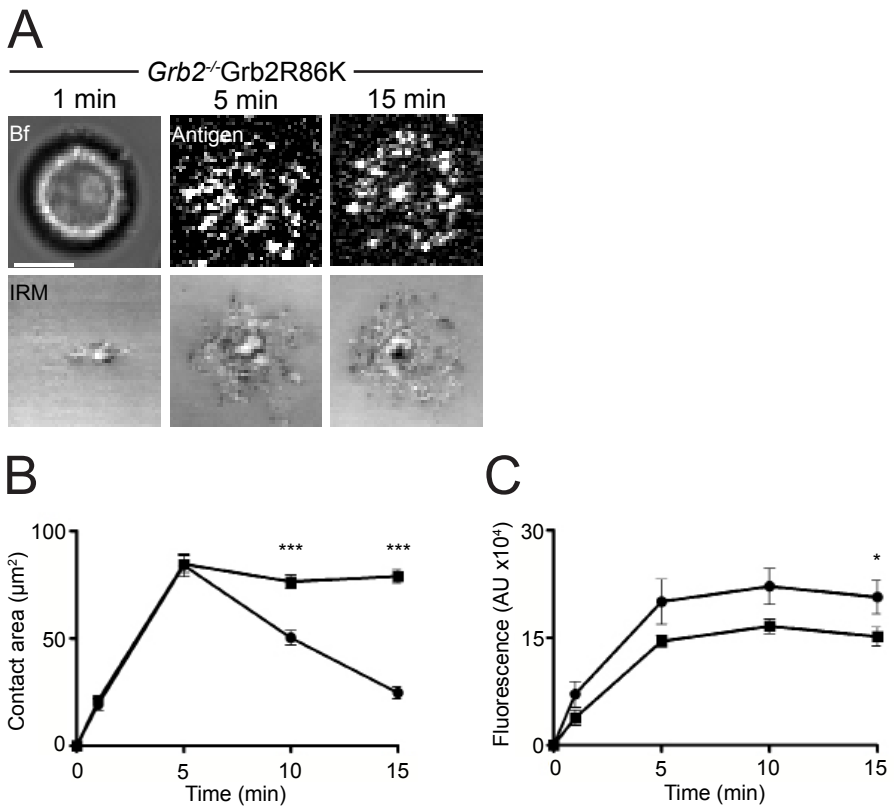

Figure 4.10. A point mutant of Grb2 shows impaired contraction and antigen gathering
(A) DT40*Grb2*$^{-/-}$ cells stably expressing a point mutant of the Grb2 SH2 domain (Grb2R86K-GFP) were settled on antigen containing bilayers and confocal images of antigen were acquired over 15 min. In parallel, the contact area between cells and the antigen-bearing lipid bilayer was monitored using IRM; cells were identified by their brightfield (Bf) image. (B) IRM data in A was used to quantify the contact area between the antigen-containing lipid bilayer and DT40*Grb2*$^{-/-}$ cells stably expressing either Grb2R86K-GFP (squares) or Grb2wt-GFP (control; circles). (G) Confocal microscopy data in A was used to quantify the amount of antigen expressed as arbitrary fluorescence units (AU) gathered over time by DT40*Grb2*$^{-/-}$ cells stably expressing either Grb2R86K-GFP (squares) or Grb2wt-GFP (control; circles). Data in B and C represents a minimum of 20 cells pooled from three independent experiments. Statistical analysis was carried using t-test; ***$p < 0.0001$; *$p < 0.02$. All scale bars equal 5 μm.

4.3.6 Grb2 acts upstream of BCR-proximal signalling molecules Syk and SLP65

As the recruitment of Grb2 to antigen-containing BCR microclusters required the expression and possibly activity of Lyn kinase, we were keen to investigate whether the expression of other key signalling molecules downstream of the BCR was required for Grb2 recruitment. We consequently focussed on the spleen tyrosine kinase Syk and the signal integrator SH2 domain-containing leukocyte adaptor protein of 65 kDa (SLP65 or BLNK). Both Syk and SLP65 act BCR-proximal and are crucial for B cell development and function (Turner et al., 1995, Turner et al., 1997, Pappu et al., 1999, Minegishi et al., 1999 and Fu et al., 1998). Syk binds to phosphorylated tyrosine residues in the Igα and Igβ subunits of the BCR once phosphorylated by Lyn. Syk has been shown to propagate the signal downstream of the BCR by phosphorylation of SLP65 and other effector molecules.

As the recruitment of Syk to antigen-containing BCR microclusters had previously been established (Weber et al., 2008), we first wanted to investigate whether SLP65 was recruited to antigen microclusters. We therefore expressed a fluorescently tagged version of SLP65-GFP in DT40*Slp65*$^{-/-}$ B cells and settled these on antigen-loaded lipid bilayers. Snapshots were taken when cells were fully spread and we observed SLP65 cluster formation upon BCR activation (Figure 4.11. A). These clusters colocalised with antigen microclusters to a high extent as could be observed by scanning fluorescence for both channels along a line (right panel in Figure 4.11. and Supplementary Video 5). Having established that SLP65 is recruited to antigen-containing microclusters in a BCR-dependent fashion, we next sought to assess whether SLP65 was needed for recruitment of Grb2 to antigen microclusters. To address this, we expressed Grb2-GFP in DT40 cells lacking SLP65 and settled them on antigen-bearing lipid bilayers. TIRF images of spread cells revealed Grb2 cluster formation and colocalisation of these clusters with antigen-containing BCR microclusters as shown by scanning fluorescence for both GFP and antigen channels along a line (Figure 4.11. B). We thus concluded that the central adaptor SLP65 was dispensable for recruitment of Grb2 to antigen-containing BCR microclusters.

We next investigated the requirement of Syk for Grb2 recruitment to antigen microclusters by expressing Grb2-GFP in DT40S*yk*$^{-/-}$ cells. When settled on antigen-containing lipid bilayers, Grb2-GFP formed clusters, which colocalised with antigen microclusters (Figure 4.11. C). When scanning fluorescence intensities for both fluorescence channels, we observed an overlay of both channels at sites of clustering. However, the enrichment of Grb2 within antigen microclusters appeared lower compared to cells lacking SLP65. This observation could possibly be explained by the hypothesis that phosphorylation by Syk was needed to increase the amount of Grb2 molecules recruited to signalling BCR microclusters. It is important to mention that B cells lacking Syk and SLP65 spread significantly less compared to wildtype cells (Weber et al., 2008). Cell spreading and subsequent contraction concomitant with antigen gathering is impaired in B cells deficient for Syk and SLP65.

To summarise, we have established a BCR-proximal role for Grb2 alternative to Syk and SLP65 as these molecules were dispensable for Grb2 recruitment to antigen-containing microclusters. Our data thus implied that Lyn kinase provided a sufficient amount of initial tyrosine phosphorylation to allow binding of Grb2 by virtue of its central SH2 domain.

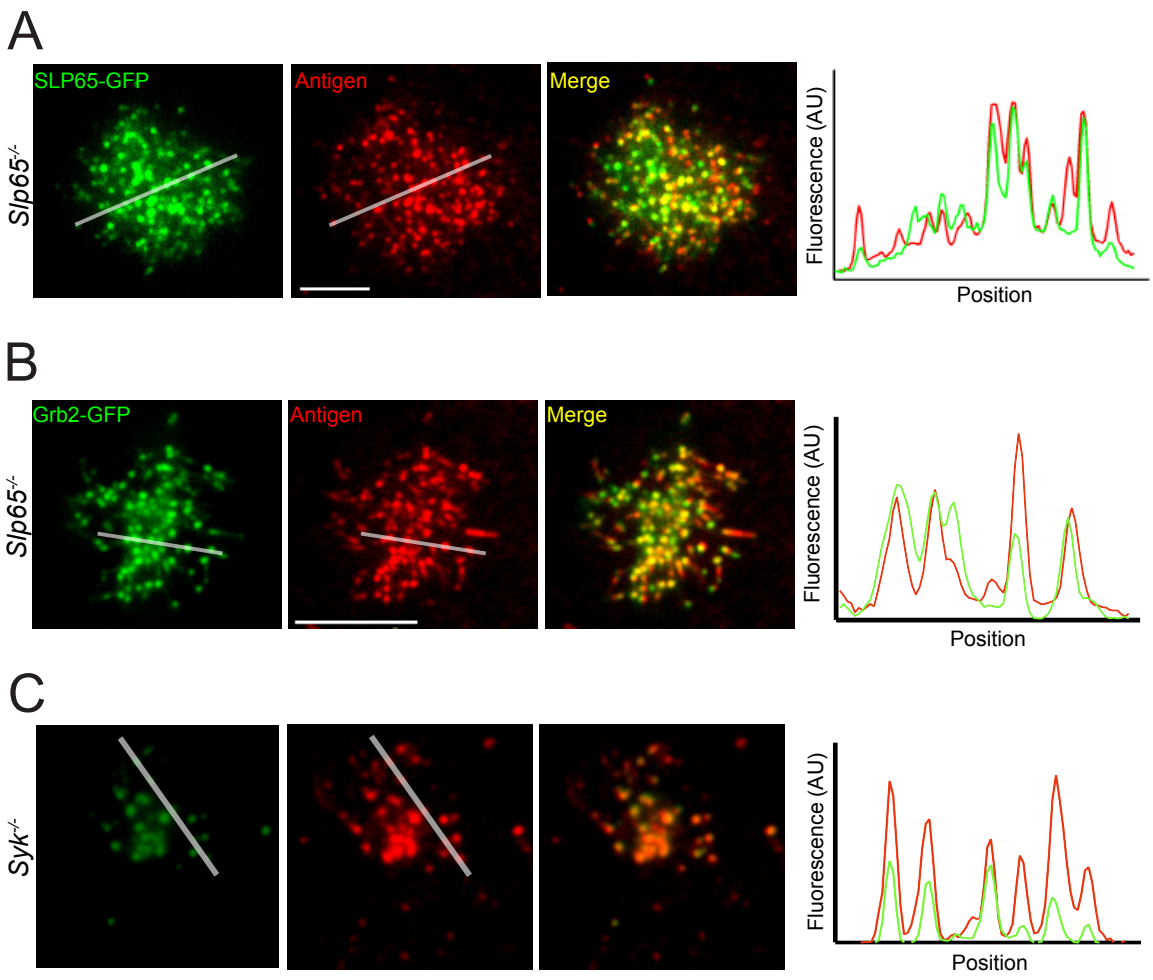

Figure 4.11. Recruitment of Grb2 to antigen-containing BCR microclusters is independent of Syk and SLP65

(A) SLP65-GFP was stably expressed in DT40*Slp65*$^{-/-}$ B cells. Cells were visualised on planar lipid bilayers containing surrogate antigen using TIRF. Images shown represent snapshots acquired five minutes after settling. Co-localisation of SLP65-GFP and antigen was assessed by measuring GFP and antigen fluorescence along the translucent lines and plotting the values in diagram on the right. (B) Grb2-GFP and antigen microclusters were visualised on planar lipid bilayers in DT40*Slp65*$^{-/-}$ cells five minutes after settling. (C) The same experiment was carried out in DT40 cells deficient for Syk. Co-localisation of Grb2-GFP and antigen was assessed by measuring GFP and antigen fluorescence along the translucent lines and plotting the values in diagrams on the right. All scale bars equal 5 µm.

4.3.7 CIN85 is recruited to antigen-containing BCR microclusters independently of SLP65

The Cbl-interacting protein of 85 kDa (CIN85) had previously been reported to bind components of the BCR signalling complex such as Grb2, SLP65 and Cbl (Take et al., 2000, Watanabe et al., 2000 and Dikic, 2002). As CIN85 binds both Grb2 and Cbl it could act as an important linker. We were therefore interested, whether CIN85 was recruited to antigen-containing BCR microclusters.

In order to address this question, we expressed CIN85-GFP in DT40 wildtype cells and seeded these on antigen-bearing lipid bilayers (Figure 4.12. A). Discrete clusters of CIN85-GFP formed and colocalised with antigen microclusters as shown by scanning fluorescence along randomly placed lines in both channels (Figure 4.12. A, right panel and Supplementary Video 6). Nevertheless, clusters of CIN85-GFP were also visible outside of regions with concentrated antigen molecules indicating that there are multiple ways to recruit CIN85 to the plasma membrane. Given our data that SLP65 was dispensable for recruitment of Grb2 to antigen-containing BCR microclusters and in light of a reported interaction of CIN85 and SLP65 (Watanabe et al., 2000), we assessed the recruitment of CIN85 in the absence of SLP65. For this purpose we expressed CIN85-GFP in DT40*Slp65*$^{-/-}$ cells and settled these on antigen-loaded lipid bilayers. Indeed, clusters of CIN85 formed and colocalised with antigen (Figure 4.12. B). This result indicated that CIN85 is recruited to the signalling BCR in a mechanism independent of the central adaptor molecule SLP65.

Our data showed recruitment of the adaptor protein CIN85 to antigen-containing BCR microclusters. As previously observed for Grb2, CIN85 recruitment was independent of SLP65 and thus potentially serves as a link between Grb2 and Cbl. The SLP65 dispensability also implies the existence of mechanisms for signalling complex formation downstream of the BCR alternative to the classical view of signal propagation by Syk and SLP65. However, more work is needed to clearly elucidate the recruitment of signalling molecules to the signalling BCR in a spatiotemporal manner.

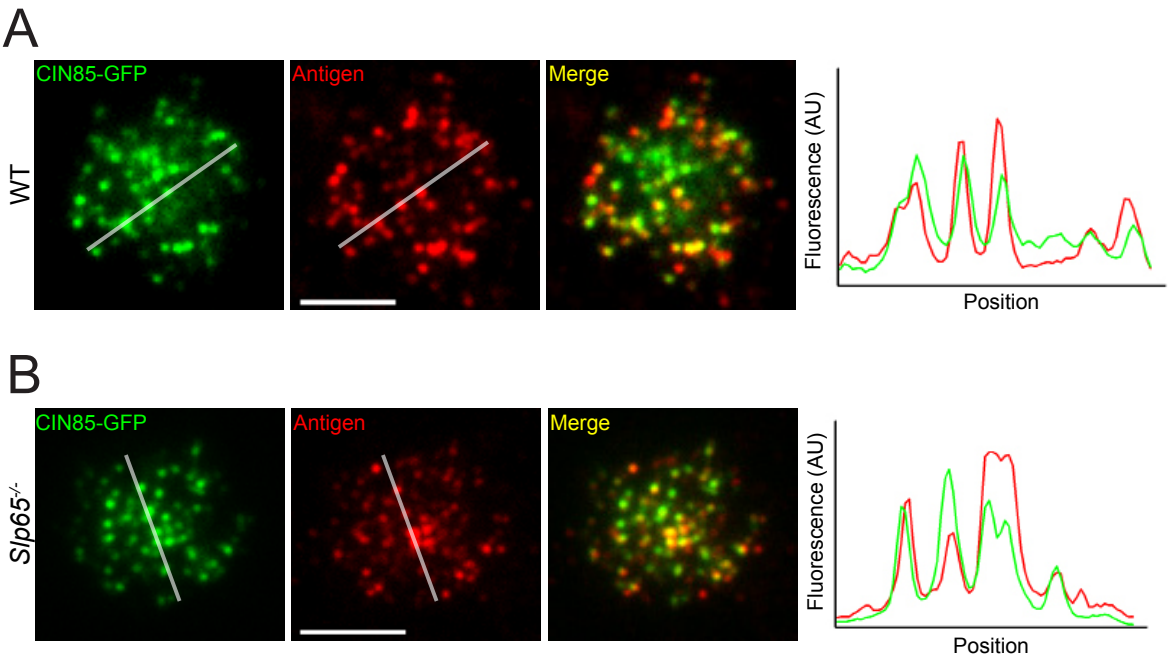

Figure 4.12. Recruitment of CIN85 to antigen-containing BCR microclusters is independent of SLP65

(A) CIN85-GFP was stably expressed in DT40 wildtype B cells. Cells were visualised on planar lipid bilayers containing surrogate antigen using TIRF microscopy. Images shown represent snapshots acquired five minutes after settling. Co-localisation of CIN85-GFP and antigen was assessed by measuring GFP and antigen fluorescence along the translucent lines and plotting the values in diagrams on the right. (B) The experimental setup in A was used to determine recruitment of CIN85-GFP to antigen-containing BCR microclusters in DT40*Slp65*$^{-/-}$ B cells. All scale bars equal 5 µm.

4.3.8 Grb2 controls intracellular signalling upon BCR ligation

Given the importance of Grb2 in antigen gathering and in the regulation of recruitment of Dok-3 and Cbl to antigen microclusters, we decided to investigate the effect of Grb2-deficiency on intracellular signalling upon BCR activation.

We used multi-well tissue culture plates and coated these with varying concentrations of an anti-chicken IgM antibody (clone M4), to mimic the surface of an antigen-presenting cell. Next, we either seeded DT40 wildtype cells or B cells lacking Grb2 on the coated surfaces. We lysed cells at different time points and processed the samples for Western blotting. An anti-tubulin antibody was used to control for equal loading among all time points. In order to assess BCR-dependent signalling in both wildtype and *Grb2*$^{-/-}$ cells, we tested samples for enrichment of phopsho-p38 and phospho-JNK. p38 and JNK belong to the MAP family of kinases and their phosphorylation indicates the activation of gene expression downstream of the BCR. Figure 4.13. shows BCR-dependent phosphorylation of both p38 and JNK as phosphorylation levels titrated with the amount of anti-chicken IgM used for plate coating (compare left and right panels). Furthermore, the phosphorylation of p38 and JNK was indeed stronger and more sustained in B cells lacking Grb2. While wildtype cells did not show any increase in phospho-p38 when seeded on a plate coated with a low concentration of anti-chicken IgM, DT40*Grb2*$^{-/-}$ cells did.

Our data on MAP kinase signalling in B cells deficient for Grb2 thus suggests an inhibitory role for Grb2 in the context of BCR signalling.

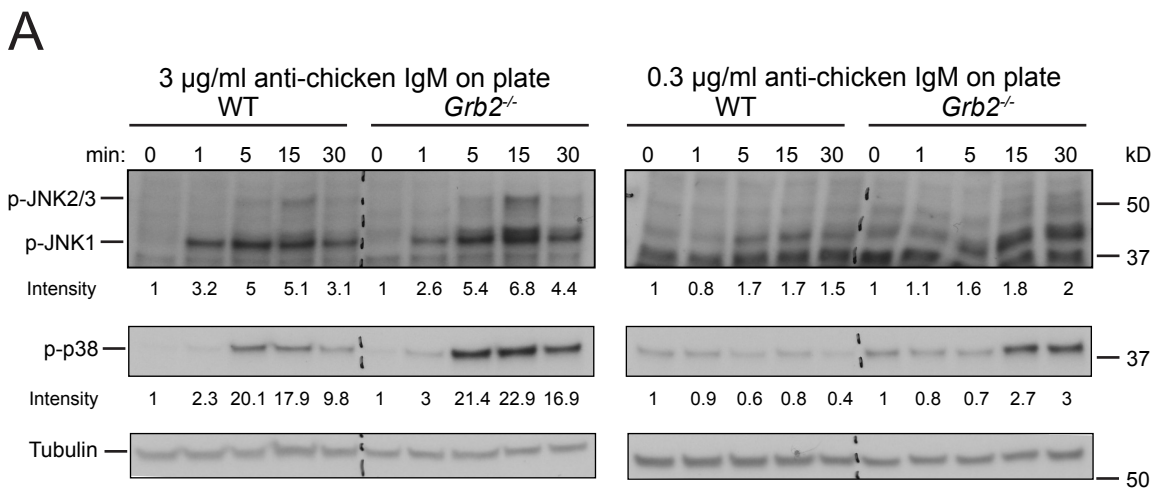

Figure 4.13. DT40 B cells lacking Grb2 show elevated intracellular signalling in response to BCR ligation

(A) DT40 wildtype (WT) or *Grb2*$^{-/-}$ cells were settled on 24-well plates coated with anti-chicken IgM antibody at either 3 µg/ml (left panel) or at 0.3 µg/ml (right panel). Cells were lysed at indicated times and an equal of 400,000 cells per condition was loaded on an SDS gel. Levels of phospho-JNK and phospho-p38 were analysed using Western blot. Tubulin served as loading control. Numbers under phospho-JNK and phospho-p38 blots indicate the band intensities relative to the first timepoint (t = 0 min). For quantification of phospho-JNK bands, band intensities for phospho-JNK1 were measured.

To conclude we have carried out a careful genetic dissection of the complex consisting of Grb2, Dok-3 and Cbl, which regulates antigen gathering in B cells. We have shown that Grb2 is essential for the recruitment of both Dok-3 and Cbl to antigen-containing BCR microclusters. The interaction of Grb2 and Dok-3 is likely to be direct and involves binding of the central SH2 domain of Grb2 to Dok-3Y331. Furthermore, our data suggests an upstream role for Grb2 as the central signalling molecules Syk and SLP65 were dispensable for Grb2 recruitment to antigen microclusters. The mechanism of Grb2 recruitment possibly involves an interaction with Lyn kinase and strongly relies on early phosphorylation events as a Grb2 variant carrying an inactivating mutation of its SH2 domain impaired recruitment of Grb2 to antigen microclusters. Importantly, expression of this Grb2 mutant in B cells lacking Grb2 was not sufficient to rescue cellular contraction and concomitant antigen gathering. In addition, we have also demonstrated recruitment of the adaptor CIN85 to antigen-containing BCR microclusters. As for Grb2, this recruitment was independent of SLP65 and might imply a collaborative role for Grb2 and CIN85 downstream of the BCR.
Our findings thereby indicate an important role for the small molecular adaptor Grb2 in the nucleation and localisation of a complex involving Dok-3 and Cbl and in the regulation of intracellular signalling through MAP kinases.

4.4 Discussion

We have used a combination of genetics and high-resolution imaging coupled to a lipid bilayer-based system for antigen presentation to show that the proteins Grb2, Dok-3 and Cbl are essential for B cell contraction and antigen gathering. Nevertheless, they appeared to be dispensable for B cell spreading and initial antigen microcluster formation. Reduced antigen gathering in cells lacking Grb2, Dok-3 or Cbl was due to impaired centripetal movement of antigen microclusters. Our data further proves recruitment of a complex consisting of Grb2, Dok-3 and Cbl to the signalling BCR. Expression of a fluorescently tagged version of either

Grb2, Dok-3 or Cbl in the respective knockout cell line was sufficient to rescue cellular contraction and concomitant antigen gathering.

We went on to genetically dissect the recruitment of Grb2, Dok-3 and Cbl to antigen microclusters and found Grb2 to be critical for complex formation involving the three mediators. The interaction of Dok-3 and Grb2 was likely to be direct and involved phosphorylation of Dok-3Y331. Grb2 recruitment itself was directly dependent on BCR signalling through the kinase Lyn. By using a chimeric protein of full-length Dok-3 and the C-terminal SH3 domain of Grb2 we showed that the latter was needed for recruitment to antigen-containing BCR microclusters as an inactivating mutation in that domain impaired recruitment. As its C-terminal SH3 domain has been reported to be in a complex with Lyn, this implied a BCR-proximal role for Grb2 (Takemoto et al., 1998). To assess this further, we found that Grb2 was recruited to antigen-containing BCR microclusters independent of the kinase Syk and the adaptor SLP65. We further established the recruitment of the Cbl-interacting protein CIN85 to antigen-containing microclusters in a mechanism independent of SLP65. CIN85 could therefore constitute a link between Grb2 and Cbl as it has been shown to interact with both proteins and was recruited to antigen-containing microclusters in a SLP65-independent way similar to Grb2 (Watanabe et al., 2000).

Given the BCR-proximal role of Grb2, we finally tested DT40*Grb2*$^{-/-}$ B cells for their ability to signal through MAP kinases and found elevated and more sustained phosphorylation of both JNK and p38.

4.4.1 Antigen gathering and negative regulation of BCR signalling

The role of phosphatases in the negative regulation of BCR signalling

One mode of negative regulation in lymphocytes is the recruitment of phosphatases to sites of immunoreceptor signalling (Mustelin et al., 2005). Phosphatases counteract the action of kinases by de-phosphorylation of target proteins or lipids. Protein phosphatases such as SHP1 have been implicated to downregulate BCR signalling by recruitment to the BCR signalosome *via* the transmembrane protein CD22 (Nitschke, 2009). A lack of CD22 in mice leads to

hyper-responsive B cells and autoimmunity (Jellusova et al., 2010). Furthermore, Dok-3 has been shown to interact with the lipid phosphatase SHIP-1 (Robson et al., 2004). Importantly, B cells from mice lacking SHIP-1 present the same phenotype as seen in Grb2-, Cbl- or Dok-3-deficient B cells with regards to elevated calcium and MAP kinase signalling. Interestingly, primary murine B cells deficient for SHIP-1 have recently been reported to show altered cellular contraction and antigen gathering (Liu et al., 2011).

Negative regulation of BCR signalling by Grb2, Dok-3 and Cbl

Our data provides insights into the mechanism regulating antigen gathering by B cells for subsequent extraction and eventual presentation to T cells. We found that three molecules Grb2, Dok-3 and Cbl are essential for the process of antigen gathering by directed movement of antigen-containing BCR microclusters towards the central region. Interestingly, all three mediators have been implicated to play a role in the negative regulation of lymphocyte signalling: BCR-induced calcium flux has been reported to be elevated in all three knockouts (Stork et al., 2004; Stork et al., 2007 and Kitaura et al., 2007). Stork and co-workers have postulated a mechanism involving the targeting of Grb2 to the same membrane compartment as Btk through Dok-3 resulting in diminished activation of PLCγ2. However, the exact mechanism how calcium signalling is inhibited by Grb2, Dok-3 or Cbl remains elusive. Correlating with the negative regulation of calcium flux, we observed a higher and more sustained phosphorylation of JNK and p38 MAP kinases in stimulated DT40*Grb2*$^{-/-}$ cells. Two independent studies have in the meantime been published using primary murine B cells lacking Grb2 to assess its role in JNK and p38 MAP kinase signalling downstream of the BCR: While Nitschke and colleagues found a lower phosphorylation of JNK and p38 in activated *Grb2*$^{-/-}$ B cells, Jang et al. reported the opposite (Ackermann et al., 2011 and Jang et al., 2011). In line with our findings using DT40 cells, MAP kinase signalling through Erk or p38 or NFAT activation has been demonstrated to be elevated in naïve B cells from mice deficient for Dok-3 and Cbl (Ng et al.; 2007, Kitaura et al., 2007 and Lemay et al., 2000). Furthermore, animals lacking Grb2, Dok-3 or Cbl all display higher levels of serum IgM indicating a hyper-

responsiveness of B cells in general (Ackermann et al., 2011; Kitaura et al., 2007 and Ng et al., 2007). It is likely that this over-activity is due to altered down-regulation of BCR from the cell surface.

Downregulation of immunoreceptor signalling by Ubiquitin ligases and associated adaptors

Our finding that the E3 ubiquitin ligase Cbl is recruited to antigen-containing BCR microclusters and participates in antigen gathering in B cells is of particular interest. While the two Cbl family members Cbl and Cbl-b are thought to regulate signalling in lymphocytes (Liu and Gu, 2002; Thien and Langdon, 2001), their precise role in BCR-mediated signalling is contentious. Genetic and biochemical data has been used to suggest Cbl proteins function both as negative and positive regulators of BCR signalling through ubiquitination of Syk and calcium signalling (Panchamoorthy et al., 1996; Shao et al., 2004; Smit et al., 1996; Sohn et al., 2003; Yasuda et al., 2000 and Yasuda et al., 2002). The apparently conflicting evidence might arise due to the partial redundancy of the Cbl family members. One recent study, utilising the same Cbl-deficient DT40 B cell line used in this thesis, found delayed BCR internalisation dependent on the ubiquitin ligase activity of Cbl early after BCR triggering (Jacob et al., 2008). In fact, on the basis of studies in mice lacking both Cbl isoforms in B cells, it was proposed that Cbl family members play a critical role in surface BCR down-regulation through ubiquitination of BCR microcluster components including Syk (Kitaura et al., 2007 and Sohn et al., 2003). In line with this, the ubiquitination of Syk by Cbl has also been demonstrated in other cellular systems such as NK cells (Paolini et al., 2001 and Peruzzi et al., 2007).

Importantly, our finding that Cbl is required for antigen gathering in B cells complements the recent discovery that ubiquitination is required for formation of the central TCR cluster following T cell stimulation (Vardhana et al., 2010). This work identified a role for TSG101, the ubiquitin-recognising component of the endosomal-sorting complex required for transport (ESCRT) II, in the down-regulation of TCR signalling. It is postulated that TCR ubiquitination, potentially mediated by E3 ubiquitin ligases such as Cbl, allows sorting of TCR into specific

degradative sites in the central cluster for internalisation and subsequent degradation. In line with this, earlier work suggested that TCR signals are sustained in peripheral microclusters and that signalling through the TCR is terminated once microclusters have fused to form a larger agglomerate (Varma et al., 2006). This model has since been modified by postulating a balance between TCR signalling and degradation, which is determined by the affinity of the TCR for the specific antigen (Cemerski et al., 2008). Correspondingly in B cells, it may be that Cbl mediates ubiquitination of the BCR microcluster to allow gathering and formation of the central antigen-rich region. Unlike T cells, however, gathering of antigen in B cells is not only important for BCR signal attenuation, but also for the acquisition of antigen and eventual presentation to specific T helper cells necessary for maximal activation.

Regarding the down-regulation of BCR from the cell surface our finding that the adaptor CIN85 is recruited to antigen-containing BCR microclusters is particularly interesting. CIN85 has been reported to act in a complex with BCR signalling molecules such as Grb2, Cbl and SLP65 (Watanabe et al., 2000). Our results showing a SLP65-independent recruitment of CIN85 to antigen microclusters resembles the phenotype observed for Grb2 recruitment in SLP65-deficient B cells and suggests a possible interaction of Grb2 and CIN85 immediately downstream of the signalling BCR. The direct interaction of CIN85 with phosphatidic acid could link CIN85 to signalling-competent membrane microdomains and provide a mechanism for plasma membrane recruitment (Zhang et al., 2009). The membrane localisation of CIN85 could also explain our results showing Cbl not only confined to antigen-microclusters. Interestingly, CIN85 associates with a range of cytoskeletal regulators such as the actin capping protein CapZ (Dikic, 2002) or Nck2 (Fu et al., 1998) and is therefore likely to link the BCR signalling complex to the actin cytoskeleton crucial for B cell spreading and endocytosis. In terms of receptor endocytosis, CIN85 and Cbl have been reported to associate with endophilins, which can induce negative membrane curvature (Petrelli et al., 2002 and Soubeyran et al., 2002). The association of Cbl and CIN85 with endophilins was crucial for endocytosis of growth factor receptors such as the EGF receptor or c-Met. Another publication has reported a role for CIN85 in the

ligand-dependent endocytosis of the high-affinity IgE receptor on Mast cells indicating a general function of CIN85 and associated Cbl in receptor endocytosis (Molfetta et al., 2005).

It is therefore conceivable that a complex involving Grb2, Dok-3, Cbl and possibly CIN85 could link the antigen-containing BCR microcluster to an endocytic machinery, which ultimately executes the down-regulation of engaged BCR molecules from the cell surface. This process is likely to lead to down-modulation of BCR-dependent signalling and might therefore explain the hyperactive phenotype of B cells lacking Grb2, Dok-3 or Cbl (Ng et al., 2007 and Kitaura et al., 2007).

4.4.2 Dynamic organisation of signalling microclusters

Here, we have extended a functional screen to reveal a role for Grb2, Dok-3 and Cbl in the process of antigen gathering and concomitant B cell contraction. Using TIRF microscopy, we have linked the function of Grb2, Dok-3 and Cbl to BCR signalling by demonstrating their recruitment to the antigen-containing BCR microcluster. Interestingly, Grb2 was critical for this recruitment independently of Syk and SLP65. Though it has been reported that the ITT motif in the tails of IgG and IgE in class-switched B cells mediates the recruitment of Grb2 to the BCR (Engels et al., 2009), it is not clear how Grb2 is recruited to BCRs lacking the ITT motif. One might expect this is at least in part due to an interaction with SLP65 (Wienands et al., 1998 and Neumann et al., 2009). In contrast, we were able to demonstrate a SLP65-independent recruitment of Grb2 to antigen-containing BCR microclusters indicating an alternative mechanism. We found that Grb2 recruitment to the BCR microcluster was dependent on early B cell signalling through the kinase Lyn and required the SH2 domain of Grb2. Importantly, our data also clearly showed stable recruitment of Grb2 to antigen-containing microclusters even in the absence of the kinase Syk. This indicated that Lyn confers a sufficient amount of tyrosine phosphorylation for binding of Grb2 to BCR-proximal proteins, which, however, remain to be identified. One possible candidate could be the hemopoietic specific protein 1 (HS1) as it binds Lyn and the C-terminal SH3 domain of Grb2 (Takemoto et al., 1998). In line with this, we

have shown recruitment of a chimeric protein consisting of full-length Dok-3 fused to the C-terminal SH3 domain of Grb2 to antigen-containing microclusters. This recruitment was impaired when we introduced a point mutation in the Grb2 SH3 domain. We thus provide evidence for the importance of both central SH2 and C-terminal SH3 domain of Grb2 for recruitment to antigen-containing BCR microclusters. Importantly, the C-terminal SH3 domain was fused to full-length Dok-3 and given our data we cannot conclude on a function of the Dok-3 entity in the recruitment of the fusion protein to antigen-containing BCR microclusters. To clearly elucidate, which domain is crucial for Grb2 recruitment to antigen microclusters one should compare the recruitment of Grb2R86K to a full-length version of Grb2 carrying the W193K mutation. The exact mechanism of Grb2 recruitment to antigen microclusters therefore remains elusive.

As Grb2-deficient mice exhibit an early embryo lethal phenotype and because a conditional Grb2 knockout mouse was not available at the time of our experiments, we have performed our experiments in DT40 chicken B cells (Cheng et al., 1998). We used this system to genetically dissect the interaction of Grb2 with the adaptor Dok-3 localised at the plasma membrane through its N-terminal PH domain (Stork et al., 2007). Dok-3 is highly expressed in several haematopoietic cells including B cells, though it is absent from T cells (Lemay et al., 2000). Consistent with previous suggestions, we observed that stable recruitment of Grb2 to the microcluster is impaired in the absence of Dok-3, but we also present data to show that Grb2 plays a pivotal role in the recruitment of Dok-3 to the microcluster. The interaction between Grb2 and Dok-3 was likely to be direct and was mediated by phosphorylation of Dok-3Y331, which in turn binds the central SH2 domain of Grb2. As the same domain is needed for Grb2 recruitment to antigen microclusters it is conceivable that the interaction of Grb2 and Dok-3 is both direct and highly dynamic.

Finally, our data demonstrating recruitment of SLP65 and CIN85 to antigen-containing BCR microclusters was part of a collaborative effort with the group of Prof Jürgen Wienands (Goettingen, Germany). This work identified Grb2 and CIN85 as stable binding partners of SLP65 in both resting and activated B cells by means of quantitative mass spectrometry (Oellerich et al., 2011). This implies the

existence of a pre-formed signal transduction complex that might be used by B cells for appropriate subcellular targeting of signalling molecules upon BCR activation.

4.4.3 Future directions

Future experiments should address the role of ubiquitin ligases and associated adaptors such as CIN85 or Grb2 in antigen gathering and BCR endocytosis. At present we do not know which molecular feature of Cbl drives these processes and it would be important to investigate whether it is the ubiquitin ligase activity or simply an adaptor function of Cbl. To answer these questions, one could use a Cbl point-mutant, which renders its ubiquitin ligase activity inactive. It is also possible to use inhibitors that specifically target E1 and E2 ubiquitin-conjugating enzymes and thereby block the ubiquitination machinery as a whole.

Furthermore, future work should focus on the exact composition of signalling microclusters. So far, questions regarding signalling molecule stoichiometry remain elusive. Our data moreover suggests that interactions among adaptors and signalling molecules downstream of the BCR are highly dynamic and it is important to investigate their associations with greater time resolution. One should moreover take advantage of the DT40 system to clearly elucidate the requirements of Grb2, Dok-3, Cbl and CIN85 recruitment to antigen-containing BCR microclusters, as our data suggests that signalling molecules can be recruited even in the absence of central proteins such as Syk or SLP65. This implies the existence of protein complexes at the signalling BCR, which are recruited in an immediate fashion dependent on the activity of Lyn kinase. Intriguingly, recent work in the T cell field has shed some light on pre-assembled TCR signalling complexes using high-resolution microscopy techniques (Schamel et al., 2005 and Lillemeier et al., 2010). The activation and integration of pre-formed signal transduction complexes in the context of immunoreceptor signalling will certainly be of great interest in the future.

Chapter 5 : A Potential Role for Myosins in the Movement of Antigen-containing BCR Microclusters

In the previous chapter we identified the three molecules Grb2, Dok-3 and Cbl as important mediators of antigen gathering and concomitant cellular contraction in B cells. The process of antigen gathering is crucial for full activation as it allows the B cell to collect sufficient amounts of antigen molecules to be extracted, processed and eventually presented to specific T cells. We had furthermore shown that antigen gathering is achieved by the directed movement of antigen-containing BCR microclusters towards the central region.

We were intrigued to know, which molecular machinery could potentially create the force to move antigen microclusters in a directed fashion. Since B cell spreading relies on actin polymerisation (Fleire et al., 2006), we focussed our attention on actin-based transport. In particular, we wanted to investigate the role of a family of molecular motors, which move on the underlying actin cytoskeleton: myosins. Myosins constitute a large family of proteins that have been implicated in numerous cellular processes such as myofibril contraction, vesicular transport and cell migration. In particular, a role for non-muscle Myosin IIa was recently reported in the stopping of T cells when encountering antigen on an antigen-presenting cell (Jacobelli et al., 2004). Importantly, Dustin and colleagues had furthermore suggested a function of Myosin IIa in the movement of TCR microclusters (Ilani et al., 2009). The study had shown impaired microcluster movement, when expression of Myosin IIa was downregulated by RNAi or when cells had been treated with the specific Myosin II inhibitor Blebbistatin. It was therefore conceivable that the actin-based molecular motor Myosin IIa could play a role in the centripetal movement of antigen-containing BCR microclusters.

Furthermore, we reasoned that actin filaments extend from the cell centre to the periphery pushing the membrane outward during B cell spreading by actin polymerisation at the leading edge. Actin filaments have a polarised structure with

a growing plus-end where polymerisation of G-actin occurs and a minus-end favouring filament disassembly. The typical centripetal movement of antigen-containing BCR microclusters implied minus-end directed transport as microclusters moved in the opposite, centripetal direction compared to the leading edge of the membrane. We therefore looked for myosin motors showing minus-end directed movement. Among the whole myosin family there is one candidate, which functions as a minus-end directed actin-based motor: Myosin VI (Wells et al., 1999 and Spudich et al., 2010). Interestingly, Myosin VI had been reported to bind the adaptor DAB2, which in turn has been shown to associate with Grb2 (Morris et al., 2002 and Inoue et al., 2002). DAB2 could therefore constitute a link between the signalling BCR and Myosin VI driving directed movement of antigen-containing BCR microclusters.

We consequently sought to investigate, whether Myosin IIa and Myosin VI had a role downstream of the signalling BCR and if they could participate in B cell antigen gathering by directed movement of antigen-containing BCR microclusters.

5.1 Interaction of Myosin IIa and Myosin VI with components downstream of the signalling BCR

5.1.1 A potential interaction of Dok-3 with Myosin IIa and Myosin VI

Given the impaired movement of antigen-containing BCR microclusters in B cells lacking Grb2, Dok-3 or Cbl and a potential role for Myosin IIa in the movement of TCR microclusters, we wanted to investigate, whether both myosins could bind to components of the signalling complex downstream of the BCR. As we had previously shown a function in antigen microcluster movement for Grb2 and Dok-3 and their involvement in BCR signalling, we sought to assess a potential interaction of either Grb2 or Dok-3 with Myosin IIa or Myosin VI.

For this purpose we took advantage of the DT40 system, as knockout cells could be easily re-constituted with a tagged version of the respective protein and this tag could be used in immunoprecipitation experiments. Furthermore, knockout cells represented a good control in those assays. We therefore used DT40 cells lacking endogenous Grb2 or stably expressing Grb2-GFP and left them to rest or stimulated them with surrogate antigen (anti-chicken IgM antibody). Cells were lysed and Myosin IIa was immunoprecipitated with a polyclonal antiserum. Immunoprecipitates were subjected to Western blot analysis probing for GFP with a monoclonal antibody originating from a different host organism than the antibody used for precipitation to reduce cross-reactivity. Grb2 has a molecular mass of 25 kDa, which was in the case of our experiments increased to 50 kDa as Grb2 was tagged with GFP. We detected the presence of Grb2-GFP in whole cell lysates from DT40*Grb2*$^{-/-}$ cells stably expressing Grb2-GFP (Figure 5.1. A). Importantly, we did not detect Grb2-GFP in whole cell lysates of DT40*Grb2*$^{-/-}$ cells. In Myosin IIa immunoprecipitates, we did observe a band of 50 kDa. However, the background also detected in DT40*Grb2*$^{-/-}$ control samples made it impossible to ascertain that Grb2 was specifically co-purified with Myosin IIa. The bands at 50 kDa in Myosin IIa immunoprecipitates might be a result of cross-reactivity, with the secondary HRP-linked antibody used to detect the anti-GFP antibody also detecting the heavy chain of the antiserum used for immunoprecipitation.

With regards to a potential interaction of Myosin VI with Grb2, we used the same experimental setup as for Myosin IIa immunoprecipitations, but used a polyclonal antiserum to precipitate Myosin VI instead. Similarly, when probing for Grb2-GFP in Myosin VI immunoprecipitates, we did observe bands of 50 kDa. However, these bands were again also visible in DT40*Grb2*$^{-/-}$ control samples (Figure 5.1. B). Again, this was presumably the result of antibody cross-reactivity and we could thus not detect copurification of Grb2 with Myosin VI.

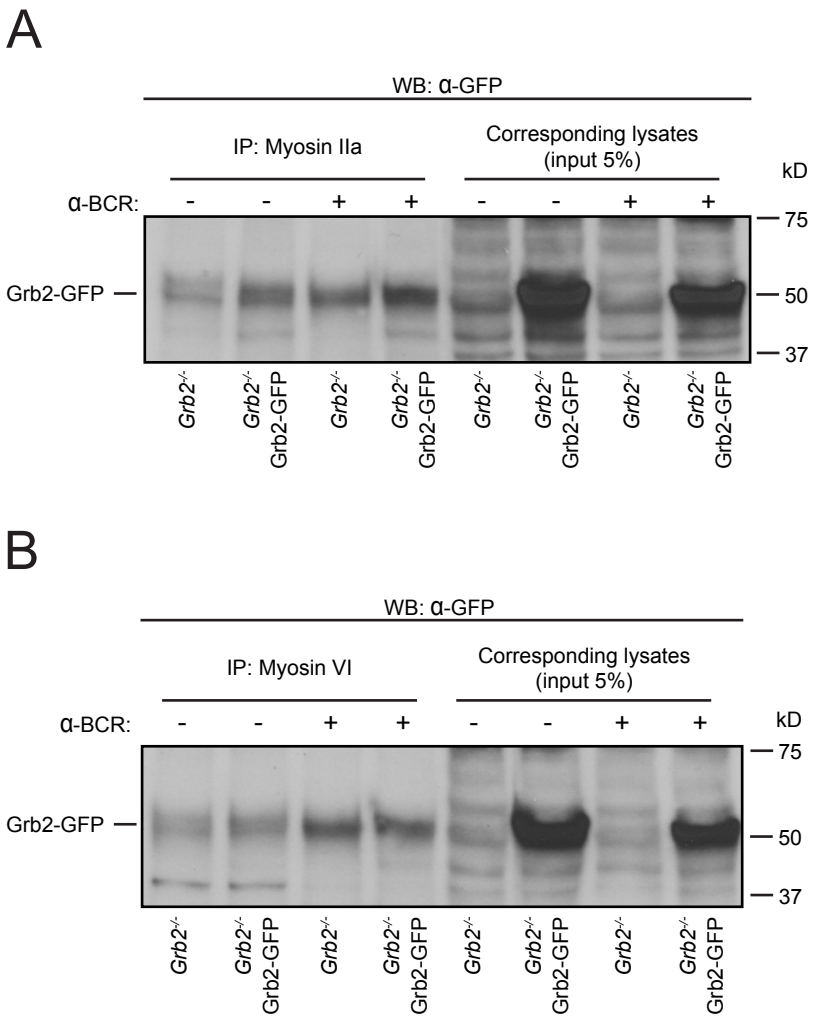

Figure 5.1. Grb2-GFP is not specifically detected in Myosin IIa and Myosin VI immunoprecipitates

(A) DT40*Grb2*$^{-/-}$ cells stably expressing Grb2-GFP were either left to rest or stimulated with an anti-chicken IgM antibody for 5 min. Cells were lysed and Myosin IIa was immunoprecipitated using a polyclonal antibody. Purified complexes were subjected to Western blot probing for the presence of GFP using a monoclonal antibody. DT40*Grb2*$^{-/-}$ cells served as control. Between lysis and immunoprecipitation 5 % (vol) of the lysate was saved to run on the same gel as immunoprecipitates to control for the expression of GFP-tagged Grb2 (4 lanes on right). The band showing at the approximate size of Grb2-GFP in immunoprecipitates is also visible in control samples and is therefore not specific. (B) The experimental setup in A was used to assess a potential interaction of Myosin VI and Grb2 using a polyclonal antiserum against Myosin VI in immunoprecipitations. As in A, a band of the size of Grb2-GFP is also visible in control immunoprecipitates, which suggest an unspecific detection by the probing antibody.

We went on to test the possible interaction between Myosin IIa or Myosin VI and Dok-3 by co-immunoprecipitation. We therefore used DT40 cells lacking endogenous Dok-3 or stably expressing Dok-3-GFP and left them to rest or stimulated them with surrogate antigen. Cells were lysed and Myosin IIa was immunoprecipitated with a polyclonal antibody as before. Chicken Dok-3 has a molecular mass of 50 kDa, resulting in a total weight of approximately 75 kDa when tagged with GFP. We detected the presence of Dok-3-GFP in whole cell lysates from DT40*Dok3*$^{-/-}$ cells stably expressing Dok-3-GFP (Figure 5.2. A). Importantly, we did not detect any Dok-3-GFP in DT40*Dok3*$^{-/-}$ cells. In Myosin IIa immunoprecipitates we indeed detected Dok-3-GFP, which was at the same time absent from DT40*Dok3*$^{-/-}$ control samples. Moreover, bands of 50 kDa were again observed in all four samples indicating a cross-reactivity of HRP-linked and precipitating antibody. Our result therefore suggested an interaction of Myosin IIa and Dok-3.

We next sought to test a possible interaction between Myosin VI and Dok-3 by co-immunoprecipitation in the same manner as before. We detected bands for Dok-3-GFP of correct size both in whole cell lysates and in Myosin VI immunoprecipitates (Figure 5.2. B). Importantly, these bands were absent from DT40*Dok3*$^{-/-}$ control samples. This result implied a potential interaction of Myosin VI and Dok-3 in B cells.

In summary, we have used immunoprecipitation experiments to investigate a potential interaction of Grb2 and Dok-3 with Myosin IIa or Myosin VI. Experiments involving Grb2-GFP were not conclusive due to background bands running at the same height as Grb2-GFP. However, we were able to detect Dok-3-GFP in both Myosin IIa and Myosin VI immunoprecipitates indicating an interaction of Dok-3 with both myosins in B cells.

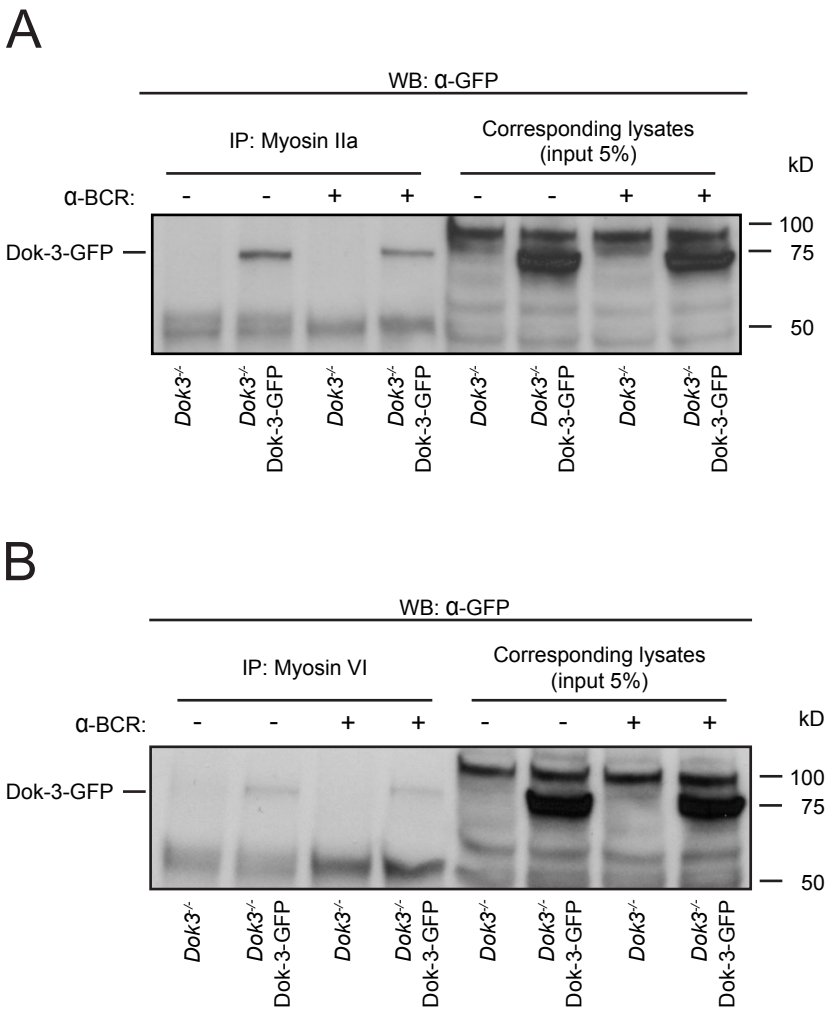

Figure 5.2. Dok-3-GFP appears in Myosin IIa and Myosin VI immunoprecipitates
(A) DT40*Dok3*$^{-/-}$ cells stably expressing Dok-3-GFP were either left to rest or stimulated with an anti-chicken IgM antibody for 5 min. Cells were lysed and Myosin IIa was immunoprecipitated using a polyclonal antibody. Purified complexes were subjected to Western blot probing for the presence of GFP using a monoclonal antibody. DT40*Dok3*$^{-/-}$ cells served as control. Between lysis and immunoprecipitation 5 % (vol) of the lysate was saved to run on the same gel as immunoprecipitates to prove expression of GFP-tagged Grb2 (4 lanes on right). (B) The experimental setup in A was used to assess a potential interaction of Myosin VI and Dok-3. Here, an antiserum against Myosin VI was used in immunoprecipitations.

5.1.2 Myosin IIa and Myosin VI are not co-purified with Dok-3 or Grb2

We wanted to verify our results indicating a possible interaction of Dok-3 and Myosin IIa and Myosin VI by carrying out the reverse experiment and subjected Dok-3 immunoprecipitates to Western blot analysis probing for the two myosins.

First, we validated our method to immunoprecipitate GFP-tagged proteins by lysing DT40 cells lacking Dok-3 or Grb2 re-constituted with Dok-3-GFP or Grb2-GFP. We immunoprecipitated Dok-3-GFP or Grb2-GFP by using a polyclonal antiserum against GFP. DT40 cells lacking Dok-3 or Grb2 served as control. We subjected immunoprecipitates to Western blot analysis detecting GFP. To minimise cross-reactivity with the antiserum used for precipitation, we used a monoclonal anti-GFP antibody from a different species. Whole cell lysates of all cell types demonstrated the expression of Grb2-GFP and Dok-3-GFP (Figure 5.3. A). With regards to GFP immunoprecipitates, we observed GFP-tagged Dok-3 or Grb2, which did not appear in control samples. We were therefore confident that immunoprecipitation of GFP-tagged proteins with a polyclonal antiserum was a suitable tool to purify Dok-3-GFP or Grb2-GFP.

We wanted to use the GFP immunoprecipitation protocol to assess a potential co-purification of Myosin IIa or Myosin VI with Grb2. We therefore used DT40 cells lacking Grb2 or stably expressing Grb2-GFP. Cells were stimulated, lysed and lysates subjected to immunoprecipitations targeting GFP. Immunoprecipitations were then followed by Western blot probing for Myosin IIa, which has a molecular mass of 220 kDa. Given the limited number of commercially available antibodies detecting Myosin IIa, we had to use a polyclonal antibody originating from the same species as the precipitating antibody. We detected bands at the correct size in whole cell lysates from cells used for immunoprecipitation indicating the expression of Myosin IIa (Figure 5.3. B). However, we observed bands in three out of the four samples representing Grb2 immunoprecipitates. We observed bands in control samples and they were generally of higher molecular weight compared to whole cell lysates. We could thus not conclude that Myosin IIa could be co-purified with Grb2.

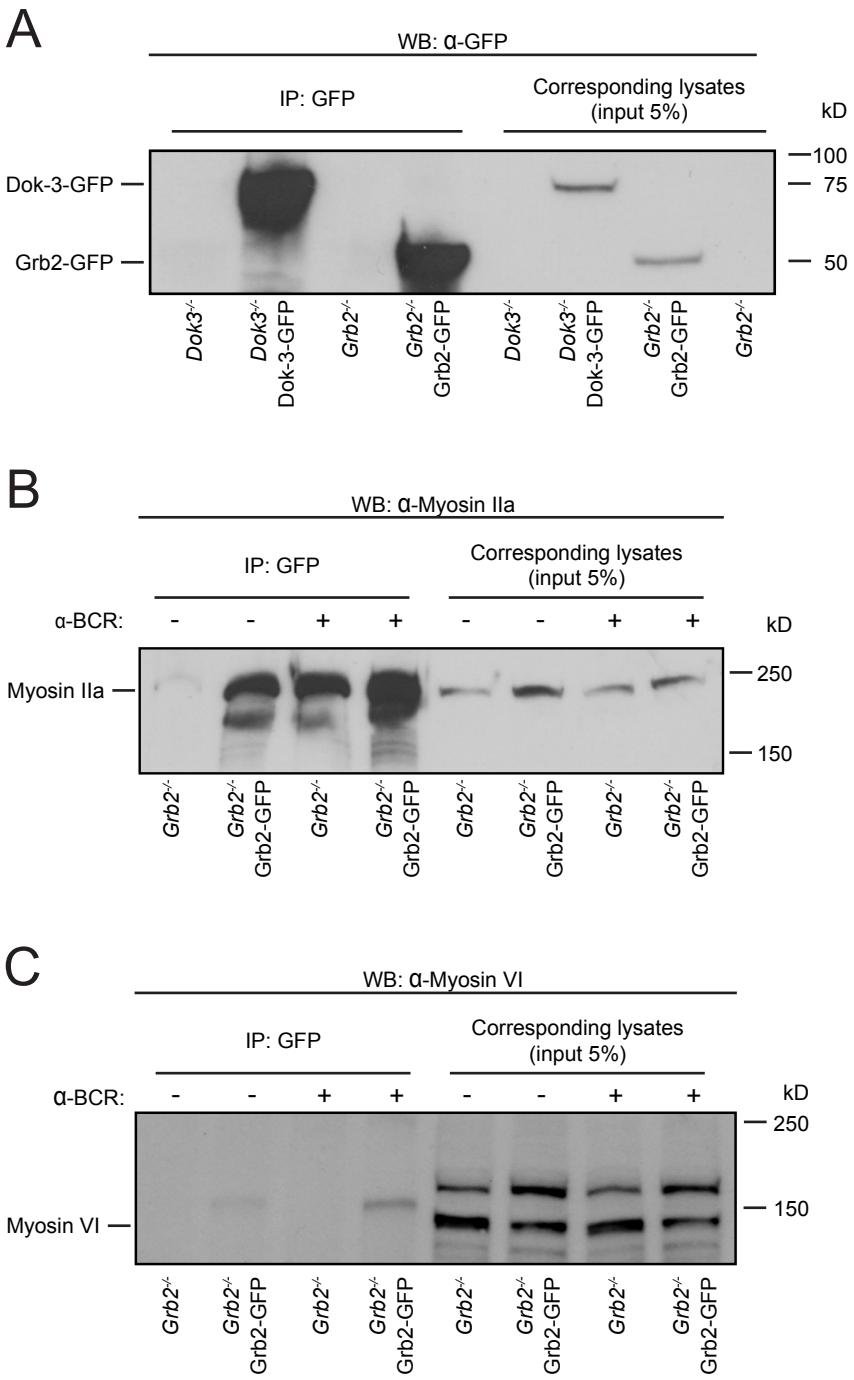

Figure 5.3. Myosin IIa and Myosin VI are not specifically co-immunoprecipitated with Grb2

(A) DT40*Grb2*$^{-/-}$ cells stably expressing Grb2-GFP or DT40*Dok3*$^{-/-}$ cells stably expressing Dok-3-GFP were lysed and GFP was immunoprecipitated using a polyclonal antibody. Purified complexes were subjected to Western blot probing for the presence of GFP using a monoclonal antibody. DT40*Grb2*$^{-/-}$ and DT40*Dok3*$^{-/-}$ cells served as control. Between lysis and immunoprecipitation 5 % (vol) of the lysate was saved to run on the same gel as immunoprecipitates to show the expression of GFP-tagged Grb2 or Dok-3 (4 lanes on right). (B) DT40*Grb2*$^{-/-}$ cells stably expressing Grb2-GFP were either left to rest or stimulated with an anti-chicken IgM antibody for 5 min. Cells were lysed and Grb2 was immunoprecipitated using a polyclonal antibody against GFP. Purified complexes were subjected to Western blot probing for the presence of Myosin IIa using a polyclonal antibody. DT40*Grb2*$^{-/-}$ cells served as control. Between lysis and immunoprecipitation 5 % (vol) of the lysate was saved to run on the same gel as immunoprecipitates to detect expression of Myosin IIa (4 lanes on right). Myosin IIa was also detected in control immunoprecipitations indicating unspecific detection by the probing antibody. (C) The experimental setup in B was applied to assess a potential interaction of Grb2 and Myosin VI using an antiserum to detect Myosin VI in Grb2 immunoprecipitates. Bands detected in immunoprecipitates are of different size compared to lysaes indicating unspecific detection by the probing antibody.

As Grb2 had been reported to bind to the adaptor DAB2, which in turn associates with Myosin VI, we next tried to co-purify Myosin VI with Grb2 applying the same experimental setup as before. We detected bands at the correct size of 140 kDa in whole cell lysates from cells used for immunoprecipitation indicating the expression of Myosin VI (Figure 5.3. C). We also observed bands in Grb2 immunoprecipitates, which were not visible in control samples. In addition, the intensity of the band increased upon stimulation with surrogate antigen. However, these bands were of slightly higher molecular weight as the bands detected in whole cell lysates. This implied problems concerning specificity either with regards to the immunoprecipitation or the antibody used to detect Myosin VI. The latter reason is unlikely, however, as the antiserum detected bands of the correct size in whole cell lysates. We could therefore not robustly establish an interaction between Myosin VI and Grb2 using this method.

Given our observation of a potential interaction between Dok-3 and Myosin IIa, we went on to assess this by immunoprecipitating Dok-3-GFP and probing for Myosin IIa using Western blot. We used DT40 cells lacking Dok-3 or stably expressing Dok-3-GFP and left them to rest or stimulated them with surrogate antigen. Cells were lysed and Dok-3-GFP was immunoprecipitated with a polyclonal antiserum. Immunoprecipitates were subjected to Western blot analysis probing for the existence of Myosin IIa. We did detect bands at the correct size in whole cell lysates from cells used for immunoprecipitation (Figure 5.4. A). Regarding Dok-3 immunoprecipitates we observed bands in all samples including controls. In addition, these bands were again of slightly higher molecular weight as the bands detected in whole cell lysates. This implied that either the antibody used to detect Myosin IIa or the immunoprecipitation itself were non-specific. The latter reason is unlikely, however, as the antiserum detected bands of the correct size in whole cell lysates. We could therefore not conclude that Myosin IIa could be co-purified with Dok-3.

We next sought to verify our results indicating a possible interaction of Dok-3 and Myosin VI by carrying out the reverse experiment and subjected Dok-3 immunoprecipitates to Western blot analysis probing for Myosin VI using DT40 cells lacking Dok-3 or stably expressing Dok-3-GFP. Chicken Myosin VI has a molecular mass of approximately 140 kDa and we detected bands at the correct size in whole cell lysates from cells used for immunoprecipitation (Figure 5.4. B). However, we did not observe any bands of the same size in Dok-3 immunoprecipitates. This indicated, that Myosin VI could not be co-purified with Dok-3 and did thus not support our earlier result showing the presence of Dok-3-GFP in Myosin VI immunoprecipitates.

In summary, we have not been able to robustly show an interaction of either Myosin IIa or Myosin VI with Grb2 or Dok-3. Although Dok-3-GFP could be co-purified with both myosins, the reverse experiment precipitating Dok-3 and probing for Myosin IIa or Myosin VI did not confirm this potential interaction. This was possibly due to unspecific binding of proteins during immunoprecipitation or unspecific antibodies used for detection in Western blots. One reason accounting for the initial detection of Dok-3 in Myosin IIa and VI immunoprecipitates could be the high expression level of DT40*Dok3*$^{-/-}$ cells re-constituted with Dok-3-GFP. The stable expression of Dok-3-GFP could be high enough to allow Dok-3-GFP to stick non-specifically to protein A/G beads used to couple the precipitating antibody. Moreover, one would anticipate a model, which assumes an interaction of Dok-3 and Myosin IIa or Myosin VI induced by BCR signalling. It was thus surprising that the amount of Dok-3 co-purified with Myosin IIa or Myosin VI did not increase upon activation of cells via their BCR.

Regarding experiments involving Grb2-GFP, we concluded that the secondary HRP-linked antibody used in the Western blot cross-reacted with the heavy chain of the antibody used for immunoprecipitations. This created background bands in all samples masking potential bands representing Grb2-GFP. Although we used cross-adsorbed antibodies from different host species this could not be avoided. In addition, the amount of antiserum used for immunoprecipitation was in the microgram range, leading to very high concentrations of antibody molecules present in all samples and thus possibly favouring cross-reactivity.

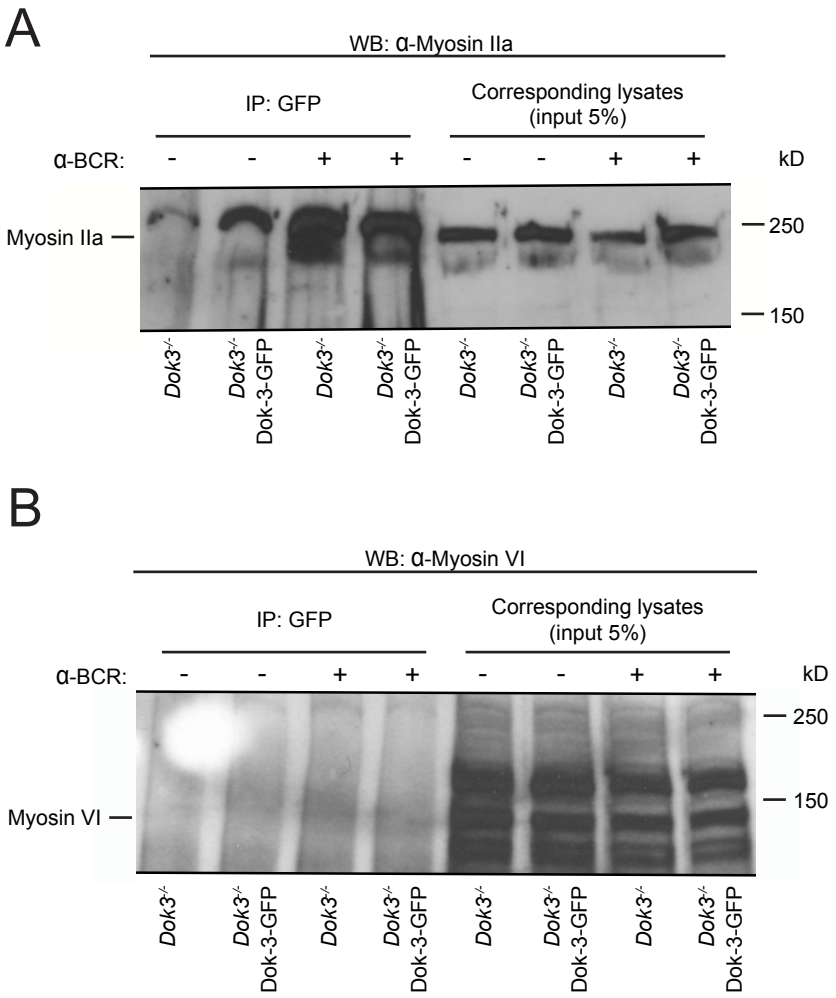

Figure 5.4. Myosin IIa and Myosin VI are not specifically co-purified with Dok-3
(A) DT40*Dok3*$^{-/-}$ cells stably expressing Dok-3-GFP were either left to rest or stimulated with an anti-chicken IgM antibody for 5 min. Cells were lysed and Dok-3 was immunoprecipitated using a polyclonal antibody against GFP. Purified complexes were subjected to Western blot probing for the presence of Myosin IIa using a polyclonal antibody. DT40*Dok3*$^{-/-}$ cells served as control. Between lysis and immunoprecipitation 5 % (vol) of the lysate was saved to run on the same gel as immunoprecipitates to show expression of MyosinVI (4 lanes on right). Bands appearing in control immunoprecipitates indicate that the probing antibody was unspecific. (B) The experimental setup in A was used to assess a potential interaction of Myosin VI and Dok-3. No significant bands of the size of Myosin VI could be detected in Dok-3 immunoprecipitates.

Thus this particular biochemical approach did not provide us with a reliable tool to investigate a potential association of Myosin IIa or Myosin VI with components of antigen-containing BCR microclusters.

5.2 Dynamic localisation of Myosin IIa and Myosin VI in activated B cells

5.2.1 Myosin IIa and Myosin VI are not recruited to antigen-containing BCR microclusters

Our immunoprecipitation experiments provided some evidence for an interaction of Myosin IIa and Myosin VI with Dok-3. However, this biochemical approach did not allow us to investigate the spatiotemporal localisation and dynamic behaviour of Myosin IIa and Myosin VI in activated B cells. We consequently applied our lipid bilayer system for antigen presentation coupled to high-resolution TIRF microscopy to assess a potential recruitment of GFP-tagged Myosin IIa and Myosin VI to antigen-containing BCR microclusters.

For this purpose, we used the murine B cell line A20 stably expressing a recombinant BCR (D1.3) recognising Hen-egg lysozyme (Hel). We transiently expressed Myosin IIa-GFP in A20 D1.3 B cells and settled them on fluorescent lipid bilayers loaded with Hel antigen. Images of fully spread cells were acquired using TIRF microscopy and revealed cluster formation of Myosin IIa-GFP (Figure 5.5. A and Supplementary Video 7). Yet, these clusters only showed very limited colocalisation with antigen-containing BCR microclusters as revealed by scanning fluorescence in both channels along a line. The low-level colocalisation was not maintained over time (Supplementary Video 7). This result showed that Myosin IIa recruitment to antigen-containing BCR microclusters was very limited and implied that Myosin IIa was possibly not linked to the directed movement of antigen microclusters.

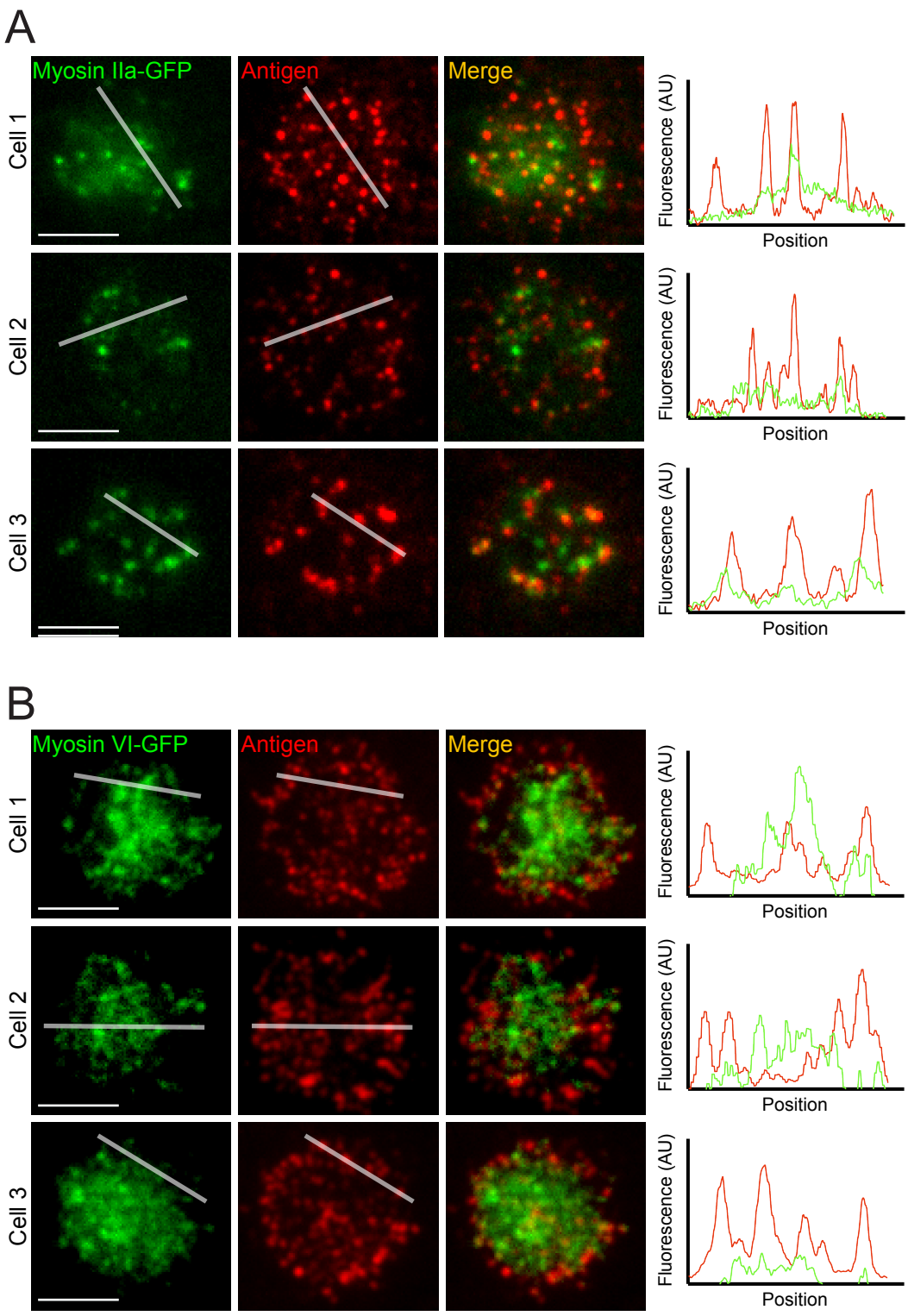

Figure 5.5. Myosin IIa and Myosin VI do not co-localise with antigen-containing BCR microclusters

(A) A20 mouse B cells stably expressing a Hen egg lysozyme (Hel)-specific BCR were transiently transfected with a vector coding for MyosinIIa-GFP. 16 hours after transfection cells were settled on lipid bilayers loaded with Hel and images were acquired 5 min after settling using TIRF microscopy. Three representative cells are shown. Co-localisation of antigen and GFP was assessed by scanning fluorescence in both channels along translucent lines. (B) The same experimental setup as in A was used to investigate the recruitment of Myosin VI-GFP to antigen-containing BCR microclusters in A20 D1.3 B cells. All scale bars equal 5 µm.

To investigate a potential recruitment of Myosin VI to antigen-containing BCR microclusters we applied the same experimental setup as before using A20 D1.3 B cells transiently expressing a GFP-tagged version of Myosin VI. Images of fully spread cells were acquired using TIRF microscopy and revealed smaller clusters and large patches of Myosin VI-GFP (Figure 5.5. B and Supplementary Video 8). Yet, these clusters and patches did not colocalise with antigen-containing BCR microclusters. This result implied that Myosin VI was not recruited to the signalling BCR microcluster. A possible link between Myosin VI and the BCR could therefore not be established.

To sum up, both Myosin IIa and Myosin VI did not show notable recruitment to antigen-containing BCR microclusters. This verified our previous results involving immunoprecipitation experiments showing that Myosin IIa and Myosin VI possibly do not directly interact with components downstream of the signalling BCR.

5.2.2 Myosin VI does not mediate antigen gathering in B cells

To investigate a potential function of Myosin VI in the directed movement of antigen-containing BCR microclusters, we used primary B cells from mice lacking Myosin VI or from wildtype littermates (Avraham et al., 1995). We settled wildtype or Myosin VI-deficient cells on lipid bilayers loaded with surrogate antigen (anti-mouse κ light-chain). As shown by TIRF microscopy, both Myosin VI knockout and wildtype cells spread over the antigen-presenting surface, formed antigen microclusters and gathered them in the central area by directed movement (Figure 5.6. A and B and Supplementary Video 9). We had thus produced additional proof that Myosin VI was not directly linked to the centripetal movement of antigen-containing BCR microclusters.

In conclusion, we have shown very limited recruitment of a GFP-tagged version of Myosin IIa to antigen-containing BCR microclusters, which was not stable over time. Furthermore, a GFP-tagged Myosin VI was not recruited to antigen-containing BCR microclusters. In addition, we examined the movement of antigen-containing BCR microclusters in primary B cells from mice lacking Myosin VI and did not observe altered antigen gathering compared to wildtype

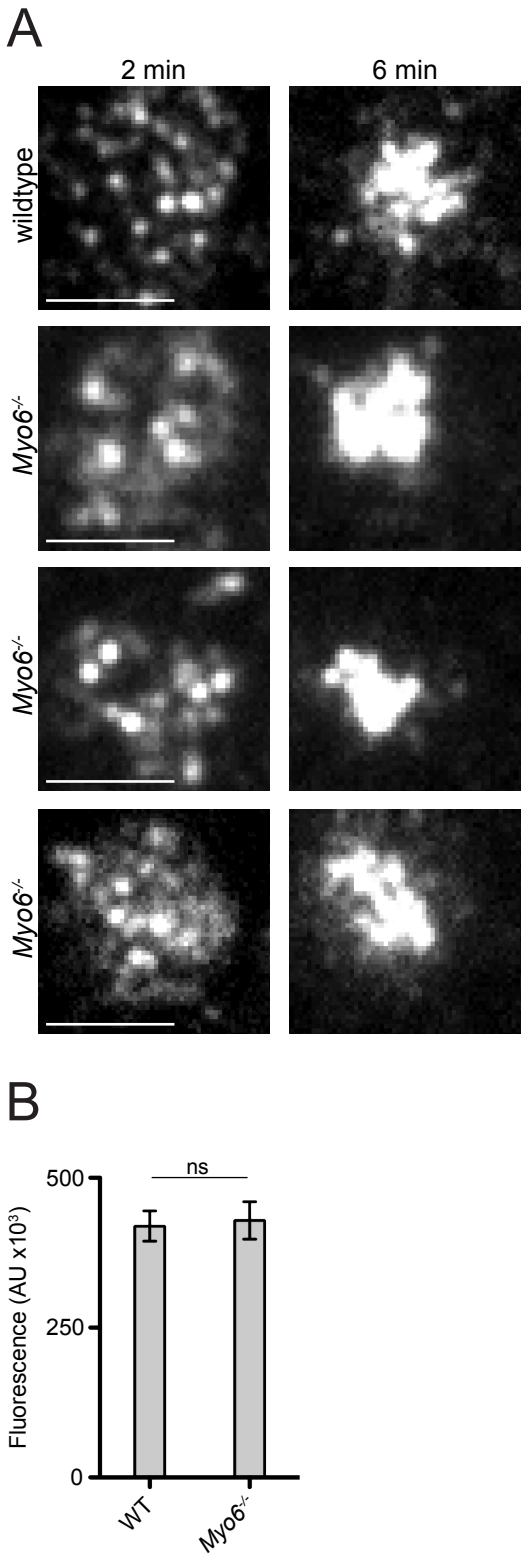

Figure 5.6. Myosin VI is not inolved in antigen gathering by B cells
(A) Primary B cells from mice lacking Myosin VI (*Myo6*$^{-/-}$) or from wildtype (WT) littermates were settled on lipid bilayers loaded with surrogate antigen (anti-mouse kappa light-chain) and images were acquired using TIRF microscopy two and six minutes after settling. Three representative knockout cells are shown. All scale bars equal 5 μm. (B) Quantification of antigen accumulation after six minutes by WT and *Myo6*$^{-/-}$ B cells. Antigen was quantified as total fluorescence.

littermates. We therefore concluded that Myosin IIa and Myosin VI did not play an essential role as part of the signalling complex downstream of the BCR as shown by high-resolution microscopy. It was thus unlikely that Myosin IIa or Myosin VI could drive the centripetal movement of antigen-containing BCR microclusters through a direct interaction with the BCR.

5.3 Discussion

By using a combination of biochemical and imaging techniques we have investigated the role two myosins in the movement of antigen-containing BCR microclusters. In particular, we have assessed a potential interaction of either Myosin IIa or Myosin VI with Grb2 and Dok-3. We have been able to detect Dok-3 in both Myosin IIa and Myosin VI immunoprecipitates. However, we could not show the reverse by detecting both Myosins in Dok-3 immunoprecipitates. We went on to test, whether GFP-tagged versions of Myosin IIa or Myosin VI could be recruited to antigen-containing BCR microclusters when expressed in A20 mouse B cells, which were settled on antigen-containing lipid bilayers. We observed clustering of both myosins at the plasma membrane when B cells were settled on the lipid bilayer. However, these myosin clusters only colocalised with antigen-containing BCR microclusters in a very limited manner indicating that Myosin IIa or Myosin VI are not responsible for the movement of antigen microlcusters. In the case of Myosin VI we obtained spleens from mice lacking Myosin VI or wildtype littermates. We isolated primary B cells and did not observe altered antigen gathering by directed antigen microcluster movement in both wildtype and Myosin VI knockout cells. We therefore conclude that Myosins IIa and VI do not play a critical role in the gathering of antigen by B cells.

5.3.1 The role of Myosins in B cell activation

Myosin IIa has been shown to be involved in the movement of TCR microclusters and thus contribute to T cell activation (Ilani et al., 2009). Apart from this finding, Myosin IIa has been implicated to play a role in other immune cell functions such as the release of cytolytic granules by NK cells (Andzelm et al., 2007 and Sanborn et al., 2009). Specifically in B cells Myosin IIa has been shown to drive the intracellular trafficking of MHC class II molecules to enable BCR-triggered antigen presentation to specific T cells (Vascotto et al., 2007). Furthermore, other myosins have also been reported in the context of B cell activation. In particular, Myosin I is a substrate of the phosphatase SHP-1 after BCR cross-linking indicating an interaction of Myosin I with the signalling complex downstream of the BCR (Baba et al., 2003). Myosin I was also found to be recruited to the B cell immune synapse and ultimately contributed to antigen presentation by B cells (Patino-Lopez et al., 2010 and Maravillas-Montero et al., 2011). It is therefore likely that myosins contribute to B cell activation by providing a platform for intracellular trafficking. Given the large size of the myosin family of motor proteins their exact functions during B cell activation remain to be explored.

5.3.2 Retrograde actin flow as a driving force for microcluster movement

Cell motility and spreading both rely on a balance between actin polymerisation at the leading edge and concomitant actin filament disassembly. The resulting phenomenon of circulating F-actin fragments is therefore called treadmilling or retrograde actin flow. Interestingly, Myosin II has been shown to participate in the disassembly of actin filaments in the uropods of motile cells thus allowing them to move (Wilson et al., 2010). Furthermore, previous work in the T cell field had shown that centripetal movement of TCR microclusters was F-actin dependent and postulated a role for retrograde actin flow (Kaizuka et al., 2007 and DeMond et al., 2008). In addition, Bunnell and colleagues introduced the impact of integrin signalling on the movement of microclusters. In this paper they showed a slower, actin flow-mediated movement of SLP-76 microclusters when the TCR and the integrin VLA-4 were coligated (Nguyen et al., 2008). However, close investigations of the directed movement of TCR microclusters proved that they

moved at only about half the speed of the underlying actin cytoskeleton. This observation implied the existence of alternative, active transport mechanisms for translocation of microclusters.

In conclusion, we do not exclude a function for myosins in B cell activation *per se*. Still, we were not able to show a function for either Myosin IIa or Myosin VI in the directed movement of antigen-containing BCR microclusters. B cells therefore gather antigen on the surface of antigen-presenting cells in a mechanism possibly independent of Myosin IIa and Myosin VI. However, this mechanism remains elusive.

Chapter 6 : Cytoplasmic Dynein Drives Antigen Gathering in B Cells

Our earlier work had established a role for Grb2, Dok-3 and Cbl in B cell antigen gathering by the directed movement of antigen-containing BCR microclusters. We had furthermore shown that Myosin IIa and Myosin VI did not interact with the signalling complex downstream of the BCR and could thus not be accounted for the force generation needed to move antigen microclusters. To gain insights into the mechanisms driving antigen microcluster movement, we therefore chose a screening approach to elucidate components of the signalling BCR complex and possibly identify novel proteins linked to movement on a subcellular level.

In collaboration with Prof Jürgen Wienands and Prof Henning Urlaub (Göttingen, Germany) we made use of a mass spectrometric approach to shed light on the signalling complex acting at the cross-linked BCR. We used a novel approach applying stable isotope labelling by amino acids in cell culture (SILAC) followed by high-end tandem mass spectrometry. We selected the kinase Syk as a marker for antigen microclusters as Syk directly binds phosphorylated Tyrosines in the ITAMs of the Igα and Igβ subunits of the BCR and is recruited to antigen microclusters upon BCR ligation. Briefly, DT40*Syk*$^{-/-}$ cells stably expressing wildtype Syk or a tagged version of Syk were cultured in medium containing either 'light' or 'heavy' amino acids, respectively. Cells were stimulated for five minutes with an anti-chicken IgM antibody, lysed and Syk was affinity purified via its tag. Purified complexes were pooled, trypsin digested and subjected to liquid chromatography-coupled tandem mass spectrometry. Detected unique peptides were then assigned to a specific protein. Importantly, the SILAC method allowed us to quantitatively measure the enrichment of peptides above background as specifically enriched peptides showed a higher mass due to heavier amino acids compared to their unlabelled counterparts originating from cells expressing untagged Syk. Figure 6.1. A illustrates the working principle of our mass spectrometric approach to elucidate the Syk interactome.

6.1 Dynein associates with the BCR signalling complex and moves antigen-containing microclusters

6.1.1 Quantitative mass spectrometry reveals a possible link between Syk and the microtubule-based motor dynein

In an attempt to identify novel proteins downstream of the BCR that might be responsible for the centripetal movement of antigen-containing BCR microclusters, we chose an approach based on quantitative mass spectrometry to elucidate the Syk interactome. This method allowed us to find new binding partners of the kinase Syk in activated B cells.

In order to obtain the Syk interactome we re-constituted DT40*Syk*$^{-/-}$ B cells either with Syk or a tagged version of Syk and cultured cells in medium containing 'light' or 'heavy' amino acids, respectively. Cells were activated and Syk subsequently purified via its tag. Purified complexes were pooled and unique peptides identified using mass spectrometry. As shown in Figure 6.1. B, peptides identifying Syk itself were found in the digested MS-MS sample. The same peptide was found twice with different masses relating to the medium cells were initially cultured in. The 'heavy' peptide identifying Syk originated from cells expressing tagged Syk, whereas the 'light' peptide was purified unspecifically as Syk was not tagged in these cells. The difference in height of the peaks for both peptides indicated that the 'heavy' peptide was purified much more efficiently than the 'light' peptide. This indicated that our purification of tagged Syk was indeed specific.

Furthermore, we also assessed the enrichment of peptides identifying proteins, which are not related to BCR signalling. In particular, we investigated the enrichment of the ribosomal protein L10 (Figure 6.1. C). Peaks for both 'heavy' and 'light' peptides uniquely identifying L10 were of similar height, thus indicating that proteins not related to BCR signalling were not specifically purified with Syk. The specific enrichment of peptides identifying Syk and the unspecific purification of peptides uniquely linked to proteins not related to BCR signalling

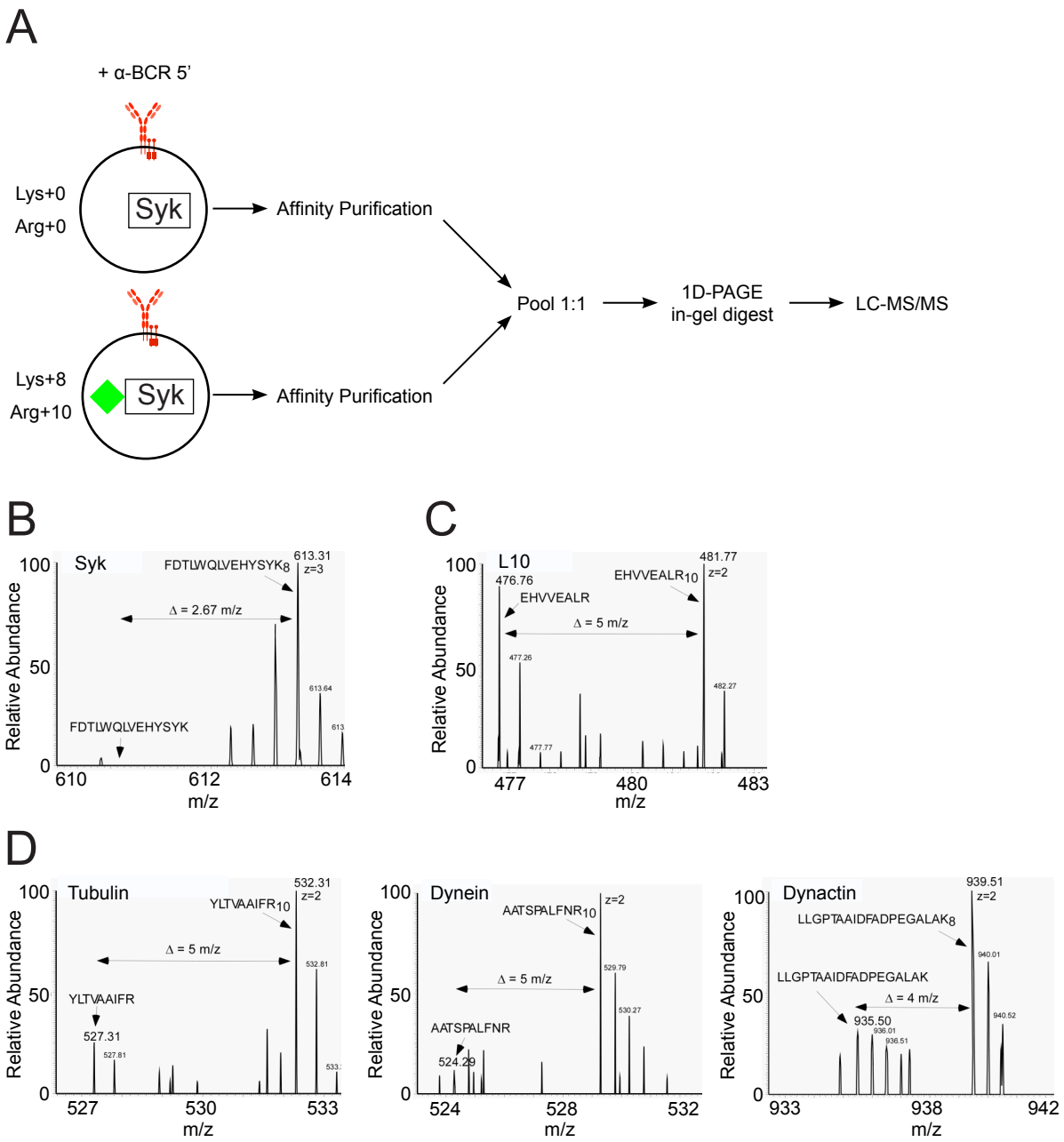

Figure 6.1. The Syk interactome reveals components of the dynein machinery and the microtubule network

(A) Schematic representing the workflow to reveal the Syk interactome. Briefly, DT40*Syk*$^{-/-}$ cells stably expressing either untagged or tagged Syk were cultured in medium containing 'heavy' and 'light' amino acids. Cell were stimulated with an anti-chicken IgM antibody for 5 min, lysed and tagged Syk was purified in a column via its tag. Samples were pooled, digested in a PAGE gel and subjected to liquid chromatography-coupled tandem mass spectrometry. (B-D) Quantitative mass spectra of peptides derived from proteins Syk, L10, Tubulin beta-2 chain, Dynein heavy chain, and Dynactin. Shown are the spectra with the mass peaks of the corresponding Lys+8 and Arg+10 labelled peptides and their non-labelled counterparts. The sequence of the peptides, the measured precursor masses (m/z values) and the charge stages (z) are listed within the spectra. The signal intensity between the labelled peptide and the non-labelled counterpart is quantitative, i.e. it reflects the abundance of the corresponding peptide and thus of the protein in the tagged or non-tagged sample. The calculated m/z differences between the labelled and non-labelled peptides are indicated in the spectra. Accordingly, Lys+8 or Arg+10 labelled peptides that showed significantly stronger signal intensity as their non-labelled counterparts derived from those proteins that specifically interact with the tagged Syk-protein (i.e. Tubulin beta-2 chain, Dynein, Dynactin). Data generated by collaborators T. Oellerich, H. Urlaub, M. Engelke and J. Wienands.

verified our mass spectrometric method to elucidate the Syk interactome as both specific and quantitative.

We listed all unique peptides and their enrichment above background and identified a plethora of proteins specifically purified with Syk from activated B cells. Within that list of proteins, our attention was drawn to the enrichment of a number of peptides derived from several tubulins, in particular Tubulin beta-2 (Figure 6.1. D, left panel). The discovery of tubulins in the Syk interactome hinted at a possible link between BCR microclusters and the microtubule network. In line with this Syk has been shown to phosphorylate α-tubulin following BCR stimulation (Peters et al., 1996). Moreover, we also observed a 13.8- and 1.8-fold enrichment of peptides corresponding to the heavy chain of cytoplasmic dynein (DYNC1H1) and the dynactin subunit 2 (DCTN2; dynamitin), respectively (Figure 6.1. D, middle and right panels). The identification of dynein was consistent with the enrichment of tubulin, as dynein is a microtubule-based minus-end directed motor protein transporting intracellular cargo along microtubules (Vale, 2003). In addition, dynamitin is a subunit of the multi-molecular dynactin complex, which links dynein to its cargo and regulates its activity (Kardon and Vale, 2009).

In summary, we have elucidated the Syk interactome by applying a quantitative mass spectrometric approach. We have validated this method by showing the specific enrichment of Syk and unspecific purification of the ribosomal protein L10, which is not linked to BCR signalling. We have furthermore found a possible link between Syk and the microtubule-based motor dynein as we co-purified peptides uniquely identifying tubulin beta-2, the cytoplasmic dynein heavy chain 1 and the dynamitin subunit of the dynactin complex.

6.1.2 Cytoplasmic dynein associates with antigen-containing BCR microclusters

Using an approach to identify the Syk interactome by mass spectrometry we had obtained initial indications that Syk interacted with the microtubule-based motor protein dynein. To test, whether this indication could potentially explain what was generating the force to move antigen-containing BCR microclusters, we used different techniques to verify a potential link between the signalling BCR and dynein.

First, we used co-immunoprecipitation to assess a possible interaction between Syk and cytoplasmic dynein. We therefore made use of the DT40 system and re-constituted Syk-deficient cells with Syk carrying a Citrine tag. Citrine is structurally very similar to GFP and could therefore be immunoprecipitated using a polyclonal anti-GFP antiserum. We consequently purified Syk from activated DT40 cells via its Citrine tag and subjected purified complexes to Western blot probing for the dynein intermediate chain of 74 kDa (DYNC1I1). DT40 wildtype cells not expressing Citrine-tagged Syk served as control (Figure 6.2. A). We observed a duplet band of approximately 75 kDa in whole cell lysates indicating that this subunit of the dynein complex was expressed in DT40 B cells. Importantly, the same duplet band was detected in Syk immunoprecipitates and not in wildtype control samples. This result confirmed our finding obtained by mass spectrometry and suggested an interaction of Syk and the dynein complex in activated B cells.

To further verify our results that dynein might interact with components of the antigen-containing BCR microcluster, we used high-resolution TIRF microscopy to investigate, whether a GFP-tagged version of the DYNC1I1 was recruited to antigen microclusters when cells were settled on artificial bilayers containing antigen. We therefore transduced primary mouse MD4 B cells with a retroviral vector coding for DYNC1I1-GFP and settled cells on lipid bilayers containing the antigen Hen egg lysozyme (Hel) and ICAM-1. MD4 B cells express a transgenic BCR, which specifically recognises Hel antigen. ICAM-1 is the natural ligand for the integrin Lfa-1 and enables primary B cells to adhere to the lipid bilayer and potentiates intracellular signalling upon BCR stimulation. We took snapshots using a TIRF microscope when cells were fully spread and observed clustering of

both antigen and DYNC1I1-GFP (Figure 6.2. B). When scanning fluorescence for both channels along a line we were able to show that clusters of DYNC1I1-GFP and antigen colocalised. By using high-resolution imaging and primary mouse B cells expressing a GFP-tagged version of the dynein intermediate chain of 74 kDa we were thus able to verify a link between the dynein machinery and the signalling BCR.

As dynein is most commonly associated with the transport of intracellular cargo along microtubules, the association with antigen-containing BCR microclusters and components such as Syk raised the intriguing possibility that dynein and dynactin participate in microcluster movement during antigen gathering. To investigate this, we used primary mouse B cells transiently expressing DYNC1I1-GFP coupled to antigen-bearing lipid bilayers and TIRF microscopy as before. We acquired image sequences to follow the distribution of DYNC1I1-GFP relative to antigen-containing BCR microclusters over time. Interestingly, clusters of DYNC1I1-GFP colocalised with antigen-containing BCR microclusters in all frames (Figure 6.2. C and Supplementary Video 10). We quantified the colocalisation of antigen and GFP for each frame and found a high degree of colocalisation over the course of image acquisition (Figure 6.2. D). Our findings thus indicated that DYNC1I1-GFP migrated with antigen-containing BCR microclusters towards the centre of the cell.

Taken together we have shown an interaction of the dynein intermediate chain of 74 kDa (DYNC1I1) with Syk in activated B cells and recruitment of DYNC1I1-GFP to antigen-containing BCR microclusters. Moreover, DYNC1I1-GFP moved with antigen microclusters over time indicating a role for the dynein machinery in the directed centripetal transport of antigen-containing BCR microclusters in B cells.

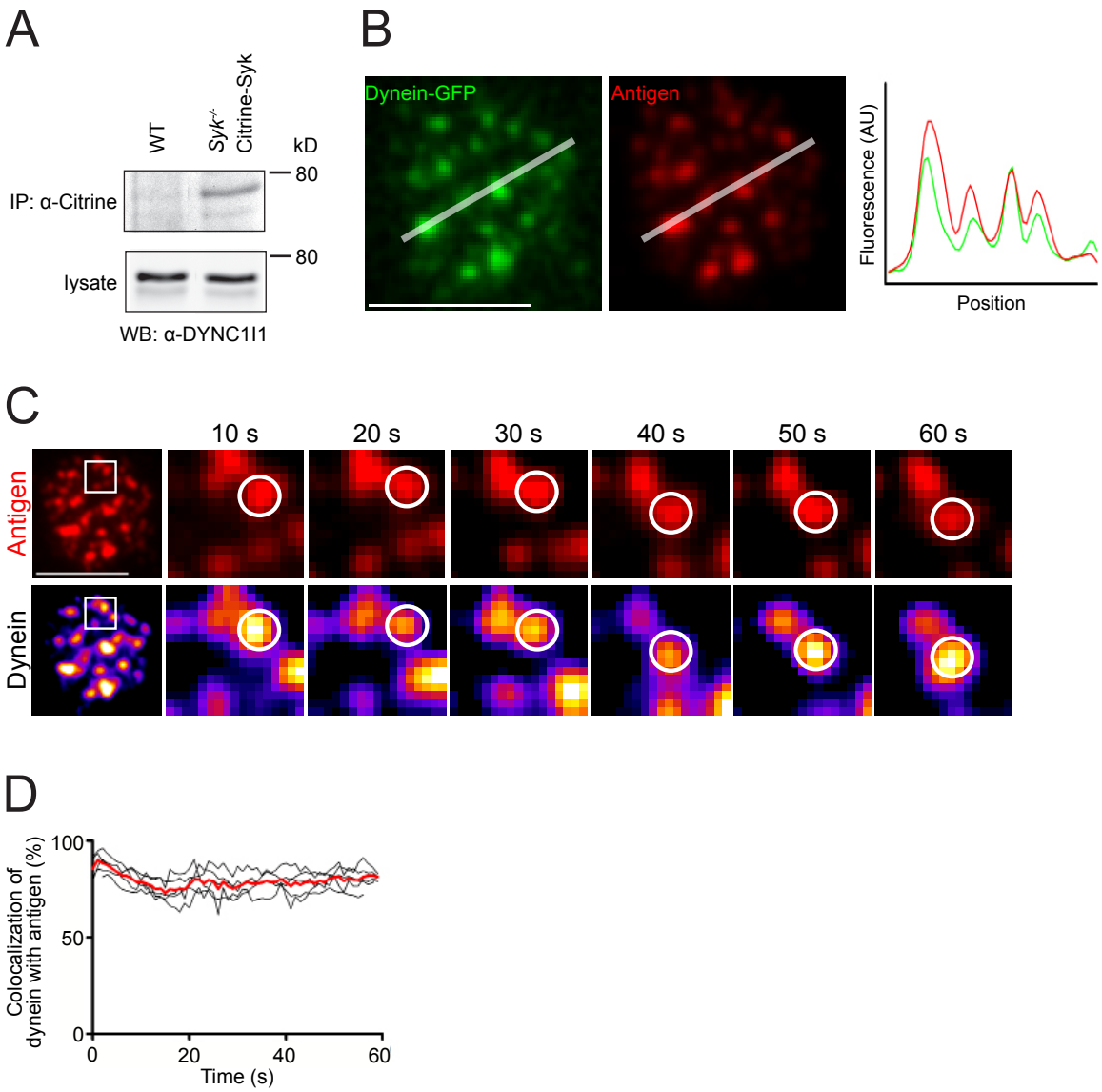

Figure 6.2. Cytoplasmic dynein binds to antigen-containing BCR microclusters
(A) DT40*Syk*$^{-/-}$ cells stably expressing Citrine-Syk were activated with 5 µg/ml of an anti-chicken IgM antibody for three minutes, lysed and Syk was immunoprecipitated using an anti-GFP antibody. Immunoprecipitates were subjected to Western blotting and the dynein intermediate chain of 74 kD (DYNC1I1) was detected with a monoclonal antibody. DT40*Syk*$^{-/-}$ cells served as control; endogeneous expression of dynein intermediate chain is shown in cell lysates (lower panels, lysate). (B) Primary murine B cells transiently expressing dynein intermediate chain-GFP (Dynein-GFP) were settled on planar lipid bilayers containing surrogate antigen and unlabelled ICAM-1. Snapshots were acquired using TIRFM when cells were fully spread. Co-localisation of antigen microclusters and dynein-GFP is visualized by plotting the respective fluorescence along the translucent lines in the diagram on the right. (C) The experimental setup in B was used to investigate dynamic movement of dynein-GFP (pseudocolor) with antigen microclusters (red). Time-lapse images show a magnified area indicated by a white box in the images on the left. White circles highlight the location of antigen and dynein-GFP at the same position in the images for each timepoint. (D) The plot shows quantification of antigen microclusters co-localising with dynein-GFP over time; black lines represent single cells, the red line shows the mean value of all cells. Co-localisation analysis was carried out using Imaris software according to methods. All scale bars equal 5 µm.

6.1.3 Cytoplasmic dynein drives centripetal movement of antigen-containing BCR microclusters for antigen gathering by B cells

To investigate the role of dynein in the directed transport of antigen-containing BCR microclusters and thus in antigen gathering by B cells, we used two alternative approaches. The first involved over-expression of the dynamitin subunit (p50) of the dynactin complex. Dynamitin over-expression has a dominant-negative effect on dynein function and leads to dissociation of the dynein complex from its cargo (Burkhardt et al., 1997). The second approach involved downregulation of dynein expression by transfection of murine B cells with shRNA targeting the cytoplasmic dynein heavy chain 1 (DYNC1H1).

We first validated both methods by expressing either a plasmid coding for Dynamitin-GFP or an shRNA targeting DYNC1H1. The shRNA expression vector included an IRES-GFP that allowed us to identify B cells expressing the construct based on GFP-fluorescence. We electroporated murine A20 B cells stably expressing a transgenic BCR (D1.3) recognising Hen egg lysozyme (Hel) with the plasmid coding for Dynamitin-GFP and assessed expression of Dynamitin by Western blot. Untransfected cells served as control. Figure 6.3. A shows expression of Dynamitin in both samples. Importantly, cells that had been transfected with Dynamitin-GFP also showed a band at 75 kDa, which corresponds to the molecular mass of Dynamitin (p50) plus the GFP-tag. We were therefore confident that we were able to express Dynamitin-GFP in A20 B cells.

Regarding the downregulation of DYNC1H1 expression, we used a construct coding for an shRNA targeting DYNC1H1 and soluble GFP. We electroporated A20 D1.3 B cells with the shRNA vector and sorted cells based on their GFP-expression 16 hours after transfection using flow cytometry (Figure 6.3. B). We left cells positive and negative for GFP for 48 hours and subsequently subjected them to Western blot analysis assessing expression of DYNC1H1 (Figure 6.3. C). We quantified the expression of DYNC1H1 in both GFP-positive and –negative populations and found a reduced expression of DYNC1H1 in B cells expressing GFP. We had thus verified that the shRNA construct provided us with a tool for DYNC1H1 downregulation in murine B cells.

If dynein played a role in the directed movement of antigen-containing BCR microclusters, A20 D1.3 B cells either over-expressing Dynamitin-GFP or showing reduced amounts of dynein heavy chain 1 protein by means of RNAi should show a defect in centripetal movement of antigen microclusters, when settled on lipid bilayers containing antigen. To test this hypothesis, we used A20 D1.3 cells expressing Dynamitin-GFP or an shRNA targeting DYNC1H1 and settled them on antigen-bearing lipid bilayers. Untransfected cells served as control. Image sequences were acquired using TIRF microscopy and we observed that all cells spread over the antigen-presenting surface forming antigen-containing BCR microclusters to the same extent. Whereas control cells showed directed movement of antigen-containing BCR microclusters, cells either expressing Dynamitin-GFP or shRNA targeting DYNC1H1 did not gather these antigen microclusters in a central agglomerate (Figure 6.3. D and Supplementary Video 11). This difference in antigen microcluster movement was strikingly similar to that observed for B cells lacking Grb2, Dok-3 or Cbl (Figure 4.2.) and became apparent when we tracked antigen microcluster movement over time and visualised this movement as vectors (Figure 6.3. D, lower panels). Vectors in control cells pointed towards the centre, whereas vectors in cells expressing Dynamitin-GFP or shRNA targeting DYNC1H1 appeared shorter and pointed in random directions. We furthermore quantified the mean net movement of antigen-containing BCR microclusters towards the centre and found this to be severely impaired following disruption of dynein expression or function (Figure 6.3. D, lower right panel). Our results therefore clearly implied a function for cytoplasmic dynein in mediating antigen gathering in B cells by directed transport of antigen microclusters.

We wanted to further validate our methods used to show a role for dynein in the movement of antigen-containing BCR microclusters and thus set up experiments that would control for the expression of shRNA or soluble GFP. We consequently used an shRNA control plasmid expressing soluble GFP by virtue of an IRES-GFP and a GFP-only test plasmid as controls. We electroporated A20 D1.3 B cells with control plasmids and a vector coding for shRNA targeting DYNC1H1 as before. Cells were lysed and GFP-expression was tested by Western blot. Untransfected

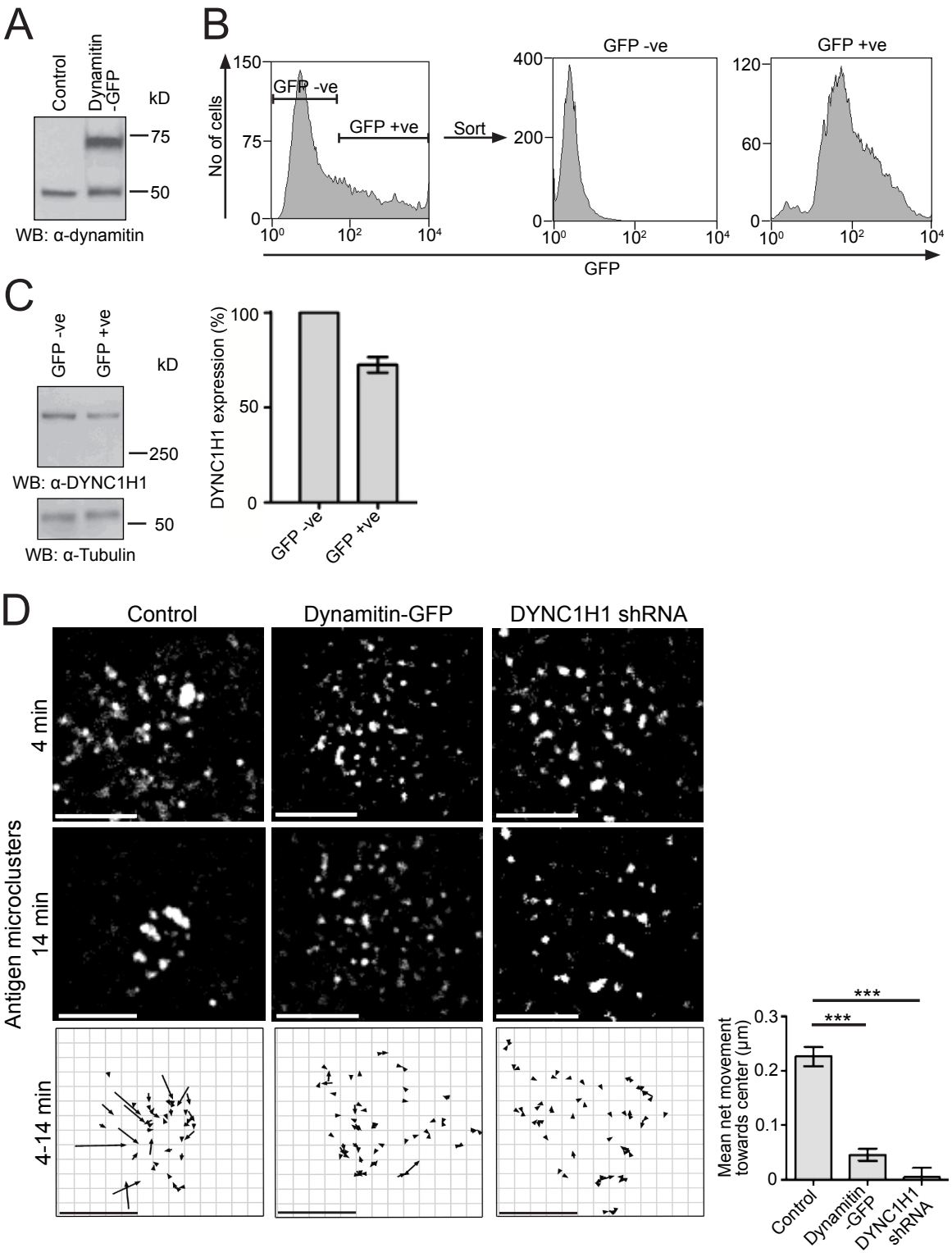

Figure 6.3. Movement of antigen-containing BCR microclusters is mediated by cytoplasmic dynein

(A) A20 mouse B cells stably expressing a Hen egg lysozyme (Hel)-specific BCR were transiently transfected with a vector coding for dynamitin-GFP. Overexpression of dynamitin-GFP was assessed 16 hours after transfection by Western blot. (B, C) A20 cells as in A were transfected with a shRNA vector to target dynein heavy chain 1 (DYNC1H1). The vector also codes for soluble GFP so cells could be sorted according to GFP expression. Sorted cells were left for 48 hours and GFP expression was measured using flow cytometry (B, right panels). DYNC1H1 expression was measured using Western blot and expression levels of GFP-positive and -negative populations were quantified (C, right panel). (D) Untreated A20 cells or cells expressing dynamitin-GFP or shRNA targeting DYNC1H1 (prepared as in A-C) were settled on Hel-loaded lipid bilayers. Antigen microclusters were visualised using TIRF microscopy and their movement over 10 min was analysed (lower panels). All scale bars equal 5 μm.

cells served as control. We observed bands indicating the expression of GFP in all but control samples (Figure 6.4. A). B cells either expressing control shRNA or shRNA targeting DYNC1H1 were lysed and the dynein heavy chain 1 protein levels were measured by Western blot. As before we detected lower levels of dynein heavy chain 1 in B cells expressing a specific shRNA compared to cells expressing a control shRNA construct (Figure 6.4. B). We next settled A20 B cells expressing the GFP-only plasmid, a control shRNA or shRNA targeting DYNC1H1 on antigen-loaded lipid bilayers and monitored the distribution of antigen-containing BCR microclusters over time (Figure 6.4. C). For all conditions we observed that B cells spread and formed antigen-containing BCR microclusters. However, only cells expressing the GFP-only or control shRNA plasmids showed antigen gathering by directed movement of antigen microclusters. In contrast to control samples, antigen microclusters formed by cells expressing the shRNA targeting DYNC1H1 stayed in the periphery over the course of the acquisition. We quantified the movement of antigen-containing BCR microclusters for all conditions as before and found a significant difference in mean net movement of antigen microclusters for cells with lower levels of DYNC1H1 (Figure 6.4. D) compared to control samples. This indicated that the expression of soluble GFP or of a control shRNA vector did not impact the centripetal movement of antigen-containing BCR microclusters.

In conclusion, we have identified tubulin beta-2 and proteins of the dynein machinery as binding partners of Syk in activated B cells by means of quantitative mass spectrometry and co-immunoprecipitation. We furthermore show recruitment and movement over time of dynein with antigen-containing BCR microclusters. Using a dominant-negative construct and RNAi we specifically show an involvement of dynein in the centripetal movement of antigen microclusters. Our results therefore clearly demonstrate a functional role for cytoplasmic dynein in the movement of antigen-containing BCR microclusters during the process of antigen gathering by B cells. Given that dynein is a microtubule-based minus-end directed molecular motor, it is likely that this movement is supported by the underlying microtubule network.

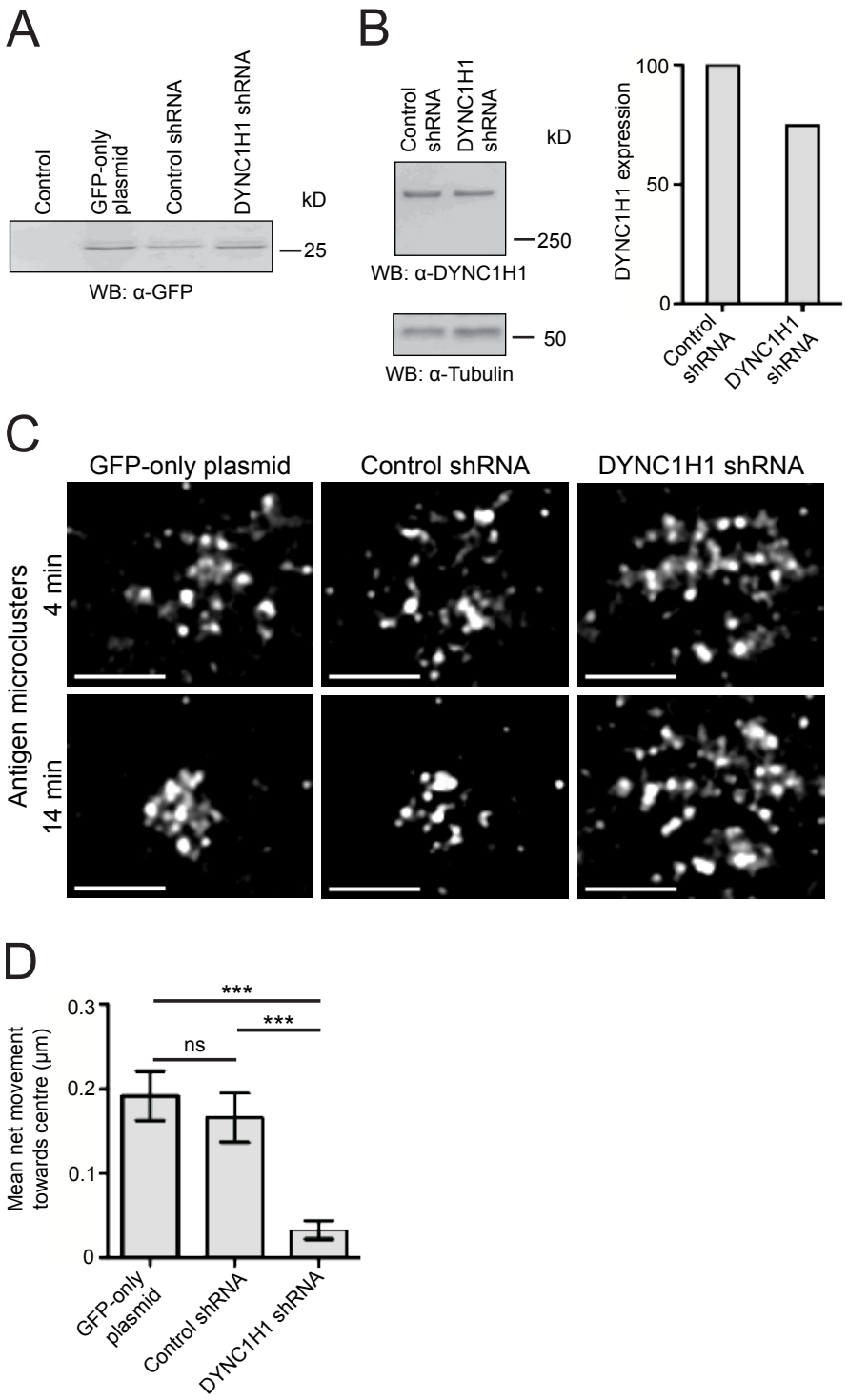

Figure 6.4. Expression of soluble GFP or of a control shRNA does not affect BCR microcluster movement

(A) A20 mouse B cells stably expressing a Hen egg lysozyme (Hel)-specific BCR were transiently transfected with vectors coding for GFP, a control shRNA or DYNC1H1 shRNA. Both shRNA vectors also code for soluble GFP. GFP expression in all tranesfected cells was compared to untransfected cells by Western blot. (B) The level of RNAi-mediated DYNC1H1 knockdown was measured by Western blot and the band intensity was quantified using ImageJ software (right panel). (C and D) A20 cells expressing soluble GFP, a control shRNA or shRNA targeting DYNC1H1 (prepared as in A and B) were settled on Hel-loaded lipid bilayers. Antigen microclusters were visualised using TIRF microscopy and their net movement towards the centre over 10 min was measured. All scale bars equal 5 µm.

6.2 Movement of antigen-containing BCR microclusters is supported by the microtubule network

Our previous work had identified a role for the molecular motor dynein in the movement of antigen-containing BCR microclusters during antigen gathering by B cells. As dynein is a minus-end directed microtubule-based motor, we were interested in assessing the function of the microtubule network in B cell antigen gathering. We therefore focussed our attention to the microtubule network and its potential role in B cell activation.

6.2.1 Inhibition of microtubule dynamics impairs antigen gathering by B cells

Mircotubules constitute a significant part of the cytoskeleton and help all cell types maintain shape, divide and transport cargo. The growth of microtubules is nucleated in the microtubule-organising centre (MTOC) where polarised fibres are extended by a constant process of α- and β-tubulin dimerisation and addition of dimers to the plus-ends of existing microtubules. The process of tubulin polymerisation and microtubule disassembly is highly dynamic and reflects an equilibrium, which can be altered by incubation of cells with microtubule-stabilising or –destabilising agents. We therefore hypothesised that treatment of B cells with microtubule-altering agents could potentially inhibit their ability to gather antigen, if the microtubule network played a functional role in that process.

To test, whether the microtubule network played a role in antigen gathering by B cells, we treated primary murine B cells with the microtubule-stabilising drug taxol prior to settling on lipid bilayers containing surrogate antigen and ICAM-1. Taxol should shift the equilibrium towards tubulin polymerisation and thus alter overall microtubule dynamics. We monitored the contact area between the lipid bilayer and the cells by IRM and recorded the distribution of fluorescent antigen molecules using confocal microscopy as before (Figure 4.1.). We settled either untreated B cells or cells pre-treated with taxol on antigen-bearing lipid bilayers and observed characteristic spreading over the course of two minutes. Within the

next four minutes untreated cells gathered antigen in a central area, whereas taxol-treated cells stayed spread and did not collect antigen in a comparable manner (Figure 6.5. A). This phenotype was in striking similarity to our observations involving DT40 B cells deficient for Grb2, Dok-3 or Cbl (Figure 4.1.). We subsequently quantified the contact area between B cells and the antigen-presenting lipid bilayer for both untreated and taxol-treated cells and found a significant difference in cellular contraction while spreading appeared not to be affected (Figure 6.5. B). In line with unaffected spreading, we did not find a difference in the number of antigen-containing BCR microclusters formed when cells were fully spread (Figure 6.5. C).

We next wanted to verify our results by using another microtubule altering agent. We chose the microtubule-depolymerising agent nocodazole, which favours the disassembly of microtubules therefore altering overall microtubule dynamics. We settled untreated cells or B cells pre-treated with nocodazole on antigen-loaded lipid bilayers and imaged contact area and distribution of fluorescent antigen molecules as before. Similar to taxol treatment, B cells pre-incubated with nocodazole spread over the antigen-presenting surface comparable to untreated cells, but failed to gather antigen molecules in a central agglomerate (Figure 6.5. D).

In summary, our experiments involving microtubule-altering agents suggest a role for the microtubule network in antigen gathering by B cells. While such agents do not influence B cells spreading or antigen microcluster formation, they do prevent B cells from gathering antigen molecules possibly by blocking the dynein-mediated movement of antigen-containing BCR microclusters on microtubules.

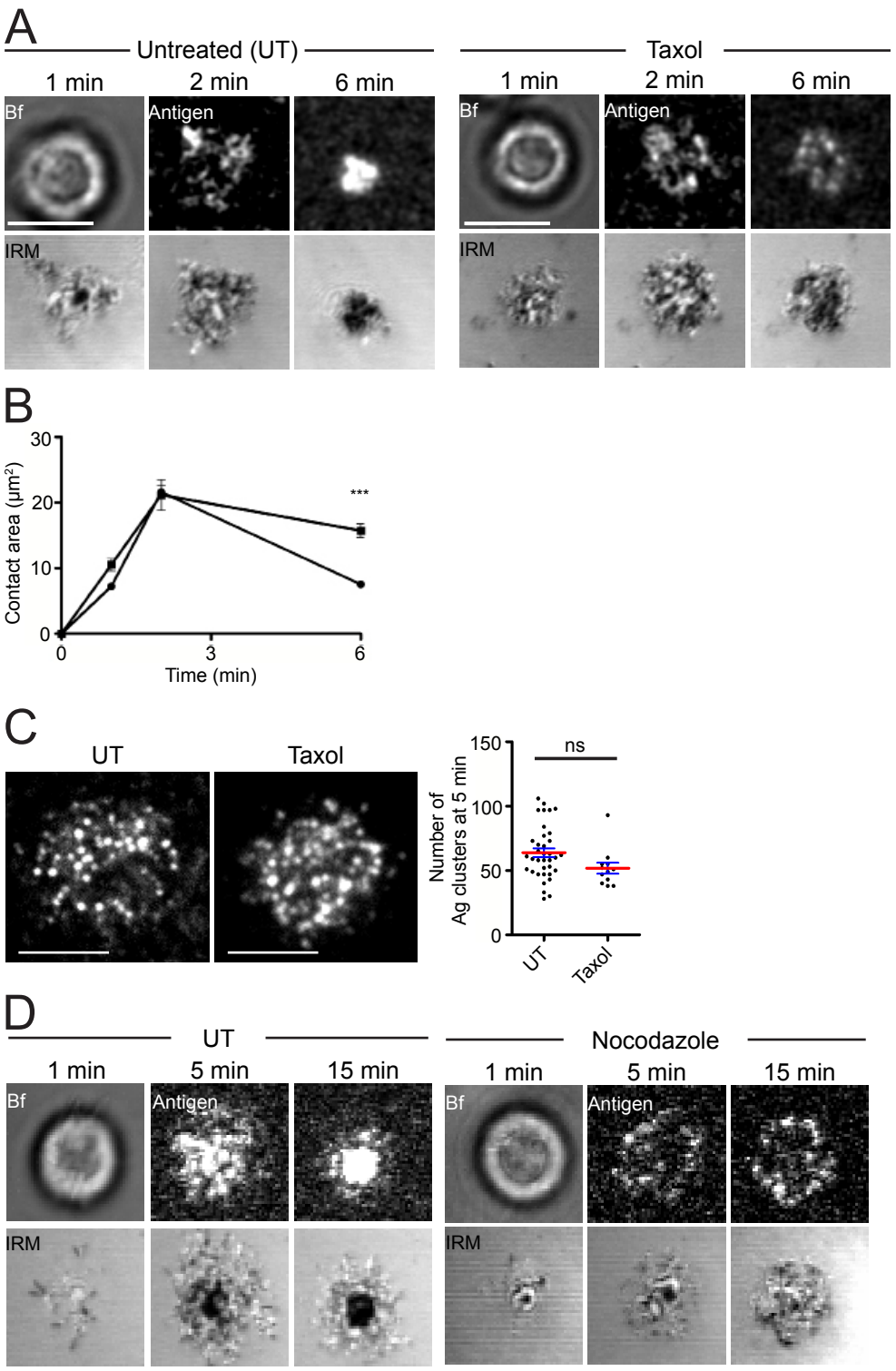

Figure 6.5. The microtubule network participates in the movement of antigen-containing BCR microclusters

(A) Primary murine B cells were either left untreated (UT) or were pre-treated with 50 μg/ml of the microtubule-stabilising drug Taxol. Cells were subsequently settled on planar lipid bilayers containing an anti-mouse kappa light chain as surrogate antigen and ICAM-1 and imaged as in Figure 4.1. (B) The plot shows a quantification of the contact area between cells and lipid bilayers over time using IRM data. Data was pooled from two independent experiments and represents a minimum of 25 cells. (C) Representative TIRF images showing B cells left untreated or treated with Taxol as described at maximum spread on planar lipid bilayers containing antigen and ICAM-1; right panel shows the number of antigen microclusters formed at this timepoint per cell. Red lines indicate the mean ± SEM (blue). (D) The experimental system in A was used to investigate the effect of the microtubule-depolymerising agent Nocodazole on antigen gathering by DT40 B cells. Cells were pre-treated with 1 μg/ml Nocodazole. Statistical analysis was carried using t-test; ***$p < 0.0001$. All scale bars equal 5 μm.

6.2.2 The microtubule network serves as a platform for BCR immobilisation and movement of antigen-containing BCR microclusters

Using microtubule inhibitors such as taxol and nocodazole we had demonstrated a functional role for the microtubule network in antigen gathering by B cells. This process possibly involved the movement of antigen-containing BCR microclusters on microtubules. The microtubule network could thus serve as a platform for antigen microcluster formation and movement.

In resting B cells, BCR molecules diffuse on the cell surface controlled by the cortical actin cytoskeleton (Treanor et al., 2010). When presented with antigen on a planar surface, BCR molecules are immobilised and the formation of signalling-competent microclusters is initiated (Depoil et al., 2008 and Treanor et al., 2011). Given an involvement of microtubules in antigen gathering following antigen microcluster formation, we were interested, whether the microtubule network could provide a platform for the initial immobilisation of BCR molecules. To address this we made use of single particle labelling of BCR molecules coupled to high-speed dual-view TIRF microscopy. By using fluorescently labelled Fab fragments of an anti-chicken IgM antibody (clone M1) at a limiting dilution we were able to visualise single particles of BCR. We labelled DT40 wildtype cells stably expressing tubulin-RFP with fluorescent anti-BCR Fab fragments and settled them on glass coverslips either coated with fibronectin or with an anti-chicken IgM antibody (clone M4). Cells spread on fibronectin- and anti-BCR coated glass triggered by integrin activation or BCR ligation, respectively. We monitored the movement of BCR particles in both conditions with respect to the distribution of tubulin at a frame rate of 20 fps for ten seconds. We observed the free diffusion of BCR particles in cells spreading on fibronectin (Figure 6.6. A, upper panels and Supplementary video 12). Interestingly, single particles of BCR were immobilised in tubulin-rich regions after settling on glass coverslips coated with anti-BCR antibody (Figure 6.6. A, lower panels). To quantify our observation, we tracked single particles of BCR using a tracking algorithm that revealed a diffusion coefficient for each particle. Single particles of BCR were scored as immobile, when their diffusion coefficient was below a threshold of 0.01 $\mu m^2 s^{-1}$. Immobile particles were counted and scored for their location with respect to tubulin as

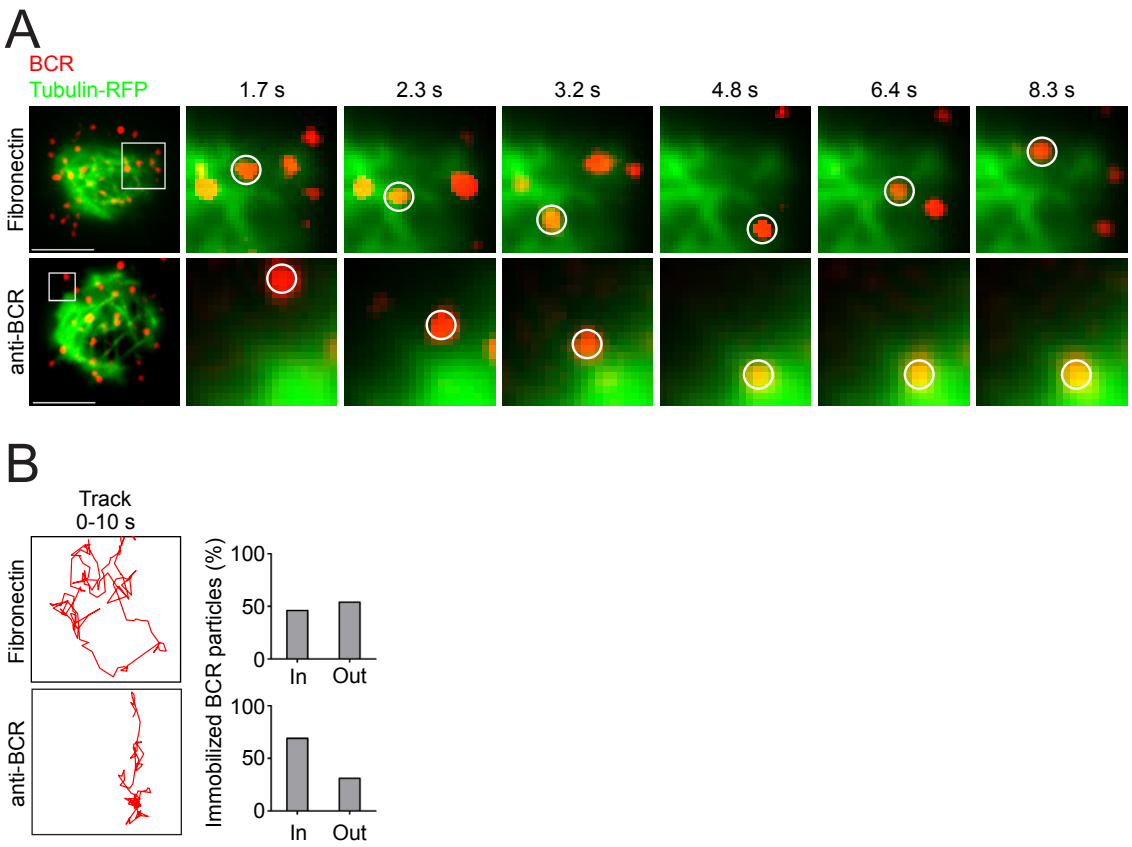

Figure 6.6. Single particles of BCR are immobilised in the microtubule network
(A) DT40 cells stably expressing tubulin-RFP (green) were labelled with a Fab fragment of an anti-chicken IgM antibody (M1) that had previously been coupled to an Atto633 fluorophore (red) at a limiting dilution. Labelled cells were settled on glass coverslips coated either with 0.5 pg/ml Fibronectin alone (upper panels) or with a mixture of 0.5 pg/ml Fibronectin and 0.1 µg/ml of a monoclonal anti-chicken IgM antibody (M4) to crosslink the BCR (lower panels). Images of tubulin and BCR particles were acquired simultaneously at high speed for 10 seconds (see Methods). Time-lapse images show a magnified area indicated by a white box in the images on the left. White circles highlight the location of one BCR particle at given time points for both conditions. (B) Left: Particles highlighted in A were tracked over time and resulting tracks are shown as red lines. Right: For quantification of BCR movement in relation to the microtubule network, particles of BCR were defined as immobile if their diffusion coefficient was below a threshold of 0.01 $\mu m^2 s^{-1}$. Immobile particles were counted and scored for their location in respect to tubulin as within ("in") an area of tubulin-RFP signal or outside ("out") of such an area. The data shown represents a minimum of 103 immobile particles pooled from two independent experiments.

within or outside of tubulin-rich areas (Figure 6.6. B). We found that the majority of single BCR particles were immobilised within tubulin-rich regions when cells were settled on glass surfaces coated with an anti-BCR antibody. This is in line with an interaction between the microtubule network and the microcluster, and suggests a potential role for tubulin during the formation of antigen microclusters triggered by BCR immobilisation.

The localisation of dynein to the signalling BCR microcluster suggested a role for microtubules in organising microcluster movement during antigen gathering. To further explore the role of the microtubule network in the directed transport of antigen-containing BCR microclusters, we transduced primary murine B cells with a plasmid coding for tubulin-RFP. Cells were settled on planar lipid bilayers containing fluorescent antigen and ICAM-1 as before. We used TIRF microscopy to record image sequences of antigen microclusters and tubulin after cells had fully spread. Antigen-containing BCR microclusters were often observed on and moving along microtubules over time (Figure 6.7. A). However, this movement was not continuous as the microtubule network was highly dynamic and frequently disappeared from the focal plane (Figure 6.7. A, lower panels and Supplementary Video 13). We quantified our observations by measuring colocalisation of tubulin-RFP and antigen over time and obtained a mean value for colocalisation of about 70 %. This indicated that antigen-containing BCR microclusters were indeed moved along microtubules.

To sum up, we have shown that single particles of BCR were immobilised in tubulin-rich regions upon BCR activation and that antigen-containing BCR microclusters moved along microtubules in primary murine B cells when settled on antigen-loaded lipid bilayers. Our results therefore support the hypothesis that the microtubule network potentially serves as a platform for BCR immobilisation, microcluster formation and subsequent centripetal transport of antigen-containing BCR microclusters for antigen gathering by B cells.

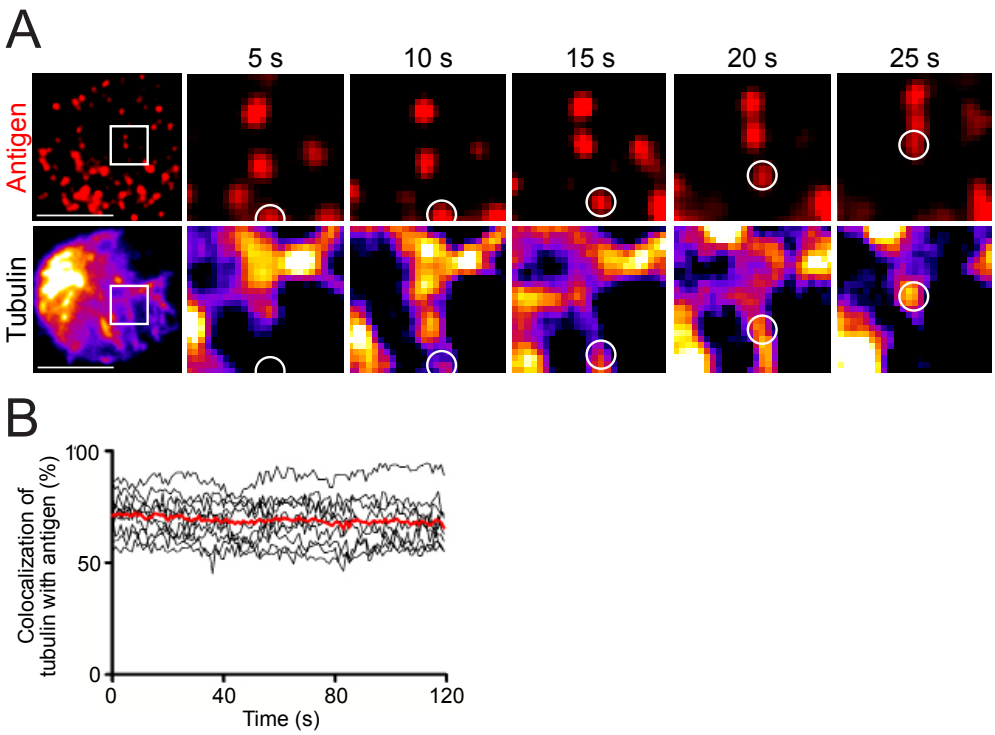

Figure 6.7. Antigen-containing BCR microclusters move along microtubules
(A) Primary murine B cells transiently expressing α-tubulin-RFP (pseudocolor) were settled on planar lipid bilayers containing surrogate antigen (red) and unlabelled ICAM-1. Images were acquired over time using TIRFM when cells were fully spread. Time-lapse images show a magnified area indicated by a white box in the images on the left. White circles highlight the location of antigen and tubulin-RFP at the same position in the images for each timepoint. (B) The plot shows a quantification of the percentage of co-localisation of antigen microclusters with tubulin-RFP over time; black lines represent single cells, the red line shows the mean value of all cells. Co-localisation analysis was carried out using Imaris software according to methods. All scale bars equal 5 µm.

6.2.3 The microtubule network is not altered in B cells lacking Grb2, Dok-3 or Cbl

Our experiments involving agents altering microtubule dynamics and the finding of antigen-containing BCR microclusters moving along microtubules suggested that while the microtubule network is not crucial during B cell spreading, it participates in subsequent antigen gathering. Thus far our observations indicate that the microtubule network makes up tracks along which antigen-containing BCR microclusters are moved by cytoplasmic dynein for antigen gathering. Inhibition of dynein expression or functionality as well as altering microtubule dynamics using pharmacological inhibitors resembled the phenotype observed in B cells lacking Grb2, Dok-3 or Cbl showing an impaired centripetal movement of antigen-containing BCR microclusters. Despite this striking similarity it was not clear, however, why the absence of Grb2, Dok-3 and Cbl impaired antigen microcluster movement. We therefore wanted to investigate, whether this was due to an alteration of the underlying microtubule network in cells deficient for Grb2, Dok-3 or Cbl.

To test this, we settled either wildtype B cells or DT40*Grb2*$^{-/-}$, *Dok3*$^{-/-}$or *Cbl*$^{-/-}$ cells stably expressing tubulin-RFP on antigen-loaded lipid bilayers. We recorded image sequences using TIRF microscopy visualising microtubules in fully spread cells at the onset of contraction. This experimental setup surprisingly revealed that the gross organisation of the microtubule network was not disrupted in wildtype B cells or cells lacking Grb2, Dok-3 or Cbl (Figure 6.8. A and Supplementary video 14). As observed before using primary murine B cells, antigen microclusters localised within tubulin-rich regions (Figure 6.7.). We therefore concluded that an alteration of the underlying microtubule network could not account for the defect observed in B cells deficient for Grb2, Dok-3 or Cbl with respect to their ability to gather antigen by directed movement of antigen-containing BCR microclusters.

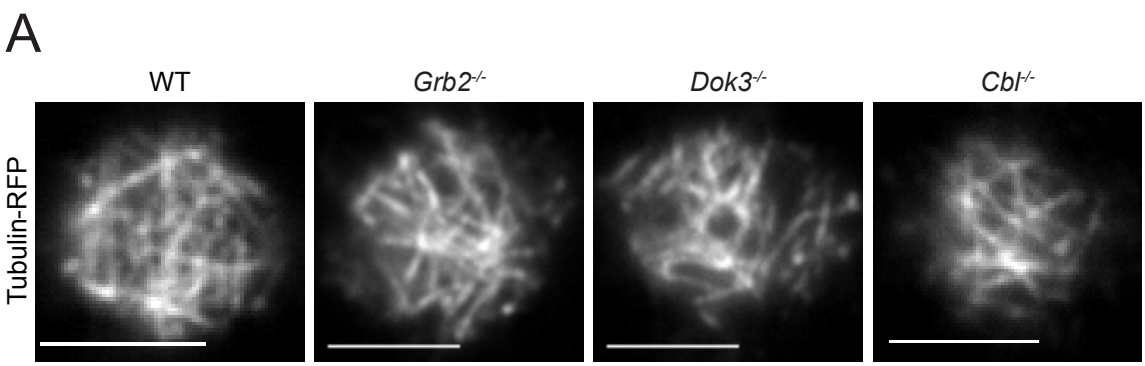

Figure 6.8. The microtubule network is not altered in DT40 cells lacking Grb2, Dok-3 or Cbl in comparison to wildtype cells

(A) DT40 wildtype (WT) cells or DT40 cells deficient in Grb2, Dok-3 or Cbl stably expressing tubulin-RFP were settled on planar lipid bilayers containing surrogate antigen. Images of tubulin-RFP were acquired using TIRFM at maximum spread three to six minutes after settling. All scale bars equal 5 µm.

In conclusion we have clearly demonstrated a role for the microtubule network in B cell antigen gathering by using microtubule-disrupting agents and by showing movement of antigen-containing BCR microclusters along microtubules. These findings are in line with our previous observations that the microtubule-based motor dynein is responsible for the centripetal movement of antigen-containing BCR microclusters. While the gross organisation of the microtubule network in B cells lacking Grb2, Dok-3 or Cbl was not altered, it remains to be elucidated why these knockout cells show impaired directional transport of antigen microclusters and concomitant antigen gathering.

6.3 Grb2, Dok-3 and Cbl recruit cytoplasmic dynein to the antigen-containing BCR microcluster

6.3.1 Grb2 and Dok-3 interact with components of the dynein machinery

We had earlier established a crucial role for the three mediators Grb2, Dok-3 and Cbl and the molecular motor dynein in the process of antigen gathering by B cells by directed movement of antigen-containing BCR microclusters. As the underlying microtubule network showed no gross alteration in B cells deficient for Grb2, Dok-3 or Cbl, we wanted to investigate, whether there was a functional link between Grb2, Dok-3 and Cbl and the dynein machinery in B cells.

To test a possible interaction of Grb2 with dynein, we used glutathione beads coated with Grb2-GST to capture dynein. DT40 B cells stably expressing a GFP-tagged version of the dynein intermediate chain of 74 kDa (DYNC1I1) were lysed and incubated with bead-bound Grb2-GST. Purified complexes were subjected to Western blot analysis probing for GFP and total cell lysates were used to verify expression of DYNC1I1-GFP in all samples. GST without Grb2 was used as control and we did not observe a co-purification of DYNC1I1 with GST on its own (Figure 6.9. A). However, when incubating cell lysates with GST-Grb2 we indeed observed a band representing DYNC1I1-GFP. This signified a co-purification of Grb2 and a subunit of the dynein complex and indicated the

potential existence of a complex of Grb2 and dynein in B cells. In addition to full length Grb2 we also coupled the three functional domains of Grb2 (C- and N-terminal SH3 and central SH2 domains) to GST and incubated these proteins with cell lysates as before followed by capture of complexes with glutathione beads. Bands representing DYNC1I1-GFP were observed in all samples, but appeared strongest for the C-terminal SH3 domain of Grb2 implying that the interaction of Grb2 and dynein could possibly be mediated by this domain (Figure 6.9. A). We had therefore provided evidence of a possible interaction between the dynein complex and Grb2.

To address a possible link between Grb2 or Dok-3 and the dynein complex in activated B cells, we next sought to assess a potential interaction of Dok-3 and dynein. We therefore activated DT40*Dok3*$^{-/-}$ cells stably expressing Dok-3-GFP and immunoprecipitated Dok-3 using its GFP-tag. Dok-3 deficient B cells served as control. We observed characteristic duplet bands for DYNC1I1 in whole cell lysates and were thus confident that DT40 B cells expressed DYNC1I1 and that the antibody used for detection was specific. Interestingly, we found the same bands in Dok-3 immunoprecipitates and not in control samples (Figure 6.9. B). This implied a potential interaction of Dok-3 and the dynein complex in activated B cells.

To confirm a potential interaction of Grb2 and Dok-3 with the dynein machinery in activated B cells, we used the same experimental system involving co-immunoprecipitation to assess if Grb2 or Dok-3 could bind other components of the multimeric dynein complex. We consequently activated DT40*Grb2*$^{-/-}$ or DT40*Dok3*$^{-/-}$ cells stably re-constituted with Grb2-GFP or Dok-3-GFP, respectively, and immunoprecipitated GFP with a polyclonal antiserum. DT40 B cells lacking Grb2 or Dok-3 served as controls. We then subjected immunoprecipitates to Western blot probing for the p150^{Glued} subunit of dynactin (DCTN1), a regulatory subunit of the dynein complex. Expression of p150^{Glued} was confirmed using whole cell lysates (Figure 6.9. C and D, lower panels). Interestingly, we observed bands representing p150^{Glued} in both Grb2- and Dok-3-immunoprecipitates (Figure 6.9. C and D, upper panels). This provided further

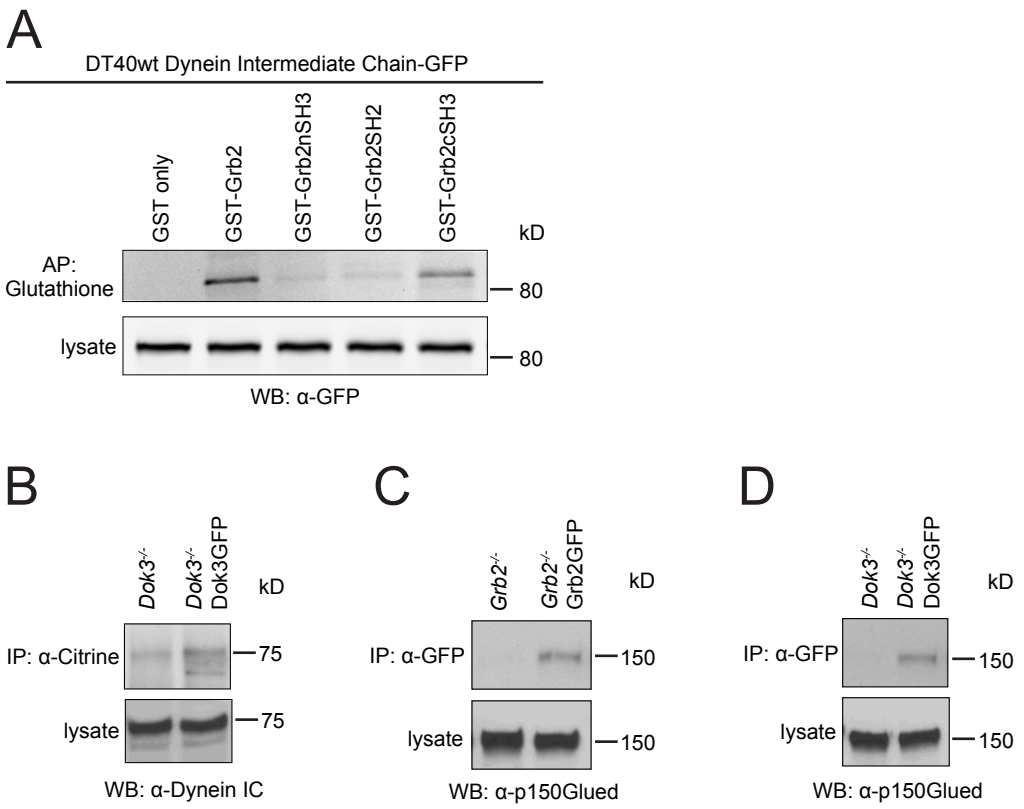

Figure 6.9. Grb2 and Dok-3 interact with subunits of the dynein complex
(A) GST pull-down assay using full length Grb2, its N-terminal SH3, central SH2, or C-terminal SH3 domain coupled to GST as bait. Purified complexes were analysed on a Western blot for dynein intermediate chain-GFP using an anti-GFP antibody for capture. GST alone served as control. Cell lysates of all samples revealed comparable dynein-GFP expression (lower panel). (B) DT40*Dok3*$^{-/-}$ cells stably expressing Dok3-GFP were activated with 5 µg/ml of an anti-chicken IgM antibody for three minutes, lysed and Dok-3 was immunoprecipitated using an anti-GFP antibody. Immunoprecipitates were subjected to Western blotting and the dynein intermediate chain of 74 kD was detected with a monoclonal antibody. DT40*Dok3*$^{-/-}$ cells served as control; endogeneous expression of dynein intermediate chain is shown in cell lysates (lower panels, WB). (C and D) The experimental strategy in B was used to immunoprecipitate Grb2 and Dok-3 from activated DT40 B cells and subsequently show a co-purification of the p150Glued subunit of Dynactin in both Grb2 and Dok-3 immunoprecipitates by Western blotting. The respective knockout cells were used to control for specificity of the immunoprecipitation.

evidence that Grb2 and Dok-3 interacted with the dynein machinery upon BCR cross-linking.

In summary, we have shown an interaction of Grb2 and Dok-3 with the dynein intermediate chain of 74 kDa (DYNC1I1) and the $p150^{Glued}$ subunit of dynactin (DCTN1) in activated B cells by biochemical means. These data support the notion that the dynein machinery is recruited to antigen-containing microclusters upon BCR triggering. While this demonstrates a potential role for dynein in the movement of antigen-containing BCR microclusters, it remains unclear whether Grb2, Dok-3 or Cbl could constitute a functional link between the signalling microcluster and dynein.

6.3.2 Recruitment of dynein to antigen-containing BCR microclusters is impaired in B cells lacking Grb2, Dok-3 or Cbl

Our previous observations clearly demonstrated a role for a complex involving Grb2, Dok-3 and Cbl in B cell antigen gathering by directed transport of antigen-containing BCR microclusters. We had furthermore shown that dynein is recruited to antigen microclusters driving their centripetal transport towards the central area. In line with this, we were able to co-purify Grb2 and Dok-3 with components of the dynein machinery. We were therefore intrigued to know, whether the recruitment of dynein to antigen-containing BCR microclusters required the expression of Grb2, Dok-3 or Cbl. This could potentially provide the molecular explanation for the observed defective phenotype in DT40*Grb2*$^{-/-}$, *Dok3*$^{-/-}$ or *Cbl*$^{-/-}$.

To address the question of dynein recruitment to antigen-containing BCR microclusters in B cells lacking Grb2, Dok-3 or Cbl, we took advantage of the DT40 system coupled to lipid bilayers for antigen presentation and high-resolution TIRF microscopy. The expression of GFP-tagged dynein intermediate chain of 74 kDa (DYNC1I1) had previously been used to show recruitment of dynein to antigen-containing BCR microclusters in primary murine B cells. We thus used the same construct and electroporated DT40 wildtype or DT40*Grb2*$^{-/-}$, *Dok3*$^{-/-}$or *Cbl*$^{-/-}$ cells to generate clones stably expressing DYNC1I1-GFP. The

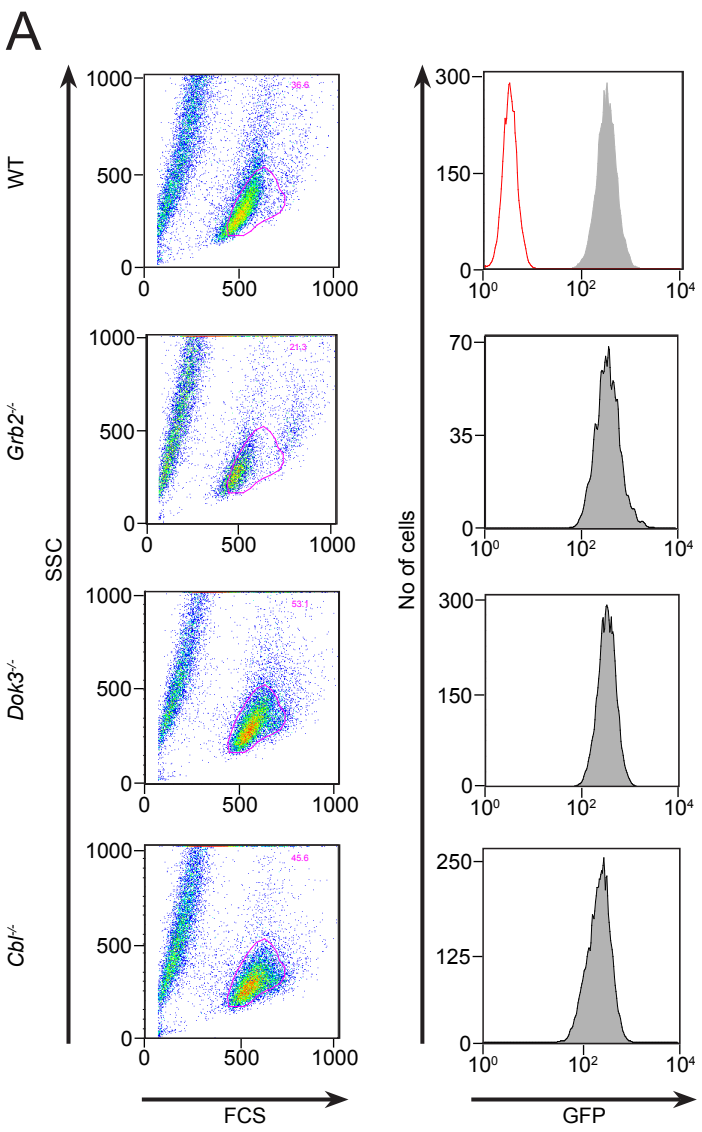

Figure 6.10. DT40 cells express the same amount of dynein-GFP
(A) DT40 wildtype (WT) cells or cells lacking Grb2, Dok-3 or Cbl were stably transfected with a construct coding for dynein intermediate chain-GFP. Stable clones were selected using Puromycin and dynein-GFP expression was measured using flow cytometry. Cell were identified based on their scatter profile (left column) and GFP-fluorescence was detected within that population (grey histograms in right column). The red peak on the top right represents non-transfected control cells.

expression of DYNC1I1-GFP was measured by flow cytometry and we chose cells showing matching expression of DYNC1I1-GFP (Figure 6.10. A).

These cells stably expressing matched amounts of DYNC1I1-GFP were settled on antigen-loaded lipid bilayers to visualise the distribution of dynein relative to antigen-containing BCR microclusters using TIRF microscopy. We recorded image sequences at a frame rate of 1 fps for one minute after cells had reached maximum spread. Regarding wildtype cells we observed dynein to be recruited to and moving with antigen-containing BCR microclusters towards the centre similar to our earlier observations in primary murine cells (Figure 6.11. A, upper panels and Supplementary Video 15). Importantly and in contrast, dynein localisation to antigen-containing BCR microclusters was impaired in DT40 B cells lacking Grb2, Dok-3 or Cbl (Figure 6.11. A, left panels and Supplementary video 16). To quantify our results we tracked antigen-containing BCR microclusters over the course of the image sequence (60 frames) and created 'masks' corresponding to antigen microcluster tracks. We subsequently measured the fluorescence intensity of DYNC1I1-GFP within these masks. As all cells expressed a matched amount of DYNC1I1-GFP this analysis provided us with a tool to quantify dynein recruitment to antigen-containing BCR microclusters over time. We measured the intensity of DYNC1I1-GFP at the antigen-containing BCR microcluster for each frame and observed significantly more recruitment of dynein to the antigen microcluster in wildtype B cells compared to cells lacking Grb2, Dok-3 or Cbl (Figure 6.11. B). When plotting all mean values for dynein intensity at the antigen microcluster over time we found that this difference even increased over the course of the acquisition (Figure 6.11. C). We have therefore clearly demonstrated that the recruitment of DYNC1I1 to antigen-containing BCR microclusters is impaired in B cells deficient for Grb2, Dok-3 or Cbl. It is consequently conceivable that Grb2, Dok-3 and Cbl are part of a complex which recruits the dynein machinery to the signalling BCR in order to drive B cell antigen gathering by directed movement of antigen-containing BCR microclusters.

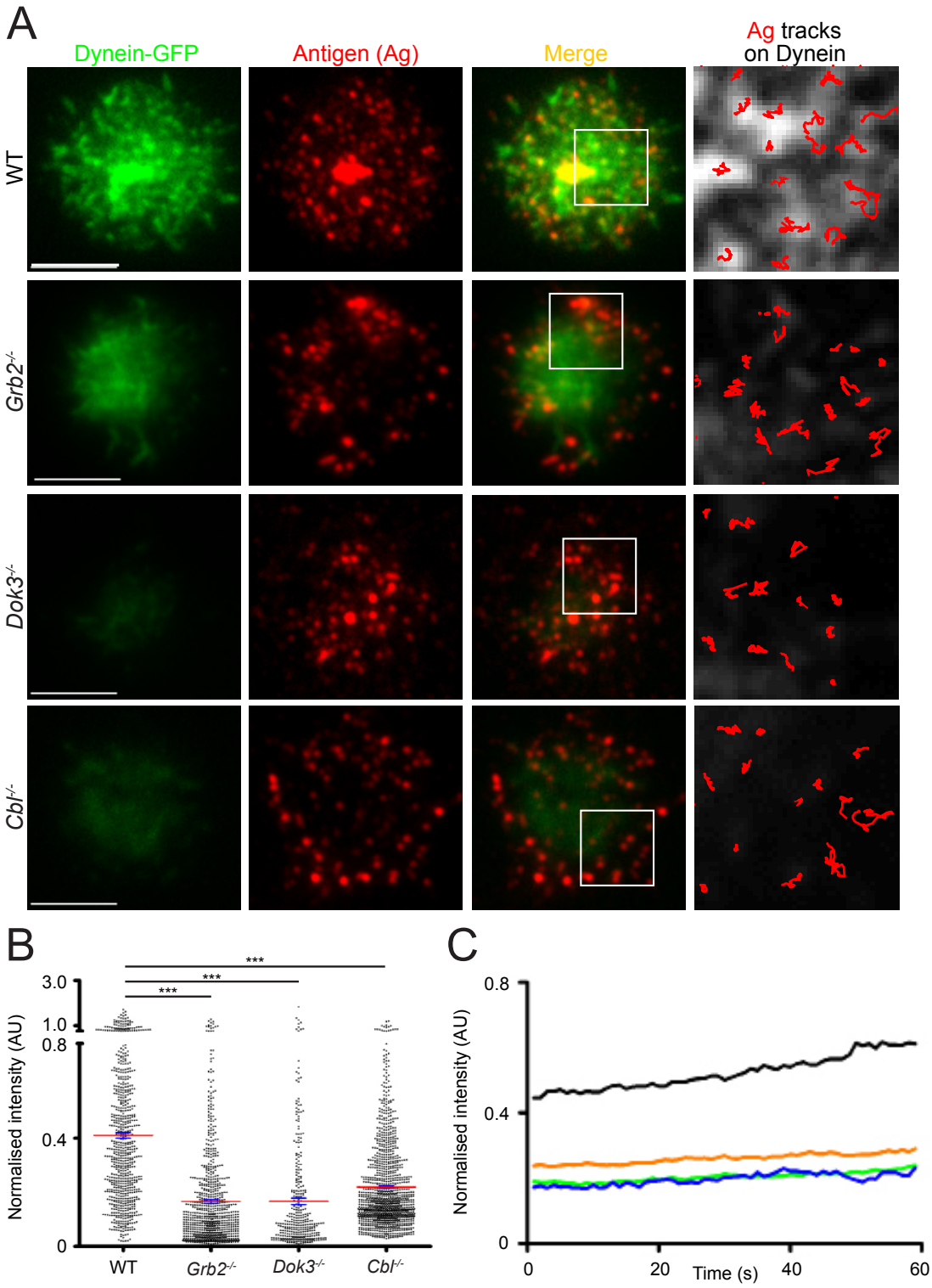

Figure 6.11. Grb2, Dok-3 and Cbl recruit dynein to antigen-containing BCR microclusters

(A) Wildtype (WT) DT40 B cells or cells deficient in Grb2, Dok-3 or Cbl stably expressing dynein-GFP were settled on planar lipid bilayers containing surrogate antigen and microclusters were tracked for one minute for all conditions. The images on the right show antigen tracks in a magnified area indicated by the white boxes in the merged images. The dynein-GFP intensity was normalised to background levels for each cell and was subsequently measured within tracks defined by antigen over time (see Methods). This yields a quantitative and comparable measure of dynein-GFP intensity in antigen microclusters over time. (B) Levels of normalised dynein-GFP intensity within antigen tracks are given in the dot plot for the first frame. Red lines indicate the mean ± SEM (blue). (C) Data on normalised dynein-GFP intensity within antigen microcluster tracks obtained as in B is visualised as a function of time. Statistical analysis was carried using the non-parametric Wilcoxon Mann-Whitney test; ***$p < 0.0001$. All scale bars equal 5 µm.

In conclusion we provide proof for an interaction between the dynein machinery and antigen-containing BCR microclusters, as subunits of the dynein complex could be co-purified with Grb2 and Dok-3 from activated B cells. We next showed impaired recruitment of DYNC1I1-GFP to antigen-containing BCR microclusters in B cells lacking Grb2, Dok-3 or Cbl over time. This reduced recruitment and/or retention of dynein to the antigen-containing BCR microcluster provides a reasonable explanation as to why antigen microcluster movement is abrogated in the absence of Grb2, Dok-3 or Cbl. It thus seems likely that a critical threshold of dynein recruitment and/or retention at the antigen microcluster must be surpassed in order to mediate efficient linkage and transport of microclusters on the microtubule network.

6.4 Discussion

Here, we have used a combination of quantitative mass spectrometry, genetics and high-resolution imaging to reveal an unexpected, but pivotal role for cytoplasmic dynein and the underlying microtubule network in antigen gathering by B cells. As the amount of antigen gathered by B cells directly correlates with the extent of T cell help, we have identified a crucial function for the dynein machinery in B cell activation.

6.4.1 Recruitment of dynein to antigen-containing BCR microclusters and the role of the microtubule network in B cell activation

Using a combination of SILAC mass spectrometry, biochemistry and imaging, we reveal that signalling BCR microclusters interact with dynein. Dynein is a homodimer of heavy chains in complex with several non-catalytic subunits and mediates the active minus-end directed movement of intracellular cargo along microtubules towards the MTOC (Kardon and Vale, 2009). We found that localisation of dynein at the BCR microcluster is dependent on Grb2, Dok-3 and Cbl and is required for BCR microcluster movement for antigen gathering. However, as we and others were unable to consistently detect direct interactions between Grb2 and dynein (Neumann et al., 2009) it seems likely that this interaction is potentially indirect or highly dynamic. Although a role for dynein during B cell activation has not been previously reported, dynein is recruited to a ring at the T cell immune synapse in a mechanism dependent on SLP-76 and ADAP (Combs et al., 2006 and Martin-Cofreces et al., 2008). Importantly, we observed that either the down-regulation of dynein expression through RNAi or the over-expression of dynamitin significantly impaired the movement of antigen microclusters. The inhibition of movement was surprisingly dramatic particularly given the residual levels of dynein expression following RNAi treatment. However, as it appears likely that dynein molecules often function in concert to mediate movement (McGrath, 2005), this may be due to a requirement for catalytic cycling to mediate effective recruitment and/or retention of dynein at the BCR microcluster.

On the basis of the interaction between BCR microclusters and dynein, we examined the role of the microtubule network in antigen gathering and visualised BCR microclusters localised to and moving on microtubules in stimulated B cells. However, we cannot definitively establish if this transport on microtubules is intracellular or extracellular. The B cell microtubule network has remained poorly characterised to date. However, a role for the network during T cell activation is implied by repositioning of the MTOC in response to TCR signalling (Lowin-Kropf et al., 1998) and the localised generation of DAG by PLCγ (Quann et al., 2009). Interestingly, it has been shown that the histone deacetylase HDAC6, capable of deacetylating α-tubulin, is also required for MTOC translocation and immune synapse formation in T cells in response to antigen (Serrador et al., 2004). This is particularly intriguing as HDAC6 associates with dynein during microtubule-mediated transport of ubiquitinated proteins to the aggresome (Kawaguchi et al., 2003). However, a role of ubiquitin-binding adaptors such as HDAC6 in B cell activation has not been shown to date.

6.4.2 Co-operation between the actin and microtubule cytoskeleton

The microtubule network and dynein participate in the movement of BCR microclusters and antigen gathering, but not in the initial phases of B cell activation. Until now it was assumed that antigen gathering, as in T cells, occurred through passive retrograde actin flow (Kaizuka et al., 2007) or Myosin IIA-mediated transport along actin filaments (Ilani et al., 2009). However, whereas sustained signalling in T cells is dependent on the continual generation of TCR microclusters, BCR microclusters are rapidly gathered concomitant with contraction to enable antigen internalisation and activation. As such, the relative contribution of the microtubule network and actin cytoskeleton in microcluster movement may differ between B and T cells, and it is therefore possible that the actin cytoskeleton and potentially Myosin IIA participate in the early movement of BCR microclusters. It remains unclear how a defect in microcluster movement towards the central region would lead to impaired B cell contraction. Given the evidence for the coupling of the actomyosin and microtubule networks (Salmon et al., 2002), it is possible that alteration of dynein or microtubule dynamics leads to

a defect in the actomyosin network thus impairing cellular retraction. Interestingly, the linker protein ezrin and its binding partner Dlg1 have recently been implicated in coordinating the various cytoskeletal reorganisations during T cell activation (Lasserre et al., 2010). In this study, Alcover and colleagues showed that while ezrin accumulates early in F-actin rich regions of the T cell immune synapse, it is also required for organization of the microtubule network and movement of TCR microclusters. However, in contrast to our findings with Grb2, Dok-3 and Cbl, silencing of ezrin was found to alter actin-mediated T cell spreading as well as movement of TCR microclusters. In light of our current findings we anticipate that the actin cytoskeleton and the microtubule network co-operate to organize the early and later events of B cell activation, respectively.

6.4.3 Conclusions

On the basis of our results we propose the following model (Figure 6.12): In response to antigen, signalling is initiated by Lyn and Syk concomitant with the formation of BCR microclusters, and is followed by recruitment of other mediators including Vav and PLCγ2 to mediate reorganisation of the actin cytoskeleton necessary for B cell spreading (Weber et al., 2008). In addition, BCR microclusters also recruit Grb2, Dok-3 and Cbl, allowing the efficient localisation of dynein and movement on microtubules after spreading. As Cbl mediates ubiquitination of BCR microcluster components including Syk we suggest that this allows association with adaptors such as HDAC6, marking the microcluster for internalisation. This type of microtubule-mediated transport mechanism is analogous to that seen in the transport of ubiquitinated proteins to the aggresome for destruction (Valenzuela-Fernandez et al., 2008). As the amount of antigen gathered determines the extent of antigen presentation to T cells, this is particularly significant in shaping the outcome of B cell activation. Interestingly, though the role of Cbl in BCR internalisation has remained unclear, a similar role for Cbl in the endocytosis of growth factor receptors has been established (Petrelli et al., 2002). Thus, this may represent a mechanism to couple movement and internalisation of numerous cell surface receptors in biology. Nonetheless, many

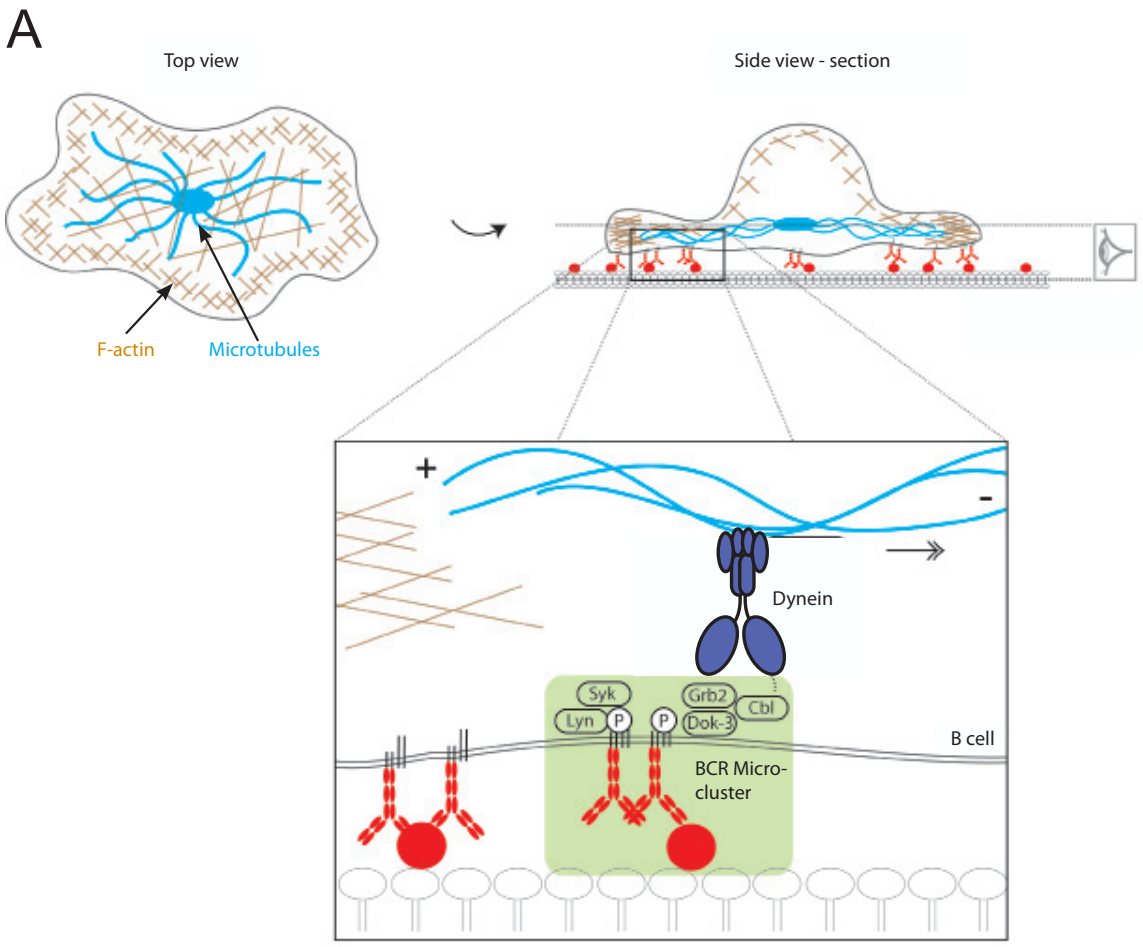

Figure 6.12. Grb2, Dok-3 and Cbl recruit dynein to antigen-containing BCR microclusters to drive antigen gathering by B cells

(A) Magnified view of a signalling microcluster being moved on the microtubule network. In the model we propose, the signalling microcluster (shown in green, containing Lyn, Syk and other mediators including SLP-65, Vav and PLCγ2) recruits the mediators Grb2, Dok-3 and Cbl. The association with the microtubule motor dynein allows minus-end directed movement on the microtubule network to form the central antigen cluster for acquisition. Schematic adapted from N. Harwood.

of the molecular details underlying the process of movement and endocytosis are yet to be established and remain the challenge of future work.

6.4.4 Future directions

We have shown that the microtubule motor dynein together with the underlying microtubule network play an important role during antigen gathering by B cells. As dynein has been previously reported in cellular processes involving receptor endocytosis and internalisation and as the amount of antigen gathered by B cells directly correlates with the extent of T cell help, it would be interesting to test, whether dynein could play a role in antigen internalisation by B cells and subsequent presentation to T cells. Cellular assays addressing this question could be based on impaired dynein function by overexpression of p50 dynamitin or by using mice that carry heterozygous mutations of the dynein heavy chain gene (DYNC1H1). The latter have been previously reported to have motorneuronal defects due to only one functional dynein heavy chain allele and could provide a useful tool to investigate dynein function in primary B cells (Hafezparast, 2003 and Chen et al., 2007). Mice carrying mutations in the dynein heavy chain gene could be used for a large set of experiments including immunisiations, *in vitro* T-B cell co-cultures to measure T cell proliferation or assessment of intracellular signalling in B cells upon BCR ligation. If dynein is indeed involved in the internalisation of the ligated BCR and the subsequent intracellular trafficking of the receptor to early endosomes, mice with only one functional dynein heavy chain allele could potentially show defects in B cell activation and in mounting an adequate immune response to antigen.

In addition to dynein functions related to internalisation, it remains unclear how dynein is recruited to the signalling BCR. HDAC6 is only one molecule that could potentially bridge the gap between microcluster proteins and the dynein machinery. Further work is therefore required to clearly elucidate the mode of action of dynein at the microcluster and the mechanism by which it is recruited.

Chapter 7 : Concluding Remarks and Perspectives

This thesis investigates the early molecular events of B cell activation. Using a combination of genetics, lipid bilayers and high-resolution microscopy we identify a role for the adaptors Grb2 and Dok-3 alongside the ubiquitin ligase Cbl in antigen gathering by B cells. Moreover, we show recruitment of Grb2, Dok-3 and Cbl to the signalling BCR and establish Grb2 as a central downstream adaptor controlling intracellular signalling. We further assess the role of several motor proteins in antigen gathering and find that dynein is recruited to the signalling BCR driving antigen gathering by the movement of antigen-containing BCR microclusters on the underlying microtubule network. Interestingly, recruitment of dynein to BCR microclusters is impaired in B cells lacking Grb2, Dok-3 or Cbl indicating that these molecules are crucial for dynein recruitment to the signalling BCR (Figure 7.1.). As the amount of antigen acquired by B cells directly correlates with the extent of T cell help, the data presented significantly contributes to our understanding of the early molecular events underlying B cell activation.

By the genetic dissection of the recruitment of Grb2, Dok-3 and Cbl to antigen-containing BCR microclusters we have provided new insights into the signalling events downstream of the BCR. According to our data the current dogma of a very hierarchical organisation of the BCR signalosome needs to be revised. For example, we were able to show recruitment of Grb2 and CIN85 to antigen-containing BCR microclusters even in the absence of the central kinase Syk. Syk has historically been regarded as one of the earliest molecules recruited to the signalling BCR and has been postulated as a signal initiator. In view of our findings this model needs re-consideration as adaptor molecules such as Grb2 can be recruited to the ligated BCR independently of Syk. Recent data by Wienands and colleagues has proposed that pre-formed signal transducer complexes might be recruited to the BCR in an immediate fashion and it is thus likely that the kinase Lyn provides sufficient phosphorylated tyrosine residues for the formation of an early signalosome consisting of both kinases and central adaptors. New high-resolution and high-speed microscopy methods will provide

valuable information on the exact composition of BCR microclusters and their spatiotemporal organisation in the near future.

In addition to Grb2, Dok-3 and Cbl we have found that the microtubule-based motor protein dynein drives B cell antigen gathering by the directed movement of BCR microclusters after spreading. Interestingly, the recruitment of dynein was dependent on the ubiquitin ligase Cbl. A whole set of papers has previously established a role for ubiquitination in the process of endocytosis and surface receptor internalisation (see above). As Cbl has been shown to ubiquitinate components of the BCR, this process could potentially mark the microcluster for internalisation. Similarly, dynein has been shown to be crucial for the recycling and internalisation of growth factor receptors in other cellular systems. Combining previous findings on ubiquitination and the dynein machinery with regards to receptor endocytosis, it is likely that both ubiquitination and force generation by dynein could represent a general mechanism for the internalisation of cell surface receptors. In particular in B cells, antigen-containing BCR microclusters could not only serve as a platform for the propagation of BCR signalling, but also as a docking site for the dynein machinery, which could potentially drive microcluster internalisation. Given our experimental data, we cannot conclude whether antigen-containing BCR microclusters observed using TIRF microscopy are indeed at the cell surface or whether they already exist as vesicular structures underneath the plasma membrane.

Given the new role for dynein and the microtubule network in B cell antigen gathering it will be of great interest to investigate the global role of dynein in B cell activation using a diverse set of experiments involving high-resolution microscopy combined with planar lipid bilayers and B cell activation using particulate antigen.

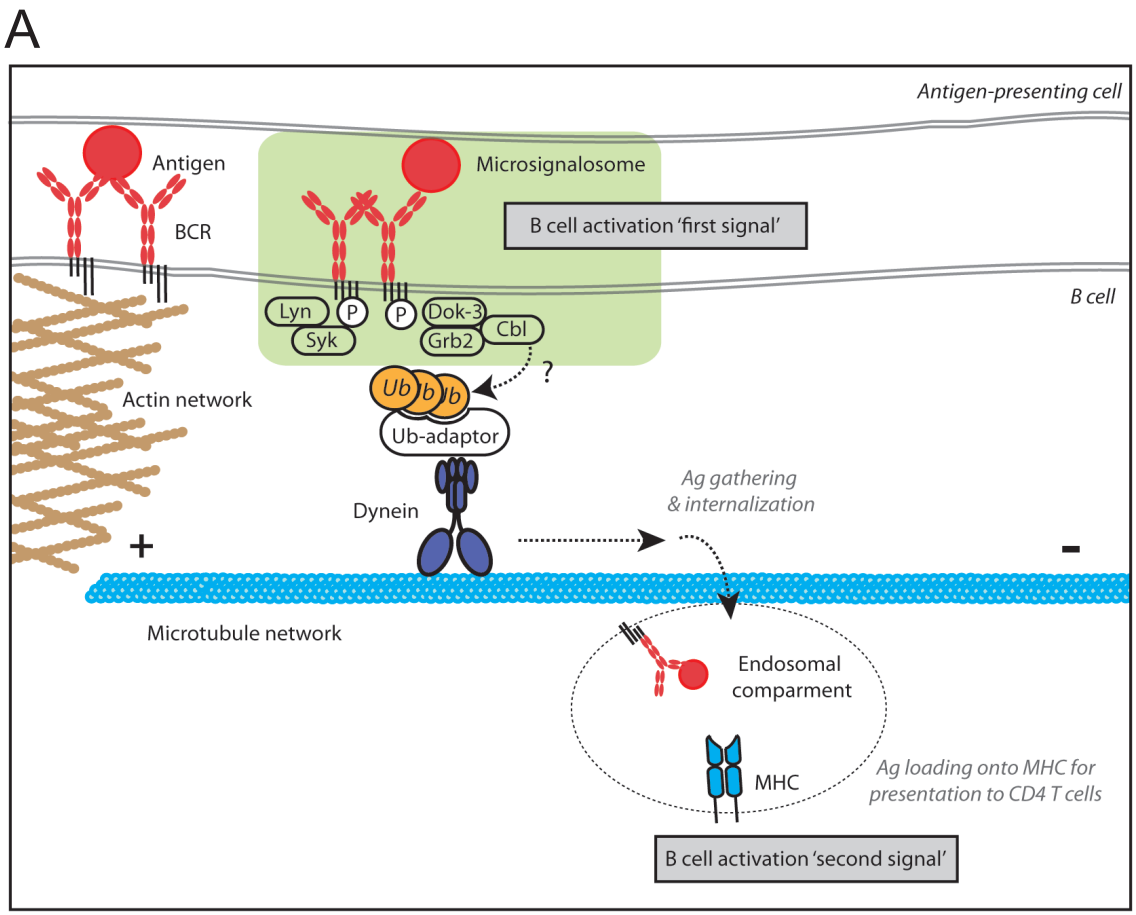

Figure 7.1. Model for antigen-containing BCR microclusters being gathered into the central cluster by dynein-mediated movement on the B cell microtubule network
(A) Magnified view of a signalling microcluster being moved on the microtubule network. In the model we propose, the signalling microcluster (shown in green, containing Lyn, Syk and other mediators including SLP-65, Vav and PLCγ2) recruits the mediators Grb2, Dok-3 and Cbl. We anticipate that ubiquitination (Ub) of microcluster components (potentially including Syk) is mediated by the ubiquitin ligase activity of Cbl and enables the association with ubiquitin-binding adaptors, such as HDAC6, and the functional dynein complex. The association with the microtubule motor dynein allows minus-end directed movement on the microtubule network to form the central antigen cluster for acquisition and presentation to T cells. Schematic adapted from N. Harwood.

Appendix 1 : List of Abbreviations

Abbreviation	Definition
Ag	Antigen
AP	Alkaline Phosphatase
APC	Antigen-presenting Cell
AU	Arbitrary units
ALV	Avian leucosis virus
BCR	B Cell Receptor
BD	Beckton Dickinson
Bf	Brightfield
Cbl	Casitas B-lineage Lymphoma
CD	Cluster of Differentiation
CFSE	Carboxyfluorescein succinimidyl ester
CIN85	Cbl-interacting protein of 85 kDa
CLP	Common lymphoid progenitor
CRUK	Cancer Research UK
DC	Dendritic cell
DC-SIGN	DC-specific ICAM3-grabbing non-integrin
DMSO	Dimethyl sulfoxide
DNA	Deoxyribonucleic acid
Dok-3	Downstream of protein kinase-3
DOPC	1,2-dioleoyl-*sn*-glycero-3-phosphocholine
dpi	Dots per inch
ECL	Enhanced Chemiluminescence
ELISA	Enzyme-linked immunosorbent assay
Erk	Extracellular signal-regulated kinase
ERM	Ezrin-radixin-moeisin
ESCRT	Endosomal sorting complex required for transport
FACS	Fluorescence-activated cell sorting
F	Phenylalanine

FC	Flow cytometry
FCS	Fetal calf serum
fps	Frames per second
FRET	Fluorescence resonance energy transfer
FSC	Forward scatter
GC	Germinal Centre
GFP	Green fluorescent protein
GST	Glutathione S-transferase
Grb2	Growth factor receptor-bound protein 2
HEL	Hen egg lysozyme
HEV	High endothelial venule
HRP	Horseradish peroxidase
IF	Immunofluorescence
IL	Interleukin
IP	Immunoprecipitation
IRES	Internal ribosome entry site
IRM	Interference reflection microscopy
IS	Immune Synapse
ITAM	Immunoreceptor tyrosine-based activation motif
ITIM	Immunoreceptor tyrosine-based inhibitory motif
JNK	c-Jun N-terminal kinase
K	Lysine
kDa	Kilodalton
LIL	Lymphocyte Interaction Laboratory
LC-MS/MS	Liquid chromatography-coupled tandem mass spectrometry
Lck	Lymphocyte-specific protein tyrosine kinase
Lfa-1	Lymphocyte function-associated antigen 1
Lyn	Lck/yes-related novel tyrosine kinase
MAC1	Macrophage receptor 1
MACS	Magnetic-activated cell sorting
MAP kinase	Mitogen-activated protein kinase
mDia	Mammalian diaphanous

MHC	Major Histocompatibility Complex
MICA	MHC 1 polypeptide-related sequence A
NEB	New England Biolabs
NFAT	Nuclear factor of activated T cells
NK cells	Natural Killer cells
ns	Not significant
PAGE	Polyacrylamide gel elctrophoresis
PAMP	Pathogen-associated molecular patterns
PCR	Polymerase chain reaction
PI	Propidium iodide
PH domain	Pleckstrin-homology domain
PLCγ2	Phospholipase C gamma 2
PRR	Pattern recognition receptor
R	Arginine
RAG	Recombination activating gene
RISC	RNA-induced silencing complex
RFP	Red Fluorescent Protein
RNA	Ribonucleic acid
RNAi	RNA interference
ROI	Region of interest
SDS	Sodium dodecyl sulfate
SH2 domain	Src Homology 2 domain
SH3 domain	Src Homology 3 domain
SHIP	SH2 domain-containing inositol 5′-phosphatase
siRNA	small interfering RNA
SLO	Secondary lymphoid organ
SLP65	SH2 domain-containing leukocyte adaptor protein of 65 kDa
SOC	Super optimal broth
Src	Sarcoma
SSC	Side scatter
Syk	Spleen tyrosine kinase
TCR	T cell receptor

TI	T-independent
TIRF	Total Internal Reflection Fluorescence
TNF	Tumor Necrose Factor
Vla-4	Very late antigen-4
W	Tryptophan
WB	Western blot
Y	Tyrosine
YFP	Yellow Fluorescent Protein

Appendix 2 : Supplementary Video Legends

Supplementary Video 1. Bjab B cells spread on anti-human IgM-coated glass
Bjab cells were settled on glass coverslips coated with of an anti-human IgM antibody. Cell spreading was monitored for 20 min using interference reflection microscopy (IRM). Dark areas represent contact sites between cells and the coated glass.

Supplementary Video 2. DT40 B cells lacking Grb2, Dok-3 or Cbl do not gather antigen-containing BCR microclusters in a central aggregate
Wildtype (WT), *Grb2*$^{-/-}$ (grb2KO), *Dok3*$^{-/-}$ (dok3KO), or *Cbl*$^{-/-}$ (cblKO) DT40 B cells were settled on antigen-containing planar lipid bilayers (red) and imaged using TIRF microscopy (TIRFM) at a frame rate of 1 fps for 60 seconds. Scale bar equals 5 μm.

Supplementary Video 3. Grb2 colocalises with antigen-containing BCR microclusters over time
DT40*Grb2*$^{-/-}$ B cells stably expressing Grb2-GFP (green) were settled on lipid bilayers containing surrogate antigen (red) and were imaged using TIRF microscopy at a frame rate of 0.5 fps. Scale bar equals 5 μm.

Supplementary Video 4. Grb2 recruitment to antigen-containing BCR microclusters is altered in *Dok-3*$^{-/-}$ B cells
(left) DT40*Grb2*$^{-/-}$ and (right) DT40*Dok-3*$^{-/-}$ B cells stably expressing Grb2-GFP (green) were settled on lipid bilayers containing surrogate antigen and were imaged using TIRF microscopy at a frame rate of 0.2 fps. Scale bar: 5 μm.

Supplementary Video 5. SLP65 colocalises with antigen-containing BCR microclusters over time

DT40*Slp65*$^{-/-}$ B cells stably expressing SLP65-GFP (green) were settled on lipid bilayers containing surrogate antigen (red) and were imaged using TIRF microscopy at a frame rate of 0.5 fps. Scale bar equals 5 μm.

Supplementary Video 6. CIN85 colocalises with antigen-containing BCR microclusters over time

DT40 B cells stably expressing CIN85-GFP (green) were settled on lipid bilayers containing surrogate antigen (red) and were imaged using TIRF microscopy at a frame rate of 0.5 fps. Scale bar equals 5 μm.

Supplementary Video 7. Myosin IIa does not colocalise with antigen-containing BCR microclusters over time

A20 B cells expressing a GFP-tagged version of Myosin IIa (MyH9-GFP, green) were settled on lipid bilayers containing surrogate antigen (red) and were imaged using TIRF microscopy at a frame rate of 0.5 fps. Scale bar equals 5 μm.

Supplementary Video 8. Myosin VI does not colocalise with antigen-containing BCR microclusters over time

A20 B cells expressing a GFP-tagged version of Myosin VI (MYO6-GFP, green) were settled on lipid bilayers containing surrogate antigen (red) and were imaged using TIRF microscopy at a frame rate of 0.5 fps. Scale bar equals 5 μm.

Supplementary Video 9. Myosin VI does not mediate centripetal movement of antigen-containing BCR microclusters

Primary murine B cells from mice lacking Myosin VI (MYO6-/-) or wildtype littermates (wildtype) were settled on lipid bilayers containing surrogate antigen (red) and were imaged using TIRF microscopy at a frame rate of 0.5 fps. Scale bar equals 5 μm.

Supplementary Video 10. Dynein colocalises with antigen-containing BCR microclusters over time

Primary murine B cells transiently expressing dynein intermediate chain-GFP (green) were settled on lipid bilayers containing antigen (red) and unlabeled ICAM-1. Images were acquired using TIRF microscopy at a frame rate of 1 fps for 70 seconds. Scale bar equals 5 μm.

Supplementary Video 11. Inhibition of dynein activity or expression affects centripetal movement of antigen-containing BCR microclusters

(left) Control A20 murine B cells or cells either expressing a (middle) shRNA construct targeting DYNC1H1 or (right) dynamitin-GFP were settled on antigen-containing lipid bilayers and imaged using TIRF microscopy at a frame rate of 0.1 fps for 10 minutes. Scale bar equals 5μm.

Supplementary Video 12. Single particles of BCR are immobilised in tubulin-rich regions upon BCR cross-linking

DT40 B cells stably expressing tubulin-RFP (green) were labelled with a fluorescent Fab-fragment (red) specific for chicken-IgM (clone M1) and were settled on glass coverslips coated with either Fibronectin alone or with an anti-chicken IgM (clone M4) to cross-link the BCR. Dual-color high-speed TIRF microscopy was used to image BCR particles and tubulin simultaneously at a frame rate of 20 fps. Scale bar equals 5 μm.

Supplementary Video 13. The microtbule network in B cells is highly dynamic

Primary murine B cells transiently expressing Tubulin-RFP (grey) were settled on lipid bilayers containing antigen (not shown) and unlabeled ICAM-1. Images were acquired using TIRF microscopy at a frame rate of 0.5 fps. Scale bar equals 5 μm.

Supplementary Video 14. The tubulin network is unaffected in cells lacking Grb2, Dok-3 or Cbl

WT, *Grb2*$^{-/-}$ (Grb2KO), *Dok3*$^{-/-}$ (Dok3KO), or *Cbl*$^{-/-}$ (CblKO) DT40 B cells stably expressing tubulin-RFP (green) were settled on antigen-containing planar lipid bilayers (red) and imaged using TIRF microscopy at a frame rate of 1 fps for 60 seconds. Scale bar equals 5 μm.

Supplementary Video 15. Dynein colocalises with antigen-containing BCR microclusters in DT40 B cells over time

Wildtype DT40 B cells stably expressing dynein intermediate chain-GFP (green) were settled on lipid bilayers containing antigen (red). Images were acquired using TIRF microscopy at a frame rate of 0.2 fps for 170 seconds. Lower panels show a magnified area within the white box indicated in upper panels. Scale bar equals 5 μm.

Supplementary Video 16. Recruitment of dynein to antigen-containing BCR microclusters requires Grb2, Dok-3 or Cbl

Wildtype (WT), *Grb2*$^{-/-}$ (grb2KO), *Dok3*$^{-/-}$ (dok3KO), or *Cbl*$^{-/-}$ (cblKO) DT40 B cells stably expressing dynein-GFP (green) were settled on antigen-containing planar lipid bilayers (red) and imaged using TIRF microscopy at a frame rate of 1 fps for one minute. Scale bar equals 5 μm.

References

Ackermann JA, Radtke D, Maurberger A, Winkler TH, Nitschke L (2011). Grb2 regulates B-cell maturation, B-cell memory responses and inhibits B-cell Ca2+ signalling. EMBO J 30(8) p1621-33

Acuto O, Di Bartolo V, Michel F (2008). Tailoring T-cell receptor signals by proximal negative feedback mechanisms. Nat Rev Immunol 8(9) p699-712.

Aderem A, Underhill DM (1999). Mechanisms of phagocytosis in macrophages. Annu Rev Immunol 17 p593-623.

Ager A, Callard R, Ezine S, Gerard C, Lopez-Botet M (1996). Immune receptor supplement. *Immunol Today* 1 p1-36.

Agrawal A, Schatz DG (1997). RAG1 and RAG2 form a stable postcleavage synaptic complex with DNA containing signal ends in V(D)J recombination. Cell 89(1) p43-53.

Akashi K, Kondo M, Cheshier S, Shizuru J, Gandy K, Domen J, Mebius R, Traver D, Weissman IL (1999). Lymphoid development from stem cells and the common lymphocyte progenitors. Cold Spring Harb Symp Quant Biol 64 p1-12.

Akira S, Takeda K (2004). Toll-like receptor signalling. Nat Rev Immunol 4(7) p499-511.

Al-Lazikani B, Lesk AM, Chothia C (1997). Standard conformations for the canonical structures of immunoglobulins. J Mol Biol 273(4) p927-48.

Allen CD, Okada T, Tang HL, Cyster JG (2007). Imaging of germinal center selection events during affinity maturation. Science 315(5811) p528-31.

Allenspach EJ, Cullinan P, Tong J, Tang Q, Tesciuba AG, Cannon JL, Takahashi SM, Morgan R, Burkhardt JK, Sperling AI (2001). ERM-dependent movement of CD43 defines a novel protein complex distal to the immunological synapse. Immunity 15(5) p739-50.

Aluvihare VR, Khamlichi AA, Williams GT, Adorini L, Neuberger MS (1997). Acceleration of intracellular targeting of antigen by the B-cell antigen receptor: importance depends on the nature of the antigen-antibody interaction. EMBO J 16(12) p3553-62.

Andzelm MM, Chen X, Krzewski K, Orange JS, Strominger JL (2007). Myosin IIA is required for cytolytic granule exocytosis in human NK cells. J Exp Med 204(10) p2285-91.

Arakawa H, Takeda S (1996). Early expression of Ig mu chain from a transgene significantly reduces the duration of the pro-B stage but does not affect the small pre-B stage. Int Immunol 8(8) p1319-28.

Arana E, Vehlow A, Harwood NE, Vigorito E, Henderson R, Turner M, Tybulewicz VL, Batista FD (2008). Activation of the small GTPase Rac2 via the B cell receptor regulates B cell adhesion and immunological-synapse formation. Immunity 28(1) p88-99.

Avraham KB, Hansson T, Steel KP, Kingsley DM, Russell LB, Mooseker MS, Copeland NG, Jenkins NA (1995). The mouse *Snell's waltzer* deafness gene encodes an unconventional myosin required for structural integrity of inner ear hair cells. Nat Genet 11(4) p369-375.

Baba T, Fusaki N, Shinya N, Iwamatsu A, Hozumi N (2003). Myosin is an in vivo substrate of the protein tyrosine phosphatase (SHP-1) after mIgM cross-linking. Biochem Biophys Res Commun 304(1) p67-72.

Baba TW, Giroir BP, Humphries EH (1985). Cell lines derived from avian lymphomas exhibit two distinct phenotypes. Virology 144(1) p139-51.

Balagopalan L, Barr VA, Sommers CL, Barda-Saad M, Goyal A, Isakowitz MS, Samelson LE (2007). c-Cbl-mediated regulation of LAT-nucleated signaling complexes. Mol Cell Biol 27(24) p8622-36.

Batista FD, Arana E, Barral P, Carrasco YR, Depoil D, Eckl-Dorna J, Fleire S, Howe K, Vehlow A, Weber M, Treanor B (2007). The role of integrins and coreceptors in refining thresholds for B-cell responses. Immunol Rev 218 p197-213.

Batista FD, Neuberger MS (1998). Affinity dependence of the B cell response to antigen: a threshold, a ceiling, and the importance of off-rate. Immunity 8(6) p751-9.

Batista FD, Neuberger MS (2000). B cells extract and present immobilized antigen: implications for affinity discrimination. EMBO J19(4) p513-20.

Batista FD, Iber D, Neuberger MS (2001). B cells acquire antigen from target cells after synapse formation. Nature 411(6836) p489-94.

Batista FD, Harwood NE (2009). The who, how and where of antigen presentation to B cells. Nat Rev Immunol (1) p15-27.

Benjamin D, Magrath IT, Maguire R, Janus C, Todd HD, Parsons RG (1982). Immunoglobulin secretion by cell lines derived from African and American undifferentiated lymphomas of Burkitt's and non-Burkitt's type. J Immunol 129(3):1336-42.

Bergtold A, Desai DD, Gavhane A, Clynes R (2005). Cell surface recycling of internalized antigen permits dendritic cell priming of B cells. Immunity 23(5) p503-14.

Bhakdi S, Tranum-Jensen J (1991). Complement lysis: a hole is a hole. Immunol Today 12(9) p318-20.

Biron CA, Nguyen KB, Pien GC, Cousens LP, Salazar-Mather TP (1999). Natural killer cells in antiviral defense: function and regulation by innate cytokines. Annu Rev Immunol 17 p189-220.

Bochenska-Marciniak M, Kupczyk M, Górski P, Kuna P (2003). The effect of recombinant interleukin-8 on eosinophils and neutrophils migration in vivo and in vitro. Allergy 58(8) p795-801.

Brack C, Hirama M, Lenhard-Schuller R, Tonegawa S (1978). A complete immunoglobulin gene is created by somatic recombination. Cell 15(1) p1-14.

Brian AA, McConnell HM (1984). Allogeneic stimulation of cytotoxic T cells by supported planar membranes. Proc Natl Acad Sci USA 81(19) p6159-63.

Brightbill HD, Libraty DH, Krutzik SR, Yang RB, Belisle JT, Bleharski JR, Maitland M, Norgard MV, Plevy SE, Smale ST, Brennan PJ, Bloom BR, Godowski PJ, Modlin RL (1999). Host defense mechanisms triggered by microbial lipoproteins through toll-like receptors. Science 285(5428) p732-6.

Brockmeyer C, Paster W, Pepper D, Tan CP, Trudgian DC, McGowan S, Fu G, Gascoigne NR, Acuto O, Salek M (2011). T cell receptor (TCR)-induced tyrosine phosphorylation dynamics identifies THEMIS as a new TCR signalosome component. J Biol Chem 286(9) p7535-47.

Brown BK, Song W (2001). The actin cytoskeleton is required for the trafficking of the B cell antigen receptor to the late endosomes. Traffic 2(6) p414-27.

Bunnell SC, Hong DI, Kardon JR, Yamazaki T, McGlade CJ, Barr VA, Samelson LE (2002). T cell receptor ligation induces the formation of dynamically regulated signaling assemblies. J Cell Biol 158(7) p1263-75.

Burkhardt JK, Echeverri CJ, Nilsson T, Vallee RB (1997). Overexpression of the dynamitin (p50) subunit of the dynactin complex disrupts dynein-dependent maintenance of membrane organelle distribution. J Cell Biol 139(2) p469-84.

Campi G, Varma R, Dustin ML (2005). Actin and agonist MHC-peptide complex-dependent T cell receptor microclusters as scaffolds for signaling. J Exp Med 202(8) p1031-6.

Carlyle JR, Zúñiga-Pflücker JC (1998). Requirement for the thymus in alphabeta T lymphocyte lineage commitment. Immunity 9(2) p187-97.

Carrasco YR, Batista FD (2006). B-cell activation by membrane-bound antigens is facilitated by the interaction of VLA-4 with VCAM-1. EMBO J 25(4) p889-99.

Carrasco YR, Batista FD (2007). B cells acquire particulate antigen in a macrophage-rich area at the boundary between the follicle and the subcapsular sinus of the lymph node. Immunity 27(1) p160-71.

Carrasco YR, Fleire SJ, Cameron T, Dustin ML, Batista FD (2004). LFA-1/ICAM-1 interaction lowers the threshold of B cell activation by facilitating B cell adhesion and synapse formation. Immunity 20(5) p589-99.

Casellas R, Shih TA, Kleinewietfeld M, Rakonjac J, Nemazee D, Rajewsky K, Nussenzweig MC (2001). Contribution of receptor editing to the antibody repertoire. Science 291(5508) p1541-1544.

Cassard S, Salamero J, Hanau D, Spehner D, Davoust J, Fridman WH, Bonnerot C (1998). A tyrosine-based signal present in Ig alpha mediates B cell receptor constitutive internalization. J Immunol 160(4) p1767-73.

Catron DM, Itano AA, Pape KA, Mueller DL, Jenkins MK (2004). Visualizing the first 50 hr of the primary immune response to a soluble antigen. Immunity 21(3) p341-7.

Cemerski S, Das J, Giurisato E, Markiewicz MA, Allen PM, Chakraborty AK, Shaw AS (2008). The balance between T cell receptor signaling and degradation at the center of the immunological synapse is determined by antigen quality. Immunity 29(3) p414-22.

Chen AA, Derfus AM, Khetani SR, Bhatia SN (2005). Quantum dots to monitor RNAi delivery and improve gene silencing. Nucleic Acids Res 33(22) pe190.

Chen XJ, Levedakou EN, Millen KJ, Wollmann RL, Soliven B, Popko B (2007). Proprioceptive sensory neuropathy in mice with a mutation in the cytoplasmic Dynein heavy chain 1 gene. J Neurosci 27(52) p14515-24.

Cheng AM, Saxton TM, Sakai R, Kulkarni S, Mbamalu G, Vogel W, Tortorice CG, Cardiff RD, Cross JC, Muller WJ, Pawson T (1998). Mammalian Grb2 regulates multiple steps in embryonic development and malignant transformation. Cell 95(6) p793-803.

Cheng PC, Steele CR, Gu L, Song W, Pierce SK (1999). MHC class II antigen processing in B cells: accelerated intracellular targeting of antigens. J Immunol 162(12) p7171-80.

Chertov O, Yang D, Howard OM, Oppenheim JJ (2000). Leukocyte granule proteins mobilize innate host defenses and adaptive immune responses. Immunol Rev 177 p68-78.

Chesnut RW, Grey HM (1981). Studies on the capacity of B cells to serve as antigen-presenting cells. J Immunol 126(3) p1075-9.

Chong R, Squires R, Swiss R, Agaisse H (2011). RNAi Screen Reveals Host Cell Kinases Specifically Involved in Listeria monocytogenes Spread from Cell to Cell. PLoS One 6(8) pe23399.

Choudhuri K, Wiseman D, Brown MH, Gould K, van der Merwe PA (2005). T-cell receptor triggering is critically dependent on the dimensions of its peptide-MHC ligand. Nature 436(7050) p578-82.

Chu J, Liu Y, Koretzky GA, Durden DL (1998). SLP-76-Cbl-Grb2-Shc interactions in FcgammaRI signaling. Blood92(5) p1697-706.

Clark SL Jr (1962). The reticulum of lymph nodes in mice studied with the electron microscope. Am J Anat 110 p217-57.

Clark R, Kupper T (2005). Old meets new: the interaction between innate and adaptive immunity. J Invest Dermatol 125(4) p629-37.

Coffman RL (1982). Surface antigen expression and immunoglobulin gene rearrangement during mouse pre-B cell development. Immunol Rev 69 p5-23.

Combs J, Kim SJ, Tan S, Ligon LA, Holzbaur EL, Kuhn J, Poenie M (2006). Recruitment of dynein to the Jurkat immunological synapse. Proc Natl Acad Sci U S A 103(40) p14883-8.

Cornall RJ, Goodnow CC, Cyster JG (1995). The regulation of self-reactive B cells. Curr Opin Immunol 7(6) p804-11.

Cox J, Mann M (2008). MaxQuant enables high peptide identification rates, individualized p.p.b.-range mass accuracies and proteome-wide protein quantification. Nat Biotechnol 26(12) p1367-72.

Cozine CL, Wolniak KL, Waldschmidt TJ (2005). The primary germinal center response in mice. Curr Opin Immunol17(3) p298-302.

Crocker JC and Grier DG (1996). Methods of Digital Video Microscopy for Colloidal Studies. J Colloid Interface Sci 179(1) p298-310.

Cyster JG (2005). Chemokines, sphingosine-1-phosphate, and cell migration in secondary lymphoid organs. Annu Rev Immunol 23 p127-59.

Cyster JG (2010). B cell follicles and antigen encounters of the third kind. Nat Immunol 11(11) p989-96.

Dal Porto JM, Gauld SB, Merrell KT, Mills D, Pugh-Bernard AE, Cambier J (2004). B cell antigen receptor signaling 101. Mol Immunol 41(6-7) p599-613.

Davanture S, Leignadier J, Milani P, Soubeyran P, Malissen B, Malissen M, Schmitt-Verhulst AM, Boyer C (2005). Selective defect in antigen-induced TCR internalization at the immune synapse of CD8 T cells bearing the ZAP-70(Y292F) mutation. J Immunol 175(5) p3140-9.

Davis DM, Chiu I, Fassett M, Cohen GB, Mandelboim O, Strominger JL (1999). The human natural killer cell immune synapse. Proc Natl Acad Sci U S A 96(26) p15062-7.

Davis RE, Ngo VN, Lenz G, Tolar P, Young RM, Romesser PB, Kohlhammer H, Lamy L, Zhao H, Yang Y, Xu W, Shaffer AL, Wright G, Xiao W, Powell J, Jiang JK, Thomas CJ, Rosenwald A, Ott G, Muller-Hermelink HK, Gascoyne RD, Connors JM, Johnson NA, Rimsza LM, Campo E, Jaffe ES, Wilson WH, Delabie J, Smeland EB, Fisher RI, Braziel RM, Tubbs RR, Cook JR, Weisenburger DD, Chan WC, Pierce SK, Staudt LM (2010). Chronic active B-cell-receptor signalling in diffuse large B-cell lymphoma. Nature 463(7277) p88-92.

Davis SJ, van der Merwe PA (2006). The kinetic-segregation model: TCR triggering and beyond. Nat Immunol 7(8) p803-9.

Deckert M, Elly C, Altman A, Liu YC (1998). Coordinated regulation of the tyrosine phosphorylation of Cbl by Fyn and Syk tyrosine kinases. J Biol Chem 273(15) p8867-74.

DeFranco AL (2001). Vav and the B cell signalosome. Nat Immunol 2(6) p482-4.

Deindl S, Kadlecek TA, Brdicka T, Cao X, Weiss A, Kuriyan J (2007). Structural basis for the inhibition of tyrosine kinase activity of ZAP-70. Cell 129(4) p735-46.

Delon J, Kaibuchi K, Germain RN (2001). Exclusion of CD43 from the immunological synapse is mediated by phosphorylation-regulated relocation of the cytoskeletal adaptor moesin. Immunity 15(5) p691-701.

DeMond AL, Mossman KD, Starr T, Dustin ML, Groves JT (2008). T cell receptor microcluster transport through molecular mazes reveals mechanism of translocation. Biophys J 94(8) p3286-92.

Depoil D, Fleire S, Treanor BL, Weber M, Harwood NE, Marchbank KL, Tybulewicz VL, Batista FD (2008). CD19 is essential for B cell activation by promoting B cell receptor-antigen microcluster formation in response to membrane-bound ligand. Nat Immunol 9(1) p63-72.

Dikic I (2002). CIN85/CMS family of adaptor molecules. FEBS Lett 529(1) p110-5.

Dintzis HM, Dintzis RZ, Vogelstein B (1976). Molecular determinants of immunogenicity: the immunon model of immune response. Proc Natl Acad Sci U S A 73(10) p3671-5.

Döhner K, Wolfstein A, Prank U, Echeverri C, Dujardin D, Vallee R, Sodeik B (2002). Function of dynein and dynactin in herpes simplex virus capsid transport. Mol Biol Cell 13(8) p2795-809.

Dong S, Corre B, Foulon E, Dufour E, Veillette A, Acuto O, Michel F (2006). T cell receptor for antigen induces linker for activation of T cell-dependent activation of a negative signaling complex involving Dok-2, SHIP-1, and Grb-2. J Exp Med 203(11) p2509-18.

Dudziak D, Kamphorst AO, Heidkamp GF, Buchholz VR, Trumpfheller C, Yamazaki S, Cheong C, Liu K, Lee HW, Park CG, Steinman RM, Nussenzweig MC (2007). Differential antigen processing by dendritic cell subsets in vivo. Science 315(5808) p107-11.

Dustin ML, Miller JM, Ranganath S, Vignali DA, Viner NJ, Nelson CA, Unanue ER (1996). TCR-mediated adhesion of T cell hybridomas to planar bilayers containing purified MHC class II/peptide complexes and receptor shedding during detachment. J Immunol 157(5) p2014-21.

Eckl-Dorna J, Batista FD (2009). BCR-mediated uptake of antigen linked to TLR9 ligand stimulates B-cell proliferation and antigen-specific plasma cell formation. Blood 113(17) p3969-77.

Edelman GM (1991). Antibody structure and molecular immunology. Scand J Immunol 34(1) p1-22.

Ehlers MR (2000). CR3: a general purpose adhesion-recognition receptor essential for innate immunity. Microbes Infect 2(3) p289-94.

Ehrlich P, Morgenroth J (1957). On haemolysins. The collected papers of Paul Ehrlich 2 p253.

Eisen HN, Siskind GW (1964). Variations in affinities of antibodies during the immune response. Biochemistry 3 p996-1008.

Engel P, Zhou LJ, Ord DC, Sato S, Koller B, Tedder TF (1995). Abnormal B lymphocyte development, activation, and differentiation in mice that lack or overexpress the CD19 signal transduction molecule. Immunity 3(1) p39-50.

Engels N, König LM, Heemann C, Lutz J, Tsubata T, Griep S, Schrader V, Wienands J (2009). Recruitment of the cytoplasmic adaptor Grb2 to surface IgG and IgE provides antigen receptor-intrinsic costimulation to class-switched B cells. Nat Immunol 10(9) p1018-25.

Fagraeus A (1948). The plasma cellular reaction and its relation to the formation of antibodies in vitro. J Immunol 58(1) p1-13.

Farr AG, Cho Y, De Bruyn PP (1980). The structure of the sinus wall of the lymph node relative to its endocytic properties and transmural cell passage. Am J Anat 157(3) p265-84.

Fearon DT, Carroll MC (2000). Regulation of B lymphocyte responses to foreign and self-antigens by the CD19/CD21 complex. Annu Rev Immunol 18 p393-422.

Fiévet B, Louvard D, Arpin M (2007). ERM proteins in epithelial cell organization and functions. Biochim Biophys Acta 1773(5) p653-60.

Flaswinkel H, Barner M, Reth M (1995). The tyrosine activation motif as a target of protein tyrosine kinases and SH2 domains. Semin Immunol 7(1) p21-7.

Fleire SJ, Goldman JP, Carrasco YR, Weber M, Bray D, Batista FD (2006). B cell ligand discrimination through a spreading and contraction response. Science 312(5774) p738-41.

Foote J, Milstein C (1991). Kinetic maturation of an immune response. Nature 352(6335) p530-2.

Fossum S, Ford WL (1985). The organization of cell populations within lymph nodes: their origin, life history and functional relationships. Histopathology 9(5) p469-99.

Fox EM, Miller TW, Balko JM, Kuba MG, Sanchez V, Smith RA, Liu S, González-Angulo AM, Mills GB, Ye F, Shyr Y, Manning HC, Buck E, Arteaga CL (2011). A kinome-wide screen identifies the Insulin/IGF-1 receptor pathway as a mechanism of escape from hormone dependence in breast cancer. Cancer Res Sep 9. [Epub ahead of print].

Frangione B, Milstein C (1967). Disulphide bridges of immunoglobin G-1 heavy chains. Nature 216(5118) p939-41.

Frangione B, Milstein C, Pink JR (1969). Structural studies of immunoglobulin G. Nature 221(5176) p145-8.

Frank MM, Fries LF (1991). The role of complement in inflammation and phagocytosis. Immunol Today 12(9) p322-6.

Fu C, Turck CW, Kurosaki T, Chan AC (1998). BLNK: a central linker protein in B cell activation. Immunity 9(1) p93-103.

Gallo RL, Murakami M, Ohtake T, Zaiou M (2002). Biology and clinical relevance of naturally occurring antimicrobial peptides. J Allergy Clin Immunol 110(6) p823-31.

Garside P, Ingulli E, Merica RR, Johnson JG, Noelle RJ, Jenkins MK (1998). Visualization of specific B and T lymphocyte interactions in the lymph node. Science 281(5373) p96-9.

Garcia KC, Teyton L, Wilson IA (1999). Structural basis of T cell recognition. Annu Rev Immunol 17 p369-97.

Gathings WE, Lawton AR, Cooper MD (1977). Immunofluorescent studies of the development of pre-B cells, B lymphocytes and immunoglobulin isotype diversity in humans. Eur J Immunol 7(11) p804-10.

Gil D, Schamel WW, Montoya M, Sánchez-Madrid F, Alarcón B (2002). Recruitment of Nck by CD3 epsilon reveals a ligand-induced conformational change essential for T cell receptor signaling and synapse formation. Cell 109(7) p901-12.

Gonzalez SF, Pitcher LA, Mempel T, Schuerpf F, Carroll MC (2009). B cell acquisition of antigen in vivo. Curr Opin Immunol 21(3) p251-7.

Goodnow CC (1996). Balancing immunity and tolerance: deleting and tuning lymphocyte repertoires. Proc Natl Acad Sci U S A 93(6) p2264-71.

Gough PJ, Gordon S (2000). The role of scavenger receptors in the innate immune system. Microbes Infect 2(3) p305-11.

Gowans JL, Knight EJ (1964). The route of re-circulation of lymphocytes in the rat. Proc R Soc Lond B Biol Sci 159 p257-82.

Grabbe A, Wienands J (2006). Human SLP-65 isoforms contribute differently to activation and apoptosis of B lymphocytes. Blood 108(12) p3761-8.

Grakoui A, Bromley SK, Sumen C, Davis MM, Shaw AS, Allen PM, Dustin ML (1999). The immunological synapse: a molecular machine controlling T cell activation. Science 285(5425) p221-7.

Grawunder U, West RB, Lieber MR (1998). Antigen receptor gene rearrangement. Curr Opin Immunol 10(2) p172-80.

Gupta N, DeFranco AL (2003). Visualizing lipid raft dynamics and early signaling events during antigen receptor-mediated B-lymphocyte activation. Mol Biol Cell 14(2) p432-44.

Gupta N, DeFranco AL (2007). Lipid rafts and B cell signaling. Semin Cell Dev Biol 18(5) p616-26.

Gupta N, Wollscheid B, Watts JD, Scheer B, Aebersold R, DeFranco AL (2006). Quantitative proteomic analysis of B cell lipid rafts reveals that ezrin regulates antigen receptor-mediated lipid raft dynamics. Nat Immunol 7(6) p625-33.

Hafezparast M, Klocke R, Ruhrberg C, Marquardt A, Ahmad-Annuar A, Bowen S, Lalli G, Witherden AS, Hummerich H, Nicholson S, Morgan PJ, Oozageer R, Priestley JV, Averill S, King VR, Ball S, Peters J, Toda T, Yamamoto A, Hiraoka Y, Augustin M, Korthaus D, Wattler S, Wabnitz P, Dickneite C, Lampel S, Boehme F, Peraus G, Popp A, Rudelius M, Schlegel J, Fuchs H, Hrabe de Angelis M, Schiavo G, Shima DT, Russ AP, Stumm G, Martin JE, Fisher EM (2003). Mutations in dynein link motor neuron degeneration to defects in retrograde transport. Science 300(5620) p808-12.

Harris LJ, Larson SB, Hasel KW, Day J, Greenwood A, McPherson A (1992). The three-dimensional structure of an intact monoclonal antibody for canine lymphoma. Nature 360(6402) p369-72.

Harrison RE, Grinstein S (2002). Phagocytosis and the microtubule cytoskeleton. Biochem Cell Biol 80(5) p509-15.

Hartley SB, Crosbie J, Brink R, Kantor AB, Basten A, Goodnow CC (1991). Elimination from peripheral lymphoid tissues of self-reactive B lymphocytes recognizing membrane-bound antigens. Nature 353(6346) p765-9.

Harwood NE, Batista FD (2008). New insights into the early molecular events underlying B cell activation. Immunity 28(5) p609-19.

Hashimoto A, Okada H, Jiang A, Kurosaki M, Greenberg S, Clark EA, Kurosaki T (1998). Involvement of guanosine triphosphatases and phospholipase C-gamma2 in extracellular signal-regulated kinase, c-Jun NH2-terminal kinase, and p38 mitogen-activated protein kinase activation by the B cell antigen receptor. J Exp Med 188(7) p1287-95.

Hauser AE, Junt T, Mempel TR, Sneddon MW, Kleinstein SH, Henrickson SE, von Andrian UH, Shlomchik MJ, Haberman AM (2007). Definition of germinal-center B cell migration in vivo reveals predominant intrazonal circulation patterns. Immunity 26(5) p655-67.

Havrylov S, Redowicz MJ, Buchman VL (2010). Emerging roles of Ruk/CIN85 in vesicle-mediated transport, adhesion, migration and malignancy. Traffic 11(6) p721-31.

Heine H, Lien E (2003). Toll-like receptors and their function in innate and adaptive immunity. Int Arch Allergy Immunol 130(3) p180-92.

Heinonen JE, Smith CI, Nore BF (2002). Silencing of Bruton's tyrosine kinase (Btk) using short interfering RNA duplexes (siRNA). FEBS Lett 527(1-3) p274-8.

Hennecke J, Wiley DC (2001). T cell receptor-MHC interactions up close. Cell 104(1) p1-4.

Hornef MW, Wick MJ, Rhen M, Normark S (2002). Bacterial strategies for overcoming host innate and adaptive immune responses. *Nat Immunol* 3(11) p1033-1040.

Hotulainen P, Lappalainen P (2006). Stress fibers are generated by two distinct actin assembly mechanisms in motile cells. J Cell Biol 173(3) p383-94.

Huang F, Gu H (2008). Negative regulation of lymphocyte development and function by the Cbl family of proteins. Immunol Rev 224 p229-38.

Huang JY, Umehara H, Inoue H, Tabassam FH, Okazaki T, Kono T, Minami Y, Tanaka Y, Domae N (2000). Differential interaction of Cbl with Grb2 and CrkL in CD2-mediated NK cell activation. Mol Immunol 37(17) p1057-65.

Ilani T, Vasiliver-Shamis G, Vardhana S, Bretscher A, Dustin ML (2009). T cell antigen receptor signaling and immunological synapse stability require myosin IIA. Nat Immunol 10(5) p531-9.

Inoue A, Sato O, Homma K, Ikebe M (2002). DOC-2/DAB2 is the binding partner of myosin VI. Biochem Biophys Res Commun 292(2) p300-7.

Irles C, Symons A, Michel F, Bakker TR, van der Merwe PA, Acuto O (2003). CD45 ectodomain controls interaction with GEMs and Lck activity for optimal TCR signaling. Nat Immunol 4(2) p189-97.

Ishiai M, Kurosaki M, Pappu R, Okawa K, Ronko I, Fu C, Shibata M, Iwamatsu A, Chan AC, Kurosaki T (1999). BLNK required for coupling Syk to PLC gamma 2 and Rac1-JNK in B cells. Immunity 10(1) p117-25.

Jacob M, Todd L, Sampson MF, Puré E (2008). Dual role of Cbl links critical events in BCR endocytosis. Int Immunol 20(4) p485-97.

Jacobelli J, Chmura SA, Buxton DB, Davis MM, Krummel MF (2004). A single class II myosin modulates T cell motility and stopping, but not synapse formation. Nat Immunol 5(5) p531-8.

Janeway CA Jr (2008). Janeway's Immunobiology, 7th edition, Garland Science, New York

Janeway CA Jr, Medzhitov R (2002). Innate immune recognition. Annu Rev Immunol 20 p197-216.

Jang IK, Cronshaw DG, Xie LK, Fang G, Zhang J, Oh H, Fu YX, Gu H, Zu Y (2011). Growth-factor receptor-bound protein-2 (Grb2) signalling in B cells controls lymphoid follicle organization and germinal center reaction. Proc Natl Acad Sci U S A 108(19) p7926-31.

Jellusova J, Wellmann U, Amann K, Winkler TH, Nitschke L (2010). CD22 x Siglec-G double-deficient mice have massively increased B1 cell numbers and develop systemic autoimmunity. J Immunol 184(7) p3618-27.

Junt T, Moseman EA, Iannacone M, Massberg S, Lang PA, Boes M, Fink K, Henrickson SE, Shayakhmetov DM, Di Paolo NC, van Rooijen N, Mempel TR, Whelan SP, von Andrian UH (2007). Subcapsular sinus macrophages in lymph nodes clear lymph-borne viruses and present them to antiviral B cells. Nature 450(7166) p110-4.

Junt T, Scandella E, Ludewig B (2008). Form follows function: lymphoid tissue microarchitecture in antimicrobial immune defence. Nat Rev Immunol 8(10) p764-75.

Kaizuka Y, Douglass AD, Varma R, Dustin ML, Vale RD (2007). Mechanisms for segregating T cell receptor and adhesion molecules during immunological synapse formation in Jurkat T cells. Proc Natl Acad Sci U S A 104(51) p20296-301.

Kardon JR, Vale RD (2009). Regulators of the cytoplasmic dynein motor. Nat Rev Mol Cell Biol 10(12) p854-65.

Kato M, Sanada M, Kato I, Sato Y, Takita J, Takeuchi K, Niwa A, Chen Y, Nakazaki K, Nomoto J, Asakura Y, Muto S, Tamura A, Iio M, Akatsuka Y, Hayashi Y, Mori H, Igarashi T, Kurokawa M, Chiba S, Mori S, Ishikawa Y, Okamoto K, Tobinai K, Nakagama H, Nakahata T, Yoshino T, Kobayashi Y, Ogawa S (2009). Frequent inactivation of A20 in B-cell lymphomas. Nature 459(7247) p712-6.

Kawaguchi Y, Kovacs JJ, McLaurin A, Vance JM, Ito A, Yao TP (2003). The deacetylase HDAC6 regulates aggresome formation and cell viability in response to misfolded protein stress. Cell 115(6) p727-38.

Kim KJ, Kanellopoulos-Langevin C, Merwin RM, Sachs DH, Asofsky R (1979). Establishment and characterization of BALB/c lymphoma lines with B cell properties. J Immunol 122(2) p549-54.

Kitamura D, Kudo A, Schaal S, Müller W, Melchers F, Rajewsky K (1992). A critical role of lambda 5 protein in B cell development. Cell 69(5) p823-31.

Kitaura Y, Jang IK, Wang Y, Han YC, Inazu T, Cadera EJ, Schlissel M, Hardy RR, Gu H (2007). Control of the B cell-intrinsic tolerance programs by ubiquitin ligases Cbl and Cbl-b. Immunity26(5) p567-78.

Kitchens CA, McDonald PR, Shun TY, Pollack IF, Lazo JS (2011). Identification of chemosensitivity nodes for vinblastine through small interfering RNA high-throughput screens. J Pharmacol Exp Ther Aug 31 [Epub ahead of print].

Koppel EA, Wieland CW, van den Berg VC, Litjens M, Florquin S, van Kooyk Y, van der Poll T, Geijtenbeek TB (2005). Specific ICAM-3 grabbing nonintegrin-related 1 (SIGNR1) expressed by marginal zone macrophages is essential for defense against pulmonary Streptococcus pneumoniae infection. Eur J Immunol 35(10) p2962-9.

Kovar DR, Harris ES, Mahaffy R, Higgs HN, Pollard TD (2006). Control of the assembly of ATP- and ADP-actin by formins and profilin. Cell 124(2) p423-35.

Kraus M, Alimzhanov MB, Rajewsky N, Rajewsky K (2004). Survival of resting mature B lymphocytes depends on BCR signaling via the Igalpha/beta heterodimer. Cell 117(6) p787-800.

Krummel MF, Sjaastad MD, Wülfing C, Davis MM (2000). Differential clustering of CD4 and CD3zeta during T cell recognition. Science 289(5483) p1349-52.

Kuhns MS, Davis MM, Garcia KC (2006). Deconstructing the form and function of the TCR/CD3 complex. Immunity 24(2) p133-9.

Kulathu Y, Hobeika E, Turchinovich G, Reth M (2008). The kinase Syk as an adaptor controlling sustained calcium signalling and B-cell development. EMBO J 27(9) p1333-44.

Kunkel EJ, Butcher EC (2002). Chemokines and the tissue-specific migration of lymphocytes. Immunity 16(1) p1-4.

Kurosaki T (1999). Genetic analysis of B cell antigen receptor signaling. Annu Rev Immunol 17 p555-92.

Kurosaki T (2002). Regulation of B cell fates by BCR signaling components. Curr Opin Immunol 14(3) p341-7.

Lam KP, Kühn R, Rajewsky K (1997). In vivo ablation of surface immunoglobulin on mature B cells by inducible gene targeting results in rapid cell death. Cell 90(6) p1073-83.

Lanzavecchia A (1985). Antigen-specific interaction between T and B cells. Nature 314(6011) p537-9.

Lasserre R, Charrin S, Cuche C, Danckaert A, Thoulouze MI, de Chaumont F, Duong T, Perrault N, Varin-Blank N, Olivo-Marin JC, Etienne-Manneville S, Arpin M, Di Bartolo V, Alcover A (2010). Ezrin tunes T-cell activation by controlling Dlg1 and microtubule positioning at the immunological synapse. EMBO J 29(14) p2301-14.

Lemay S, Davidson D, Latour S, Veillette A (2000). Dok-3, a novel adapter molecule involved in the negative regulation of immunoreceptor signaling. Mol Cell Biol 20(8) p2743-54.

Li X, Sandoval D, Freeberg L, Carter RH (1997). Role of CD19 tyrosine 391 in synergistic activation of B lymphocytes by coligation of CD19 and membrane Ig. J Immunol 158(12) p5649-57.

Lillemeier BF, Mörtelmaier MA, Forstner MB, Huppa JB, Groves JT, Davis MM (2010). TCR and Lat are expressed on separate protein islands on T cell membranes and concatenate during activation. Nat Immunol 11(1) p90-6.

Lillemeier BF, Pfeiffer JR, Surviladze Z, Wilson BS, Davis MM (2006). Plasma membrane-associated proteins are clustered into islands attached to the cytoskeleton. Proc Natl Acad Sci U S A 103(50) p18992-7.

Liu D, Bryceson YT, Meckel T, Vasiliver-Shamis G, Dustin ML, Long EO (2009). Integrin-dependent organization and bidirectional vesicular traffic at cytotoxic immune synapses. Immunity 31(1) p99-109.

Liu C, Miller H, Hui KL, Grooman B, Bolland S, Upadhyaya A, Song W (2011). A balance of Bruton's tyrosine kinase and SHIP activation regulates B cell receptor cluster formation by controlling actin remodeling. J Immunol 187(1) p230-9.

Liu YC, Gu H (2002). Cbl and Cbl-b in T-cell regulation. Trends Immunol 23(3) p140-3.

Liu Q, Oliveira-Dos-Santos AJ, Mariathasan S, Bouchard D, Jones J, Sarao R, Kozieradzki I, Ohashi PS, Penninger JM, Dumont DJ (1998). The inositol polyphosphate 5-phosphatase ship is a crucial negative regulator of B cell antigen receptor signaling. J Exp Med 188(7) p1333-42.

Loder F, Mutschler B, Ray RJ, Paige CJ, Sideras P, Torres R, Lamers MC, Carsetti R (1999). B cell development in the spleen takes place in discrete steps and is determined by the quality of B cell receptor-derived signals. J Exp Med 190(1) p75-89.

Löffert D, Ehlich A, Müller W, Rajewsky K (1996). Surrogate light chain expression is required to establish immunoglobulin heavy chain allelic exclusion during early B cell development. Immunity 4(2) p133-44.

Lowin-Kropf B, Shapiro VS, Weiss A (1998). Cytoskeletal polarization of T cells is regulated by an immunoreceptor tyrosine-based activation motif-dependent mechanism. J Cell Biol 140(4) p861-71.

Lupher ML Jr, Rao N, Lill NL, Andoniou CE, Miyake S, Clark EA, Druker B, Band H (1998). Cbl-mediated negative regulation of the Syk tyrosine kinase. A critical role for Cbl phosphotyrosine-binding domain binding to Syk phosphotyrosine 323. J Biol Chem 273(52) p35273-81.

MacLennan IC (1994). Germinal centers. Annu Rev Immunol 12 p117-39.

Maeda A, Scharenberg AM, Tsukada S, Bolen JB, Kinet JP, Kurosaki T (1999). Paired immunoglobulin-like receptor B (PIR-B) inhibits BCR-induced activation of Syk and Btk by SHP-1. Oncogene 18(14) p2291-7.

Makowska A, Faizunnessa NN, Anderson P, Midtvedt T, Cardell S (1999). CD1high B cells: a population of mixed origin. Eur J Immunol 29(10) p3285-94.

Manders E, Verbeek F, and Aten J. (1993). Measurement of co-localization of objects in dual-colour confocal images. J Microscopy 169, 375-382.

Maravillas-Montero JL, Gillespie PG, Patiño-López G, Shaw S, Santos-Argumedo L (2011). Myosin 1c participates in B cell cytoskeleton rearrangements, is recruited to the immunologic synapse, and contributes to antigen presentation. J Immunol 187(6) p3053-63.

Martín-Cófreces NB, Robles-Valero J, Cabrero JR, Mittelbrunn M, Gordón-Alonso M, Sung CH, Alarcón B, Vázquez J, Sánchez-Madrid F (2008). MTOC translocation modulates IS formation and controls sustained T cell signaling. J Cell Biol 182(5) p951-62.

Martínez-Pomares L, Kosco-Vilbois M, Darley E, Tree P, Herren S, Bonnefoy JY, Gordon S (1996). Fc chimeric protein containing the cysteine-rich domain of the murine mannose receptor binds to macrophages from splenic marginal zone and lymph node subcapsular sinus and to germinal centers. J Exp Med 184(5) p1927-37.

McCann FE, Eissmann P, Onfelt B, Leung R, Davis DM (2007). The activating NKG2D ligand MHC class I-related chain A transfers from target cells to NK cells in a manner that allows functional consequences. J Immunol 178(6) p3418-26.

McGrath JL (2005). Dynein motility: four heads are better than two. Curr Biol 15(23) pR970-2.

McHeyzer-Williams MG, McLean MJ, Lalor PA, Nossal GJ (1993). Antigen-driven B cell differentiation in vivo. J Exp Med 178(1) p295-307.

Mebius RE (2003). Organogenesis of lymphoid tissues. Nat Rev Immunol 3(4) p292-303.

Medzhitov R, Janeway CA Jr (2000). How does the immune system distinguish self from nonself? Semin Immunol 12(3) p185-8.

Medzhitov R, Janeway C Jr (2000). The Toll receptor family and microbial recognition. Trends Microbiol 8(10) p452-6.

Minegishi Y, Rohrer J, Coustan-Smith E, Lederman HM, Pappu R, Campana D, Chan AC, Conley ME (1999). An essential role for BLNK in human B cell development. Science 286(5446) p1954-7.

Mitchell GF, Chan EL, Noble MS, Weissman IL, Mishell RI, Herzenberg LA (1972). Immunological memory in mice. 3. Memory to heterologous erythrocytes in both T cell and B cell populations and requirement for T cells in expression of B cell memory. Evidence using immunoglobulin allotype and mouse alloantigen theta markers with congenic mice. J Exp Med 135(2) p165-84.

Mizuno K, Tagawa Y, Mitomo K, Arimura Y, Hatano N, Katagiri T, Ogimoto M, Yakura H (2000). Src homology region 2 (SH2) domain-containing phosphatase-1 dephosphorylates B cell linker protein/SH2 domain leukocyte protein of 65 kDa and selectively regulates c-Jun NH2-terminal kinase activation in B cells. J Immunol 165(3) p1344-51.

Molfetta R, Belleudi F, Peruzzi G, Morrone S, Leone L, Dikic I, Piccoli M, Frati L, Torrisi MR, Santoni A, Paolini R (2005). CIN85 regulates the ligand-dependent endocytosis of the IgE receptor: a new molecular mechanism to dampen mast cell function. J Immunol 175(7) p4208-16.

Monks CR, Freiberg BA, Kupfer H, Sciaky N, Kupfer A (1998). Three-dimensional segregation of supramolecular activation clusters in T cells. Nature 395(6697) p82-6.

Morita S, Kojima T, Kitamura T (2000). Plat-E: an efficient and stable system for transient packaging of retroviruses. Gene Ther 7(12) p1063-6.

Morris SM, Arden SD, Roberts RC, Kendrick-Jones J, Cooper JA, Luzio JP, Buss F (2002). Myosin VI binds to and localises with Dab2, potentially linking receptor-mediated endocytosis and the actin cytoskeleton. Traffic 3(5) p331-41.

Mosier D, Subbarao D (1982). Thymus-independent antigens: complexity of B-lymphocyte activation revealed. Immunol Today 3 p217.

Mustelin T, Vang T, Bottini N (2005). Protein tyrosine phosphatases and the immune response. Nat Rev Immunol 5(1) p43-57.

Nagasawa T, Hirota S, Tachibana K, Takakura N, Nishikawa S, Kitamura Y, Yoshida N, Kikutani H, Kishimoto T (1996). Defects of B-cell lymphopoiesis and bone-marrow myelopoiesis in mice lacking the CXC chemokine PBSF/SDF-1. Nature 382(6592) p635-8.

Nemazee DA, Bürki K (1989). Clonal deletion of B lymphocytes in a transgenic mouse bearing anti-MHC class I antibody genes. Nature 337(6207) p562-6.

Neumann K, Oellerich T, Urlaub H, Wienands J (2009). The B-lymphoid Grb2 interaction code. Immunol Rev 232(1) p135-49.

Ng CH, Xu S, Lam KP (2007). Dok-3 plays a nonredundant role in negative regulation of B-cell activation. Blood 110(1) p259-66.

Nguyen K, Sylvain NR, Bunnell SC (2008). T cell costimulation via the integrin VLA-4 inhibits the actin-dependent centralization of signaling microclusters containing the adaptor SLP-76. Immunity 28(6) p810-21.

Nichols BJ, Kenworthy AK, Polishchuk RS, Lodge R, Roberts TH, Hirschberg K, Phair RD, Lippincott-Schwartz J (2001). Rapid cycling of lipid raft markers between the cell surface and Golgi complex. J Cell Biol 153(3) p529-41.

Niiro H, Clark EA (2002). Regulation of B-cell fate by antigen-receptor signals. Nat Rev Immunol 2(12) p945-56.

Nitschke L (2005). The role of CD22 and other inhibitory co-receptors in B-cell activation. Curr Opin Immunol 17(3) p290-7.

Nitschke L (2009). CD22 and Siglec-G: B-cell inhibitory receptors with distinct functions. Immunol Rev 230(1) p128-43.

North B, Lehmann A, Dunbrack RL Jr (2011). A new clustering of antibody CDR loop conformations. J Mol Biol 406(2) p228-56.

Nossal GJ, Abbot A, Mitchell J, Lummus Z (1968). Antigens in immunity. XV. Ultrastructural features of antigen capture in primary and secondary lymphoid follicles. J Exp Med 127(2) p277-90.

Odegard VH, Schatz DG (2006). Targeting of somatic hypermutation. Nat Rev Immunol 6(8) p573-83.

Oellerich T, Bremes V, Neumann K, Bohnenberger H, Dittmann K, Hsiao HH, Engelke M, Schnyder T, Batista FD, Urlaub H, Wienands J (2011). The B-cell antigen receptor signals through a preformed transducer module of SLP65 and CIN85. EMBO J 30(17) p3620-34.

Oellerich T, Grønborg M, Neumann K, Hsiao HH, Urlaub H, Wienands J (2009). SLP-65 phosphorylation dynamics reveals a functional basis for signal integration by receptor-proximal adaptor proteins. Mol Cell Proteomics 8(7) p1738-50.

Ohno H, Stewart J, Fournier MC, Bosshart H, Rhee I, Miyatake S, Saito T, Gallusser A, Kirchhausen T, Bonifacino JS (1995). Interaction of tyrosine-based sorting signals with clathrin-associated proteins. Science 269(5232) p1872-5.

Okada T, Miller MJ, Parker I, Krummel MF, Neighbors M, Hartley SB, O'Garra A, Cahalan MD, Cyster JG (2005). Antigen-engaged B cells undergo chemotaxis toward the T zone and form motile conjugates with helper T cells. PLoS Biol 3(6) pe150.

Orange JS, Fassett MS, Koopman LA, Boyson JE, Strominger JL (2002). Viral evasion of natural killer cells. Nat Immunol 3(11) p1006-12.

Panchamoorthy G, Fukazawa T, Miyake S, Soltoff S, Reedquist K, Druker B, Shoelson S, Cantley L, Band H (1996). p120cbl is a major substrate of tyrosine phosphorylation upon B cell antigen receptor stimulation and interacts in vivo with Fyn and Syk tyrosine kinases, Grb2 and Shc adaptors, and the p85 subunit of phosphatidylinositol 3-kinase. J Biol Chem 271(6) p3187-94.

Papamichail M, Gutierrez C, Embling P, Johnson P, Holborow EJ, Pepys MB (1975). Complement dependence of localisation of aggregated IgG in germinal centres. Scand J Immunol 4(4) p343-47.

Paolini R, Molfetta R, Piccoli M, Frati L, Santoni A (2001). Ubiquitination and degradation of Syk and ZAP-70 protein tyrosine kinases in human NK cells upon CD16 engagement. Proc Natl Acad Sci USA 98(17) p9611-6.

Pape KA, Catron DM, Itano AA, Jenkins MK (2007). The humoral immune response is initiated in lymph nodes by B cells that acquire soluble antigen directly in the follicles. Immunity 26(4) p491-502.

Pappu R, Cheng AM, Li B, Gong Q, Chiu C, Griffin N, White M, Sleckman BP, Chan AC (1999). Requirement for B cell linker protein (BLNK) in B cell development. Science 286(5446) p1949-54.

Patino-Lopez G, Aravind L, Dong X, Kruhlak MJ, Ostap EM, Shaw S (2010). Myosin 1G is an abundant class I myosin in lymphocytes whose localization at the plasma membrane depends on its ancient divergent pleckstrin homology (PH) domain (Myo1PH). J Biol Chem 285(12) p8675-86.

Peruzzi G, Molfetta R, Gasparrini F, Vian L, Morrone S, Piccoli M, Frati L, Santoni A, Paolini R (2007). The adaptor molecule CIN85 regulates Syk tyrosine kinase level by activating the ubiquitin-proteasome degradation pathway. J Immunol 179(4) p2089-96.

Peters JD, Furlong MT, Asai DJ, Harrison ML, Geahlen RL (1996). Syk, activated by cross-linking the B-cell antigen receptor, localizes to the cytosol where it interacts with and phosphorylates alpha-tubulin on tyrosine. J Biol Chem 271(9) p4755-62.

Petrelli A, Gilestro GF, Lanzardo S, Comoglio PM, Migone N, Giordano S (2002). The endophilin-CIN85-Cbl complex mediates ligand-dependent downregulation of c-Met. Nature 416(6877) p187-90.

Pfeffer K (2003). Biological functions of tumor necrosis factor cytokines and their receptors. Cytokine Growth Factor Rev 14(3-4) p185-91.

Pham TH, Okada T, Matloubian M, Lo CG, Cyster JG (2008). S1P1 receptor signaling overrides retention mediated by G alpha i-coupled receptors to promote T cell egress. Immunity 28(1) p122-33.

Phan TG, Grigorova I, Okada T, Cyster JG (2007). Subcapsular encounter and complement-dependent transport of immune complexes by lymph node B cells. Nat Immunol 8(9) p992-1000.

Plotz PH (2003). The autoantibody repertoire: searching for order. Nat Rev Immunol 3(1) p73-8.

Poljak RJ (1991). Structure of antibodies and their complexes with antigens. Mol Immunol 28(12) p1341-5.

Porter RR (1991). Lecture for the Nobel Prize for physiology or medicine 1972: Structural studies of immunoglobulins. 1972. Scand J Immunol 34(4) p381-9.

Potter TA, Grebe K, Freiberg B, Kupfer A (2001). Formation of supramolecular activation clusters on fresh ex vivo CD8+ T cells after engagement of the T cell antigen receptor and CD8 by antigen-presenting cells. Proc Natl Acad Sci U S A 98(22) p12624-9.

Potworowski EF, Nairn RC (1967). Specific antigenicity of thymocytes. Nature 213(5081) p1135-6.

Pulvertaft JV (1964). Cytology of Burkitt's Tumour (African Lymphoma). Lancet1(7327) p238-40.

Quann EJ, Merino E, Furuta T, Huse M (2009). Localized diacylglycerol drives the polarization of the microtubule-organizing center in T cells. Nat Immunol 10(6) p627-35.

Rajewsky K (1996). Clonal selection and learning in the antibody system. Nature 381(6585) p751-8.

Rao N, Dodge I, Band H (2002). The Cbl family of ubiquitin ligases: critical negative regulators of tyrosine kinase signaling in the immune system. J Leukoc Biol 71(5) p753-63.

Reth M (1989). Antigen receptor tail clue. Nature 338(6214) p383-4.

Reth M, Wienands J (1997). Initiation and processing of signals from the B cell antigen receptor. Annu Rev Immunol 15 p453-79.

Rickert RC, Rajewsky K, Roes J (1995). Impairment of T-cell-dependent B-cell responses and B-1 cell development in CD19-deficient mice. Nature 376(6538) p352-5.

Riedl J, Crevenna AH, Kessenbrock K, Yu JH, Neukirchen D, Bista M, Bradke F, Jenne D, Holak TA, Werb Z, Sixt M, Wedlich-Soldner R (2008). Lifeact: a versatile marker to visualize F-actin. Nat Methods 5(7) p605-7.

Robbins SH, Brossay L (2002). NK cell receptors: emerging roles in host defense against infectious agents. Microbes Infect 4(15) p1523-30.

Robson JD, Davidson D, Veillette A (2004). Inhibition of the Jun N-terminal protein kinase pathway by SHIP-1, a lipid phosphatase that interacts with the adaptor molecule Dok-3.Mol Cell Biol 24(6):2332-43.

Rolli V, Gallwitz M, Wossning T, Flemming A, Schamel WW, Zürn C, Reth M (2002). Amplification of B cell antigen receptor signaling by a Syk/ITAM positive feedback loop. Mol Cell 10(5) p1057-69.

Rose R, Weyand M, Lammers M, Ishizaki T, Ahmadian MR, Wittinghofer A (2005). Structural and mechanistic insights into the interaction between Rho and mammalian Dia. Nature 435(7041) p513-8.

Roumier A, Olivo-Marin JC, Arpin M, Michel F, Martin M, Mangeat P, Acuto O, Dautry-Varsat A, Alcover A (2001). The membrane-microfilament linker ezrin is involved in the formation of the immunological synapse and in T cell activation. Immunity 15(5) p715-28.

Salmon WC, Adams MC, Waterman-Storer CM (2002). Dual-wavelength fluorescent speckle microscopy reveals coupling of microtubule and actin movements in migrating cells. J Cell Biol 158(1) p31-7.

Sanborn KB, Rak GD, Maru SY, Demers K, Difeo A, Martignetti JA, Betts MR, Favier R, Banerjee PP, Orange JS (2009). Myosin IIA associates with NK cell lytic granules to enable their interaction with F-actin and function at the immunological synapse. J Immunol 182(11) p6969-84.

Sbalzarini IF, Koumoutsakos P (2005). Feature point tracking and trajectory analysis for video imaging in cell biology. J Struct Biol 151(2) p182-95.

Schamel WW, Arechaga I, Risueño RM, van Santen HM, Cabezas P, Risco C, Valpuesta JM, Alarcón B (2005). Coexistence of multivalent and monovalent TCRs explains high sensitivity and wide range of response. J Exp Med 202(4) p493-503.

Schamel WW, Reth M (2000). Monomeric and oligomeric complexes of the B cell antigen receptor. Immunity 13(1) p5-14.

Schamel WW, Risueño RM, Minguet S, Ortíz AR, Alarcón B (2006). A conformation- and avidity-based proofreading mechanism for the TCR-CD3 complex. Trends Immunol 27(4) p176-82.

Scharenberg AM, Humphries LA, Rawlings DJ (2007). Calcium signalling and cell-fate choice in B cells. Nat Rev Immunol 7(10) p778-89.

Schatz DG, Oettinger MA, Baltimore D (1989). The V(D)J recombination activating gene, RAG-1. Cell 59(6) p1035-48.

Schnyder T, Castello A, Feest C, Harwood NE, Oellerich T, Urlaub H, Engelke M, Wienands J, Bruckbauer A, Batista FD (2011). B cell receptor-mediated antigen gathering requires ubiquitin ligase Cbl and adaptors Grb2 and Dok-3 to recruit dynein to the signaling microcluster. Immunity 34(6) p905-18.

Schwickert TA, Lindquist RL, Shakhar G, Livshits G, Skokos D, Kosco-Vilbois MH, Dustin ML, Nussenzweig MC (2007). In vivo imaging of germinal centres reveals a dynamic open structure. Nature 446(7131) p83-7.

Secrist JP, Burns LA, Karnitz L, Koretzky GA, Abraham RT (1993). Stimulatory effects of the protein tyrosine phosphatase inhibitor, pervanadate, on T-cell activation events. J Biol Chem 268(8) p5886-93.

Serrador JM, Cabrero JR, Sancho D, Mittelbrunn M, Urzainqui A, Sánchez-Madrid F (2004). HDAC6 deacetylase activity links the tubulin cytoskeleton with immune synapse organization. Immunity 20(4) p417-28.

Shao Y, Yang C, Elly C, Liu YC (2004). Differential regulation of the B cell receptor-mediated signaling by the E3 ubiquitin ligase Cbl. J Biol Chem 279(42) p43646-53.

Shimizu T, Mundt C, Licence S, Melchers F, Mårtensson IL (2002). VpreB1/VpreB2/lambda 5 triple-deficient mice show impaired B cell development but functional allelic exclusion of the IgH locus. J Immunol 168(12) p6286-93.

Shlomchik MJ, Marshak-Rothstein A, Wolfowicz CB, Rothstein TL, Weigert MG (1987). The role of clonal selection and somatic mutation in autoimmunity. Nature 328(6133) p805-11.

Smit L, van der Horst G, Borst J (1996). Formation of Shc/Grb2- and Crk adaptor complexes containing tyrosine phosphorylated Cbl upon stimulation of the B-cell antigen receptor. Oncogene 13(2) p381-9.

Smith KG, Hewitson TD, Nossal GJ, Tarlinton DM (1996). The phenotype and fate of the antibody-forming cells of the splenic foci. Eur J Immunol 26(2) p444-8.

Sohn HW, Gu H, Pierce SK (2003). Cbl-b negatively regulates B cell antigen receptor signaling in mature B cells through ubiquitination of the tyrosine kinase Syk. J Exp Med 197(11) p1511-24.

Song W, Cho H, Cheng P, Pierce SK (1995). Entry of B cell antigen receptor and antigen into class II peptide-loading compartment is independent of receptor cross-linking. J Immunol 155(9) p4255-63.

Sokol CL, Chu NQ, Yu S, Nish SA, Laufer TM, Medzhitov R (2009). Basophils function as antigen-presenting cells for an allergen-induced T helper type 2 response. Nat Immunol 10(7) p713-20.

Soubeyran P, Kowanetz K, Szymkiewicz I, Langdon WY, Dikic I (2002). Cbl-CIN85-endophilin complex mediates ligand-induced downregulation of EGF receptors. Nature 416(6877) p183-7.

Spudich JA, Sivaramakrishnan S (2010). Myosin VI: an innovative motor that challenged the swinging lever arm hypothesis. Nat Rev Mol Cell Biol 11(2) p128-37.

Stavnezer J (1996). Immunoglobulin class switching. Curr Opin Immunol 8(2) p199-205.

Stinchcombe JC, Bossi G, Booth S, Griffiths GM (2001). The immunological synapse of CTL contains a secretory domain and membrane bridges. Immunity 15(5) p751-61.

Stinchcombe JC, Majorovits E, Bossi G, Fuller S, Griffiths GM (2006). Centrosome polarization delivers secretory granules to the immunological synapse. Nature 443(7110) p462-5.

Stork B, Engelke M, Frey J, Horejsí V, Hamm-Baarke A, Schraven B, Kurosaki T, Wienands J (2004). Grb2 and the non-T cell activation linker NTAL constitute a Ca(2+)-regulating signal circuit in B lymphocytes. Immunity 21(5) p681-91.

Stork B, Neumann K, Goldbeck I, Alers S, Kähne T, Naumann M, Engelke M, Wienands J (2007). Subcellular localization of Grb2 by the adaptor protein Dok-3 restricts the intensity of Ca2+ signaling in B cells. EMBO J 26(4) p1140-9.

Suzuki K, Grigorova I, Phan TG, Kelly LM, Cyster JG (2009). Visualizing B cell capture of cognate antigen from follicular dendritic cells. J Exp Med 206(7) p1485-93.

Szakal AK, Holmes KL, Tew JG (1983). Transport of immune complexes from the subcapsular sinus to lymph node follicles on the surface of nonphagocytic cells, including cells with dendritic morphology. J Immunol 131(4) p1714-27.

Takata M, Sabe H, Hata A, Inazu T, Homma Y, Nukada T, Yamamura H, Kurosaki T (1994). Tyrosine kinases Lyn and Syk regulate B cell receptor-coupled Ca2+ mobilization through distinct pathways. EMBO J 13(6) p1341-9.

Take H, Watanabe S, Takeda K, Yu ZX, Iwata N, Kajigaya S (2000). Cloning and characterization of a novel adaptor protein, CIN85, that interacts with c-Cbl. Biochem Biophys Res Commun 268(2) p321-8.

Takemoto Y, Furuta M, Sato M, Findell PR, Ramble W, Hashimoto Y (1998). Growth factor receptor-bound protein 2 (Grb2) association with hemopoietic specific protein 1: linkage between Lck and Grb2. J Immunol 161(2) p625-30.

Talmage DW (1957). Allergy and immunology. Annu Rev Med 8 p239-56.

Tanaka M, Gupta R, Mayer BJ (1995). Differential inhibition of signaling pathways by dominant-negative SH2/SH3 adapter proteins. Mol Cell Biol 15(12) p6829-37.

Taniguchi T, Kobayashi T, Kondo J, Takahashi K, Nakamura H, Suzuki J, Nagai K, Yamada T, Nakamura S, Yamamura H (1991). Molecular cloning of a porcine gene syk that encodes a 72-kDa protein-tyrosine kinase showing high susceptibility to proteolysis. J Biol Chem 266(24) p15790-6.

Tedder TF, Clement LT, Cooper MD (1984). Discontinuous expression of a membrane antigen (HB-7) during B lymphocyte differentiation. Tissue Antigens 24(3) p140-9.

Tew JG, Phipps RP, Mandel TE (1980). The maintenance and regulation of the humoral immune response: persisting antigen and the role of follicular antigen-binding dendritic cells as accessory cells. Immunol Rev 53 p175-201.

Tew JG, Wu J, Fakher M, Szakal AK, Qin D (2001). Follicular dendritic cells: beyond the necessity of T-cell help. Trends Immunol 22(7) p361-7.

Thien CB, Langdon WY (2001). Cbl: many adaptations to regulate protein tyrosine kinases. Nat Rev Mol Cell Biol 2(4) p294-307.

Tiegs SL, Russell DM, Nemazee D (1993). Receptor editing in self-reactive bone marrow B cells. J Exp Med 177(4) p1009-1020.

Tiselius A, Kabat EA (1938). Electrophoresis of immune serum. Science 87(2262) p416-7.

Tolar P, Hanna J, Krueger PD, Pierce SK (2009). The constant region of the membrane immunoglobulin mediates B cell-receptor clustering and signaling in response to membrane antigens. Immunity 30(1) p44-55.

Tolar P, Sohn HW, Pierce SK (2005). The initiation of antigen-induced B cell antigen receptor signaling viewed in living cells by fluorescence resonance energy transfer. Nat Immunol 6(11) p1168-76.

Tomlinson S (1993). Complement defense mechanisms. Curr Opin Immunol 5(1) p83-9.

Treanor B, Depoil D, Bruckbauer A, Batista FD (2011). Dynamic cortical actin remodeling by ERM proteins controls BCR microcluster organization and integrity. J Exp Med 208(5) p1055-68.

Treanor B, Depoil D, Gonzalez-Granja A, Barral P, Weber M, Dushek O, Bruckbauer A, Batista FD (2010). The membrane skeleton controls diffusion dynamics and signaling through the B cell receptor. Immunity 32(2) p187-99.

Tsai JW, Bremner KH, Vallee RB (2007). Dual subcellular roles for LIS1 and dynein in radial neuronal migration in live brain tissue. Nat Neurosci 10(8) p970-9.

Turner M, Gulbranson-Judge A, Quinn ME, Walters AE, MacLennan IC, Tybulewicz VL (1997). Syk tyrosine kinase is required for the positive selection of immature B cells into the recirculating B cell pool. J Exp Med 186(12) p2013-21.

Turner M, Mee PJ, Costello PS, Williams O, Price AA, Duddy LP, Furlong MT, Geahlen RL, Tybulewicz VL (1995). Perinatal lethality and blocked B-cell development in mice lacking the tyrosine kinase Syk. Nature 378(6554) p298-302.

Tuveson DA, Carter RH, Soltoff SP, Fearon DT (1993). CD19 of B cells as a surrogate kinase insert region to bind phosphatidylinositol 3-kinase. Science 260(5110) p986-9.

Vale RD (2003). The molecular motor toolbox for intracellular transport. Cell 112(4) p467-80.

Valenzuela-Fernández A, Cabrero JR, Serrador JM, Sánchez-Madrid F (2008). HDAC6: a key regulator of cytoskeleton, cell migration and cell-cell interactions. Trends Cell Biol 18(6) p291-7.

Vardhana S, Choudhuri K, Varma R, Dustin ML (2010). Essential role of ubiquitin and TSG101 protein in formation and function of the central supramolecular activation cluster. Immunity 32(4) p531-40.

Varma R, Campi G, Yokosuka T, Saito T, Dustin ML (2006). T cell receptor-proximal signals are sustained in peripheral microclusters and terminated in the central supramolecular activation cluster. Immunity 25(1) p117-27.

Vascotto F, Lankar D, Faure-André G, Vargas P, Diaz J, Le Roux D, Yuseff MI, Sibarita JB, Boes M, Raposo G, Mougneau E, Glaichenhaus N, Bonnerot C, Manoury B, Lennon-Duménil AM (2007). The actin-based motor protein myosin II regulates MHC class II trafficking and BCR-driven antigen presentation. J Cell Biol 176(7) p1007-19.

von Andrian UH, Mempel TR (2003). Homing and cellular traffic in lymph nodes. Nat Rev Immunol 3(11) p867-78.

Warner CL, Stewart A, Luzio JP, Steel KP, Libby RT, Kendrick-Jones J, Buss F (2003). Loss of myosin VI reduces secretion and the size of the Golgi in fibroblasts from Snell's waltzer mice. EMBO J 22(3) p569-79.

Watanabe S, Take H, Takeda K, Yu ZX, Iwata N, Kajigaya S (2000). Characterization of the CIN85 adaptor protein and identification of components involved in CIN85 complexes. Biochem Biophys Res Commun 278(1) p167-74.

Weber M, Treanor B, Depoil D, Shinohara H, Harwood NE, Hikida M, Kurosaki T, Batista FD (2008). Phospholipase C-gamma2 and Vav cooperate within signaling microclusters to propagate B cell spreading in response to membrane-bound antigen. J Exp Med 205(4) p853-68.

Wei Q, Adelstein RS (2000). Conditional expression of a truncated fragment of nonmuscle myosin II-A alters cell shape but not cytokinesis in HeLa cells. Mol Biol Cell 11(10) p3617-27.

Wells AL, Lin AW, Chen LQ, Safer D, Cain SM, Hasson T, Carragher BO, Milligan RA, Sweeney HL (1999). Myosin VI is an actin-based motor that moves backwards. Nature 401(6752) p505-8.

West MA, Lucocq JM, Watts C (1994). Antigen processing and class II MHC peptide-loading compartments in human B-lymphoblastoid cells. Nature 369(6476) p147-51.

Wiedemann A, Müller S, Favier B, Penna D, Guiraud M, Delmas C, Champagne E, Valitutti S (2005). T-cell activation is accompanied by an ubiquitination process occurring at the immunological synapse. Immunol Lett 98(1) p57-61.

Wienands J, Schweikert J, Wollscheid B, Jumaa H, Nielsen PJ, Reth M (1998). SLP-65: a new signaling component in B lymphocytes which requires expression of the antigen receptor for phosphorylation. J Exp Med 188(4) p791-5.

Wilson CA, Tsuchida MA, Allen GM, Barnhart EL, Applegate KT, Yam PT, Ji L, Keren K, Danuser G, Theriot JA (2010). Myosin II contributes to cell-scale actin network treadmilling through network disassembly. Nature 465(7296) p373-7.

Xu C, Gagnon E, Call ME, Schnell JR, Schwieters CD, Carman CV, Chou JJ, Wucherpfennig KW (2008). Regulation of T cell receptor activation by dynamic membrane binding of the CD3epsilon cytoplasmic tyrosine-based motif. Cell 135(4) p702-13.

Yang J, Reth M (2010). Oligomeric organization of the B-cell antigen receptor on resting cells. Nature 467(7314) p465-9.

Yasuda T, Maeda A, Kurosaki M, Tezuka T, Hironaka K, Yamamoto T, Kurosaki T (2000). Cbl suppresses B cell receptor-mediated phospholipase C (PLC)-gamma2 activation by regulating B cell linker protein-PLC-gamma2 binding. J Exp Med 191(4) p641-50.

Yasuda T, Tezuka T, Maeda A, Inazu T, Yamanashi Y, Gu H, Kurosaki T, Yamamoto T (2002). Cbl-b positively regulates Btk-mediated activation of phospholipase C-gamma2 in B cells. J Exp Med 196(1) p51-63.

Yokosuka T, Sakata-Sogawa K, Kobayashi W, Hiroshima M, Hashimoto-Tane A, Tokunaga M, Dustin ML, Saito T (2005). Newly generated T cell receptor microclusters initiate and sustain T cell activation by recruitment of Zap70 and SLP-76. Nat Immunol 6(12) p1253-62.

Yoshida K, van den Berg TK, Dijkstra CD (1993). Two functionally different follicular dendritic cells in secondary lymphoid follicles of mouse spleen, as revealed by CR1/2 and FcR gamma II-mediated immune-complex trapping. Immunology 80(1) p34-9.

Yoshimoto T, Yasuda K, Tanaka H, Nakahira M, Imai Y, Fujimori Y, Nakanishi K (2009). Basophils contribute to T(H)2-IgE responses in vivo via IL-4 production and presentation of peptide-MHC class II complexes to CD4+ T cells. Nat Immunol 10(7) p706-12.

Zhang J, Zheng X, Yang X, Liao K (2009). CIN85 associates with endosomal membrane and binds phosphatidic acid. Cell Res 19(6) p733-46.

Zhu JW, Brdicka T, Katsumoto TR, Lin J, Weiss A (2008). Structurally distinct phosphatases CD45 and CD148 both regulate B cell and macrophage immunoreceptor signaling. Immunity 28(2) p183-96.

Zinkernagel RM, Bachmann MF, Kündig TM, Oehen S, Pirchet H, Hengartner H (1996). On immunological memory. Annu Rev Immunol 14 p333-67.

Zinkernagel RM, Callahan GN, Klein J, Dennert G (1978). Cytotoxic T cells learn specificity for self H-2 during differentiation in the thymus. Nature 271(5642) p251-3.

Publications

The work presented in this thesis has contributed to the following publications:

Schnyder T, Castello A, Feest C, Harwood NE, Oellerich T, Urlaub H, Engelke M, Wienands J, Bruckbauer A, Batista FD (2011). B cell receptor-mediated antigen gathering requires ubiquitin ligase Cbl and adaptors Grb2 and Dok-3 to recruit dynein to the signaling microcluster. **Immunity** 34(6) p905-18.

Oellerich T, Bremes V, Neumann K, Bohnenberger H, Dittmann K, Hsiao HH, Engelke M, **Schnyder T**, Batista FD, Urlaub H, Wienands J (2011). The B-cell antigen receptor signals through a preformed transducer module of SLP65 and CIN85. **EMBO J** 30(17) p3620-34.